ADSORPTIVE PROPERTIES

OF

CHROMIUM OXIDES AND SILICA

Thesis submitted for the degree of

Doctor of Philosophy

by

Frederick Stanley Baker

March 1974

The School of Chemistry,
Brunel University,
Kingston Lane,
Uxbridge,
Middlesex.

TO

VIVIENNE

and the

MEMORY OF MY PARENTS

C O N T E N T S

ACKNOWLEDGEMENTS v

ABSTRACT vii

CHAPTER 1 1

INTRODUCTION 1

1.1 The Influence of Texture on the Catalytic Properties of Chromia 2

1.2 Preparation of Chromia 7

1.3 Structure of Chromia 9

1.4 Thermal Decomposition of Chromia Gels 10

References 14

CHAPTER 2 21

THEORETICAL ASPECTS OF PHYSICAL ADSORPTION 21

2.1 Introduction 21

2.2 Physical Interaction Energies 24

2.3 The BET Method for the Determination of Surface Area 26

2.4 Empirical Methods of Isotherm Analysis 31

The α_s-Method 32

The Frenkel-Halsey-Hill Method 35

References 38

Figures 43

CHAPTER 3 46

EXPERIMENTAL 46

A. THE MATERIALS 46

3.1 Chromium Oxide Gels 46

	A Series	47
	B Series	50
	S Series	51
3.2	Chromium Oxy-hydroxide and Chromium Dioxide Samples	53
3.3	Silica Samples	53
B.	METHODS OF CHARACTERISATION	54
3.4	Differential Thermal Analysis (DTA)	54
3.5	Differential Scanning Calorimetry (DSC)	54
3.6	X-Ray Diffraction	55
3.7	Electron Microscopy	55
	Transmission	55
	Scanning	56
3.8	Mass Spectrometry	56
3.9	Atomic Absorption	56
3.10	Heat of Immersion	57
C.	LOW TEMPERATURE GAS ADSORPTION	57
3.11	Design and Construction of the Volumetric Apparatuses	58
3.12	Calibration of the Gas Adsorption System	60
	Gas Burette Bulbs	60
	The "Adsorption" Manometer	60
	Dead Space Volumes V_a, V_b and V_c	62
	Dead Space Volumes V_a and V_t	65
	Dead Space Volume V_c	66
	Absolute Nature of the Calibrations	71
3.13	The Pressure-Sensitive Transducer	73
	Calibration of the Transducers	75
	Comparison of Manometric and Transducer Pressure Data	77
3.14	The Oxygen Vapour Pressure Thermometer	77
3.15	Sample Outgassing Procedure	79
3.16	Isotherm Determination	79

D. WATER AND MERCURY VAPOUR ADSORPTION 81

THE SPRING BALANCE 82

3.17 Design and Technique 82

3.18 Calibration of the Spring Balance 84

3.19 Sample Outgassing Procedure 85

3.20 Isotherm Determination 85

THE GULBRANSEN MICROBALANCE 86

References 88

Figures 90

CHAPTER 4 110

RESULTS AND DISCUSSION I

GAS ADSORPTION AND RELATED STUDIES ON THE SILICA SAMPLES 110

4.1 The Adsorption Isotherms 110

4.2 Comparison of the Water Adsorption Data 117

4.3 Surface Concentration of Hydroxyl Groups 120

4.4 Heats of Immersion in Water 122

4.5 The Frenkel-Halsey-Hill Plots 123

References 129

Figures 132

CHAPTER 5 148

RESULTS AND DISCUSSION II

MERCURY VAPOUR ADSORPTION ON CHROMIUM OXIDES 148

5.1 Mercury Vapour Adsorption on Chromium Oxide Gels 148

5.2 Mercury Vapour Adsorption on Chromium Dioxide 150

5.3 Interaction of Chromium Oxides and Mercury Vapour 155

5.4 Mercury Vapour Adsorption on Other Adsorbents 157

References 159

Figures 161

CHAPTER 6 166

RESULTS AND DISCUSSION III

GAS ADSORPTION AND RELATED STUDIES OF THE CHROMIUM OXIDES 166

A. CHARACTERISATION OF THE HYDROUS CHROMIUM OXIDES 166

6.1 Preparation and Purity of the Chromium Oxide Gels 166

6.2 Differential Thermal Analysis (DTA) and
Differential Scanning Calorimetry (DSC) 170

Chromia Gels 170

Orthorhombic Oxy-hydroxide and Chromium Dioxide 178

6.3 Thermal Dehydration of the Chromia Gels 181

6.4 X-Ray Powder Diffraction and Electron Microscopy Studies 185

X-Ray Powder Diffraction 185

Electron Microscopy 186

B. GAS ADSORPTION ON THE HYDROUS CHROMIUM OXIDES 188

6.5 Sorptive Properties of Chromia Gels Outgassed at 25°C 188

The Adsorption Isotherms 189

Comparison of the Nitrogen, Argon and Water BET Surface
Areas of the Gels 195

6.6 Sorptive Properties of Chromia Gel A3 Outgassed at
Various Temperatures up to 1000°C 200

Interpretation and Analysis of the Adsorption Isotherms 201

The Frenkel-Halsey-Hill (FHH) Plots 208

References 213

Figures 218

CHAPTER 7 238

GENERAL DISCUSSION AND CONCLUSIONS 238

References 246

APPENDICES A1

A C K N O W L E D G E M E N T S

The work described in this Thesis was carried out under the guidance of Professor K.S.W. Sing, to whom the author wishes to express deep gratitude for his patience, understanding and constant encouragement throughout the past four years.

Appreciation is extended to Dr. S.J. Gregg for many helpful discussions during the course of writing this Thesis, and in which the author was introduced to the subject of "Dangling Participles".

Life for a research worker is made that much easier by good technical assistance: the author has been especially fortunate to encounter the friendly help and cooperation of many members of the Technical Staff of Brunel University. These are too numerous to mention all by name, but particular thanks are due to Bill Wilkings(who turned my pennies into pounds), Alan Higdon, Dick Bird, and the 'boys in the back room', Doug and Ted. The expertise of a Glass Blower is an invaluable assistance to the Surface Chemist and Brunel' is able to boast one of the best; the photographs included in this Thesis are testimony to the glassworking skill of Tony Williams, to whom the author extends sincere thanks for his considerable help (and unfailing provision of 'Page 3' in the Surface Chemistry 'Rest Room').

During the course of this work the author was a member of the staff of Glaxo Research Ltd., to whom sincere thanks are extended for the company's generous financial support given throughout the author's university career. Acknowledgement is also due to the

Science Research Council for the Industrial S.R.C. Award to the author.

I am particularly grateful to my very good friends Peter and Jean Warren for their generous hospitality and understanding, which helped me through some difficult periods during the course of this work. Appreciation is extended to Mr. Denzil Plomer for the excellent photography of the adsorption apparatus described in this Thesis.

Last but not least, the author wishes to recognise an irremunerable debt of gratitude owed to Mrs Doreen Wray, who worked so hard and conscientiously late into many nights to type this Thesis. Without "Dodo's" help, perseverance and skill (and her understanding husband "Charlie" who took over all domestic chores), this Thesis may not have made typed form.

A B S T R A C T

The adsorption of nitrogen, argon and water vapour was studied on various well-characterised chromium oxides and silicas outgassed at selected temperatures between 25° and 1000°C. Standard data derived on non-porous oxides provided a basis for the analysis of the isotherms by the α_s-method, which has been found especially useful for the identification of the various physisorption processes, e.g. micropore filling and capillary condensation. The Frenkel-Halsey-Hill (FHH) method has also been used to analyse the multilayer region of the isotherms.

Chromia gels precipitated at about pH 6 were found to be microporous. These gels,when outgassed at 25°C, exhibited molecular sieve properties; the sorption capacity for water was high, whereas the pore volume available to nitrogen and argon was small. It is suggested that cavities were formed in the gel in the vicinity of the Cr^{3+} ions through the removal of water ligands under conditions where the hydroxide structure was slow to develop. The molecular sieve character was considerably reduced in the case of gels precipitated at high pH (about 10.5), presumably because of the more efficient replacement of water ligands by hydroxyl ions.

Chromia gels outgassed at high temperature retained a strong affinity for water vapour, and gave argon and water vapour

isotherms which exhibited some slight stepwise character. On the other hand, silicas outgassed at 1000°C were found to be strongly hydrophobic.

Mercury vapour adsorption was found to take place very readily on some outgassed chromium oxides. This presents a problem in both volumetric and gravimetric adsorption measurements unless special precautions are taken to exclude mercury vapour from the system. Pressure-sensitive transducers have been used to overcome this problem in the case of the water vapour adsorption studies.

C H A P T E R 1

INTRODUCTION

Chromium oxides and hydrous chromium oxides are widely employed for diverse applications and have consequently been the subject of considerable investigation for over a century. Much of the interest in recent decades has been stimulated by the use of oxides in ceramics and semiconductors, but perhaps the most important role of the chromium oxide system is in the field of catalysis. With the exception of alumina, silica and group VIII metals, chromium oxide has probably received more attention than any other catalyst. Nevertheless, although a number of surface chemical studies have been made of chromium oxide gels, two particular problems merit further attention: (1) the difficulty of controlling the complex textural and surface chemical changes, which involve both surface hydration and oxidation state, and (2) the identification of catalytically active sites for particular reactions. For convenience, reference is usually made to 'chromia' to denote a hydrated chromium oxide of unspecified degree of hydration, but it must also be borne in mind that chromium may be present in different oxidation states.

The present work was undertaken in an attempt to gain an increased understanding of the bulk and surface chemistry of the Cr—O—H_2O system. In particular, attention has been given to the origin of porosity in chromia gels in relation to conditions of preparation, dehydration and calcination. For this purpose gas adsorption has provided the main experimental method of investigation, but the techniques of differential thermal analysis (DTA), differential scanning calorimetry (DSC), heat of

immersion, electron microscopy and x-ray diffraction have also been used to assist in the characterisation of the gels and the products of thermal decomposition. In addition, the adsorption properties of certain standard silicas have been studied: hydroxylated and dehydroxylated silicas may be expected to provide useful reference surfaces in the analysis of the adsorption data.

Nitrogen adsorption measurements are generally employed for the determination of surface area and pore size distribution. It is now recognised, however, that nitrogen undergoes a specific physisorption interaction with some surfaces. The degree of specificity of water vapour adsorption is very great, but on the other hand, the adsorption of argon involves only nonspecific interactions. A comparative study of the adsorption of these three adsorptive molecules is therefore likely to provide useful information concerning the chemistry of the chromia surface. A direct study of the second major problem associated with chromia (i.e. characterisation of the catalytically active sites) was, unfortunately, beyond the scope of the present work.

1.1 The influence of texture on the catalytic properties of chromia

The ability of chromia to act as a catalyst was recognised as early as 1852, when Wohler[1] reported that chromia catalysed the oxidation of sulphur dioxide to the trioxide. The classical work of Sabatier[2,3] some sixty years later established the usefulness of certain metal oxides as dehydrogenation catalysts, amongst which chromia was listed as a catalyst of "mediocre activity". However, the later work of Lazier and Vaughen[4] revealed that chromia is, in fact, a hydrogenation catalyst possessing a high activity. Early workers frequently failed to recognise the importance of pre-treatment conditions or, for example, the poisoning action of water

vapour in many catalytic reactions.[5-7] Similarly, there are many references to gas adsorption studies on chromia catalysts with "clean surfaces", although it appears that insufficient precautions have been taken to avoid the possible contamination of the surface by grease or oil vapour; indeed, under certain outgassing conditions employed,[8] the undetected chemisorption of mercury vapour would almost certainly have occurred.

The versatility of chromia as a catalyst is demonstrated by its use in a wide variety of reactions, many of industrial importance; e.g. hydrogenation,[9] dehydrogenation,[10] dehydration,[11] dehydrocyclisation,[12] hydrodealkylation,[13] dealkylation,[14] dehydrocracking,[15] aromatisation,[16] oxidation,[17] dehalogenation[18] and fluorination.[19] Other industrial uses include the removal of sulphur-containing gases from automobile exhaust systems,[20] as pigments in colour printing[21] and for the detection and removal of oxygen from olefin streams without polymerisation of the olefin.[22] There is now a strong tendency towards the industrial use of supported chromia catalysts, e.g. chromia dispersed on alumina or silica. Chromia - alumina is a particularly important catalyst in the manufacture of butadiene from butane for the synthetic rubber industry. Chromia supported on silica - alumina, is an active catalyst for the polymerisation of ethylene to give crystalline, orientated polymers.[23] Chromia-based catalysts will probably continue to play a major role in the heavy chemicals industry and in the reduction of atmospheric pollution.

The major function of the support of a dispersed chromia catalyst is generally to prevent loss in surface area that occurs when chromia is heated at temperatures above about 400°C.[24] Supported chromia catalysts exhibit certain properties which can be predicted from a consideration of the parent oxides. However, although supported chromia catalysts may, at least to a first approximation, be regarded as dual-function catalysts,[25] they also

possess properties which are attributed to a synergistic interaction of the two phases.[26]

Chromia is unusual in the respect that it displays both n and p-type semiconductivity.[27] The nature of the conductivity is dependent upon a number of factors, e.g. mode of preparation, pretreatment, temperature and reaction atmosphere. Chapman[28] has found that chromia behaves as a p-type semiconductor in oxygen and a n-type semiconductor in hydrogen. Weller and Voltz[6,29] have confirmed the findings of earlier workers[30,31] that chromium (III) oxide contains excess oxygen after oxidation and adsorbed hydrogen after reduction. Extensive studies by Dereń and Haber[32,33] suggest that the conduction mechanism is essentially the same in both the amorphous and crystalline oxide, at least for the annealing (in air) temperature range of 200 - 700°C.

Chromia annealed in air below 200°C is a poor conductor:[32] the conductivity increases on raising the annealing temperature, reaching a maximum at about 400°C and thereafter declining with higher annealing temperatures. Several workers[34,35] have noted that the degree of oxidation of the gel increases with the temperature of annealing in air. Dereń and Haber[32] have postulated that this will result in an increase of the concentration of Cr^{6+} acceptor centres and consequently in the increase of conductivity. Crystallisation of Cr_2O_3 at about 400°C probably results in a crystal lattice that is highly disordered and therefore exhibits high conductivity: on increasing the annealing temperature above 400°C the lattice becomes progressively more ordered, the concentration of Cr^{6+} ions decreases and so does the conductivity. Several workers[36,37] have suggested that above 400°C, chromium (III) oxide changes from a predominantly p-type semiconductor to predominantly n-type. It is interesting to note that

although it has been proposed that conductivity in polycrystalline oxides is a function of the surface conductivity of the grains,[38] Dereń and Haber[32] found similar conductivities for chromias of widely different surface areas. However, there are insufficient data in the reported work to indicate whether the external surface areas of the gels were also dissimilar.

Many studies[39-41] have indicated that chromium ions may exist in chromia systems in oxidation states from +2 to +6. In addition, Shelef[42] has reported electron paramagnetic resonance (epr) evidence of the univalent state in a reduced chromia-alumina catalyst. The relative amounts of the various states present on the chromia surface may strongly influence its catalytic properties. The surface layer of an 'oxidised' chromia catalyst will contain predominantly the higher oxidation states, i.e. Cr^{6+}, Cr^{5+} and Cr^{4+}, and apparently promotes reactions such as hydrogen peroxide decomposition and ethylene polymerisation etc. A 'reduced' chromia, containing Cr^{3+} (and possibly Cr^{2+}) in the surface layers, apparently favours reactions such as hydrogen - deuterium exchange and olefin hydrogenation etc.

In many cases, chromia may simultaneously catalyse more than one reaction, e.g. both the dehydration and dehydrogenation of alcohols. In such cases, the selectivity of the catalyst is a particularly salient feature. Garner[43] has suggested that cation vacancies favour dehydration whilst anion vacancies favour dehydrogenation. There are different opinions as to the origin of p-type semiconductivity in Cr_2O_3, but Voltz and Weller[6,29,44,45] have postulated that at least in the surface layers, the conductivity is due to cation deficiency. It was shown by Dowden et al[46] that in the case of propan-2-ol, dehydration was favoured by p-type semiconductors and dehydrogenation by n-type. Kuriacose and co-workers[47-52] have observed a similar relationship in a series of studies of propan-2-ol on chromia and chromia - alumina catalysts; a puzzling feature of a few of their papers is,

however, the fact that they have also stated the reverse to be the case,[50,52]

In any assessment of the catalytic activity of chromia it is inherently difficult to distinguish clearly between surface chemical and textural contributions. The analysis is further confused by the extreme sensitivity of the adsorptive and catalytic properties of chromia to the conditions of preparation, storage and heat-treatment of the gel. Nevertheless, the texture of the chromia surface may also play an important part in determining the dehydration/dehydrogenation selectivity of the catalyst. Kuriacose et al[51] have shown that the activity of chromia, in respect of alcohol dehydration, is closely related to the pore structure of the catalyst. The dehydration activity is completely destroyed when the catalyst is sintered: pore size distribution analysis revealed that the micropore structure of the catalyst was considerably reduced after sintering. Conversely, Schwab et al[53] have found that dehydrogenation is facilitated by non-porous catalysts: a reduction (by sintering) or increase (by powdering) of the external surface area of the catalyst, decreases[54] or enhances,[51] respectively, the dehydrogenation activity. Several workers[51,55] have observed that there is a correlation between the loss of dehydration activity and the progressive removal of water from the surface of a chromia catalyst. Dowden[55] suggested that the active centres for dehydration are protons originating from water located at cation vacancies in the oxide lattice. Sintering of the catalyst results in the predominantly irreversible loss of surface hydroxyl groups: in the absence of pores, a rehydroxylated chromia surface imparts only a fraction of the original dehydration activity.[51] However, Topchieva[56] has shown that in the case of yttrium oxide, the original dehydration/dehydrogenation selectivity is restored if the dehydration process can be carried out reversibly; a reduced surface hydroxyl concentration enhances dehydrogenation at the expense of dehydration.

Burwell[9,57] and Zecchina[58] have applied the concept of "surface coordinative unsaturation" to the active sites formed on the surface of chromia by dehydration. Loss of water by condensation involving surface hydroxyl groups will, in general, generate coordinatively unsaturated sites (cus) of Cr^{3+},O^{2-} and possibly OH^- species. In the case of α-Cr_2O_3, water loss can generate sites of different geometries and degrees of coordinative unsaturation, and either one or two exposed Cr^{3+}: one cannot be so specific for the case of amorphous chromia, but it is suggested[24] that similar considerations will apply.

Burwell and his co-workers[59] have suggested that the microporous structure found in many amorphous chromias may impart special catalytic activity. For example, the ratio of isomerisation to hydrogenation of hex-1-ene was very low in the presence of a microporous chromia gel; when however, the gel was suitably treated to give a mesoporous texture, the ratio was high. Cross and Leach[60] have observed a similar relationship for the isomerisation of but-1-ene to cis and trans but-2-ene respectively. Gurevich et al[61] observed that the diffusion (and subsequent desorption) of polyethylene macromolecules formed on the surface of a chromia catalyst, was hindered in the presence of a predominantly microporous structure and subsequent catalytic activity was lost: a macroporous structure represented an insufficient surface area, but a pore diameter range of 50 - 150 Å was found to be the optimum. Thus, the surface area available, and its nature, frequently play an important role in the type of catalytic activity displayed by chromia.

1.2 Preparation of Chromia

Generally speaking, supported chromia catalysts are made using either co-precipitation or impregnation techniques, whilst unsupported catalysts are obtained by the requisite activation of amorphous chromia gels.

Lazier and Vaughen[4] studied the catalytic properties (in respect of ethylene hydrogenation) of some twenty chromia gels, prepared from a number of chromium salts and basic precipitating agents. They, and later Köhlschutter,[62] concluded that the precipitation of chromia gel from chromium nitrate and ammonium hydroxide was the most reliable and convenient method for preparing an active chromia catalyst. Various other early preparations of chromia gel have been summarised by Turkevich et al.[63] These include the addition of ammonium hydroxide to chromium (III) acetate and the reduction of aqueous solutions of chromic acid by sucrose, oxalic acid or ethanol.[64] The production of chromium oxyhydroxide by the carbohydrate reduction of sodium dichromate is now an important process for the manufacture of α-Cr_2O_3 pigment.[65] Perhaps one of the most widely used and currently popular methods of preparing chromia gels is that developed by Burwell and his co-workers:[11,66] this relies upon the uniform generation of ammonia in a refluxed aqueous solution of urea and chromium nitrate. The Burwell preparation invariably results in a highly microporous gel of small particle size, but a gel of more open texture may be obtained by autoclaving the product in water or pentane.[67]

More recently, techniques have been developed for the production of chromium oxides with 'tailor-made' characteristics: Peri[68] has prepared a "self-sustaining" α-Cr_2O_3 aerogel film of unusually high surface area; Teichner[69] has similarly patented a process aimed at producing high surface area oxides (including chromium oxide), where hydrated metal salts are reacted with anhydrous bases in organic media, under conditions which ensure that the minimum amount of water is present; similarly, Lohmann[70] has prepared metal hydroxides by reacting metal sulphates with sodium hydroxide in such a manner that the water is effectively removed from the reaction sphere as the decahydrate of sodium sulphate. Such methods recognise the

important role played by water during the formation, and propagation, of the chromia gel polymer and on its subsequent textural properties. Matijević[71,72] has extensively investigated the properties of chromium hydroxide hydrosols. Similar sols have been employed[73,74] in "sol-gel processes" to produce gels of controlled particle size and high surface area. These systems are likely to be the subject of much future work.

1.3 Structure of Chromia Gels

Weiser and Milligan[75] supported the early view of van Bemmelen[76] that a hydrous oxide gel consists essentially of agglomerates of minute crystals of oxide, hydrate or hydroxide, rather than of polymerised species of condensation products. However, many other workers, notably Willstätter et al[77] and Morley et al,[78] held the latter view, and that the freshly precipitated hydrous oxide is subject to an ageing process to yield polyhydroxides of increasing complexity. This is basically the opinion that is now widely accepted.[9,79]

It is generally regarded by many investigators that chromia gel has a "brush heap" structure, made up of a complex network of fibre-like particles.[80] The exact structure of the chromia fibres is unknown, although Selwood[79] has presented one picture of the gel as a chain polymer extending along the hexagonal axis, but the properties of the gel are consistent with those of large polymers:[81,82] for example, extremely low solubility and the resolubilisation of freshly precipitated gel by the addition of a small amount of chromium nitrate. In general, freshly precipitated chromia gels are amorphous, but Ratnasamy and Léonard[83] have recently claimed the identification of crystalline $Cr(OH)_3$ in a gel prepared according to the high pH method of the present author.[84]

Burwell[9,24] has proposed that chromia gel fibres are condensation polymers of $Cr(H_2O)_3(OH)_3$,

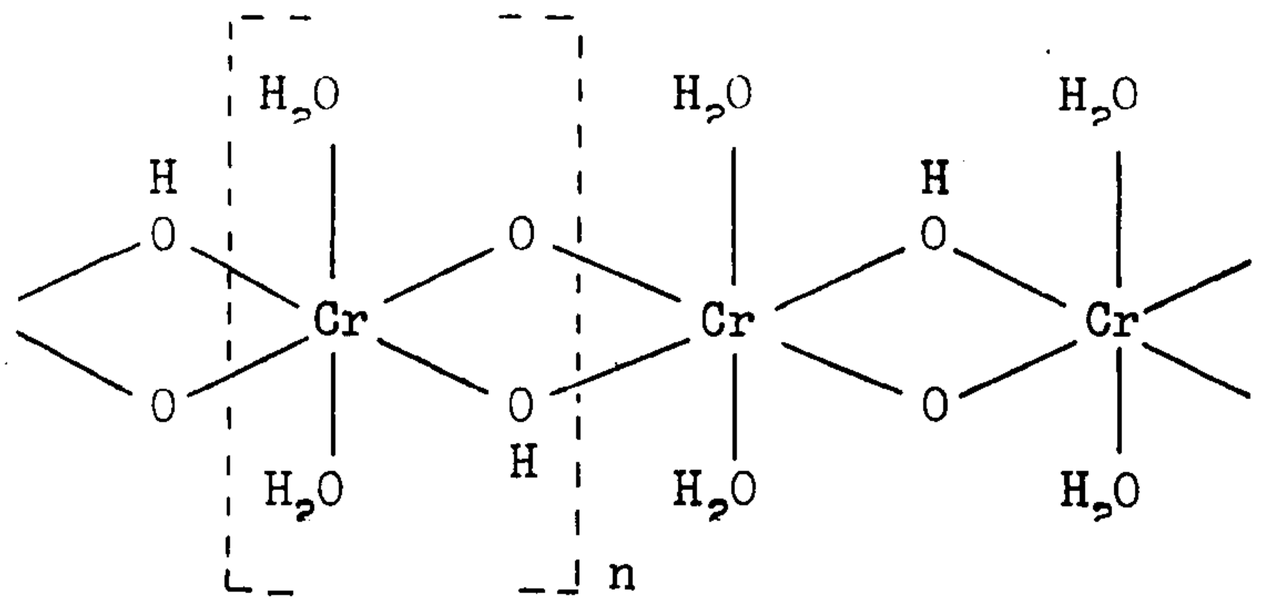

formed by the neutralisation of the hexaquo-ion, $[Cr(H_2O)_6]^{3+}$, upon the addition of a base, e.g. ammonia. The hexaquo ion forms at least the dimer and trimer,[85-87] but the polymerisation reaction is thought to involve species such as $[Cr(H_2O)_5(OH)]^{2+}$ etc., which undergo condensation much more rapidly than $[Cr(H_2O)_6]^{3+}$. When air-dried at 25°C, nearly all chromia gels, and particularly those prepared using the Burwell method,[11,66] retain appreciable quantities of physisorbed water of composition approximating to the formula, $Cr_2O_3.7H_2O$. However, Selwood[79] and Berg[88] have reported gels, dried under similar conditions, that analyse very closely to $Cr_2O_3.5H_2O$, i.e. the empirical formula of the hypothetical polymer shown above.

1.4 Thermal Decomposition of Chromia Gels

Many authors[34-37,88-95] have noted that the thermal decomposition of chromia gels is a complex process. Dereń and Haber[33] have proposed that at least three different simultaneous processes are involved: (a) dehydration, leading to the formation of chromium (III) oxide hydrates (and oxy-hydroxide) which subsequently decompose at higher temperatures; (b) redox processes involving chromium ions in different oxidation states, and (c) formation of crystalline α-Cr_2O_3 as the stable end product. Generally, for temperatures $< 250^{\circ}C$, the thermal effects observed by DTA are a result of gel-hydration

changes, and are independent of the surrounding atmosphere; for temperatures > 250°C, the thermal effects are associated with redox processes and, as such, are dependent upon the nature of the surrounding atmosphere, i.e. inert, oxidising or reducing.

The dehydration process, (a), will effectively vary the coordination state of O^{2-}. For example, in the hypothetical polymer the coordination number (n) of Cr^{3+} with respect to O^{2-} is 6, whilst that of O^{2-} with respect to Cr^{3+} is 1.5. During progressive heating, the polymer loses water which may result in the bridging of chains and, at the extreme, to an average coordination of n = 2 for O^{2-}; further loss of water by condensation from bridging OH groups will lead to a coordination of 3, i.e. that found in chromium oxy-hydroxide, CrOOH.[96a] Finally, total elimination of water results in an O^{2-} coordination of 4, i.e. that found in α-Cr_2O_3.[96d] In an amorphous gel the average coordination of O^{2-} appears[24] to be always < 4.

During the redox process, (b), CrOOH (orthorhombic[97]), CrO_2 (rutile structure[96b]), CrO_3 (chain structure of linked CrO_4 tetrahedra[96c]) and α-Cr_2O_3 (corundum structure[96d]) may, at least in the surface layers, co-exist. Recent work by Ratnasamy and Léonard,[83] using x-ray scattering techniques, has identified the presence of CrOOH, CrO_3 and α-Cr_2O_3: Fenerty,[95] using magnetic susceptibility measurements, has confirmed the presence of ferromagnetic CrO_2 in amorphous chromia gels. The subsequent 'glow' of the gel, a phenomenon first described by Berzelius[98] in 1818, results in the formation of macro-crystalline α-Cr_2O_3.[99]

DTA, in addition to thermogravimetric analysis (TG), has been widely employed to investigate the decomposition of chromia gels. Bhattacharyya et al[37,93,94] have attributed the endotherms at 160° and 250°C to the expulsion of 'loosely bound' and 'rigidly bound' water respectively. Narasimha Rao and Kesavulu[100] correlated DTA observations with parallel oxygen

adsorption/evolution studies (indicated below in parentheses) and reached a similar conclusion; the evolution of water from the gel pores is responsible for the first endotherm (no oxygen adsorbed or evolved), whilst the second dehydration endotherm (oxygen adsorbed by exposed surface chromium ions) is associated with the oxide structure, i.e. condensation of hydroxyl groups. Dereń and Haber[32] assigned the two endotherms to the loss of water to form $Cr_2O_3.3H_2O$ (trihydrate) and $Cr_2O_3.H_2O$ (monohydrate) respectively, a view that is widely accepted. However, Sing and his co-workers[34,35] have found for certain gels, that the DTA may also exhibit an exotherm at about 230°C as a result of the formation of crystalline orthorhombic CrOOH. Fenerty[95] has confirmed the presence of micro-crystalline orthorhombic CrOOH in certain calcined gels. Apparently, the crystalline monohydrate is only formed if the gel contains sufficient water trapped in the pores of large granules. The mechanism for the formation of the oxy-hydroxide structure is probably very similar to the hydrothermal process involved in the formation of boehmite (γ-AlOOH), which has been characterised by Tertian and Papée[101] and by de Boer et al.[102] The crystalline orthorhombic CrOOH is probably the principal source of CrO_2 in an amorphous gel: the interconversion of orthorhombic CrOOH and tetragonal CrO_2 is known to proceed via a topotactic reaction.[103-105] Subsequent decomposition of CrO_2 to α-Cr_2O_3 may also proceed via a topotactic reaction.[106]

The exact mechanism of the glow phenomenon is still largely a matter for conjecture. The temperature at which the strongly exothermic transformation of amorphous Cr_2O_3 into macro-crystalline α-Cr_2O_3 occurs is dependent on the mode of gel preparation,[107] thermal history of the gel[34,95] and on the nature of the surrounding atmosphere:[35] the glow phenomenon occurs at about 400°C in an oxidising atmosphere, at about 500°C in hydrogen and up to 600°C in an inert atmosphere, e.g. nitrogen or vacuum; the crystallisation

temperature under vacuum is a function of pressure.[88,92,108] The actual temperature of the sample may rise to at least 800°C during the glow phenomenon,[95] which is slightly more in line with the temperature of > 1000°C required for large scale crystallisation of γ-alumina to the corundum structure.[109]

Chromium (VI) assists the crystallisation process by lowering the energy barrier to nucleation, but in itself, is not a prerequisite for the glow phenomenon.[95] Alternative sites for nucleation[110] may be provided by the micro-crystalline α-Cr_2O_3 which is present in amorphous gels.[83,95] In such cases, the situation is analogous to that of $Fe(OH)_3$, where Weiser[111] has shown that the form of Fe_2O_3 is α-Fe_2O_3 before and after the glow. Sorrentino et al[112] have correlated the incidence of the glow phenomenon with the particle size of the hydrous oxide: they postulate that the glow is a visible manifestation of the coalescence of primary particles into larger masses, with the consequent release of surface energy. Supporting evidence for this view is, in part, derived from their confirmation of the earlier findings of Milligan et al[113,114] that only single oxide systems exhibit the glow phenomenon. When mixed with another hydrous oxide the glow is quelled, a fact attributed to the adsorption of one oxide on the surface of the other; the effect is independent of whether or not the second hydrous oxide itself exhibits the glow phenomenon, e.g. $Fe(OH)_3$ and $Al(OH)_3$ respectively.

Perhaps the one certain feature related to the glow phenomenon is that the abrupt crystallisation of α-Cr_2O_3 invariably causes a large reduction in surface area and catalytic activity.[4] However, it does not, as some authors have stated,[100] render the oxide completely inactive as a catalyst.

REFERENCES

1. F. Wohler and F. Mahla, Ann. Chem., (1852) 81, 255.
2. P. Sabatier, "La Catalyse en Chimie Organique", Béranger, Paris, 2nd Edt., (1920).
3. P. Sabatier and E. Emmet Reid, "Catalysis in Organic Chemistry", D. Van Nostrand Co., New York, (1923) 252.
4. W.A. Lazier and J.V. Vaughen, J. Amer. Chem. Soc., (1932), 54, 3080.
5. D.J. Salley, H. Fehrer and H.S. Taylor, J. Amer. Chem. Soc., (1941) 63, 1131.
6. S.W. Weller and S.E. Voltz, J. Amer. Chem. Soc., (1954) 76, 4695.
7. S.E. Voltz and S.W. Weller, J. Phys. Chem., (1965) 59, 566.
8. L. White, Jr., and C.H. Schneider, J. Amer. Chem. Soc., (1949) 71, 2593.
9. R.L. Burwell, Jr., A.B. Littlewood, M. Cardew, G. Pass and C.T.H. Stoddart, J. Amer. Chem. Soc., (1960) 82, 6272.
10. R.L. Burwell, Jr., and A.B. Littlewood, J. Amer. Chem. Soc., (1956) 78, 4170.
11. R.L. Burwell, Jr., J. Amer. Chem. Soc., (1937) 59, 1609.
12. R.E. Kline and W.C. Starnes, U.S. 3,240,719 (1966).
13. B. Notari, P.D. Valentini and M. Malde, "Proc. 3rd Int. Congr. Catalysis", Amsterdam, 1964. Eds. W.M.H. Sachtler, G.C.A. Schuit and P. Zwietering; North-Holland Pub. Co., Amsterdam, (1965) 2, 1034.
14. W.M. Swanson, U.S. 3,222,410 (1965).
15. V.T. Skylar, E.V. Lebedev and V.A. Zakupra, Neftekhimiya, (1964) 4, 209.
16. M. Yasuda, J. Chem. Soc., Japan, Ind. Chem. Sect., (1952) 55, 123.
17. B. Dmuchovsky, M.C. Freerks and F.B. Zienty, J. Catalysis, (1965) 4, 577.
18. H. Noller, W. Loew and P. Andreu, Ber. Bunsenges, Physik Chem., (1964) 68, 663.

19. E.I. du Pont de Nemours & Co., Fr. 1,372,549(1964).

20. J.W. Benedict, Brit. 1,281,247 (1972).

21. G.E. Cagle and D.R. Witt, U.S. 3,663,176 (1972).

22. V.E. Sivanov, V.I. Deinezhenko, B.P. Sereda, A.K. Chirva, N.A. Okhotnikova and I.Z. Sagdeev, U.S.S.R. 340,675 (1972).

23. A. Clark, J. Hogan, R. Banks and W. Lansing, Ind. Eng. Chem., (1956) 48, 1152.

24. R.L. Burwell, Jr., G.L. Haller, K.C. Taylor and J.F. Read, "Advances in Catalysis", Academic Press, New York, (1969) 20, 1.

25. C.P. Poole, Jr., and D.S. Mac Iver, "Advances in Catalysis", Academic Press, New York, (1967) 17, 223.

26. L.M. Webber, J. Phys. Chem., (1972) 76, 2694.

27. R. Chaplin, P.R. Chapman and R.H. Griffith, Nature, (1953) 172, 77.

28. P.R. Chapman, R.H. Griffith and J.D.F. Marsh, Proc. Roy. Soc., (1954) A224, 419.

29. S.E. Voltz and S.W. Weller, J. Amer. Chem. Soc.,(1954) 76, 4701; Z. Phys. Chem. (Frankfurt), (1955) 5, 100.

30. G.N. Maslyanskii and N.R. Bursian, J. Gen. Chem. (U.S.S.R.), (1947) 17, 208.

31. J. Givaudon, E. Nagelstein and R. Leygonie, J. Chim. Phys., (1950) 47, 304.

32. J. Dereń, J. Haber, A. Podgórecka and J. Burzyk, J. Catalysis, (1963) 2, 161.

33. J. Dereń and J. Haber, Ceramika, (1969) No 13, 5.

34. J.D. Carruthers, Ph.D. Thesis, Brunel University, (1968).

35. J.D. Carruthers, J. Fenerty and K.S.W. Sing, "Proc. 6th Int. Symp. Reactivity Solids", Schenectady, 1968. Eds. J.W. Mitchell, R.C. DeVries, R.W. Roberts and P. Cannon; Wiley Interscience, New York, (1969) 127.

36. J.F. García de la Banda, J. Catalysis, (1962) 1, 136.

37. S.K. Bhattacharyya, V.S. Ramachandran and J.C. Ghosh, "Advances in Catalysis", Academic Press, New York, (1957) 9, 114.

38. A. Bielanski, J. Dereń, J. Haber and J.Sloczyński, "Proc. 2nd Int. Congr. Catalysis", Paris, 1960. Technip, Paris, (1961) 2, 1653.

39. P. Cossee and L.L. Van Reijen, "Proc. 2nd Int. Congr. Catalysis", Paris, 1960. Technip, Paris, (1961) 2, 1679.

40. D.E. O'Reilly and D.S. Mac Iver, J. Phys. Chem., (1962) 66, 276.

41. L.L. Van Reijen and P. Cossee, Discussions Faraday Soc., (1966) No 41, 277.

42. M. Shelef, J. Catalysis, (1969) 15, 289.

43. W.E. Garner, "Advances in Catalysis", Academic Press, New York, (1957) 9, 184.

44. S.E. Voltz and S.W. Weller, J. Amer. Chem. Soc., (1953) 75, 5227, 5231.

45. S.E. Voltz and S.W. Weller, "Advances in Catalysis", Academic Press, New York, (1957) 9, 215.

46. B.C. Alsop and D.A. Dowden, J. Chim. Phys., (1954) 51, 678.

47. J.C. Kuriacose and M.V.C. Sastri, "Proc. 3rd Int. Congr. Catalysis", Amsterdam, 1964. Eds. W.M.H. Sachtler, G.C.A. Schuit and P. Zwietering; North-Holland Pub. Co., Amsterdam, (1965) 1, 507.

48. M.C. Upreti, J.C. Kuriacose and M.V.C. Sastri, Bull. Acad. Pol.Sci., Ser. Sci. Chim., (1965) 11, 651.

49. C. Daniel and J.C. Kuriacose, Indian J. Chem., (1968) 6, 645.

50. J.C. Kuriacose, C. Daniel and R. Swaminathan, J. Catalysis, (1968) 12, 19.

51. J.C. Kuriacose and C. Daniel, J. Catalysis, (1969) 14, 77.

52. J.C. Kuriacose, Metals Miner. Rev., (1970) 9, 5.

53. G.M. Schwab and E.S. Agallidis, J. Amer. Chem. Soc., (1949) 71, 1806.

54. J.R. Owens, J. Amer. Chem. Soc., (1947) 69, 2559.

55. D.A. Dowden, J. Chem. Soc., (1950) 242.

56. K.V. Topchieva, "Proc. 3rd Int. Congr. Catalysis", Amsterdam, 1964. Eds. W.M.H. Sachtler, G.C.A. Schuit and P. Zwietering; North-Holland Pub. Co., Amsterdam, (1965) 1, 518.

57. R.L. Burwell, Jr., and C.J. Loner, "Proc. 3rd Int. Congr. Catalysis", Amsterdam, 1964. Eds. W.M.H. Sachtler, G.C.A. Schuit and P. Zwietering; North-Holland Pub. Co., Amsterdam, (1965) 2, 804.

58. A. Zecchina, S. Coluccia, E. Guglielminotti and G. Ghiotti, J. Phys. Chem., (1971) 75, 2774.

59. R.L. Burwell, Jr., K.C. Taylor and G.L. Haller, J. Phys. Chem., (1967) 71, 4580.

60. N.E. Cross and H.F. Leach, J. Catalysis, (1971) 21, 239.

61. V.R. Gurevich, M.A. Dalin, K.M. Arutyunova and I.A. Lagernaya, "Proc. 4th Int. Congr. Catalysis", Moscow, 1968. Ed. G.K. Boreskov; Akad. Kiado, Budapest, (1972) 491.

62. H.W. Köhlschutter, Z. Anorg. Allg. Chem., (1934) 220, 370.

63. J. Turkevich, H. Fehrer and H.S. Taylor, J. Amer. Chem. Soc., (1941) 63, 1129.

64. F.C. Fernelius, Ed., "Inorganic Synthesis", (1946) 2, 190.

65. R.G. Robins, Aust. Chem. Process. Eng., (1972) 25, 21.

66. R.L. Burwell, Jr., and H.S. Taylor, J. Amer. Chem. Soc., (1936) 58, 697.

67. K.C. Taylor, Ph.D. Thesis, Northwestern University, Evanston, Illinois, U.S.A., (1968).

68. J.B. Peri, U.S. 3,434,912 (1969).

69. S.J. Teichner, U.S. 2,888,323 (1959).

70. P. Lohmann, Ger. 1,136,674 (1963).

71. R. Demchak and E. Matijević, J. Colloid Interface Sci., (1969) 31, 257.

72. E. Matijević, A.D. Lindsay, S. Kratohvil, M.E. Jones, R.I. Larson and N.W. Cayey, J. Colloid Interface Sci., (1971) 36, 273.

73. C.J. Hardy, "Sol-Gel Processes for Ceramic Nuclear Fuels", Proc. of A Panel, Vienna, (1968) 33.

74. R.M. Dell, "Proc. 7th Int. Symp. Reactivity Solids", Bristol, 1972. Eds. J.S. Anderson, M.W. Roberts and F.S. Stone; Chapman and Hall, London, (1972) 553.

75. H.B. Weiser and W.O. Milligan, Chem. Revs., (1939) 25, 1.

76. J.M. van Bemmelen, Rec. Trav. Chim., (1888) 7, 106.

77. R. Willstätter and H. Kraut, Ber., (1923) 56B, 149 and 1117; ibid, (1924) 57B, 1082; ibid, (1925) 58B, 2451; ibid, (1926) 59B, 2541.

78. A.M. Morley and J.K. Wood, J. Soc. Dyers Colourists, (1923) 39, 100; J. Chem. Soc., (1924) 125, 1626.

79. P.W. Selwood, M. Ellis and C.F. Davis, Jr., J. Amer. Chem. Soc., (1950) 72, 3549.

80. P.H. Hermans, in "Colloid Science", Ed. H.R. Kruyt; Elsevier, Amsterdam, (1949) 2, Chap. 12.

81. J.J. Hermans, in "Colloid Science", Ed. H.R. Kruyt; Elsevier, Amsterdam, (1949) 2, 77ff.

82. A.E. Alexander and P. Johnson, in "Colloid Science", Clarendon Press, Oxford, (1949) 2, 786.

83. P. Ratnasamy and A.J. Léonard, J. Phys. Chem., (1972) 76, 1838.

84. F.S. Baker, J.D. Carruthers, R.E. Day, K.S.W. Sing and L.J. Stryker, Discussion Faraday Soc., (1971) No 52, 173.

85. M. Kilpatrick, J. Electrochemical Soc., (1953) 100, 85.

86. J.A. Laswick and R.A. Plane, J. Amer. Chem. Soc., (1959) 81, 3564.

87. D. Cornet and R.L. Burwell, Jr., J. Amer. Chem. Soc., (1968) 90, 2489.

88. L.G. Berg, K.P. Pribylov and R.A. Abdurakhmanov, Zh. Neorg. Khim., (1970) 15(10), 2618.

89. A. Simon and T. Schmidt, Z. Anorg. Chem., (1926) 153, 191.

90. W. Milligan, J. Phys. Colloid Chem., (1951) 55, 497.

91. M. Shafer and R. Roy, Z. Anorg. Chem., (1954) 276, 275.

92. T.W. Rode, Ph.D. Thesis, Institute of General and Inorganic Chemistry, Academy of Sciences, U.S.S.R., (1956); "Kislorodnyie Soiedinienia Chroma i Chromowyie Katalizatory" ("Oxygen Compounds of Chromium and Chromium Catalysts"), Izdat. Akad. Nauk, S.S.S.R., Moscow, (1962).

93. S.K. Bhattacharyya and V.S. Ramachandran, Bull. Nat. Inst. Sci. (India), (1959) 12, 23.

94. S.K. Bhattacharyya, J. Thermal Analysis, (1969) 1, 75.

95. J. Fenerty, Ph.D. Thesis, Liverpool Polytechnic, (1971).

96. (a) A.F. Wells, "Structural Inorganic Chemistry", Oxford University Press, London, 3rd Edt. (1962) 559;
(b) ibid., 469; (c) ibid., 442; (d) ibid., 457.

97. N.C. Tombs, W.J. Croft, J.R. Carter and J.F. Fitzgerald, Inorg. Chem., (1964) 3, 1791.

98. J. Berzelius, J. Chem. Physik., (1818) 22, 60.

99. J.D. Carruthers, J. Fenerty and K.S.W. Sing, Nature, (1967) 213, 66.

100. T.L. Narasimha Rao and V. Kesavulu, Indian J. Appl. Chem., (1967) 30, 25.

101. R. Tertian and D. Papée, J. Chim. Phys., (1958) 55, 341.

102. J.H. de Boer, J.J. Steggerda, J.M.H. Fortuin and P. Zwietering, "Proc. 2nd Int. Congr. Surface Activity", London, 1957. Butterworths, London, (1957) 2, 93.

103. M.A. Alario Franco and K.S.W. Sing, J. Thermal Analysis, (1972) 4, 47.

104. M.A. Alario Franco, J. Fenerty and K.S.W. Sing, "Proc. 7th Int. Symp. Reactivity Solids", Bristol, 1972. Eds. J.S. Anderson, M.W. Roberts and F.S. Stone; Chapman and Hall, London, (1972) 327.

105. Y. Shibasaki, Mat. Res. Bull., (1972) 7, 1125.

106. R.D. Shannon, J. Amer. Ceram. Soc., (1967) 50, 53.

107. T.W. Rode, "Trudy 1-GO Soveshchaniya Termografii", Kazan, 1953. Izdat. Akad. Nauk, S.S.S.R., (1955) 154; Referat. Zh. Khim., (1957) Abstr. No. 369.

108. M.A. Khachvankyan and B.F. Ormont, Zh. Fiz. Khim., (1947) 21, 575.

109. S.J. Gregg and K.S.W. Sing, J. Phys. Chem., (1952) 56, 388.

110. L.V. Azaroff, "Introduction to Solids", McGraw Hill, (1960) 198.

111. H. Weiser, "Inorganic Colloid Chemistry", Wiley, New York, (1935) 2, 35.

112. M. Sorrentino, L. Steinbrecher and F. Hazel, J. Colloid Interface Sci., (1969) 31, 307.

113. W.O. Milligan and L. Merten, J. Phys. Chem., (1947) 51, 521.

114. H.B. Weiser and W.O. Milligan, J. Phys. Chem., (1948) 52, 942.

C H A P T E R 2

THEORETICAL ASPECTS OF PHYSICAL ADSORPTION

The theory of gas adsorption by solids has been extensively developed and discussed in recent years.[1-5] This chapter is, therefore, concerned only with certain theoretical aspects of physisorption which are relevant to the present work. Emphasis is placed on the utilisation and interpretation of gas adsorption data, in both the monolayer and multilayer regions of the adsorption isotherm.

2.1 Introduction

Physisorption occurs whenever a gas, or vapour, (the adsorptive) is brought into contact with an outgassed solid (the adsorbent). The phenomenon, often termed van der Waals adsorption, is dependent on molecular interaction forces similar in type to those responsible for the condensation of a vapour to a liquid (or solid). Since physisorption is related to this process, it occurs to an appreciable extent only at pressures and temperatures close to those required for liquefaction. In physisorption, as distinct from chemisorption, there is no electron exchange between the adsorbed species (the adsorbate) and the adsorbent.

In principle, the amount, x, of gas adsorbed per unit mass of the adsorbent may be expressed as a function of the equilibrium pressure, P, the temperature, T, and the nature of the adsorptive and adsorbent:

$$x = f\ (P, T, \text{gas}, \text{solid}) \qquad (2.1)$$

The adsorption data are generally recorded in the form of an adsorption isotherm, i.e. the adsorption measured at various equilibrium pressures, all other variables being held constant. If, as is usually the case in practice, the gas is below its critical temperature then the amount adsorbed is conveniently expressed as a function of the relative pressure, P/Po, where Po is the saturated vapour pressure of the adsorptive:

$$x = f\ (P/Po)_{T,\ gas,\ solid} \qquad (2.2)$$

The majority of published isotherms may be assigned to one of the five types originally proposed by Brunauer, Deming, Deming and Teller,[6] but now more frequently referred to as the Brunauer Classification.[1] This classification is illustrated in Fig. 2.1 In practice, many isotherms show an upward deviation (represented by dotted lines in Fig. 2.1) as the saturated vapour pressure is approached. Hysteresis loops (the desorption branch of an isotherm) are frequently encountered with the various types of isotherms, notably in the case of a Type IV isotherm. de Boer[7] developed a useful classification of hysteresis loops; this will be referred to in succeeding chapters concerned with the discussion of the adsorption isotherms.

As with most classifications, there are borderline cases which possess the characteristics of one or more types, and are therefore difficult to assign to a particular group. In addition, there are many isotherms, notably stepwise isotherms, which are difficult to fit into the Brunauer classification at all.

The underlying reasons and the significance and interpretation of the various isotherm types have been discussed in detail by Brunauer[1] and Gregg and Sing.[4] Briefly, the type I isotherm is usually associated with micropore filling. Types II and III with monolayer-multilayer adsorption and Types IV and V with capillary condensation. Only those types particularly

relevant to the present work, namely Type I and Type II, will be discussed in any further detail (Section 2.3). Some discussion on step-wise isotherms is included in Chapter 6.

Most adsorbents of high surface area are porous, possessing both internal and external surface area.[8] The pore systems are of many different kinds, the pores varying greatly both in size and shape for any given adsorbent. To discuss the interpretation of adsorption isotherms, it is helpful to classify pores according to their effective width. The classification is necessarily arbitrary and is still the subject of much discussion. However, for the purpose of the present work, the recent IUPAC classification[9] (similar to an earlier classification by Dubinin[10]) has been adopted: namely, the narrowest pores of width not exceeding about 20 Å (2.0 nm) are called "MICROPORES"; pores of width exceeding about 500 Å (50 nm) are called "MACROPORES". The pores of intermediate width, which have previously been termed intermediate or transitional pores,[11] are referred to as "MESOPORES".

Adsorption in the relative pressure region of P/Po ~ 0.05 to ~ 0.5 may depend on three different mechanisms:[12] (a) monolayer-multilayer coverage, (b) micropore filling, and (c) capillary condensation. Dubinin[10] proposed that the whole of the accessible micropore volume may be pictured as adsorption space, since in pores of these dimensions the adsorption potentials of opposite walls overlap. The micropore volume is thus filled at low relative pressure and no well-defined monolayer is formed. Mechanisms (a) and (b) may therefore be considered as primary processes of adsorption. On the other hand, capillary condensation in mesopores (involving the formation of a liquid-like meniscus) is preceded by the formation of an adsorbed layer on the pore walls, and is, therefore, a secondary process.

In practice, it is difficult to resolve the different processes occurring in micropores and mesopores. Frequently, the above processes, (a), (b) and (c), may all contribute to the measured adsorption. Sing[13] has pointed out that in any real system, there are two main problems: first, the adsorption properties of the solid are determined by its texture and by the adsorbent-adsorbate and adsorbate-adsorbate interactions, which occur in a unique way in each adsorption system; secondly, as already mentioned, the pores in a real solid are generally distributed over a wide range of size and shape. The interpretation of isotherms, in terms of monolayer-multilayer adsorption and micropore filling, is therefore frequently very difficult.

2.2 Physical Interaction Energies

The detailed studies of Kiselev[14,15] and Barrer[16] have revealed that, in addition to non-specific interactions, physisorption is frequently associated with specific adsorbent-adsorbate interactions. The adsorption potential, ϕ, (i.e. interaction energy) for a polar adsorbate molecule on a heteropolar or ionic surface may be expressed[16] as the sum of the number of energy contributions:

$$\phi = \phi_D + \phi_P + \phi_{F\mu} + \phi_{FQ} + \phi_R \qquad (2.3)$$

The dispersion energy, ϕ_D, and the short range repulsion energy, ϕ_R, may be regarded as originating from non-specific interactions; the polarisation, ϕ_P, the field-dipole, $\phi_{F\mu}$, and the field gradient-quadrupole, ϕ_{FQ}, terms represent the specific interaction energy contributions. The contribution of ϕ_P is usually small, but that of ϕ_F or ϕ_{FQ} may be very important in the case of adsorbate molecules possessing permanent dipole or quadrupole moments.

In general, the specific interactions are the result of the concentration of charge density on the periphery of the adsorbate molecule.

Oxide surfaces are generally energetically heterogeneous; they are hydrated (or hydroxylated) unless they have been outgassed at a high temperature, i.e. at about 1000°C. The degree of surface hydroxylation may have pronounced effect on the adsorbent-adsorbate interactions, notably the specific contributions. Kiselev and his co-workers[14,15,17,18] have studied the effect of the surface dehydroxylation of silica on the physisorption of a number of polar and non-polar vapours. Their investigations revealed that the differential heats of adsorption for adsorptives with π-bonds (e.g. benzene, nitrogen) or lone pairs of electrons (e.g. pyridine, diethyl ether) were considerably reduced by a decrease in the number of hydroxyl groups per unit surface area of silica. Conversely, the differential heats of adsorption for comparable non-polar adsorptives (e.g. n-hexane, argon) were not significantly affected. Thus, the ϕ_D, ϕ_P and ϕ_R contributions are insensitive to the degree of surface hydroxylation, but the $\phi_{F\mu}$ and ϕ_{FQ} terms are dependent on the concentration of the surface hydroxyl groups.

In view of the differences in the differential heats of adsorption for certain adsorptives on hydroxylated and dehydroxylated oxide surfaces,[19] it is not surprising that the shape of the isotherms may also be significantly affected. For example, the similarity of their molecular size and polarisability would suggest that argon and nitrogen should be alike in their physisorption behaviour. In fact, dehydroxylation of a silica surface has very little effect on argon adsorption,[20] but for nitrogen adsorption the specific nitrogen quadrupole interaction, ϕ_{FQ}, is considerably reduced. The statistical monolayer for nitrogen adsorption on a hydroxylated silica surface is usually a well-defined point on the isotherm; dehydroxylation of

the surface has been shown[20,21] to result in a nitrogen isotherm that is very similar in shape to that for argon, where point B (section 2.3) is frequently poorly defined (for hydroxylated and dehydroxylated silica surfaces).

2.3 The BET Method for the Determination of Surface Area

The Langmuir theory[22,23] established the classical model of localised monolayer adsorption on a uniform surface, and may be represented by the equation:

$$\frac{V}{V_m} = \frac{bP}{1 + bP} \qquad (2.4)$$

where V is the amount of gas adsorbed (mass, volume or mole) at an equilibrium pressure P: V_m is the monolayer capacity (i.e. the amount of gas adsorbed in a completed monolayer), and the constant b is a function of the heat and the entropy of adsorption.[24] The model was designed for application to adsorption on an open surface freely exposed to the gas phase, the plateau of the Langmuir isotherm[24] (Type I in Fig. 2.1) representing a completed monolayer. It is now generally agreed, however, that if a Type I isotherm is obtained, then the adsorbent must be predominantly microporous in nature; furthermore, the plateau does not necessarily represent a completed monolayer and therefore the specific surface of the adsorbent.[25]

Brunauer, Emmett and Teller developed Langmuir's suggestion[23] that the dynamic condensation-evaporation mechanism might apply to second, and subsequent, adsorbate layers. Since its inception in 1938, the BET theory[26] has occupied a central position in the use of gas adsorption studies for surface area determination.

The BET equation is usually applied in the form:

$$\frac{P}{V(Po - P)} = \frac{1}{V_m C} + \frac{(C - 1)}{V_m C} \cdot \frac{P}{Po} \qquad (2.5)$$

where V, V_m and P are the quantities defined for equation (2.4) and Po is the saturated vapour pressure of the adsorptive. According to the simplified theory, C is a constant related to the net heat of adsorption, but in fact it is a free energy term which is dependent on both the enthalpy and entropy of adsorption.[27] It is clear from equation (2.5) that there should be a linear relationship between P/V (Po - P) and P/Po. In practice, however, the linearity of the BET plot rarely extends beyond the relative pressure range of 0.05 - 0.3, even with non-porous adsorbents. Indeed, the range of linearity is often much more restricted,[28] and with uniform surfaces, notably graphitised carbon,[29] may not extend beyond P/Po = 0.1.

From the linear region of the BET plot, the slope, S, and intercept, I, may be derived. The BET parameters, V_m and C, may then be readily calculated by application of the equations:

$$V_m = \frac{1}{S + I} \qquad (2.6)$$

$$C = \frac{S}{I} + 1 \qquad (2.7)$$

The main criticisms levelled at the BET model may be summarised as follows:

(1) It assumes that all adsorption sites are exactly equivalent. In fact, the variation of the heat of adsorption with coverage for many adsorbents implies that the surface is energetically heterogeneous;[30] in many cases, the range of linearity of the BET plot is better for heterogeneous surfaces than for uniform surfaces.[31]

(2) Lateral interactions of adsorbate molecules are neglected; only those interactions normal to the adsorbent surface are considered. As the degree of coverage increases the inter-adsorbate distance decreases, and therefore the lateral interactions must become significant. Further, the neglect of the lateral adsorbate interactions is in conflict with the most basic assumption of the BET theory - that the evaporation-condensation properties of the second and subsequent adsorbate layers are the same as those of the surface of the bulk liquid.[32]

(3) Adsorbate molecules in second and subsequent layers are treated as completely equivalent. It would be expected that the adsorption potential would diminish as a function of the distance from the adsorbent surface.[33]

(4) The model assumes that the number of adsorbate layers is infinite at the saturated vapour pressure of the adsorptive. In fact, there are many cases where the number of adsorbate layers is finite in the presence of the saturated vapour.[34]

Nevertheless, in spite of the limitations of the BET theory, it has provided a remarkably successful method for the analysis of adsorption isotherms. Many refined theories have been presented over recent years, but very few retain the essence of the BET theory - its practical utility.

Brunauer and his co-workers[35] have recently modified the BET equation in an attempt to improve the agreement with experimental isotherm data over a wider range of relative pressure. A third parameter, k, was introduced to allow for the finite number of adsorbate layers on a non-porous adsorbent as $P \longrightarrow Po$:

$$\frac{kP}{V(Po - kP)} = \frac{1}{V_m C} + \frac{(C - 1)}{V_m C} \cdot \frac{kP}{Po} \qquad (2.8)$$

As an empirical relationship, equation (2.8) was found to give a considerably better fit for nitrogen adsorption on several non-porous oxides.[35] The deviation of k from unity is an approximate measure of the inadequacy of the basic BET assumption - that the second and subsequent adsorbate layers possess the properties of the bulk liquid.

On empirical grounds, Emmett and Brunauer[36] suggested that the completion of the monolayer is indicated by point B on the isotherm, i.e. the point corresponding to the beginning of the almost linear region exhibited by many Type II isotherms (Figs. 2.1 and 2.2). Halsey[37] supported this view by suggesting that this point is located where the affinity of the surface for the adsorptive is changing most rapidly, and it is reasonable to identify this change in adsorptive power with the completion of the first layer. However, it is now clear that reasonable agreement between point B and the BET monolayer capacity, V_m, is only found if point B lies within the linear region of the BET plot.[38]

The characteristic 'knee' of a Type II isotherm is dependent on the numerical value of C; as the value of C increases (i.e. as the value of the net heat of adsorption increases) so the shape of the knee becomes progressively sharper (Fig. 2.2). Many workers[3,4,32,37,39] have suggested that the BET method for the evaluation of monolayer capacity, should only be used if the isotherm exhibits a clear point B, i.e. in general, the value of C exceeds about 50.

The specific surface area, S_{BET} (expressed in m^2g^{-1}), of an adsorbent may be calculated from the monolayer capacity, V_m (expressed in cm^3g^{-1}), by application of the equation:

$$S_{BET} = \frac{V_m \cdot N \cdot A_m \times 10^{-20}}{22414} \qquad (2.9)$$

where N is Avogadro's constant (6.023×10^{23} molecules $mole^{-1}$) and A_m (expressed in $Å^2$) is the assumed average area occupied by the adsorbate molecule in the completed monolayer.

The main difficulty associated with the calculation of S_{BET} from V_m, is the lack of independent evidence on the correct value of A_m. Most workers have followed the example of Emmett and Brunauer,[36] in assuming that the close-packing of the adsorbate molecules in the monolayer is very similar to that in the bulk liquid state. For the case of nitrogen as the adsorptive, such as assumption leads to a molecular cross-sectional area (i.e. A_m) of 16.2 $Å^2$ at 77 K: McClellan and Harnsberger,[40] in a recent comprehensive survey of the literature on assumed cross-sectional areas of adsorbed molecules, concluded that this is the most reliable recommended value. On a priori grounds, however, one might expect some degree of localisation of the adsorbate molecules in the monolayer and a variation in the area occupied per molecule from one surface to another. Indeed, recent investigations[21,41-43] have indicated that the nitrogen monolayer may be slightly more open than in the liquid state and consequently, the value of A_m may be as high as about 20 $Å^2$.

For many other adsorbates, there is a greater degree of uncertainty attached to the assumed value of the cross-sectional area of the adsorbate molecule.[40] Extensive studies have indicated that the value of A_m to be adopted is dependent on the value of the BET C constant,[44] and therefore, the net heat of adsorption. Since the net heat of adsorption is a function of the degree of adsorbent-adsorbate interaction, a particular adsorptive may yield different values of C (and therefore, A_m) on different adsorbents.[45] This is particularly the case for water adsorption, where the degree of adsorbent-adsorbate interaction will be dependent on the extent of the hydrophobicity of the adsorbent surface;[46] water adsorption on a hydrophilic

surface is highly specific.[43] The assumed value of A_m for water is, therefore, particularly sensitive to changes on the adsorbent surface; for the purposes of the present work, the value[47] of 10.6 Å² (representing close-packing of the adsorbate molecules) has been adopted.

In the case of argon adsorption, there is a two-fold problem: first, a similar question of the cross-sectional area for an adsorbate molecule where BET C values are frequently below 50; secondly, whether one assumes the adsorbate is in a solid or liquid-like state at temperatures below the bulk triple point of argon. These problems are discussed in Sections 4.1 and 6.5.

2.4 Empirical Methods of Isotherm Analysis

In recent years, the t-method of Lippens and de Boer[48] has attracted considerable attention[49-53] as a simple and direct means of interpreting nitrogen isotherm data. The amount, V, of nitrogen adsorbed on the test adsorbent is plotted against t, the statistical thickness[54] of the adsorbed layer of nitrogen at corresponding relative pressures (t is obtained from the standard isotherm on a non-porous reference adsorbent, and is given by $t = (V/V_m)\,\sigma$, where σ is the statistical thickness of the monolayer). A deviation in shape from the standard isotherm may be interpreted in terms of the porosity of the test adsorbent, and is detected as a departure of the t-plot from linearity; furthermore, the slope of a linear t-plot is directly proportional to the surface area of the test adsorbent. Much of the early work[41,54-56] was directed at obtaining a common or "universal" multilayer thickness (t-curve) for nitrogen on different adsorbents, but with the growing awareness of specific interactions with nitrogen adsorption (cf. Section 2.2), it is now recognised[12,27,39,57,58] that this is not possible. Instead, it may be possible[39] to establish a set of t-tables for

the adsorption of nitrogen (and other adsorptives)on different adsorbents. Brunauer and his co-workers[27,49,50,53] have suggested that the correct t-curve should be based on a reference adsorbent that gives a similar value of the BET C constant as the adsorbent under analysis; furthermore, there should be a close agreement between the surface area obtained from the slope of the t-plot and the BET area.

Other limitations of the t-plot are: (1) it is necessarily dependent on the evaluation of the BET monolayer capacity, since t is itself calculated from V/V_m (i.e. for nitrogen, $t = 3.54. V/V_m$), and (2) it cannot be readily applied where adsorption isotherms have low C-values. To avoid these difficulties, the t-method was modified by Sing[12,59] and the empirical α_s-method introduced.

The α_s-Method

α_s is defined[12,13] as V/V_s, where V_s is the amount of vapour adsorbed at a selected relative pressure, $(P/Po)_s$. The values of α_s are calculated from the reduced standard isotherm for an appropriate non-porous reference adsorbent. For the isotherm under analysis, the α_s-plot is constructed as the amount adsorbed, V, against the α_s value obtained at the corresponding relative pressure, $(P/Po)_s$.

In principle, the value of α_s may be placed equal to unity at any convenient point on the standard isotherm. In practice, however, it is usually convenient to place $\alpha_s = 1$ at $(P/Po)_s = 0.4$; with nitrogen adsorption at 77 K, both monolayer coverage and micropore filling occur at $P/Po < 0.4$, whereas any hysteresis loop (associated with capillary condensation) is generally located at $P/Po > 0.4$. Furthermore, greater precision is achieved[59] by placing $\alpha_s = 1$ in the middle range of the isotherm, especially in the case of a Type III (or near Type III) isotherm.

Deviation of the α_s-plot from linearity provides a convenient diagnostic test for both micropore filling and capillary condensation. Examples of hypothetical α_s-plots, curves (d), (e) and (f), are shown in Fig. 2.3, together with the corresponding isotherms, curves (a), (b) and (c), respectively, from which they could possibly be derived. The linear plot in (d) is the result of unrestricted monolayer - multilayer adsorption on a non-porous or macroporous adsorbent. The upward deviation of curve (e) from linearity indicates that capillary condensation is taking place within mesopores of an adsorbent; a similar downward deviation from linearity may indicate the occurrence of inter-particle condensation. The restricted adsorption in the case of curve (f) is typical of a microporous adsorbent, with pronounced micropore filling followed by multilayer adsorption (the upper linear branch) on a small external surface.

The α_s-method may also be used for the assessment of surface area[12] (internal and external) and micropore volume.[60,61] The surface area, S_s, is readily calculated from the slope, m, of the linear region of the α_s-plot by the use of a proportionality (or normalising) factor; the factor, f, is obtained from the standard isotherm on the non-porous reference adsorbent of known BET surface area:

$$f = \frac{(S_{BET})_{ref}}{(V_{0.4})_{ref}} \qquad (2.10)$$

where $(S_{BET})_{ref}$ is the BET surface area of the non-porous reference standard, and $(V_{0.4})_{ref}$ is the amount adsorbed on the reference standard at a relative pressure of 0.4 (assuming α_s is placed equal to unity at P/Po = 0.4). The surface area S_s, is then given by:

$$S_s = f \cdot m \qquad (2.11)$$

In the cases where the linear region of the α_s-plot passes through the origin (i.e. curve (d), and the lower linear region of curve (e), in Fig. 2.3), equation (2.11) may be rewritten in the form:

$$S_s = f \cdot \frac{V}{\alpha_s} \qquad (2.12)$$

where V is the amount on the test adsorbent at a particular value of α_s. Clearly, in cases such as curves (e) and (f) in Fig. 2.3, the slope, m, of the upper linear region is given by:

$$m = \frac{\Delta V}{\Delta \alpha_s} \qquad (2.13)$$

and therefore, the <u>external</u> surface area, S_{ext}, is given by:

$$S_{ext} = f. \frac{\Delta V}{\Delta \alpha_s} \qquad (2.14)$$

The pore volume, V_p, or micropore volume, V_{mic}, may be assessed by the back-extrapolation of the upper linear region of the respective α_s-plots (curves (e) and (f) in Fig. 2.3) to the intercept at $\alpha_s = 0$. If the uptake at the intercept is V_y, and assuming liquid close-packing of the adsorbate molecules, then for nitrogen adsorption[60] V_p (or V_{mic}) is given by:

$$V_p = 0.00156 \cdot V_y \qquad (2.15)$$

Occasionally, a compensating effect (between micropore filling and reversible capillary condensation[62]) may occur with certain isotherms, giving rise to an almost linear α_s-plot over a very wide range of relative pressure. Such a compensating effect can be detected by means of a systematic study employing adsorptives of different size and polarisability, in order to check the constancy of S_s and the linearity of the different α_s-plots on the same adsorbent.[12]

A particular advantage of the α_s-method is that it may be employed for Type III isotherms, or Type II isotherms with a small or indistinct knee, where the calculation of the BET surface area is unreliable; e.g. adsorption of carbon tetrachloride on silica.[12] In such cases, the surface area, S_s, of the adsorbent (with respect to a particular adsorptive) may be obtained from the α_s-plot on a comparative basis, usually with respect to a standard nitrogen surface area. Equation (2.10) is rewritten in the form:

$$f = \frac{(S^N_{BET})_{ref}}{(V_{0.4})_{ref}} \qquad (2.16)$$

where $(S^N_{BET})_{ref}$ is the BET <u>nitrogen</u> surface area of the non-porous reference standard, and $(V_{0.4})_{ref}$ is the amount of the adsorptive in question adsorbed on the reference standard at a relative pressure of 0.4. The surface area, S_s, (with respect to the test adsorptive) is then calculated in the usual manner, by application of either equation (2.12) or (2.14).

In principle, the α_s-method can be made entirely independent of the BET procedure; however, no <u>absolute</u> method of surface area determination has yet been developed that incorporates the necessary degree of accuracy and reliability.

<u>The Frenkel - Halsey - Hill Method</u>

Frenkel,[63] Halsey[32] and Hill[64,65] independently suggested that at high relative pressures, where an adsorbed film is several molecular layers in thickness and its properties approach those of the bulk liquid, the adsorption isotherm may be described by an equation of the form:

$$2.303 \log \left(\frac{Po}{P}\right) = \frac{k}{\theta^r} \qquad (2.17)$$

where k is a constant related to the energy of adsorption in the first layer, r is an exponent based on the decay of surface forces with distance, and θ is the surface coverage (i.e. $\theta = V/V_m$). Equation (2.17) may readily be transformed to give:

$$\log V = \frac{1}{r}(\log k - \log 2.303) + \log V_m - \frac{1}{r}\left[\log\left\{\log\left(\frac{Po}{P}\right)\right\}\right] \qquad (2.18)$$

Either equation (2.17) or (2.18) may be used to analyse adsorption data by plotting, log log (Po/P) either against log θ or against log V. From the slope of the plot the value of r may be readily determined.

The Frenkel - Halsey - Hill (FHH) treatment assumes that in the multilayer region of an adsorption isotherm, the periodicity due to the structure of the adsorbent may be regarded as effectively smoothed out and that the adsorbed film may be treated as a uniform slab of liquid similar to the bulk liquid. According to the 'slab model',[65,66] at an appreciable distance from the surface the adsorbent-adsorbate interaction energy decays with the third power of distance and r = 3. The slab theory is strictly only applicable to adsorbates having spherically symmetrical molecules, but even for these adsorbates wide variations from the value of r = 3 are found.[32,46,67,68]

Halsey[32] has suggested that the magnitude of r characterises the type of interaction between a vapour and the adsorbent surface: specific adsorbent - adsorbate interactions are indicated by a high value of r. In addition, Pierce and Ewing[69] have shown that if a log-log plot of log (Po/P) against V does not give a straight line of approximately normal slope for a particular adsorptive, then it may be concluded that there is

not unrestricted free surface adsorption. An upward deviation of the plot from linearity may be interpreted[67,69,70] in terms of capillary condensation, whilst a generally curved plot (or a linear plot of too low a slope) may indicate[69] the occurrence of micropore filling.

Zettlemoyer and his co-workers[46,71,72] have extended the earlier work of Pierce[67,69,70] and studied the applicability of the FHH plot to nitrogen and water adsorption isotherms on a range of non-porous adsorbents. In the case of nitrogen adsorption, it was noted that oxides and other high energy (polar) surfaces gave r values in the range 2.5 - 2.75, whereas low energy polymer surfaces gave r = 2.12. Zettlemoyer[46] has endorsed the opinion of Pierce[41,67] that the "ideal nitrogen isotherm" on a polar surface is represented by a linear FHH plot for which the value of r = 2.75; for a non-polar surface, Zettlemoyer has proposed that the ideal value of r is 2.12. In the case of water adsorption on hydrophilic surfaces (e.g. hydroxylated Fe_2O_3, SiO_2, TiO_2), the FHH plots gave r values around 2.5; water adsorption on hydrophobic surfaces (e.g. dehydroxylated SiO_2 etc.) gave much lower r values in the range 1.3 - 1.9.

REFERENCES

1. S. Brunauer, "The Adsorption of Gases and Vapours", Oxford University Press, London (1944).
2. J.H. de Boer, "The Dynamical Character of Adsorption", Clarendon Press, Oxford, 1st Edt., (1953), 2nd Edt., (1968).
3. D.M. Young and A.D. Crowell, "Physical Adsorption of Gases", Butterworths, London, (1962).
4. S.J. Gregg and K.S.W. Sing, "Adsorption, Surface Area and Porosity", Academic Press, London,(1967).
5. E. Allison Flood, Ed., "The Solid-Gas Interface", Marcel Dekker, New York, (1967).
6. S. Brunauer, L.S. Deming, W.S. Deming and E. Teller, J. Amer. Chem. Soc., (1940) 62, 1723.
7. J.H. de Boer, "The Structure and Properties of Porous Materials", Butterworths, London, (1958) p.68.
8. S.J. Gregg, "The Surface Chemistry of Solids", Chapman and Hall, London, 2nd Edt., (1965) p.25.
9. IUPAC Manual of Symbols and Terminology, Appendix 11, Part 1, Colloid and Surface Chemistry; Pure and Appl. Chem., (1972) 31, 578.
10. M.M. Dubinin, J. Colloid Interface Sci., (1967) 23, 487.
11. M.M. Dubinin, Quat. Rev. Chem. Soc., (1955) 9, 101.
12. K.S.W. Sing, "Proc. Int. Symp. Surface Area Determination", Bristol, 1969. Eds. D.H. Everett and R.H. Ottewill; Butterworths, London, (1970) 25
13. K.S.W. Sing, Specialist Periodical Report, Colloid Science. Senior Reporter, D.H. Everett; The Chemical Society, London, (1973) 1, 1.
14. A.V. Kiselev, Discussions Faraday Soc., (1965) No 40, 205.

15. A.V. Kiselev, J. Colloid Interface Sci., (1968) 28, 430.

16. R.M. Barrer, J. Colloid Interface Sci., (1966) 21, 415.

17. A.V. Kiselev, J. Chromatography, (1970) 49, 84.

18. A.V. Kiselev, A.V. Kuznetsov, I. Yu. Filatova and K.D. Scherbakova, Zh. Fiz. Khim., (1970) 44, 1272.

19. K.S.W. Sing, J. Oil Col. Chem. Assoc., (1971) 54, 731.

20. B.G. Aristov and A.V. Kiselev, Zh. Fiz. Khim., (1963) 37, 2520; ibid., (1964) 38, 1984.

21. D.R. Bassett, E.A. Boucher and A.C. Zettlemoyer, J. Colloid Interface Sci., (1968) 27, 649.

22. I. Langmuir, J. Amer. Chem. Soc., (1916) 38, 2221.

23. I. Langmuir, J. Amer. Chem. Soc., (1918) 40, 1361.

24. Reference 3, page 106.

25. Reference 4, page 200.

26. S. Brunauer, P.H. Emmett and E. Teller, J. Amer. Chem. Soc., (1938) 60, 309; for errata see P.H. Emmett and J.W. DeWitt, Ind. Eng. Chem. (Anal), (1941) 13, 28.

27. S. Brunauer, "Proc. Int. Symp. Surface Area Determination, Bristol, 1969. Eds. D.H. Everett and R.H. Ottewill; Butterworths, London, (1970) 63.

28. Yu. F. Berezkina, M.M. Dubinin and A.I. Sarakhov, Izv. Akad. Nauk. S.S.S.R., Ser. Khim., (1969) 2653; Bull. Acad. Sci. U.S.S.R., Chem. Sci., (1969) 2495.

29. A.A. Isirikyan and A.V. Kiselev, J. Phys. Chem., (1961) 65, 601; ibid., (1962) 66, 210.

30. Reference 4, page 59.

31. S. Ross, "Proc. Int. Symp. Surface Area Determination", Bristol, 1969. Eds. D.H. Everett and R.H. Ottewill; Butterworths, London, (1970) 143 and 205.

32. G.D. Halsey, J. Chem. Phys., (1948) 16, 931.

33. R.M. Barrer, N. MacKenzie and D. McLeod, J. Chem. Soc., (1952) 1736.

34. J.H. Singleton and G.D. Halsey, Can. J. Chem., (1955) 33, 184.

35. S. Brunauer, J. Skalny and E.E. Bodor, J. Colloid Interface Sci., (1969) 30, 546.

36. P.H. Emmett and S. Brunauer, J. Amer. Chem. Soc., (1937) 59, 153.

37. G.D. Halsey, Discussions Faraday Soc., (1950) No 8, 54.

38. K.S.W. Sing, Chem. and Ind., (1964) 321.

39. J.H. de Boer, "Proc. Int. Symp. Surface Area Determination", Bristol, 1969. Eds. D.H. Everett and R.H. Ottewill; Butterworths, London, (1970) 7.

40. A.L. McClellan and H.F. Harnsberger, J. Colloid Interface Sci., (1967) 23, 577.

41. C. Pierce, J. Phys. Chem., (1968) 72, 3673; ibid., (1969) 73, 813.

42. B.W. Davis and R.G. Varsanik, J. Colloid Interface Sci., (1971) 37, 870.

43. J.D. Carruthers, D.A. Payne, K.S.W. Sing and L.J. Stryker, J. Colloid Interface Sci., (1971) 36, 205.

44. Reference 4, page 78.

45. A.V. Kiselev and Y.A. Eltekov, "Proc. 2nd Int. Congr. Surface Activity", London, 1957. Butterworths, London, (1957) 2, 228.

46. A.C. Zettlemoyer, J. Colloid Interface Sci., (1968) 28, 343.

47. W.D. Harkins and G. Jura, J. Amer. Chem. Soc., (1944) 66, 919, 1362 and 1366.

48. B.C. Lippens and J.H. de Boer, J. Catalysis, (1965) 4, 319.

49. R. Sh. Mikhail, S. Brunauer and E.E. Bodor, J. Colloid Interface Sci., (1968) 26, 45 and 54.

50. J. Hagymassy, Jr., S. Brunauer and R. Sh. Mikhail, J. Colloid Interface Sci., (1969) 29, 485.

51. R.B. Gammage, E.L. Fuller, Jr., and H.F. Holmes, "Proc. Int. Symp. Surface Area Determination", Bristol, 1969. Eds. D.H. Everett and R.H. Ottewill; Butterworths, London (1970) 161.

52. M.M. Dubinin, "Proc. Int. Symp. Surface Area Determination", Bristol, 1969. Eds. D.H. Everett and R.H. Ottewill; Butterworths, London, (1970) 75

53. J. Skalny, E.E. Bodor and S. Brunauer, J. Colloid Interface Sci., (1971) 37, 476.

54. C.G. Shull, J. Amer. Chem. Soc., (1948) 70, 1405 and 1410.

55. J.H. De Boer, B.G. Linsen and Th. J. Osinga, J. Catalysis, (1965) 4, 643.

56. J.H. De Boer, B.C. Lippens, B.G. Linsen, J.C.P. Broekhoff, A van den Heuvel and Th. J. Osinga, J. Colloid Interface Sci., (1966) 21, 405.

57. R.B. Gammage, E.L. Fuller, Jr., and H.F. Holmes, J. Colloid Interface Sci., (1970) 34, 428.

58. G.D. Parfitt, D. Urwin and T. Wiseman, J. Colloid Interface Sci., (1971) 36, 217.

59. K.S.W. Sing, Chem. and Ind., (1968) 1520.

60. K.S.W. Sing, Chem. and Ind., (1967) 829.

61. G.A. Nicolaon and S.J. Teichner, J. Chim. Phys., (1969) 66, 1816.

62. G.C. Bye and K.S.W. Sing, Chem. and Ind., (1967) 1139.

63. J. Frenkel, "Kinetic Theory of Liquids", Clarendon Press, Oxford, (1946).

64. T.L. Hill, J. Chem. Phys., (1946) 14, 263 and 441; ibid., (1947) 15, 767; ibid., (1949) 17, 580 and 668.

65. T.L. Hill, "Advances in Catalysis", Academic Press, New York, (1952) 4, 211.

66. Reference 3, page 167.

67. C. Pierce, J. Phys. Chem., (1960) 64, 1184.

68. D. Lando and L.J. Slutsky, J. Chem. Phys., (1970) 52, 1510.

69. C. Pierce and B. Ewing, J. Amer. Chem. Soc., (1962) 84, 4070.

70. C. Pierce, J. Phys. Chem., (1968) 72, 1955.

71. E. McCafferty and A.C. Zettlemoyer, J. Colloid Interface Sci., (1970) 34, 452.

72. E. McCafferty and A.C. Zettlemoyer, Discussions Faraday Soc., (1971) No 52, 239.

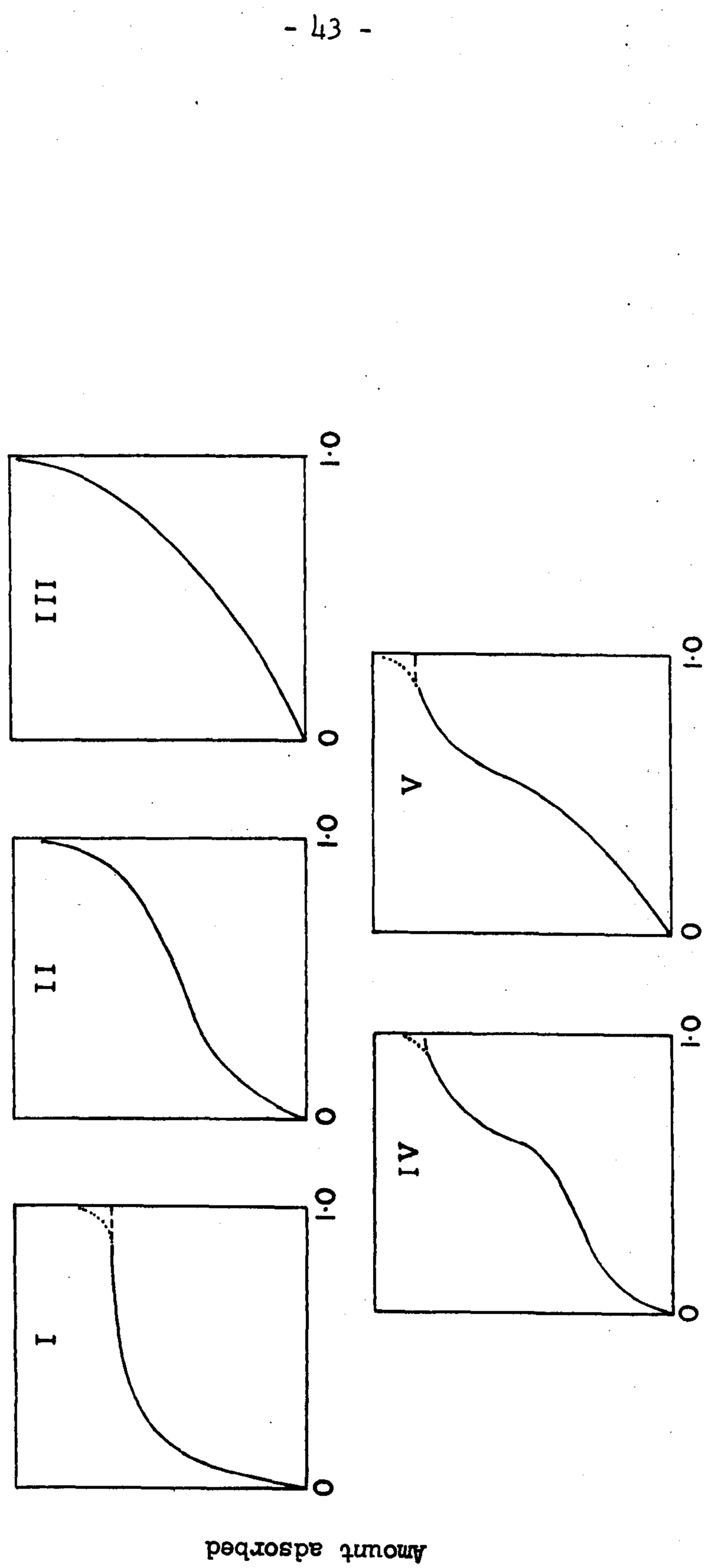

FIG 2.1 The Five Types of Adsorption Isotherm in the Classification of Brunauer, Deming, Deming and Teller (also called the BET classification)

FIG 2.2 Curves of V/V_m Against P/Po Calculated from the BET Equation (2.5) for Different Values of C

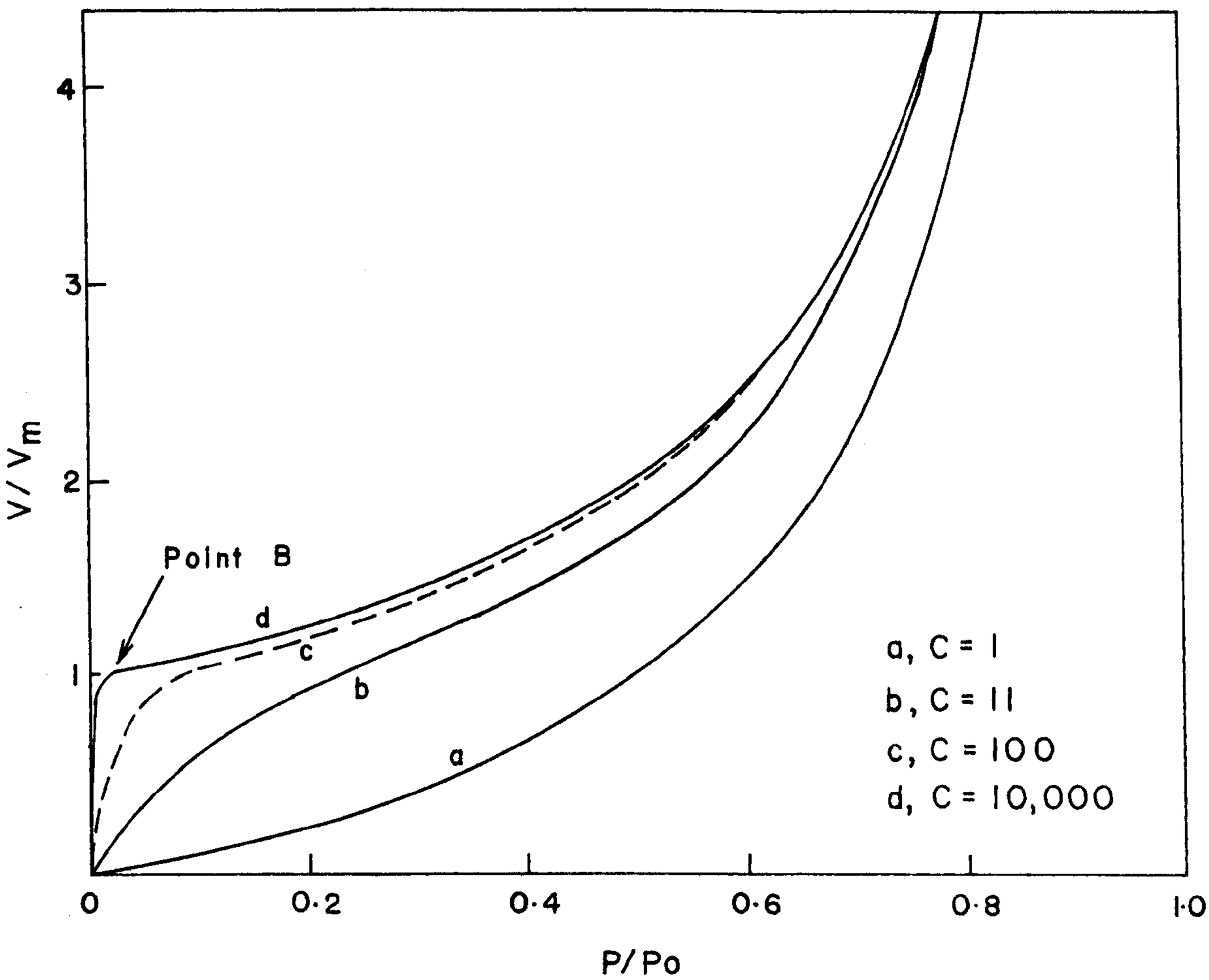

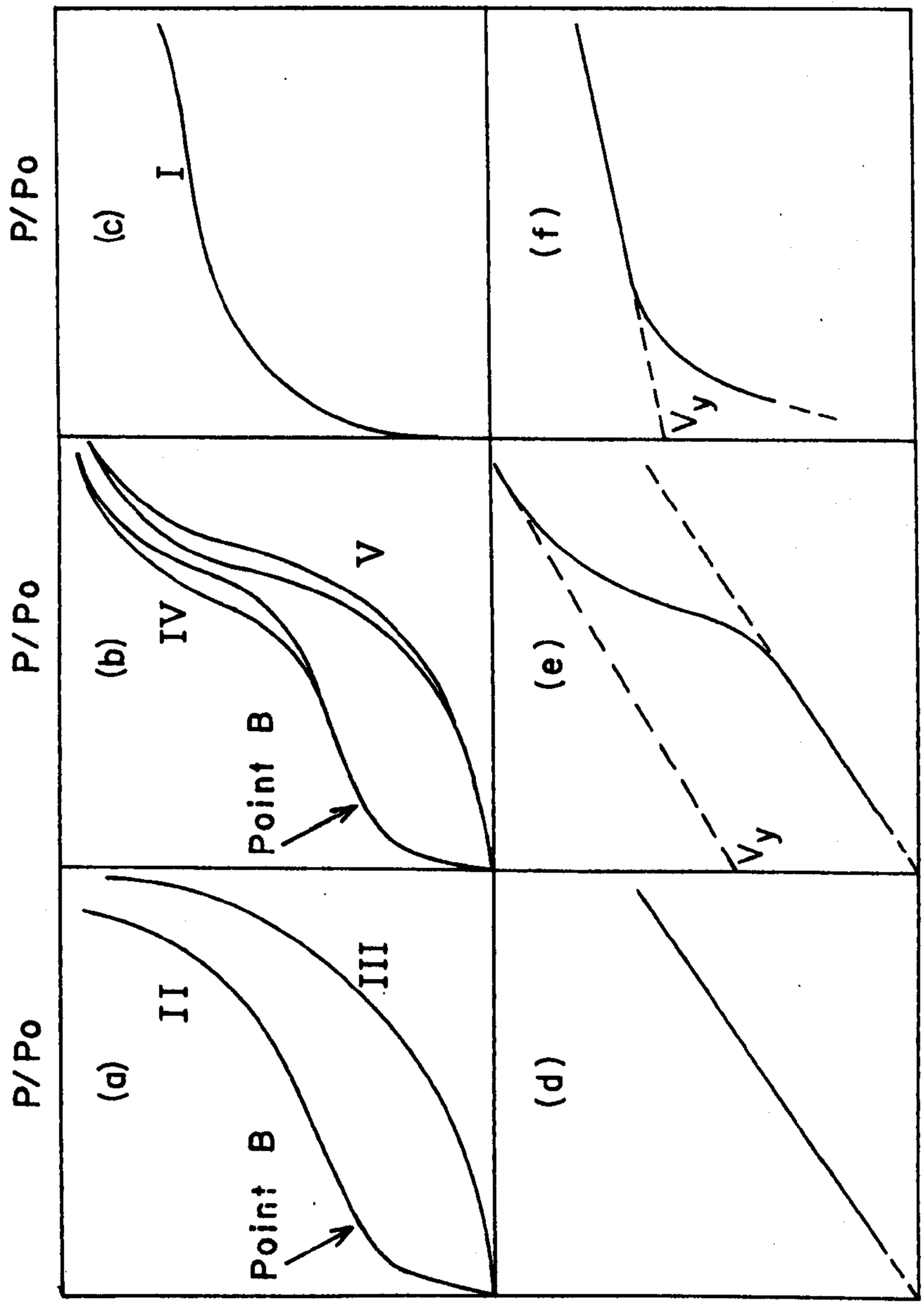

FIG 2.3 Types of Adsorption Isotherms and α_s-Plots

C H A P T E R 3

EXPERIMENTAL

In the present chapter the materials studied and the methods used in their general characterisation and study, will be described.

A. THE MATERIALS

3.1 Chromium Oxide Gels

The chromium oxide gels were prepared from aqueous chromium(III) nitrate in three ways: (a) by the slow addition of chromium nitrate to vigorously stirred ammonia solution (A series); (b) by the method of Burwell[1,2] utilising the slow hydrolysis of urea (B series); and (c) by the simultaneous addition of solutions of chromium nitrate and ammonia under conditions of controlled pH and concentration (S series).

The single electrode pH meter employed for the gel preparations was carefully calibrated over the operational pH range of the respective gel preparations. The pH values quoted in the present work have been corrected, where necessary, by reference to the appropriate calibration plot. However, no account has been taken of a possible 'suspension effect', i.e. the difference between the pH of a suspension and that of its isolated mother liquor.[3] For example, in the case of gel S2 the precipitation pH of 8.6 is very close to the point of zero charge (pzc) for freshly precipitated chromia gel[4,5] (about pH 8.5), and the suspension effect may, therefore, be assumed to be absent.[4] However, in the case of gel A1, precipitated at a mean pH value of 10.5, the pH of the suspension may be approximately 0.2 pH units lower than that of the mother liquor,[4]

i.e. the precipitation process is actually taking place at a slightly different pH value than that observed. When compared, however, with the overall wide range of precipitation pH (notably for the A series preparations), the effect is of little significance.

With the exception of chromium nitrate, all materials employed in the preparation of the chromia gels were of Analytical Reagent (AR) grade. Analytical grade chromic nitrate was not commercially available and it was therefore necessary to use the BDH Laboratory Reagent (LR) grade material; in the case of chromic nitrate, i.e. $Cr(NO_3)_3.9H_2O$, the purity of the LR grade material is at least 98% w/w, with less than 0.05% w/w Fe content.

The freshly prepared gels were washed with aliquots of distilled water (redistilled under nitrogen immediately prior to use) until tests[6] for NH_4^+ and NO_3^- gave negative responses. The gel was then treated according to the individual methods described below. In the cases where the gels were washed with acetone and ether, a total volume of approximately 7 dm^3 of each solvent per mole of chromic nitrate employed in the gel preparation, was used in the washing process. Each gel was dried at room temperature in a cylindrical drying chamber (35 cm x 8 cm), through which dry air was continuously passed at a flow rate of about 300 $cm^3\ min^{-1}$. The gel was placed in a 'boat' (28 cm x 6 cm) and, unless otherwise stated, the 'boat' was periodically removed from the chamber in order to redisperse the wet gel, thereby allowing the gel to dry fairly uniformly.

The conditions for each preparation are summarised in Table 3.1.

A Series

The A series gels were prepared under a dynamic atmosphere of nitrogen in a 5 dm^3 reaction vessel equipped with a mechanical stirrer. The pH of

the reaction medium was constantly monitored during the slow addition of the chromium nitrate solution to the ammonia solution. The addition was made below the surface of the ammonia solution (accompanied by vigorous stirring) in order to minimise localisation of the precipitation process. The initial pH of the ammonia solution was generally 11.2; upon commencement of the addition of the chromium nitrate solution, the pH rapidly fell to a value close to the mean pH value quoted in table 3.1 for the respective preparations. Thus, gels of this series were not prepared under conditions of constant pH and concentration; preliminary experiments revealed, however, that an S series-type preparation was difficult to control when the required pH was greater than about 10.

Gel A1

The gel was prepared by the addition of 0.1M chromium nitrate to 0.25M ammonia. The pH range for approximately 90% of the precipitation was 10.3 to 10.7, and the mean pH of the preparation therefore assumed to be 10.5. The gel was harvested by vacuum filtration and successively washed with aliquots of water, acetone and diethyl ether, using a slurry technique for each wash. The gel was dried to constant weight over a period of 16 hours.

Gel A2

The gel was prepared in a very similar manner to that of gel A1, but the ratio of 0.25M ammonia solution to 0.1M chromium nitrate solution was decreased in order to lower the minimum pH value of the preparation. Approximately 85% of the precipitation occurred in the pH range of 9.0 to 9.2, and the mean pH of the preparation was therefore assumed to be 9.1. The time taken for the harvesting and washing of the gel was considerably reduced (four-fold) with the aid of a large-capacity centrifuge. Using a

45° angle head, it was possible to centrifuge 3 dm^3 of the gel suspension (or wash) at 4,500 r.p.m., and thereby reduce the total harvesting and washing time to about 1.5 hours.

Gel A3

In order to maintain the pH of the precipitation medium as high as possible, the concentration of the ammonia solution was increased to 1M for this preparation. In addition, 1M ammonia solution was simultaneously added with the chromium nitrate solution, to the ammonia solution already present in the reaction vessel. Thus, the overall mole ratio of ammonia to chromium nitrate was increased approximately six-fold (compared to gel A1) for gel A3. In this manner, approximately 95% of the gel precipitation was confined to the pH range of 10.4 to 10.6, i.e. a mean pH of 10.5. The gel was harvested by centrifugation, thoroughly washed with water, and dried to constant weight over a period of 7 days.

Thus,gels A1 and A3 were each prepared at about pH 10.5, but contrast in the respect that gel A3 was prepared using a much higher concentration of ammonia and only water was used to wash the gel.

Gel A4

With the exception of gel A3, the mother liquors of all the gel preparations (A, B and S series) were colourless; for gel A3, the mother liquor was a light-violet in colour. Such a colour is typical of a hexaquochromium (III) compound, e.g. $[Cr(H_2O)_6](OH)_3$, (cf. Chapter 6). The clear mother liquor was placed in a dark cupboard in order to investigate the reason for the colour in this instance. However, after a period of three days, a precipitate resulted leaving a colourless mother liquor. The precipitate was isolated, washed and dried as per gel A3, and the blue-grey powder designated gel A4.

B Series

Gels B6 - B9 were prepared from a single Burwell-type preparation, as follows:

A vigorously stirred solution, containing 0.15 mole of chromium (III) nitrate and 1.0 mole of urea in 4 dm^3 of water, was refluxed at 100°C over a period of 4 hours. Gelation commenced after refluxing for about 1.5 hours. The resulting suspension was cooled to room temperature over a period of 1 hour and the precipitate isolated by centrifugation. The wet gel was split into two equal portions (by weight): gel B6 was isolated from the first portion, whilst gels B7 - B9 were isolated from the second portion.

Gel B6

The wet gel was successively washed with aliquots of water, acetone and diethyl ether, and dried to constant weight over a period of 16 hours.

Gels B7 - B9

The wet gel was thoroughly washed with water and dried to constant weight over a period of 8 days. However, instead of periodically redispersing the wet gel in the drying boat, the gel was left undisturbed during the drying process (apart from periodic removal of the boat to check the weight of the gel). During the drying of all the previous gels, a gradient in the rate at which the gels dried (particularly those washed with organic solvents) was observed to exist along the length of the drying chamber. Naturally, such a gradient was to be expected and therefore the gel was periodically redispersed. However, it was surprising to find that the rate at which the gel dried increased with distance from the dry air inlet, i.e. the rate apparently increased with increasing humidity through the drying chamber.

In order to investigate whether the phenomenon affected the subsequent surface properties of the gel, the vitreous dark green solid was split into three portions (ratio by weight of about 1 : 3 : 1) upon removal from the drying chamber. The portions were designated as follows:

Gel B7 - the portion furthest away from the air inlet.

Gel B8 - the major portion, removed from the centre of the drying chamber.

Gel B9 - the portion nearest to the air inlet.

S Series

Gel S2

The mixing apparatus employed for the preparation of gel S2 was based on an earlier design of Harris and Sing.[7] The modified apparatus incorporated a number of new features which enabled a relatively large scale preparation to be carried out, with sensitive control on the flow rates of the reactants and constant monitoring of the pH of the reaction medium. The reaction medium was vigorously stirred magnetically, and was maintained under a dynamic atmosphere of nitrogen.

The gel was prepared at pH 8.6 ($\pm$ 0.05) by the simultaneous addition of 0.1M chromium (III) nitrate and 1M ammonia to the reaction vessel. The desired fraction (pH 8.6) of the gel was isolated by vacuum filtration, successively washed with aliquots of water, acetone and diethyl ether, and dried to constant weight over a period of 16 hours.

TABLE 3.1

Conditions for the Preparation of the Chromia Gels

GEL	PREPN. NO.	MEAN pH	CHROMIUM NITRATE		AMMONIA		YIELD (g)
			MOLARITY	MOLE USED	MOLARITY	MOLE USED	
A1	FSB/G2	10.5	0.1	0.07	0.25	0.44	9.0
A2	FSB/G3	9.1	0.1	0.09	0.25	0.5	13.8
A3	FSB/G4	10.5	0.1	0.1	1	4	12.7
A4	FSB/G4/2 (a)	10.5	0.1	0.1	1	4	2.5
B6	FSB/G5/1	~6 (b)	0.038	0.15	0.25 (c)	1	8.9
B7	FSB/G5/2/1 (d)	~6	0.038	0.15	0.25	1	2.1
B8	FSB/G5/2/2 (d)	~6	0.038	0.15	0.25	1	5.6
B9	FSB/G5/2/3 (d)	~6	0.038	0.15	0.25	1	1.7
S2	FSB/G1	8.6	0.1	0.07	1	0.5	8.7

Footnotes:

(a) Gel A4 was obtained from the preparation of gel A3.

(b) The gel precipitation pH of a Burwell-type preparation is thought[8] to be about 6. When the precipitation of the gel is complete, the pH of the medium rises to about 8.5 when the above concentrations are employed.

(c) The figures in the 'ammonia' column for gels B6 - B9 refer to urea: each mole of urea, upon hydrolysis, generates two moles of ammonia.

(d) Gels B7 - B9 were obtained from the preparation of gel B6.

3.2 Chromium Oxy-hydroxide and Chromium Dioxide Samples

Pure samples of orthorhombic oxy-hydroxide (CrOOH) and chromium dioxide (CrO_2) were supplied by Dr. E.F. Hockings of the RCA Laboratories, Princeton, USA. No impurities could be detected by x-ray powder diffraction.

3.3 Silica Samples

The silica samples were obtained from commercial sources.

Fransil, a non-porous hydroxylated silica produced by a plasma process, was supplied by Fransol S.A. of France. The surface area determined by transmission electron microscopy (36 m^2g^{-1}) was in fairly good agreement with the BET nitrogen surface area (38.7 m^2g^{-1}).[9] This material was used as a reference standard for the calibration of the volumetric apparatuses.

Silica Gels E and J, prepared by a gelation process, were supplied by the Unilever Chemical Development Centre, England. The two gels were specially selected to provide a microporous reference adsorbent (gel E) and a mesoporous reference adsorbent (gel J), respectively.

TK 800, a non-porous hydroxylated silica produced by a plasma process, was supplied by Degussa Forschung Chemie, Rheinfelden, West Germany. This product has been found[9] to consist of discrete spherical particles, the degree of aggregation being lower than in the commercial grades of Aerosil (Degussa products), e.g. Aerosil 200. Two samples of TK 800, namely TK 800 - II and TK 800 - III respectively, have been employed in the present work. The latter sample, TK 800 - III, has been widely distributed by the National Physical Laboratory, England, to laboratories participating in the Surface Area Standards Scheme[10] (sample reference No. NPL 6A/32/31).

B. METHODS OF CHARACTERISATION

3.4 Differential Thermal Analysis (DTA)

The DTA experiments on the chromia gels were performed on a Standata Model 6.25 instrument (Stanton Instruments, London), under a static atmosphere of air. The experiments on the samples of CrOOH and CrO_2 were carried out under a static atmosphere of air, and also, dynamic atmospheres of pure hydrogen, nitrogen and oxygen (flow rates of 200 $cm^3\ min^{-1}$ at STP). The differential temperature, ΔT, and the reference temperature, T (of the sample), were recorded by a twin-pen potentiometric recorder. Freshly calcined α-Al_2O_3 was used as the reference solid and the rate of heating was standardised at $10^oC\ min^{-1}$. Previous work[11] on chromia gels has shown that a variation in the rate of heating, within the range $2.5^oC\ min^{-1}$ to $10^oC\ min^{-1}$, has very little effect on the DTA curve.

In each DTA run, 100 mg of sample and of reference solid were placed in the respective dimpled platinum crucibles which were mounted on the two Pt - Pt/Rh thermocouples inside the vertical cylindrical furnace. The chromia gel samples were ground, prior to examination, using an agate mortar and pestle.

3.5 Differential Scanning Calorimetry (DSC)

A Perkin Elmer differential scanning calorimeter, Model DSC-1B, was employed for the DSC study of the chromia gels. The instrument was fitted with a thermal conductivity gas detector for the analysis of the sample effluent.

This instrument, unlike the DTA apparatus, maintains a sample isothermal with a reference material (or the furnace block) by supplying heat to the sample or reference material according to demand. The energy required to maintain an isothermal condition is recorded as a function of temperature (or time). The temperature of a transition was assumed to be the temperature at which the first evidence of the change appeared, i.e. a departure of the

recordor pen from the baseline calibration. A twin-pen potentiometric recorder, fitted with a fiducial marker, was used to simultaneously record the calorimetric, thermal conductivity and temperature output signals, respectively. The thermal conductivity trace provided information which related an exothermic or endothermic change to gas evolution at a particular temperature.

The use of the thermal conductivity gas detector requires the presence of a carrier gas; the chromia gel samples were therefore examined under a dynamic atmosphere of nitrogen (flow rate of 30 cm^3 min^{-1} at STP).

3.6 X-Ray Diffraction

The Debye - Scherrer x-ray powder diffraction technique[12] was employed for the examination of the chromium oxide samples. The samples were finely ground, using an agate mortar and pestle, and packed into Lindemann silica glass tubes of 0.03 cm internal diameter. Each specimen was mounted in a powder camera of 11.48 cm diameter, so that its longitudinal axis was concentric with a cylinder of 35 mm photographic film on which the diffraction pattern was recorded. The Cu K_α radiation (λ = 1.541 Å) was obtained using a Philips 11704 x-ray unit, and was filtered by a nickel foil. The exposure time was varied between 4 and 12 hours.

3.7 Electron Microscopy

Transmission

Electron micrographs of the chromium oxide samples were obtained using a JEM-7 electron microscope (manufactured by Japan Electron Optics Laboratory, Japan). The finely ground samples were ultrasonically dispersed in absolute alcohol and the specimen prepared by placing a drop of the resulting suspension on a carbon film supported by a copper grid. The specimen was dried at ambient temperature and pressure before insertion into the instrument.

Scanning

The chromium oxide samples were sequentially scattered (in the dry state) on segments of double-sided sellotape affixed to an aluminium mounting stub. The samples were then vacuum coated with a layer of carbon, followed by a layer of gold/palladium alloy, to a total thickness of about 200 Å. The specimens were examined using a Stereoscan S4 scanning electron microscope (manufactured by Cambridge Scientific Instruments, England).

3.8 Mass Spectrometry

A Hitachi Perkin Elmer mass spectrometer, Model RMS-4, (coupled to an SE Laboratories oscillograph recorder, Model 3006) was employed to assess the purity of the chromia gels. The gels were examined by direct insertion of the sample into the ion source chamber of the instrument. In addition, the gases evolved from the gels, on outgassing at room temperature and 250°C respectively, were identified by using a sampling technique similar to that described by Murphy and his co-workers.[13] The effluent gas sample was inserted into the ion source chamber of the instrument and the gases identified by their respective fragmentation patterns.

3.9 Atomic Absorption

A Perkin Elmer double beam atomic absorption spectrophotometer, Model 303, was employed to determine the mercury content of a number of chromium oxides outgassed in the presence of mercury vapour. The absorption at λ = 2537 Å was measured, with a mercury detection limit of 0.5 μ g cm^{-3} (aqueous solution).

The weighed sample was extracted with a standard volume of 3.8M nitric acid by vigorous mechanical shaking over a period of 16 hours. The solid was isolated from the extract by centrifugation and carefully washed with aliquots of distilled water. The extract and washes were combined and the solution clarified by filtration through a quartz wool plug. The solution was diluted

with water to a standard volume, such that the estimated mercury content was within the optimum working range of 20 - 200 $\mu g\ cm^{-3}$ and the strength of the acid was 0.1M HNO_3.

The mercury contents of the respective solutions (and therefore the original chromium oxide samples) were determined by atomic absorption, with reference to a calibration plot of % absorption against mercury concentration.

3.10 Heat of Immersion

The heats of immersion of a number of chromium oxide and silica samples were determined in a simple diathermal calorimeter similar to the type designed by Zettlemoyer and his co-workers.[14] It consisted of a glass Dewar vessel fitted with a lid of tufnol, which carried supports for an ampoule holder, a thermistor, a heater coil and a stirrer. The stirrer incorporated a device for breaking the glass ampoule. The thermistor was connected into a Wheatstone bridge circuit and the out-of-balance current was registered as the deflection of a sensitive galvanometer. The details of the apparatus and method of operation have been described by Gregg and his co-workers.[15]

The author is indebted to Dr. R.R. Mather and Mr. C. Phillips for carrying out the heats of immersion studies.

C. LOW TEMPERATURE GAS ADSORPTION

The two volumetric apparatuses employed for the present study of argon and nitrogen adsorption were designed and built by the author. Although a number of refinements were made to the design and construction technique of each apparatus, the principle of operation was very similar to that described by Harris and Sing.[16]

3.11 Design and Construction of the Volumetric Apparatuses

Traditionally, gas adsorption apparatus has generally been constructed on the 'rod and clamp' principle. Although such apparatuses have been very successfully applied to gas adsorption studies, they are usually fragile and cannot be moved without substantial re-building (and frequently, re-calibration) During the course of the present work, the surface chemistry research laboratories at Brunel University were scheduled to be relocated from the site in Acton on to the new university campus. It was, therefore, an essential pre-requisite that the design and construction of the new apparatuses should allow the complete assembly to be moved with the minimum of difficulty and subsequent re-building.

The design requirements for the attainment of a high vacuum in a particular apparatus contrast sharply with the requirements for successful gas adsorption studies: the design of any gas adsorption system is, therefore, a compromise between pumping speed (and ultimate vacuum) on one hand, and 'dead space' volume on the other. Particular attention was given to this problem when drafting the design of the present apparatuses.

The general view of the front of the two volumetric apparatuses is shown in Fig. 3.1. The general arrangement of the left hand apparatus (L.H.A.) is shown in diagrammatic form in Fig. 3.4; the arrangement of the right hand apparatus (R.H.A.) was very similar. The significant difference between the two apparatuses was only one of convenience: the R.H.A. was designed to handle samples of surface area less than about 150 m^2g^{-1}, whilst the L.H.A. could more easily handle samples with surface areas in excess of 150 m^2g^{-1}. The lower limit of each apparatus was about 1 m^2g^{-1}. In addition, the L.H.A. was designed to allow high temperature outgassing of the sample (up to 1100°C). The two apparatuses were carefully mounted on a common back-plate, but were otherwise totally independent of one another. The vapour diffusion pumps,

cold traps, argon and nitrogen reservoirs, together with a Townson and Mercer thermostatic bath (and ancillary water pumps) were located on the rear of the back-plate; the rotary pumps, together with the low vacuum reservoir, were located beneath the base of the assembly. The cathetometers were placed on a heavy, purpose built, table securely anchored to the base of the assembly and located immediately in front of the apparatuses.

Each diffusion pump was protected against accidental over-heating by incorporation of both an Edwards 'Flowtrol' (monitoring the flow of the cooling water) and an Edwards 'Thermal Snap Switch' (activated by an excessive pump-body temperature) in the power supply circuits of the pumps. Edwards MS Silicone Fluid 704 was employed as the diffusion pump fluid. The gas adsorption system was protected against backstreaming of the pump fluid by sorption traps (at -196°C) containing a mixed zeolite bed of Linde molecular sieves, type 5A (to adsorb water vapour) and type 13X (to adsorb silicone oil vapour) respectively.

The essential differences between the design of the present apparatuses and those previously described,[11,17-20] were: (a) with the exception of the two-way stopcocks in the low vacuum line, greaseless stopcocks (supplied by Springham and Co. Ltd.) were employed throughout; (b) pressure-sensitive transducers (supplied by the Electronics and Instruments Group of Bell and Howell Ltd.) were incorporated in the dead space sections, and (c) the flexibility of the gas burette of each apparatus was considerably increased by the inclusion of 12 calibrated bulbs to vary the volume of the dead space. The calibration of the left hand limb of the "adsorption" manometer (M1 in Fig. 3.4) permitted an even finer control of the frequency and number of isotherm points. The characteristics of these particular features are discussed in the following sections.

3.12 Calibration of the Gas Adsorption System

The total volume of the adsorption system was composed of (a) the volume of the gas burette bulbs; (b) the volume of the left hand limb of the adsorption manometer (M1 in Fig. 3.4) and, (c) the dead space volumes, designated as V_a, V_b and V_c respectively, in Fig. 3.5. The calibration of the three main sections will be discussed separately and, unless otherwise stated, the discussion equally applies to both apparatuses.

Gas Burette Bulbs

Each set of six bulbs, complete with the outer water jacket, was calibrated before being carefully welded into position on the apparatus. The volumes of the bulbs were determined gravimetrically by weighing the amount of triple-distilled mercury necessary to fill each bulb to its fiducial mark (see Fig. 3.5). The calibrations were carried out in triplicate, with the bulbs maintained at a temperature of $25^{\circ} \pm 0.01^{\circ}C$; the magnitude of the variation of the individual calibrations was less than 0.004 cm^{-3}. The volumes of the respective bulbs for each apparatus are recorded in Table 3.2.

The "Adsorption"Manometer

The adsorption manometer was constructed from high precision bore glass tubing, supplied by Jencons Scientific Ltd. The internal diameter of the manometer for the L.H.A. was 1.0 cm, whilst that for the R.H.A. was 0.5cm; the bore tolerances were each $\pm$ 0.001 cm. The left hand limb of each manometer was machine-calibrated, and scaled in divisions of 0.1 cm^3 for the L.H.A. and 0.05 cm^3 for the R.H.A the zero graduation was placed at the top of the limb and the numerical markings engraved in an inverted position, such that the gaseous volume reading could be directly observed through the telescope of the cathetometer (simultaneously

TABLE 3.2

Gas Burette Bulb Volumes at 25.0°C

BULB No	L.H.A. (cm^3)	R.H.A. (cm^3)
1	20.17	15.95
2	20.70	13.10
3	20.71	10.34
4	19.71	8.07
5	19.84	5.94
6	21.25	3.82
7	20.91	13.93
8	16.54	11.08
9	13.48	7.85
10	13.21	6.03
11	10.89	3.94
12	9.95	2.02

L.H.A. = Left Hand Apparatus

R.H.A. = Right Hand Apparatus

with the height of the mercury column). The calculated machine error in the volume of the left hand limb of each manometer was $\pm$ 0.2% for the L.H.A. and $\pm$ 0.4% for the R.H.A. The manometer was carefully welded into position on the apparatus, such that the dead space volume immediately above the zero graduation of the left hand limb was as small as possible without damaging the calibrated section.

Dead Space Volumes, V_a, V_b and V_c

The assembled apparatuses were thoroughly outgassed (to a pressure of less than 10^{-5} torr) over a period of several weeks, before in situ calibration measurements were made. Where possible, sections of the systems were 'baked' at about 250°C during the outgassing process by means of an Electrothermal heating tape wound around the glassware. However, the operational areas of the mercury manometers (M1 - M4 in Fig. 3.4) were not raised above ambient temperature. The Viton A diaphragms for the greaseless stopcocks were outgassed at 250°C over a period of four days, prior to insertion into the barrels of the stopcocks on the assembled apparatuses: Viton A is the tradename of a fluorocarbon rubber. Triple-distilled mercury was placed in each of the mercury reservoirs upon termination of the outgassing period.

The argon and nitrogen reservoirs were outgassed to a pressure of about 10^{-5} torr before being filled, to a pressure of one atmosphere, with pure argon (99.995% purity) and 'white spot' nitrogen (99.9% purity) respectively. The reservoir-filling system was designed to allow all lines (including the cold trap) leading to the regulator of the gas cylinder, to be outgassed to a pressure of about 10^{-2} torr. The gas was slowly passed through a cold trap immersed in liquid nitrogen to remove residual impurities, e.g. carbon dioxide, water and oxygen. Before the

gas was actually collected in the appropriate reservoir, the system was flushed with gas (at a pressure of about 20 torr) over a period of about 30 minutes. The manometer, M4 in Fig. 3.4, monitored the residual pressure in the gas reservoirs during operation of the apparatus, as well as serving as a safety valve.

The component sections, V_a, V_b and V_c respectively, of the dead space volume are shown in Fig. 3.5. The dead space volume, V_a, is bounded by stopcock 'A' (in the closed position), stopcock 'B' (in the closed position), the transducer 'F', the upper fiducial marks of the gas burette (i.e. Nos. 6 and 12 respectively) and the zero graduation of the adsorption manometer, M1: this volume is shown enclosed by broken lines in Fig. 3.5. The dead space volume, V_b, is the volume enclosed by stopcock 'A' (in the open position) and the datum line 'L' on the sample bulb. V_c is the volume of the sample bulb below the datum line 'L', i.e. the volume of the sample bulb below the surface of the liquid nitrogen in the cryostat bath. The datum line on the sample bulb is assumed to be the arbitrary point at which there is a sharp transition between the temperature of the refrigerant and the ambient temperature. Such an assumption is necessary in order to apply a 'non-ideality' correction to the volume of gas contained below the level of the refrigerant. In practice, however, a temperature gradient will exist along this region of the sample bulb; by maintaining the refrigerant level at the datum line for both the calibration and the test runs, the error arising from this assumption is negligible.

It is important to note that the operation of the type of greaseless stopcock employed in the present apparatuses results in a volume change within the barrel of the stopcock. Normally, such an effect is of no significance, but for stopcocks 'A' and 'B' in the dead space region the

consequences of the volume change must be taken into account. The volume change occurs only within the barrel of the stopcock; where the raised centre of the diaphragm seats on the bore of the opposite limb of the stopcock, there is no measurable volume change with the limb during normal operation of the stopcock. For the stopcocks employed in the adsorption region of each apparatus (i.e. stopcocks 'A', 'B', 'C', 'D' and 'E' respectively, in Fig. 3.2), the volume change occurring between the extreme limits of movement of the diaphragm was about 0.45 cm^3. In practice, the diaphragm was always manipulated well within the extreme positions and the corresponding volume change was, therefore, much less.

It is obvious, therefore, that each greaseless stopcock may be positioned in one of two opposite directions. During the assembly of the apparatuses, the stopcocks were positioned such that the barrel-limb was joined to the part of the system where the undesirable features of the stopcock would have the least effect. In addition to the volume change, the barrel of the stopcock is also the side with the greatest potential leak risk. The limb joined to the bore of the stopcock was designated the 'safe-side' and is represented by a small arrow in the symbol for the stopcock in Fig. 3.5.

The manipulation of stopcock 'A' (the sample stopcock) was particularly critical in respect of the volume change within the barrel: the diaphragm was always moved through the same distance for successive operations in order to ensure that the dead space volume, V_b, remained constant.

The programme for the studies of argon and nitrogen adsorption on chromia and silica samples respectively, included the in situ outgassing of the sample at temperatures of up to 1100°C. The sample bulb, shown in Fig. 3.2, was therefore fabricated from silica glass, and included a

condenser-type jacket to cool the neck of the bulb (by water circulation) during the high temperature outgassing process. The empty silica glass bulb was necessarily subjected to the maximum temperature outgassing conditions (1100°C for 16 hours on the L.H.A.) prior to calibration of the dead space volume. The pyrex glass bulb (without condenser), for use on the L.H.A. at outgassing temperatures of up to 450°C, was similarly treated prior to calibration.

The calibrations were carried out by admitting a charge of nitrogen to the adsorption region and then measuring the pressure as the gas was compressed by either (a) raising the mercury in the gas burette bulbs to successive fiducial marks, and checking by emptying the bulbs in succession, or (b) maintaining the mercury in the gas burette at the upper fiducial marks, and compressing the gas by progressively raising the mercury in the adsorption manometer. Both methods were adopted, using several charges of nitrogen, such that the full operational pressure range was covered in detail. The total dead space volume, V_t (i.e. $V_a + V_b + V_c$), was determined with stopcock 'A' in the open position; V_c was also determined with stopcock 'A' open, but with the sample bulb immersed (to the datum line) in liquid nitrogen. V_a was determined with stopcock 'A' closed, whilst V_b was determined by difference.

Dead Space Volumes, V_a and V_t:

It has been shown[21] that under the conditions employed for the determination of V_a and V_t, nitrogen does not deviate to any significant extent from ideal behaviour; equation (3.1), based on Boyle's Law, was therefore applied to calculate the dead space volumes, V_a and V_t:

$$V_a \text{ (or } V_t) = \frac{T}{P} \cdot \frac{V_o \times 76}{273.16} - V_g \qquad (3.1)$$

where V_a (or V_t) = the dead space volume(in cm^3)

T = the temperature of the measurement (in ^oK)

P = the measured pressure (in cm of mercury)

V_o = the volume of the charge admitted, which is a constant for a series of compression readings

V_g = the combined volume of the gas burette bulbs, and the left hand limb of the adsorption manometer, not filled with mercury.

From equation (3.1), it is clear that a plot of V_g against T/P should be a straight line with a negative intercept equal to the dead space volume, V_a or V_t. For each of the determinations, a satisfactory straight line plot was obtained; the least squares method was used to evaluate the intercept. The various determinations for each apparatus are summarised in Table 3.3

Dead Space Volume, V_c:

In order to calculate the dead space volume, V_c, it was necessary to apply a non-ideality correction factor to the volume of nitrogen contained below the level of the refrigerant. Madeley[18] has shown that V_c may be expressed by an equation of the form:

$$V_c = \frac{\left[P_2 (V_t + V_{g2}) - P_1 (V_t + V_{g1})\right] 77.3}{T(P_1' - P_2') + 77.3 (P_2 - P_1)} \qquad (3.2)$$

where P_1 and P_2 are the first and second pressure measurements respectively, of a pair of compression readings (in cm of mercury).

P_1' and P_2' are the values of P_1 and P_2 respectively, corrected for non-ideality.

V_{g_1} and V_{g_2} are the first and second gas burette volumes respectively, of a pair of compression readings (in cm^3).

V_t is the total dead space volume, as given by equation (3.1).

T is the temperature of the measurement (in ^oK).

The non-ideality correction factor, α, for nitrogen at 77.3^oK, was applied in the form:

$$P' = P + \alpha P^2 \qquad (3.3)$$

where, for a pressure measurement expressed in cm of mercury, $\alpha = 6.58 \times 10^{-4}$; i.e. the value reported by Emmett and Brunauer,[22] and confirmed by Harris.[17]

The determinations of V_c for each apparatus are summarised in Table 3.3. From the respective mean values of V_a, V_c and V_t, the value of V_b was obtained by difference.

The variable dead space volumes (i.e. V_a <u>plus</u> the volume of the gas burette bulbs <u>not</u> filled with mercury), for each apparatus are shown in Tables 3.4 and 3.5 respectively. For any combination of gas burette bulbs filled with mercury, the residual dead space volume may be obtained by reference to the appropriate table. The fiducial mark numbers in the left hand column of each table correspond to the first set of gas burette bulbs (i.e. Nos. 1 - 6),whilst those across the top of the table correspond to the second set of bulbs (i.e. Nos. 7 - 12). The fiducial marks, and the corresponding gas burette bulbs, are shown in Fig. 3.5.

TABLE 3.3

Summary of Dead Space Volume Determinations

LEFT HAND APPARATUS SAMPLE BULB B10				RIGHT HAND APPARATUS SAMPLE BULB B1		
V_a	V_c	V_t		V_a	V_c	V_t
7.73	2.96	17.01		6.54	2.87	16.42
7.89	3.00	16.88		6.59	2.84	16.74
7.84	2.97	16.96		6.58	2.81	16.70
7.75	2.96	16.76		6.49	2.89	16.48
7.82	3.02	17.09		6.50	2.86	16.57
7.86	2.99	17.10		6.55	2.83	16.61
7.78	3.04	16.89		6.48	2.82	16.68
7.74	3.04	16.82		6.51	2.84	16.74
7.90	2.97	17.06		6.53	2.85	16.54
7.91	3.03	16.93		6.52	2.88	16.51
Mean	7.82	3.00	16.95	6.53	2.85	16.60

$V_t = V_a + V_b + V_c$; volumes are expressed in cm^3.

L.H.A., with Sample Bulb B10:

$V_a = 7.82\ cm^3$

$V_b = 6.13\ cm^3$

$V_c = 3.00\ cm^3$

R.H.A., with Sample Bulb B1:

$V_a = 6.53\ cm^3$

$V_b = 7.22\ cm^3$

$V_c = 2.85\ cm^3$

TABLE 3.4

LEFT HAND VOLUMETRIC APPARATUS

Dead Space Volumes @ 25.0°C (in cm^3)

Fiducial Mark No.	0	7	8	9	10	11	12
0	215.18	194.27	177.73	164.25	151.04	140.15	130.20
1	195.01	174.10	157.56	144.08	130.87	119.98	110.03
2	174.31	153.40	136.86	123.38	110.17	99.28	89.33
3	153.60	132.69	116.15	102.67	89.46	78.57	68.62
4	133.89	112.98	96.44	82.96	69.75	58.86	48.91
5	114.05	93.14	76.60	63.12	49.91	39.02	29.07
6	92.80	71.89	55.35	41.87	28.66	17.77	7.82

TABLE 3.5

RIGHT HAND VOLUMETRIC APPARATUS

Dead Space Volumes @ 25.0°C (in cm^3)

Fiducial Mark No.	0	7	8	9	10	11	12
0	108.60	94.67	83.59	75.74	69.71	65.77	63.75
1	92.65	78.72	67.64	59.79	53.76	49.82	47.80
2	79.55	65.62	54.54	46.69	40.66	36.72	34.70
3	69.21	55.28	44.20	36.35	30.32	26.38	24.36
4	61.14	47.21	36.13	28.28	22.25	18.31	16.29
5	55.20	41.27	30.19	22.34	16.31	12.37	10.35
6	51.38	37.45	26.37	18.52	12.49	8.55	6.53

Under experimental conditions, V_b was decreased by an amount equal to the volume (V_b^1) of the glass wool plug inserted in the neck of the sample bulb; similarly, V_c was decreased by an amount equal to the volume (V_c^1) of the sample under investigation. These decreases in the dead space volumes were taken into account during the derivation of the isotherm data. Values of V_b^1 and V_c^1 were estimated from the outgassed weight and density of the plug and sample respectively. Earlier workers have shown[11,17,18,20] that an error of less than 1% in the surface area is incurred by assuming a mean value for the density of the sample over a range of outgassing temperatures. Thus, since the majority of the present work was comparative, rather than absolute, in nature, it was not considered necessary to carry out an actual measurement of V_c^1 (using helium) but to assume a constant value for the density of the sample: e.g. chromia, 6.0 g cm^{-3}; silica (Fransil), 2.5 g cm^{-3}; silica (TK 800), 2.1 g cm^{-3}.

Absolute Nature of the Calibrations

The validity of the calibrations for each apparatus was checked by determining both the nitrogen and argon isotherms on samples of Fransil and TK 800-II respectively. The values of the nitrogen and argon BET surface areas so obtained are shown in Table 3.6, together with the published[9,23,24] values for Fransil and TK 800. Following the recent recommendation of Sing,[25] the BET C-constant values are recorded alongside the corresponding BET surface area values. It is evident from Table 3.6, that the respective surface area values obtained using each apparatus are in good agreement for a particular adsorbent; furthermore, the absolute nature of the calibrations is confirmed by the agreement of the experimental data with those reported for Fransil and TK 800.

TABLE 3.6

COMPARISON OF PUBLISHED AND EXPERIMENTAL CALIBRATION SURFACE AREAS

	FRANSIL				TK 800			
	NITROGEN		ARGON		NITROGEN		ARGON	
	C	S_{BET}^{N}	C	S_{BET}^{Ar}	C	S_{BET}^{N}	C	S_{BET}^{Ar}
Published Data[a,b]	-	38.4- 38.7	-	38.7 38.8	-	163- 166	-	161- 168
Found[b]								
L.H.A.	131	38.6	30	39.0	99	164.1	33	162.6
R.H.A.	138	38.7	37	39.2	110	162.9	37	162.1

a see reference Nos. 9, 23 and 24.

b Surface area expressed in m^2g^{-1}; taking 16.2 $Å^2$ and 18.2 $Å^2$ as the apparent cross sectional areas of nitrogen and argon, respectively. The silica samples were outgassed at 140°C over a period of 16 hours.

Fig. 3.6. clearly demonstrates the excellent agreement between the experimental isotherm data obtained in the present work, and the isotherm data previously reported[9] for a particular standard adsorbent. The isotherm obtained using the L.H.A. for nitrogen adsorption on TK 800-II (outgassed at 140°C) has been taken as an example: the adsorption points are shown superimposed on the isotherm reported by Turk (determined using another volumetric apparatus), for a sample of TK 800-II taken from the same bulk batch. For the sake of clarity, desorption points have not been included in Fig. 3.6, but each isotherm was almost totally reversible and characteristic of a non-porous adsorbent. The complete isotherm data for Fig. 3.6 are recorded in Appendix 7.

3.13 The Pressure-Sensitive Transducers

A pressure-sensitive transducer converts fluid pressures experienced by the diaphragm of the instrument, to a controlled strain in the strain-gauge windings that form an integral part of an excited Wheatstone bridge in which all four arms are active. A rod welded to the centre of the force-summing diaphragm transmits its displacement to a spring element. The resulting flexure of the spring tilts the sapphire posts on which the strain gauge windings are mounted, increasing the strain and hence the resistance in the two windings at one end of the posts, and decreasing the strain and resistance in the windings at the other end. The thermal and mechanical symmetry of the unit ensure that the output is a linear function of the pressure applied to the diaphragm. A diagram of the pressure-sensing element is shown in Fig. 3.7.

Each volumetric apparatus was equipped with a Bell and Howell pressure-sensitive transducer (type 4-366) with an operation range of 0.1 - 776 torr (absolute). The resolution of this transducer is infinite,

but in practice, the ultimate sensitivity of the complete system is governed by the resolution of the potentiometric device that is employed to measure the output of the transducer. In the present work, an API Instruments Co., (Chesterland, Ohio, USA) Model 4304, digital voltmeter was used to measure the output voltage of the transducer (full range output of the transducer was about 40 mV). The resolution of the digital voltmeter (DVM) was $\pm$ 0.005 mV; in terms of absolute pressure, the sensitivity of the complete system was about $\pm$ 0.1 torr, i.e., an order of magnitude lower than a corresponding manometer measurement.

The excitation potential for the transducer (10 V $\pm$ 0.02%) was provided by a purpose built power supply, the circuit diagram of which is shown in Fig. 3.8. The zero and span of the transducer itself were set to within very fine tolerances at the time of manufacture; adjustments in the electrical zero were therefore made in an external circuit, i.e. by the potentiometer, P1, in Fig. 3.8. The zero and span of the DVM were adjustable by controls on the instrument; a high quality, low thermal e.m.f., multiway switch was incorporated into the circuit, such that the output signal of the transducer could be short-circuited in order to check the zero setting of the DVM. The multiway switch also served to share a single DVM between the two transducers.

It is worth noting that a negligible change in the dead space volume is incurred with movement of the transducer diaphragm in response to pressure changes within the system. For example, if the least-favourable case is considered, namely for that of the minimum dead space volume, V_a, the <u>total</u> variation in the volume resulting from movement of the diaphragm over the full operational range of the transducer (0.1 - 776 torr) was less than 0.009%.

Calibration of the Transducers

Each unit of the complete pressure-measuring system was thoroughly tested for electrical stability, and reproducibility, prior to the calibration measurements. These tests were made over a period of several weeks, and showed that the respective stabilities of the power supply, transducer and DVM were entirely satisfactory. The output of the transducers employed in the present work was relative to absolute pressure and was, therefore, unaffected by variations in the ambient pressure.

The calibration curve was constructed as a plot of the transducer's open circuit output voltage as a function of pressure (measured by the mercury manometer, M1 in Fig. 3.4). Measurements were made for both increasing and decreasing pressure excursions over the full range output of the transducer. The calibration plots are shown in Figs. 3.9 and 3.10 respectively; for the sake of clarity, only a small proportion of the calibration points have been reproduced in the figures. Several different pressure excursions were made to confirm the reproducibility of the transducer's response. The slope of each plot, and hence the transducer calibration factor, was computed using the method of least mean squares to analyse about 120 calibration points for each transducer: the calibration factors, expressed as cm of mercury per mV, are recorded in Table. 3.7.

TABLE 3.7

TRANSDUCER CALIBRATION FACTORS

L.H.A. TRANSDUCER		R.H.A. TRANSDUCER	
Hg Temp °C	Factor cm Hg/mV	Hg Temp °C	Factor cm Hg/mV
26.7	2.081	24.6	1.921
0	2.071	0	1.913

Each calibration factor was corrected for the density of mercury at the mean temperature of the calibration measurements, thereby allowing the factor to be expressed in terms of cm of mercury at 0°C. The "corrected" factor was used in the computer program written for the analysis of volumetric adsorption data derived from transducer-pressure measurements (Appendix 1). The "original" factor, expressed in terms of cm of mercury at the mean temperature of the calibration measurements, was used to formulate various conversion tables of relative pressure, manometric pressure and transducer pressure; manipulation of the volumetric apparatus was optimised during the determination of an isotherm by reference to the conversion tables. Examples of the conversion tables are recorded in Appendix 2.

It is evident from Figures 3.9 and 3.10 that hysteresis and non-linearity effects respectively, of each transducer are negligible. Furthermore, the calibration measurements were made using both nitrogen and argon respectively: no significant difference in the calibration factors for each gas was observed.

Comparison of Manometric and Transducer Pressure Data

Isotherm data were always computed using manometric pressure measurements; the digital display of the transducer pressure provided a very useful means of assessing the moment at which the adsorption system had attained an "equilibrium pressure". However, by way of an example of the possible applications of a transducer in a volumetric apparatus, the isotherm data for nitrogen adsorption on a standard silica sample (TK 800 -III) were also computed on the basis of transducer pressure measurements: the comparison of the manometric and transducer pressure data respectively, is shown in Fig. 3.11. The transducer pressure data lead to a BET surface area value which is lower by less than 4% of the corresponding area derived from the manometric data.

It is worth noting that the application of a single wide-range transducer to an accumulative volumetric technique, is the least-favourable example of the use of a transducer in the present type of adsorption experiments. Nevertheless, the present work has shown that such a transducer may be usefully employed in a volumetric apparatus for the routine study of nitrogen adsorption, especially if the studies are required to be made in the absence of mercury vapour.

3.14 The Oxygen Vapour Pressure Thermometer

The temperature of the liquid nitrogen in the cryostat bath surrounding the sample bulb, and therefore the saturated vapour pressure of the adsorbate (Po), was measured with a conventional oxygen vapour pressure thermometer. The thermometer bulb was located as closely as possible to the sample bulb, leaving just sufficient space to slide an outgassing furnace into position around the sample bulb. Two thermometers of different lengths were necessary for the L.H.A. (shown in Fig. 3.2), for use with the low and high temperature sample bulbs respectively. Each thermometer

contained 'grade X' oxygen (purity greater than 99.96%) at a pressure of about 700 torr, providing sufficient condensate at -196°C to register a reliable vapour pressure. The outgassed thermometers were filled with oxygen using a procedure very similar to that described by Payne.[20]

Plots of the saturated vapour pressure (SVP) of liquid oxygen against the SVP of liquid nitrogen[26] and solid argon[20] respectively, were constructed: the plots were used to evaluate the SVP of the adsorbate from the readings of the appropriate oxygen vapour pressure thermometer, taken at frequent intervals during the course of an adsorption isotherm determination. Equivalent SVP data (taken from the SVP plots) for oxygen, argon and nitrogen respectively, are recorded in Table 3.8.

TABLE 3.8

Equivalent Values of Saturated Vapour Pressure Data

SVP	(Expressed in torr)	
Oxygen	Argon	Nitrogen
151.0	191.0	740.8
152.0	192.5	744.8
153.0	194.1	748.8
154.0	195.7	752.8
155.0	197.3	756.8
156.0	198.9	760.8
157.0	200.5	764.8
158.0	202.1	768.7
159.0	203.7	772.7
160.0	205.3	776.7
161.0	206.9	780.6
162.0	208.4	784.6
163.0	210.0	788.5
164.0	211.6	792.4

3.15 Sample Outgassing Procedure

The chromium oxide samples were outgassed over a period of at least 15 hours at the desired temperature; the time of outgassing for the silica samples generally varied between 2 and 20 hours, according to the outgassing temperature. In all cases, samples were outgassed to a pressure of about 2×10^{-4} torr. The outgassing conditions for a particular sample are recorded in the notation for the sample specimen: for example, S2(25)20V was a sample of chromia gel S2 outgassed at 25°C over a period of 20 hours; similarly, CrO_2(100)17V was a sample of chromium dioxide outgassed at 100°C over a period of 17 hours. Unless otherwise stated, samples were outgassed in the presence of mercury vapour.

A typical arrangement for the outgassing of a sample is shown for the R.H.A. in Fig. 3.1. The temperature of the furnace was controlled (to better than $\pm$ 1% up to 1100°C) by a Linear Variable Programmer, with a potentiometric chart recorder placed in parallel with the thermocouple, thereby providing a permanent record of the outgassing conditions. An industrial air blower was employed to maintain the greased joint of the sample bulb at ambient temperature. When outgassing at temperatures in excess of about 400°C, using the L.H.A. in Fig. 3.1, additional cooling for the neck of the sample bulb was provided by a flow of water through the condenser jacket of the silica sample bulb.

3.16 Isotherm Determination

In the following outline of the procedure for making adsorption measurements, the stopcocks specifically referred to are those shown in Fig. 3.2, or alternatively, those depicted in the diagram in Fig. 3.4.

After outgassing the sample at the desired temperature, stopcock 'A' was closed and, where appropriate, the sample allowed to cool to

ambient temperature; with the exception of the main pumping system, all other stopcocks were also closed. The mercury in the gas burette bulbs was lowered to the zero fiducial marks. A controlled charge of nitrogen (or argon) was admitted, via stopcocks 'C' and 'B' respectively, to the dead space section; the pressure of the charge (optimised by reference to the conversion tables discussed in Section 3.13) was measured using the adsorption manometer, M1, and also, the transducer 'F'. The temperature of the manometric measurement was noted from the mercury thermometer ($\pm$ 0.1°C). The gas charge was then shared with the sample bulb section, by opening stopcock 'A', and the liquid nitrogen cryostat bath then raised into position around the sample bulb. This procedure differs from those previously described[9,11,20] for low temperature gas adsorption (where the cryostat bath was raised into position before admittance of the adsorptive charge), and was introduced to considerably reduce the risk of "gettering" effects by the reactive samples. After the system had attained a state of apparent equilibrium, the pressure and temperature of the adsorptive were again recorded (generally with stopcock 'A' open). Further points on the isotherm were obtained by progressively raising the mercury in the burette bulbs to successive fiducial marks, and, as necessary, admitting a further charge of the adsorptive.

Desorption points were obtained by either lowering the mercury in the gas burette bulbs, or, as necessary, removing a proportion of the adsorptive from the dead space section (stopcock 'A' closed) via stopcock 'B'.

Equilibration times generally varied between 15 minutes and 2 hours, depending on the nature of the adsorbent and the magnitude of the equilibrium pressure. The majority of the isotherms were determined in detail, necessitating the recording of the adsorption points over a period

of 16 hours on one day, whilst the desorption points were recorded over a similar period on the following day: the readings were held in abeyance for about 8 hours, with a constant level device monitoring, and maintaining, the level of liquid nitrogen in the cryostat bath.

The arrangement for the simple constant level device employed in the present work, based on a gas thermometer connected to a mercury cut-off, is shown in Fig. 3.3. The device was used both for the dead space calibrations and throughout the determination of the isotherms, and was capable of controlling the level of liquid nitrogen in the cryostat bath to within about ± 1 mm of the sample bulb datum line. A similar constant level device has been described in detail by Feld and Klein.[27]

The experimental adsorption data were processed using an Elliot 803 computer. The programs, for manometric and transducer pressure measurements respectively, were written in Autocode language and are recorded in Appendix 1. The following quantities were computed, using the <u>outgassed</u> sample weight:

(a) the relative pressure, P/Po

(b) The amount of vapour adsorbed at the equilibrium pressure, P, expressed in cm^3 (STP) g^{-1}, and

(c) the 'BET factor', P/V(Po-P).

The experimental data for nitrogen and argon adsorption on chromium oxides and silicas respectively, are recorded in Appendices 3,4,7 and 8.

D. <u>WATER AND MERCURY VAPOUR ADSORPTION</u>

Two gravimetric apparatuses were employed in the present work to study the adsorption of water and mercury vapour respectively, on chromium oxides, and of water vapour on silicas. A quartz-spring balance of the McBain-Bakr type[28] was designed and built by the author, and used for the majority of the gravimetric studies. A Gulbransen manual microbalance,[29]

built by Payne,[20] was employed for a number of the mercury vapour adsorption studies and for the study of water vapour adsorption on chromium oxy-hydroxide.

THE SPRING BALANCE

3.17 Design and Technique

General views of the spring balance are shown in Fig. 3.12 (high temperature sample outgassing arrangement) and Fig. 3.13 (adsorption measurement arrangement) respectively: the general arrangement of the balance is depicted in diagrammatic form in Fig. 3.16. Essentially the spring balance comprised a tapered helical quartz spring (sensitivity about 100 cm g^{-1}, maximum load of 1g) suspended inside a water jacket maintained at a temperature of $26.5^{o} \pm 0.05^{o}C$ by water pumped from a B.T.L. 'Circon' thermostatic bath. A silica glass bucket (weight about 0.2g), containing the sample, was attached to the spring by means of a thin silica glass sliver: silica wool was placed in the narrow neck of the bucket to prevent loss of the sample by "spurting" during the outgassing process. The sliver, bucket and sample are just discernible in Fig. 3.14. The sample bucket was enclosed in a separate water jacket maintained at $25^{o} \pm 0.01^{o}C$ by water pumped from a Townson and Mercer thermostatic bath. The upper and lower joints on the balance "case" were each made by means of a clamped 'Rotulex' spherical greaseless joint, with a Viton A 'O'-ring employed as the seal. In order to permit high temperature outgassing of the sample (up to $1100^{o}C$), the sample section of the balance case was fabricated from transparent 'Vitreosil' silica galss.

The total weight of the bucket, plug and sliver suspension was about 0.4g, thereby allowing sample weights of about 0.3 - 0.5g to be used, depending on the expected uptake of water (or mercury) vapour. Occasionally, for silica samples of low bulk-density, additional silica glass weights

were hung on the bucket suspension in order to restrict the overall movement of the bucket to the lower region of the sample jacket. By arranging that the bucket was always as near as possible to the base of the sample jacket at the SVP of water vapour, thermal transpiration effects[30] were reduced to a minimum.

The balance case was connected, via greaseless stopcocks, to (a) a vacuum pumping system which was protected against failure of the cooling water supply etc., in a manner similar to that described in Section 3.11, (b) a pressure-measurement system comprising a mercury manometer, a silicone oil manometer (Edwards MS 704 silicone fluid), and a pressure-sensitive transducer, and (c) a water storage reservoir, containing triple distilled water, which was outgassed for about 10 minutes prior to each experiment (using a freeze-thaw cyclic process).

The vacuum pumping system comprised both oil and mercury vapour diffusion pumps respectively, arranged in parallel with a common rotary pump such that each could be selected at will. A polyphenyl ether (Edwards 'Santovac 5') was employed as the fluid for the oil diffusion pump, in preference to a silicone fluid. The pressure-measurement system allowed a particular manometer, or the transducer, to be employed for an experiment whilst the remainder of the system was isolated from the balance case; each manometer was used in conjunction with the corresponding diffusion pump.

Silicone oil vapour is known[31,32] to reduce certain chromium oxide surfaces; furthermore, it may even result in the deposition of silica on an active oxide surface, e.g. chromia or titania.[33] In addition, the present work has revealed that certain chromium oxides have a high affinity for mercury vapour[34,35] (Chapter 5). Ideally, therefore, silicone oil (or mercury) should be excluded from manometric systems employed for the

study of chromium oxides. In practice, however, there are very few alternative low vapour pressure fluids, possessing a greater chemical inertness, which also satisfy the requirements of a manometric fluid: for example, the viscosity of 'Santovac 5' at 25°C is greater than 500 cSt, consequently resulting in intolerable "drainage times". The flexibility of the pressure-measurement system in the present apparatus permitted a study of mercury vapour adsorption to be made. The study of water vapour adsorption per se was made in the strict absence of either silicone oil vapour or mercury vapour: pressure measurements were made using the sensitive transducer.

3.18 Calibration of the Spring Balance

The quartz spring was calibrated, at a temperature of 26.5° ± 0.05°C, against precision milligramme weights (conforming to NPL 'grade A' specifications) with the balance case under high vacuum (10^{-5} torr). The calibration plot is shown in Fig. 3.18: the extension of the spring was both elastic, and linear, with load. All spring extension measurements were taken with a cathetometer (± 0.001 cm) and were referred to a fixed point, in the form of very fine cross-wires, on the balance case.

The silicone oil manometer (M2 in Fig. 3.16) was calibrated against the precision wide-bore mercury manometer (M1 in Fig. 3.16): the calibration factor, expressed in terms of cm of mercury (at 0°C) per cm of silicone oil (at the temperature of the calibration), was written into the appropriate computer program for manometric pressure measurements.

A Bell and Howell pressure-sensitive transducer (type 4-353) with an operational range of 0.01 - 26 torr (absolute), was employed in the present apparatus. The principle of operation and calibration etc., of this transducer is very similar to that described for the type 4-366 transducer

(Section 3.13). However, in terms of absolute pressure, the sensitivity of the type 4-353 transducer system for water adsorption was about $\pm 6.2 \times 10^{-3}$ torr, i.e. about 16 times greater than the sensitivity of the type 4-366 system for nitrogen adsorption. Thus, the tranducer pressure measurements on the spring balance were more sensitive than mercury-manometric measurements and could therefore be confidently employed for isotherm determinations. The calibration plot for the transducer is shown in Fig. 3.19; the calibration factor, expressed in terms of cm of mercury (at $0^{o}C$) per mV, was written into the computer program for transducer pressure measurements (Appendix 1). A conversion table of relative pressure, manometric pressure and transducer pressure respectively, was constructed to optimise the manipulation of the spring balance; the table is recorded in Appendix 2.

3.19 Sample Outgassing Procedure

A typical arrangement for the outgassing of a sample is shown in Fig. 3.12. The procedure was similar in many respects to that described for the volumetric apparatuses in Section 3.15. However, unless otherwise stated, samples were outgassed in the absence of either mercury or silicone oil vapour, generally to a pressure of about 5×10^{-5} torr. Helium ('grade X', purity greater than 99.9997%), at a pressure of about 2 torr, was generally admitted to the balance case during the cooling period following completion of the outgassing of chromium oxide samples; the sample was re-evacuated (at $25.0^{o}C$) immediately prior to the isotherm determinations.

3.20 Isotherm Determination

The uptake of water vapour was simply followed by measuring the extension of the spring with progressive increase of pressure.

Equilibration times were very dependent upon the nature of the adsorbents, generally varying between about 1 and 6 hours: in some cases, equilibration times were much longer and the isotherm points so recorded did not necessarily represent a state of true equilibrium.

A correction for the buoyancy effect[36] was incorporated into the computer program (Algol language) written for the processing of the experimental data, by application of the equation:

$$\delta w = \frac{Mv}{RT} \cdot P \qquad (3.4)$$

where δw = the upthrust on the load of the spring

M = the molecular weight of water

v = the volume of the load, i.e. the sum of the volumes of the bucket, plug, sample and adsorbate respectively

R = the gas constant

T = the temperature in ^{o}K

and P = the pressure of the water vapour.

The sorption of water vapour by the spring, bucket and plug respectively, was found to be negligible when determined in the absence of a sample.

The experimental data for water adsorption on chromium oxides and silicas, are recorded in Appendices 5 and 9 respectively: the experimental data for mercury vapour adsorption on chromium oxides are recorded in Appendix 6.

THE GULBRANSEN MICROBALANCE

Apart from a small number of the mercury vapour adsorption studies, the use of the Gulbransen microbalance was limited to a single experiment involving the study of water vapour adsorption on low-area chromium oxy-hydroxide. In the latter case, the advantage of the microbalance lay

in the fact that the sensitivity of the microbalance ($\pm$ 1 μg) was an order of magnitude greater than that of the spring balance.

The Gulbransen microbalance employed in the present work has been described in considerable detail by Payne[20] and will not, therefore, be discussed further here.

REFERENCES

1. R.L. Burwell, Jr., and H.S. Taylor, J. Amer. Chem. Soc., (1936) 58, 697.
2. R.L. Burwell, Jr., J. Amer. Chem. Soc., (1937) 59, 1609.
3. T. Gatowskaja and P. Wassiliew, Acta Physicochim., (1936) 4, 37; P. Wassiliew, T. Gatowskaja and A. Rabinowitsch, ibid., (1936) 4, 1.
4. Yu. M. Chernoberezhskii, S.N. Zubkova, S.D. Usanova and L.V. Afanaseva, Kolloid. Zh., (1965) 27,(5), 780.
5. G.C. Bye and G.T. Simpkin, Chem. and Ind., (1970) 532.
6. A.I. Vogel, "Macro and Semimicro Qualitative Inorganic Analysis", Longmans, 4th Edt., (1964) pages 318 and 363.
7. M.R. Harris and K.S.W. Sing, J. Appl. Chem., (1957) 7, 397.
8. L.J. Stryker, Personal Communication.
9. D.H. Turk, Ph.D. Thesis, Brunel University, (1972).
10. R. Wilson, SCI/IUPAC/NPL Surface Area Standards, National Physical Laboratory, England.
11. J.D. Carruthers, Ph.D. Thesis, Brunel University, (1968).
12. P. Debye and P. Scherrer, Physica, (1916) 17, 272.
13. C.B. Murphy, J.A. Hill and G.P. Schacher, Analyt. Chem., (1960) 32, 1374.
14. A.C. Zettlemoyer, G.J. Young, J.J. Chessick and F.H. Healey, J. Phys. Chem., (1953) 57, 649.
15. S.J. Gregg, S. Nashed and M.T. Malik, Powder Technology, (1973) 7, 15.
16. M.R. Harris and K.S.W. Sing, J. Appl. Chem., (1955) 5, 223.
17. M.R. Harris, Ph.D. Thesis, London University, (1957).
18. J.D. Madeley, Ph.D. Thesis, London University, (1957).
19. G.W.A. Newton, Res. Dip., Liverpool, (1962).
20. D.A. Payne, Ph.D. Thesis, Brunel University, (1970).
21. International Critical Tables, (1928) 3, pages 6, 8 and 18.

22. P.H. Emmett and S. Brunauer, J. Amer. Chem. Soc., (1937) 59, 1553.

23. M.R. Bhambhani, P.A. Cutting, K.S.W. Sing and D.H. Turk, J. Colloid Interface Sci., (1972) 38, 109.

24. D.A. Payne, K.S.W. Sing and D.H. Turk, J. Colloid Interface Sci., (1973) 43, 287.

25. K.S.W. Sing, Specialist Periodical Report, Colloid Science. Senior Reporter, D.H. Everett; The Chemical Society, London, (1973) 1, 1

26. A. Farkas and H.W. Melville, "Experimental Methods in Gas Reactions", Macmillan, London, (1939) 106.

27. M. Feld and F.S. Klein, J. Scientific Instruments, (1954) 31, 474.

28. J.W. McBain and A.M. Bakr, J. Amer. Chem. Soc., (1926) 48, 690.

29. E.A. Gulbransen, Rev. Sci. Instruments, (1944) 15, 201.

30. S.J. Gregg and K.S.W. Sing, "Adsorption, Surface Area and Porosity"; Academic Press, London, (1967) page 333.

31. P.B. Ayscough, C. Eden and H. Steiner, J. Catalysis, (1965) 4, 278.

32. C. Eden, H. Feilchenfeld and Y. Haas, J. Catalysis, (1967) 9, 367.

33. R.E. Day, Personal Communication.

34. F.S. Baker and K.S.W. Sing, Nature (Phys. Sci.), (1971) 229, 27.

35. M.A. Alario Franco, F.S. Baker and K.S.W. Sing, "Progress in Vacuum Microbalance Techniques", Eds. S.C. Bevan, S.J. Gregg and N.D. Parkyns; Heyden and Son Ltd., London, (1973) 2, 51.

36. Reference 30, page 337.

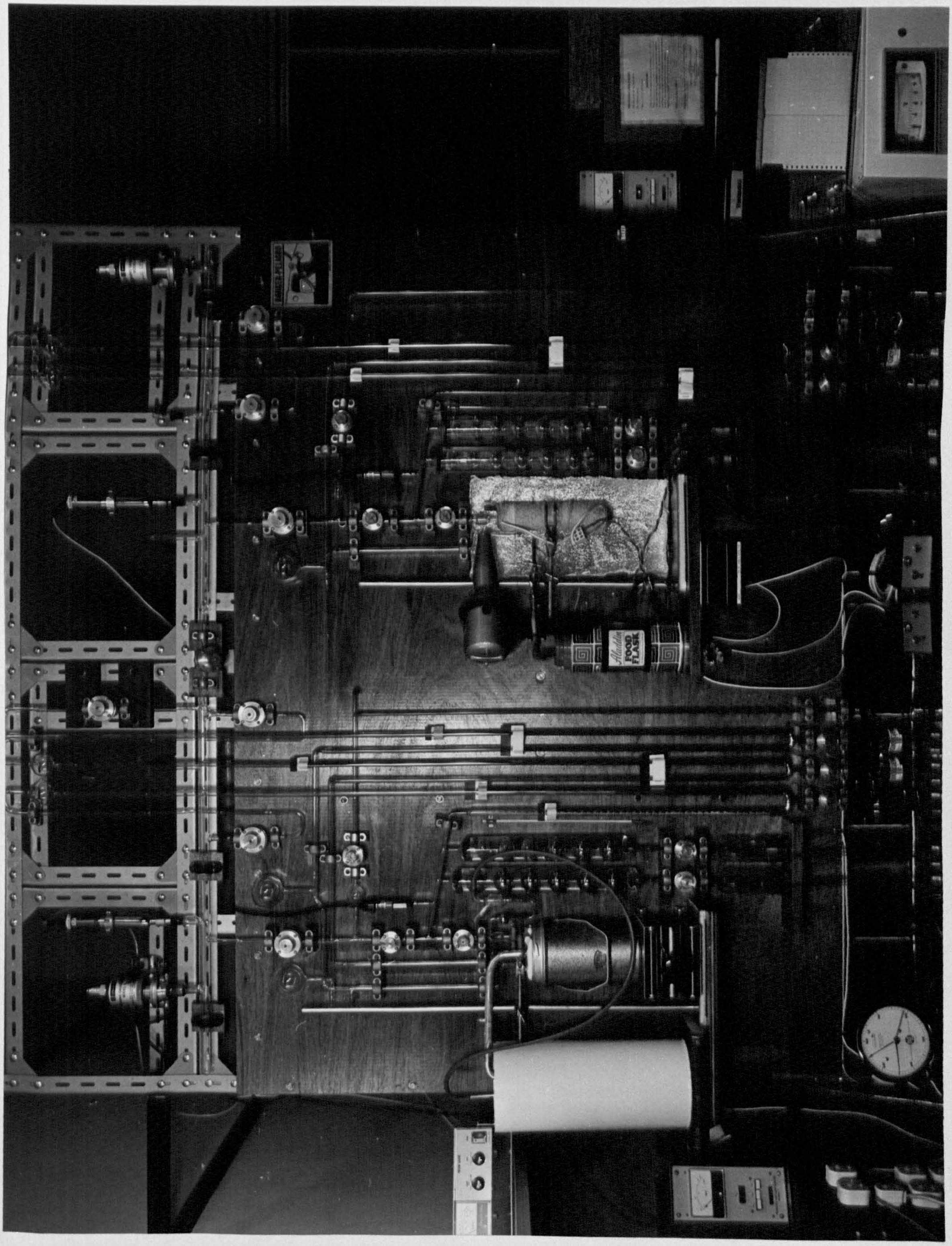

FIG 3.1

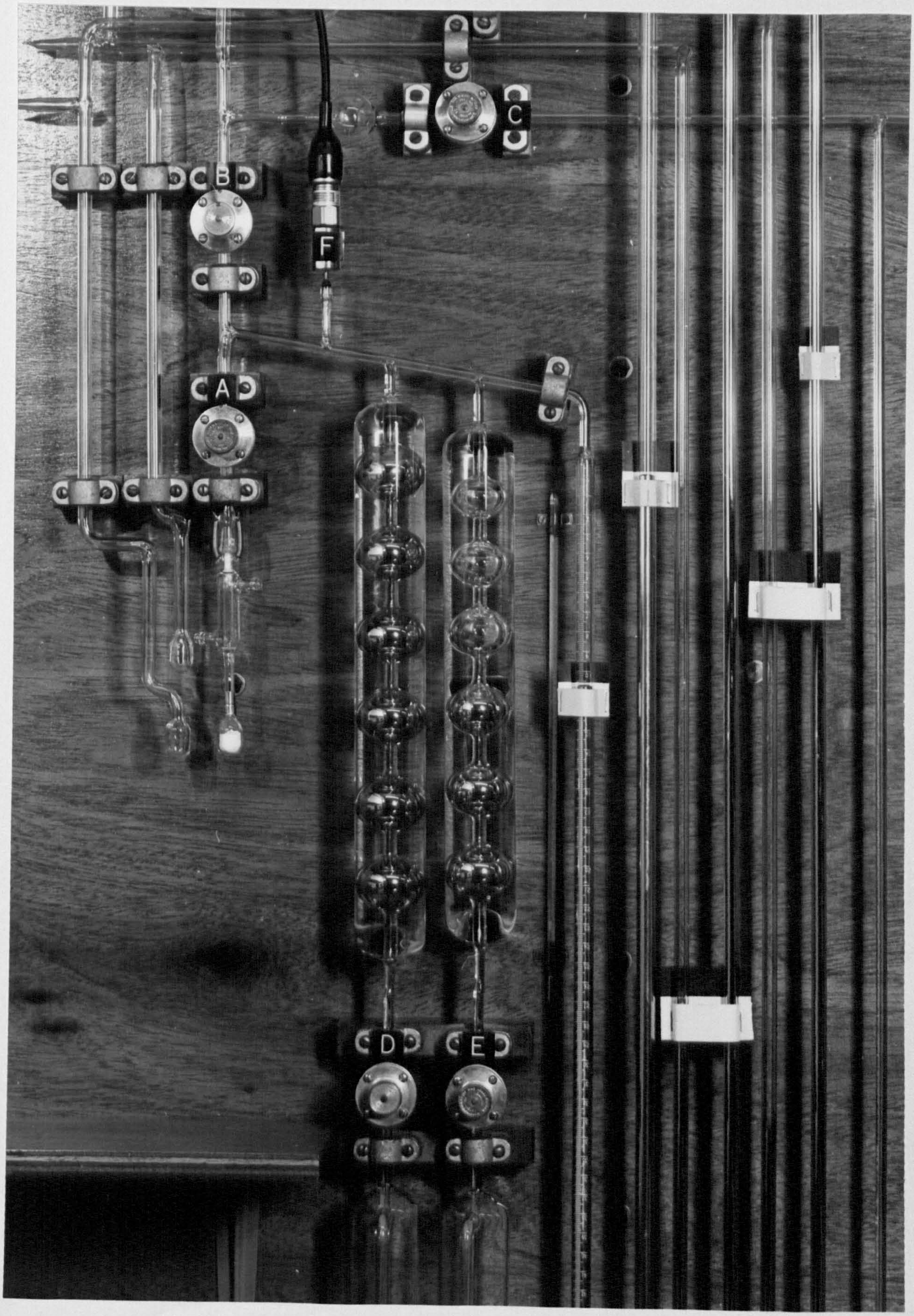

FIG 3.2

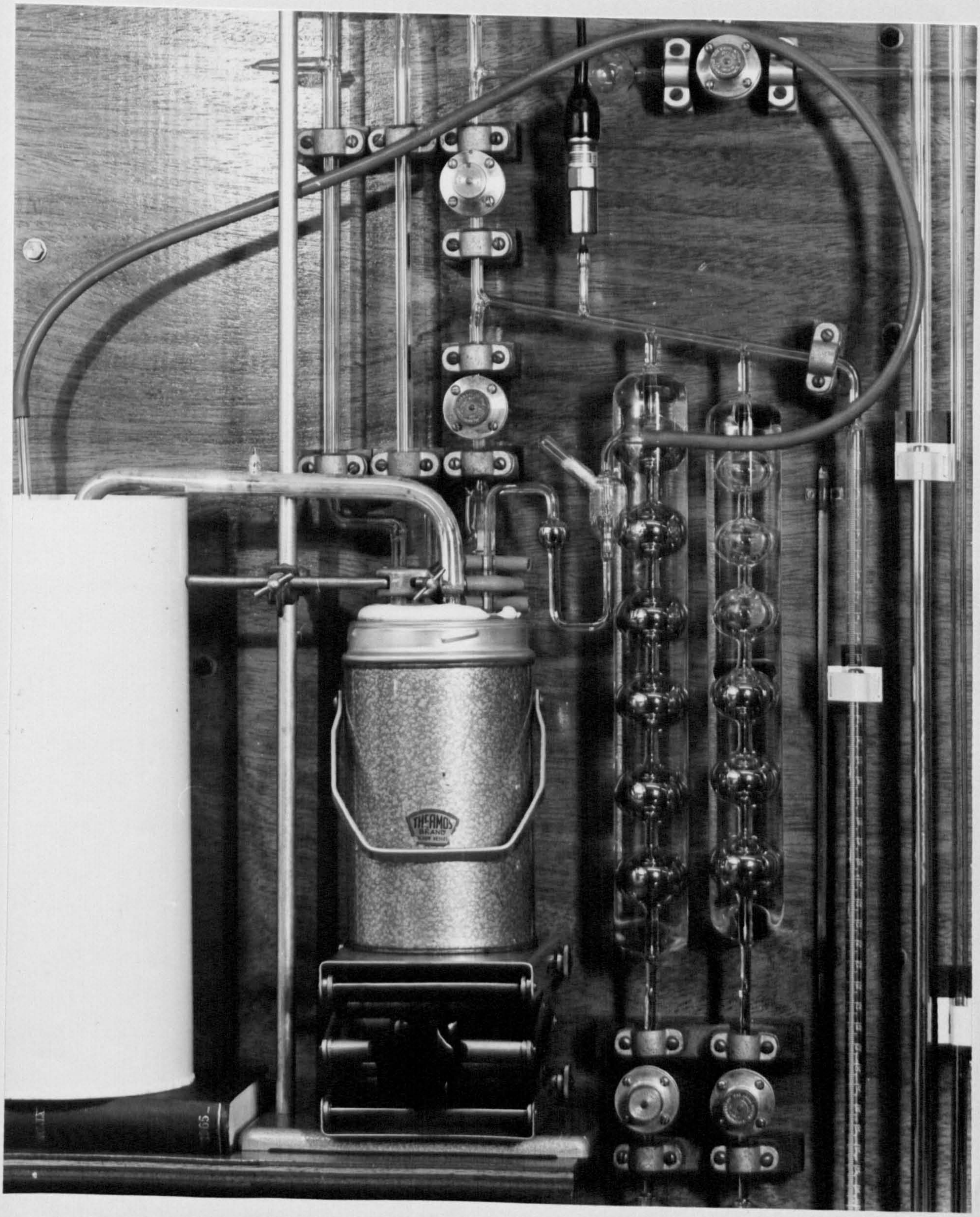

FIG 3.3

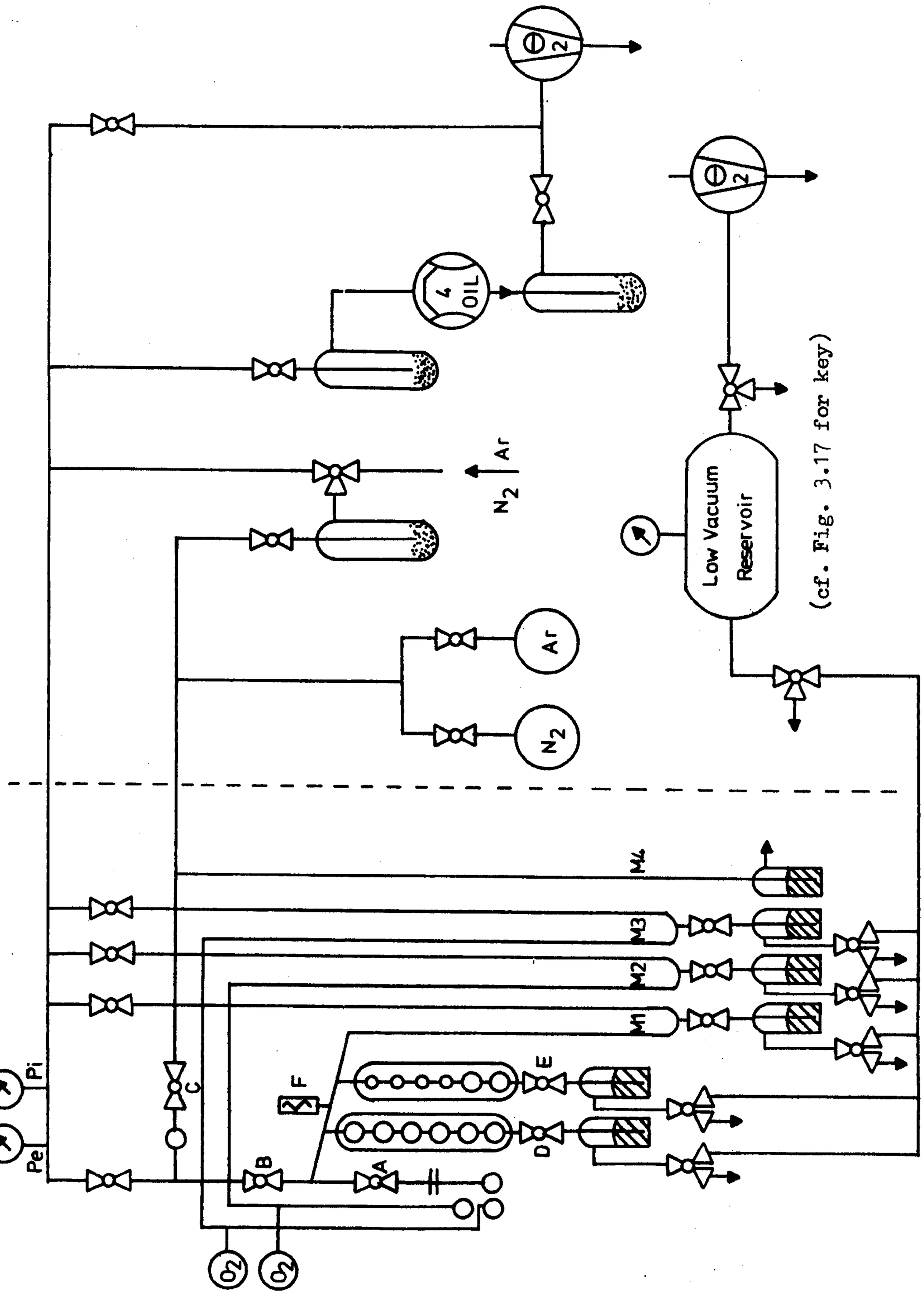

FIG 3.4 Layout of the Volumetric Apparatus (L.H.A.) for the Study of Nitrogen and Argon Adsorption

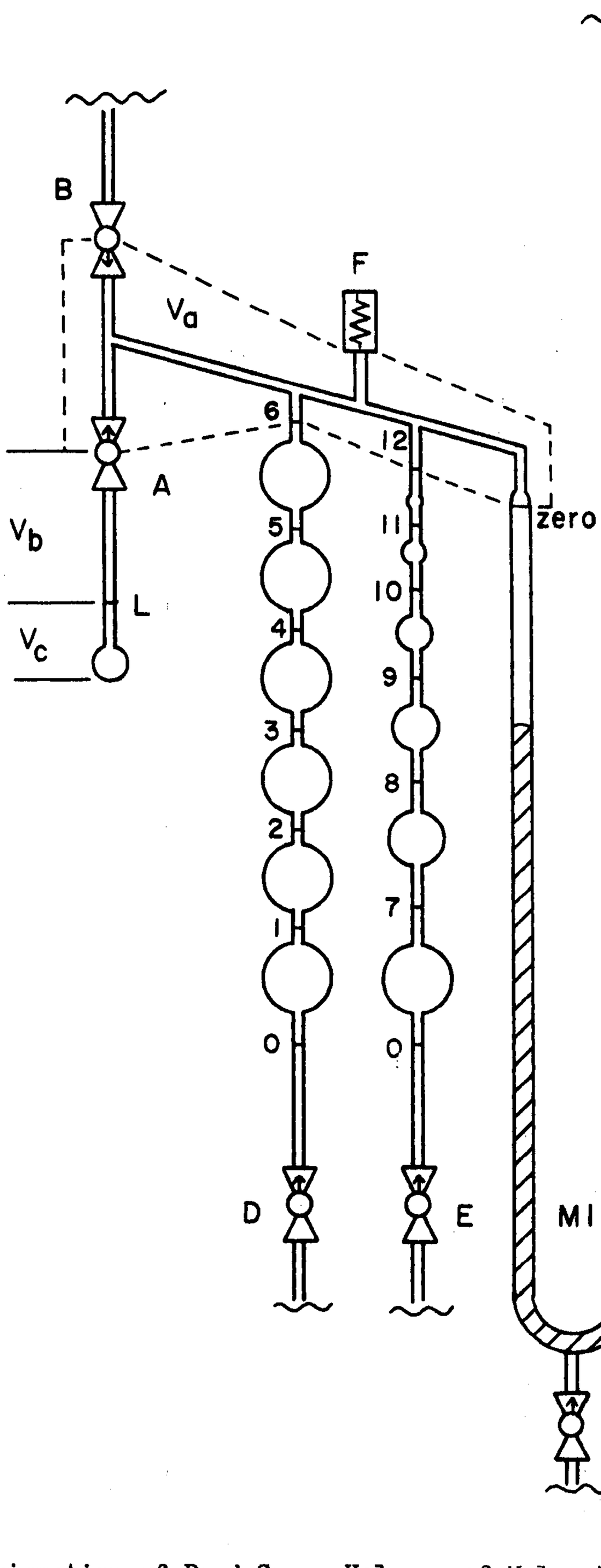

FIG 3.5 Designation of Dead Space Volumes of Volumetric Apparatus

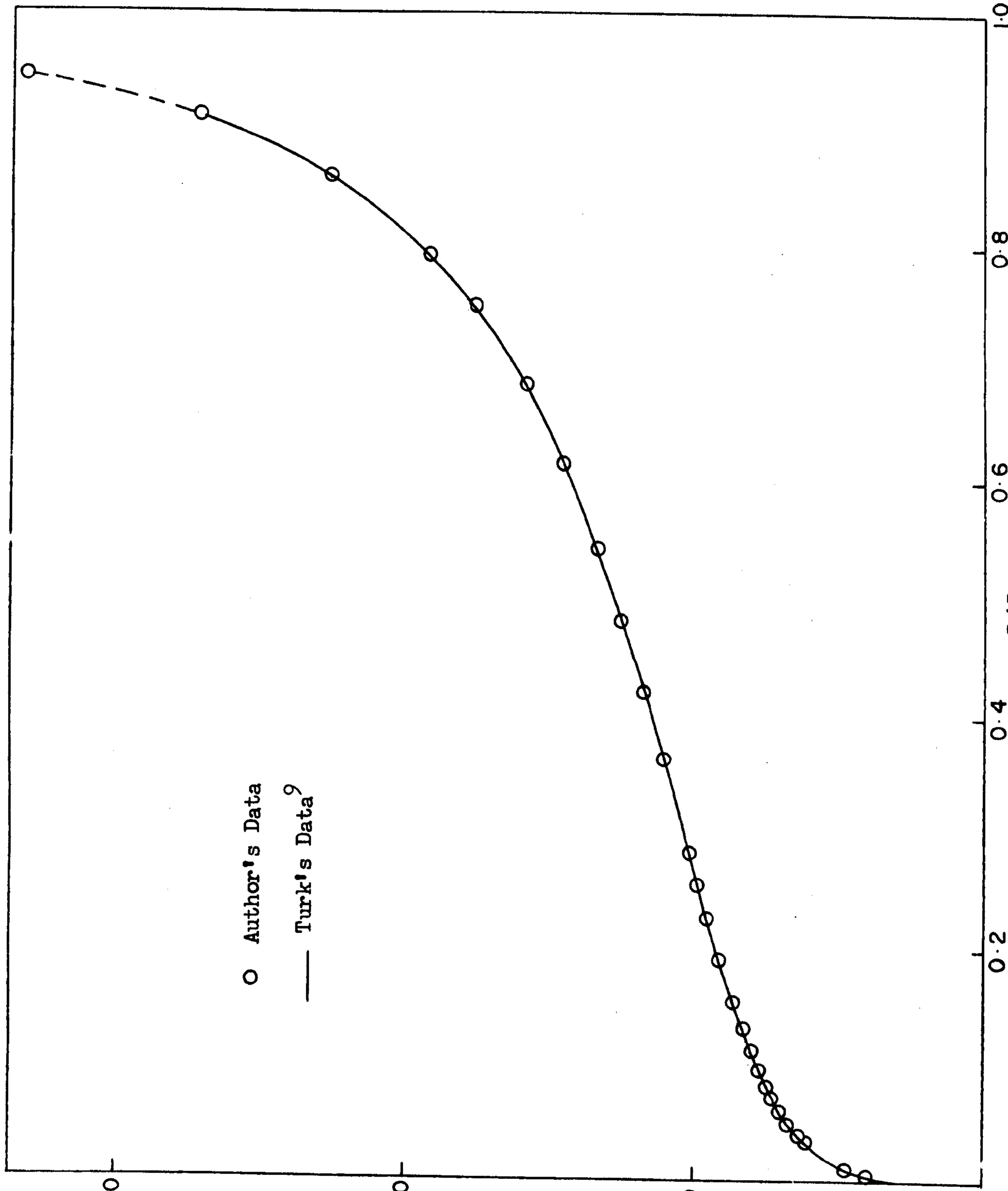

FIG 3.6 Volumetric Apparatus Calibrations Check: Nitrogen Adsorption on TK 800-II

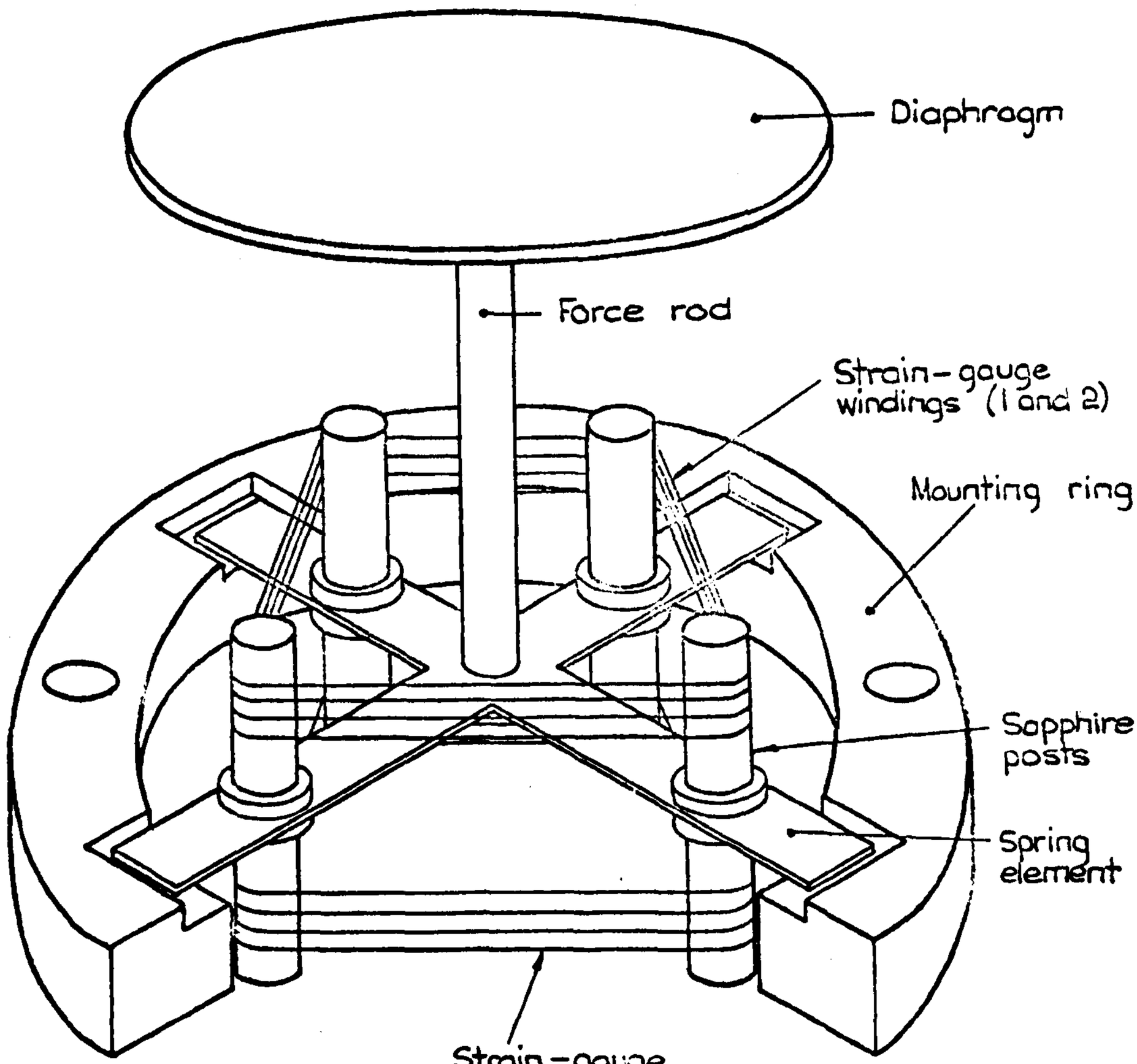

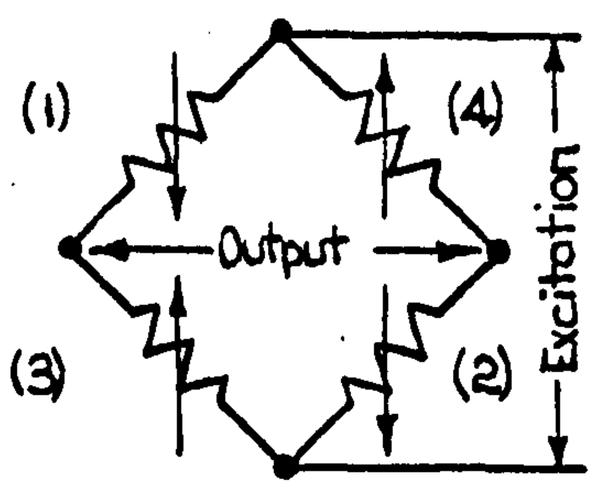

Wheatstone bridge

FIG 3.7 Transducer Pressure-Sensing Element

(Courtesy of Bell and Howell Ltd.)

FIG 3.8 Transducer Power Supply

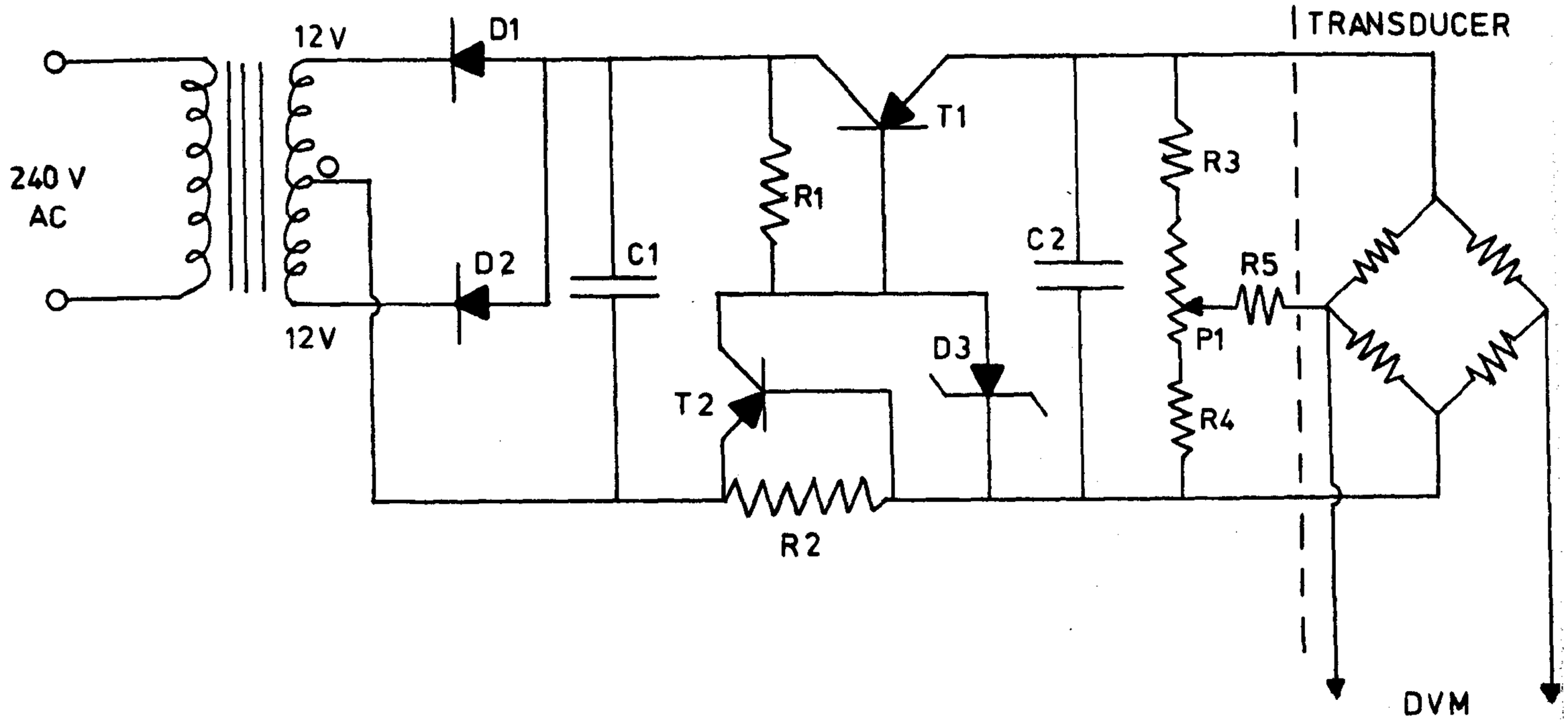

D1 & D2 - Silicon Diode
150 V PIV (peak inverse voltage)
I_f 90 mA (forward current)
(Radiospares Cat. No. 1SJ 150)

D3 - Zener Diode
10 V

T1 & T2 - p-n-p Junction Transistor
160 mW
Vc max -32 V
Ic max 500 mA
(Mullard OC 84)

C1 - 100 µF

C2 - 50 µF

R1 - 470 Ω

R2 - 2.7 Ω

R3 & R4 - 3.9 K Ω

R5 - 68 K Ω

P1 - 5 K Ω, 10 turn potentiometer.

The output is 10 V with a maximum peak to peak ripple of 2 mV full load.

FIG 3.9 L.H.A. Transducer Calibration Curve

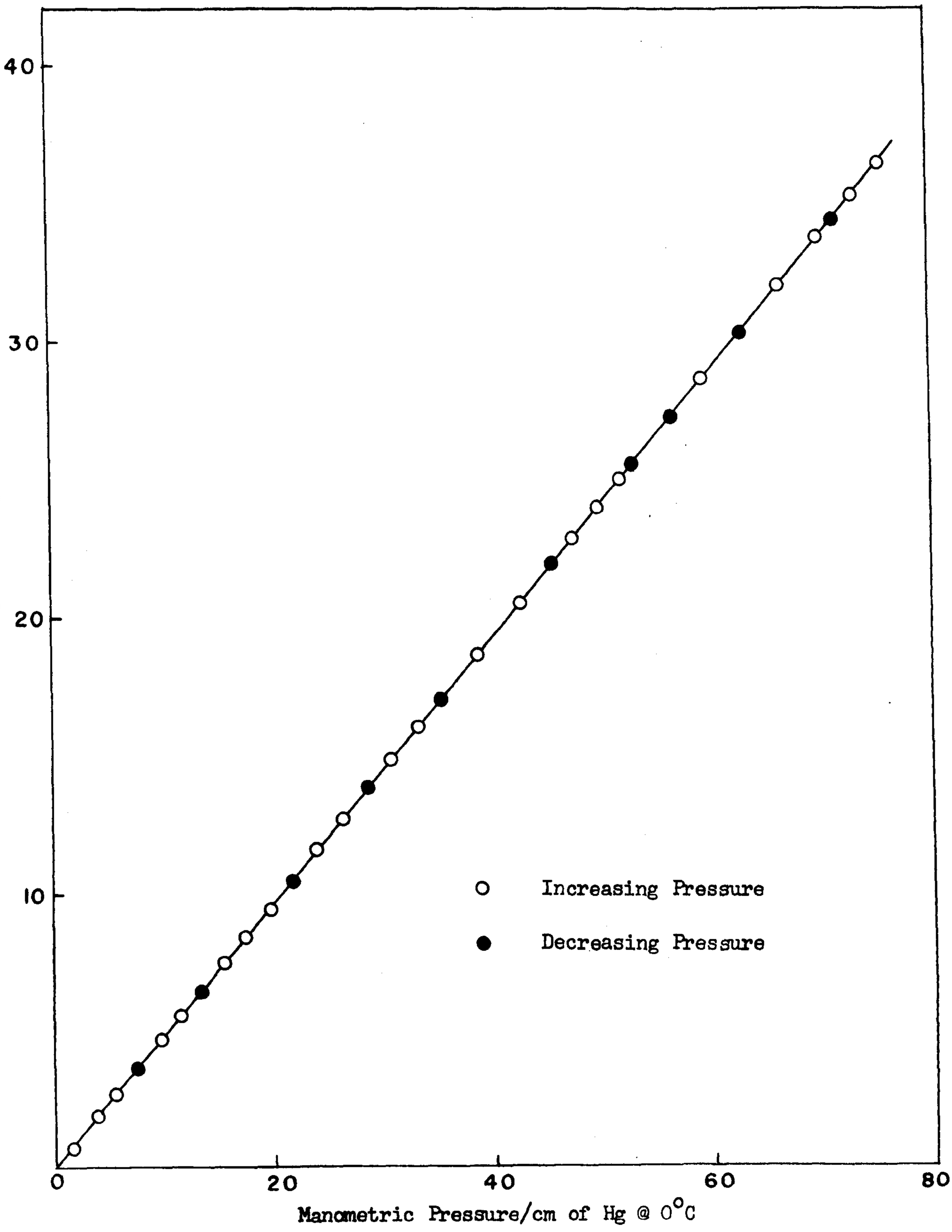

FIG 3.10 R.H.A. Transducer Calibration Curve

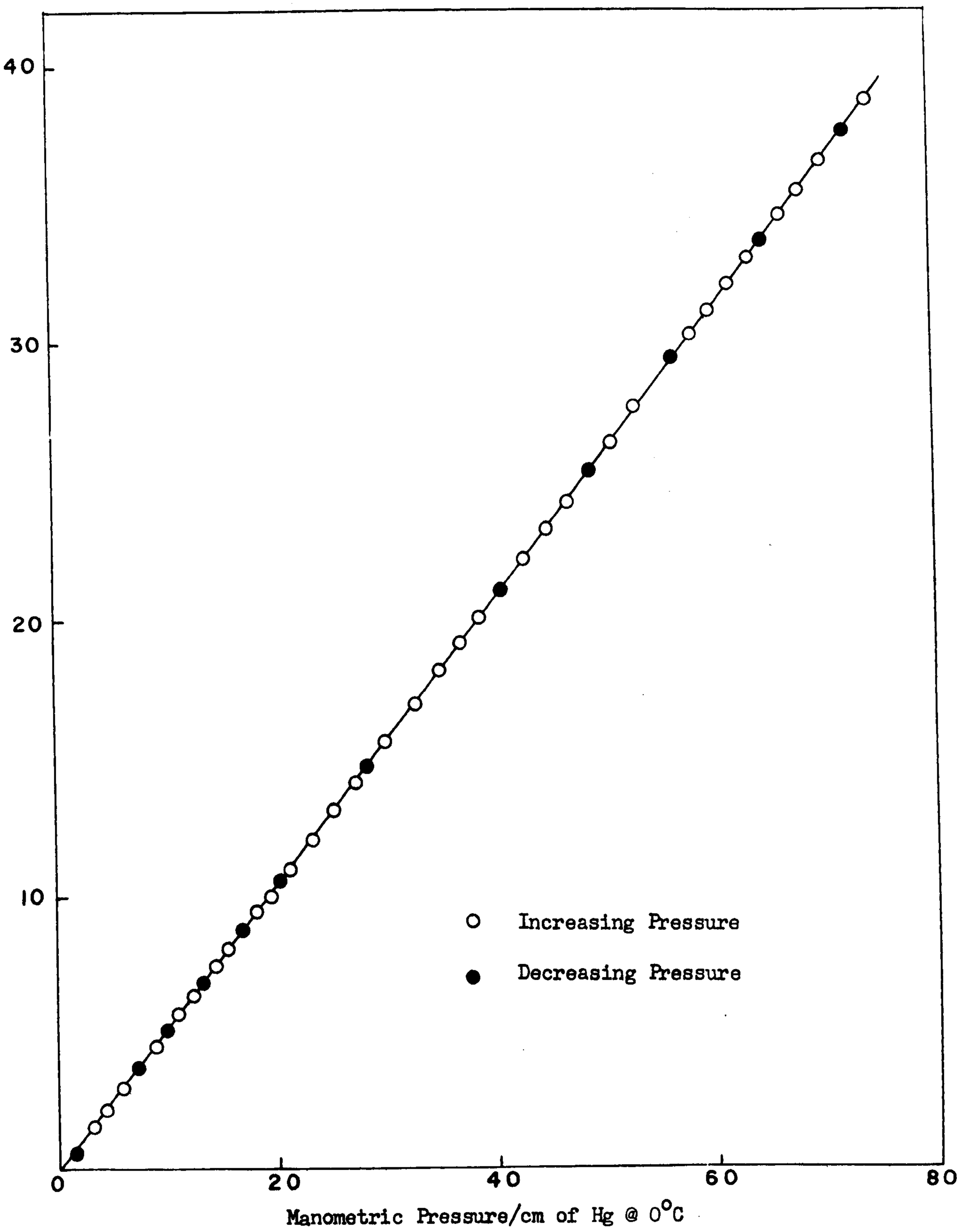

FIG.3.11 Comparison of Manometric and Transducer Pressure Data (Nitrogen on TK 800-III)

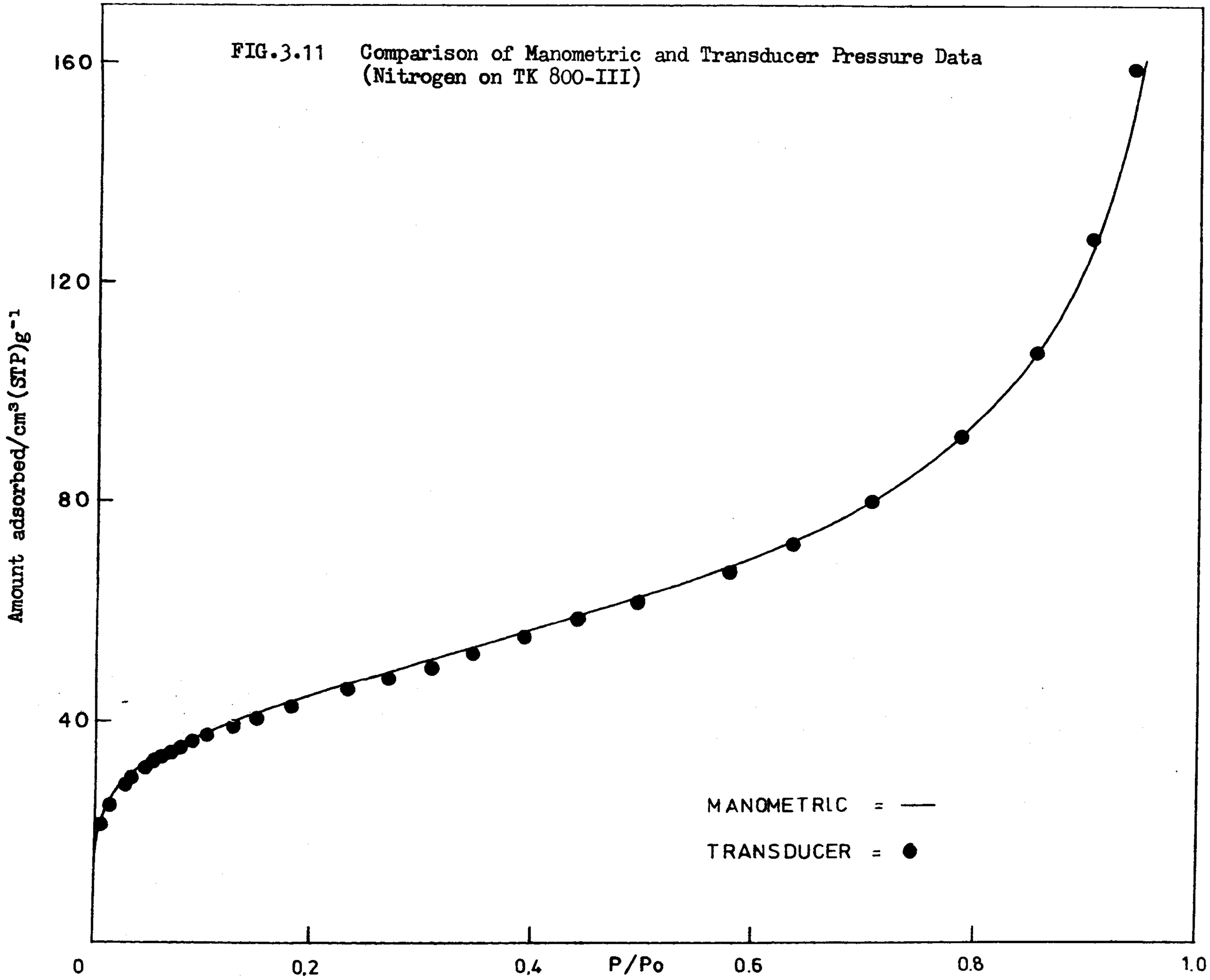

S^{N}_{BET} VALUES.

MANOMETRIC = 161

TRANSDUCER = 155

$m^2 g^{-1}$

FIG 3.12

FIG 3.13

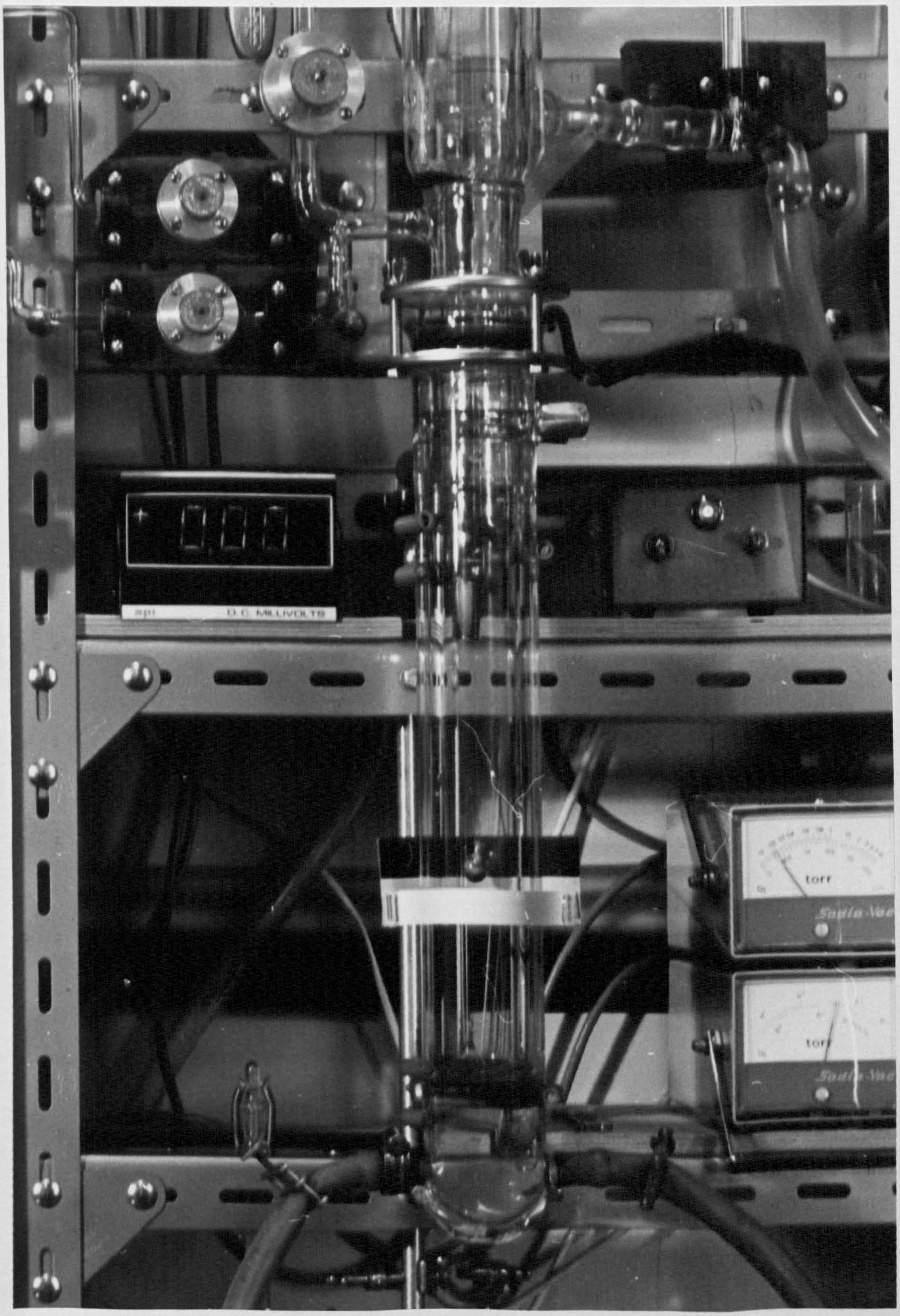

FIG 3.14

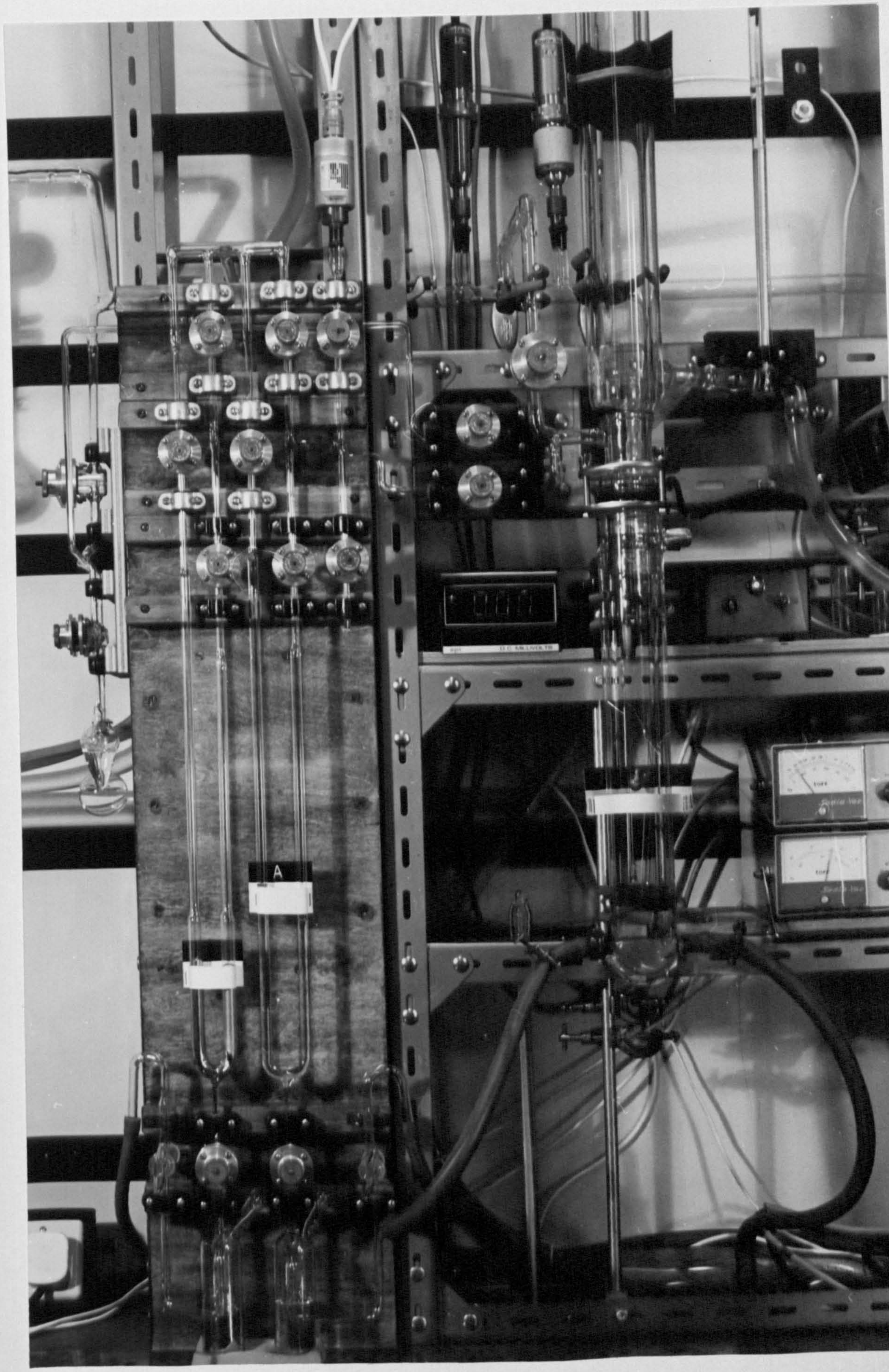

FIG 3.15

FIG 3.16 Layout of the Quartz Spring Balance for the Study of Water and Mercury Vapour Adsorption.

(cf. Fig. 3.17 for key)

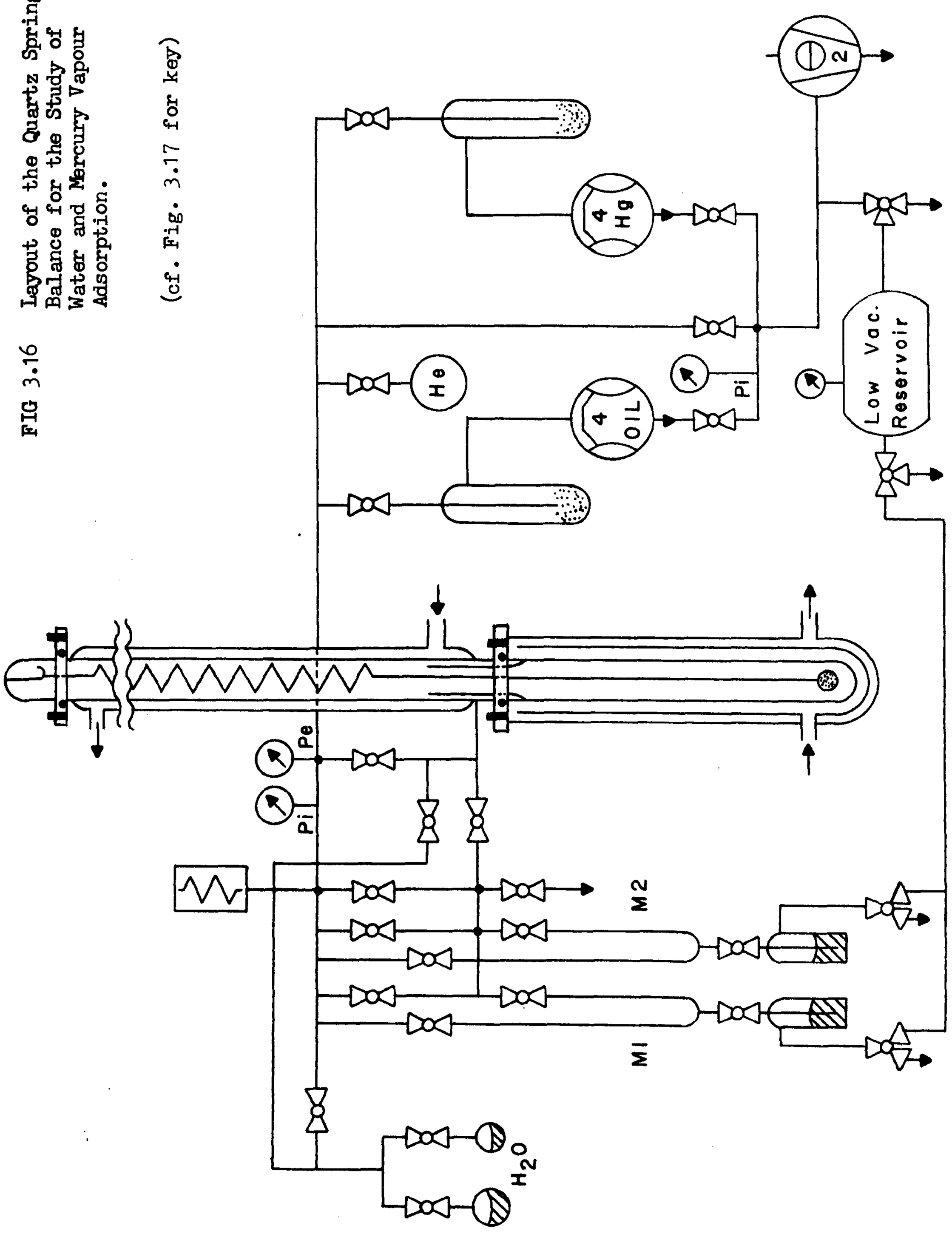

FIG 3.17 Key for Diagrams Shown in Figs. 3.4, 3.5 and 3.16

Straight-through stopcock.

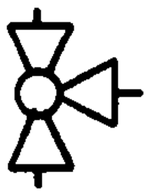

Three-way stopcock.

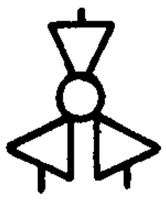

Two-way stopcock.

B7 ground glass joint.

"Rotulex" joint with 'O' ring seal.

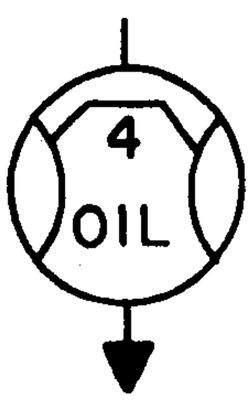

4-stage oil diffusion pump.

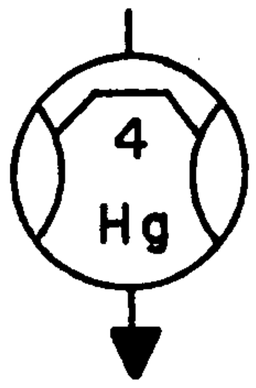

4-stage mercury diffusion pump.

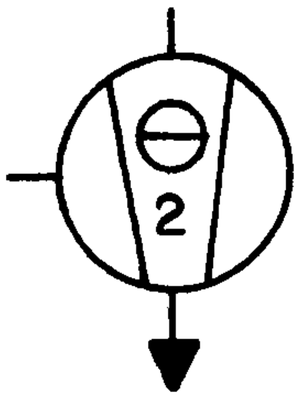

2-stage rotary vane pump.

Vacuum gauge - general.

Pirani gauge.

Penning gauge.

FIG 3.17 Key for Diagrams Shown in Figs. 3.4, 3.5 and 3.16 (cont)

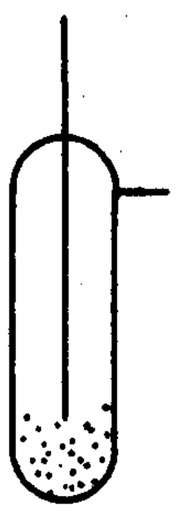

Liquid nitrogen cold trap containing molecular sieve.

Pressure-sensitive transducer.

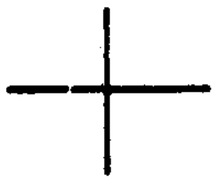

Crossing of glass lines <u>without</u> connection.

Crossing of glass lines <u>with</u> connection.

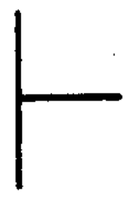

Branch connection.

Gas inlet.

FIG 3.18 Calibration Curve for Quartz Spring

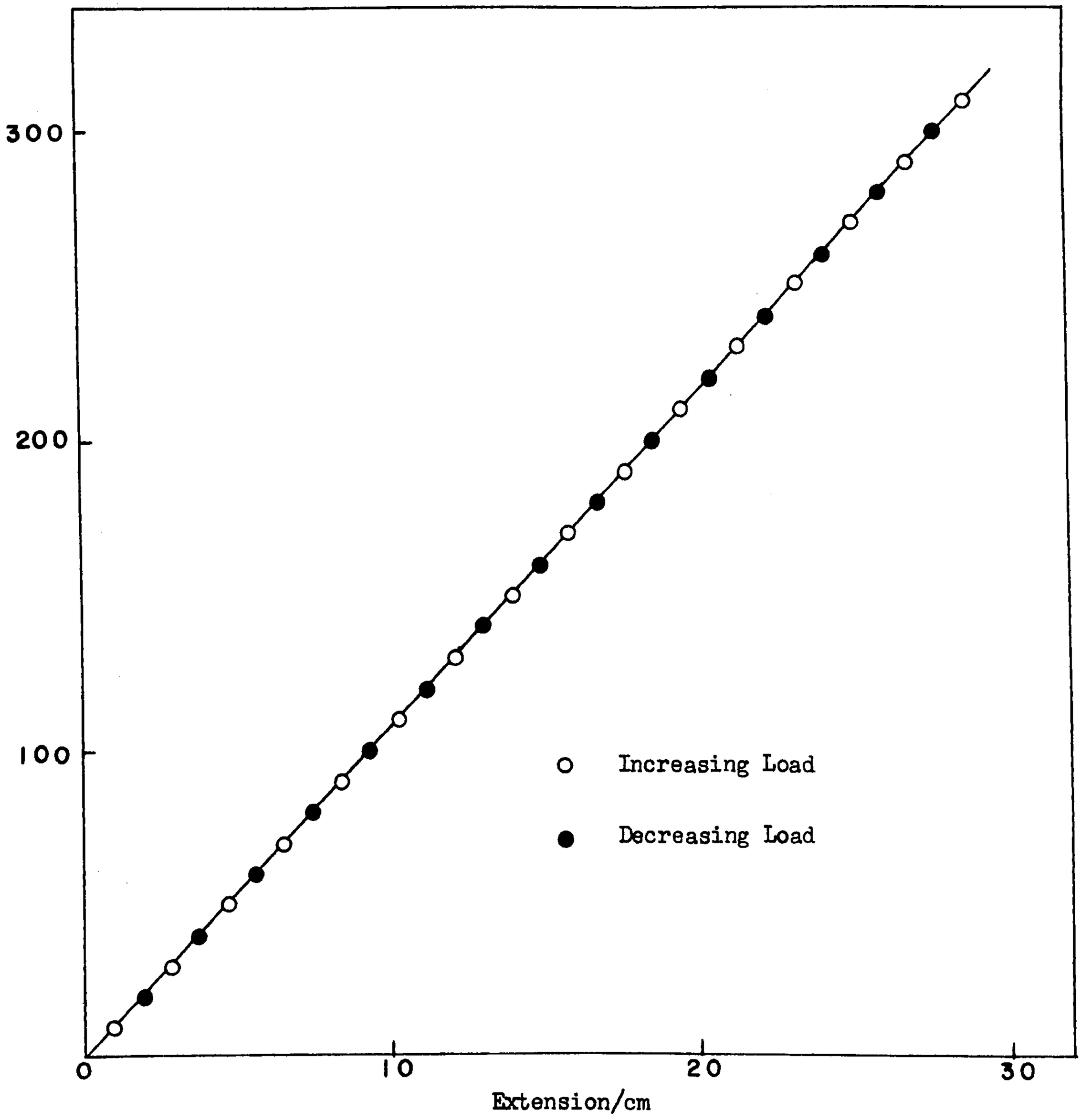

FIG 3.19 Spring Balance Transducer Calibration Curve

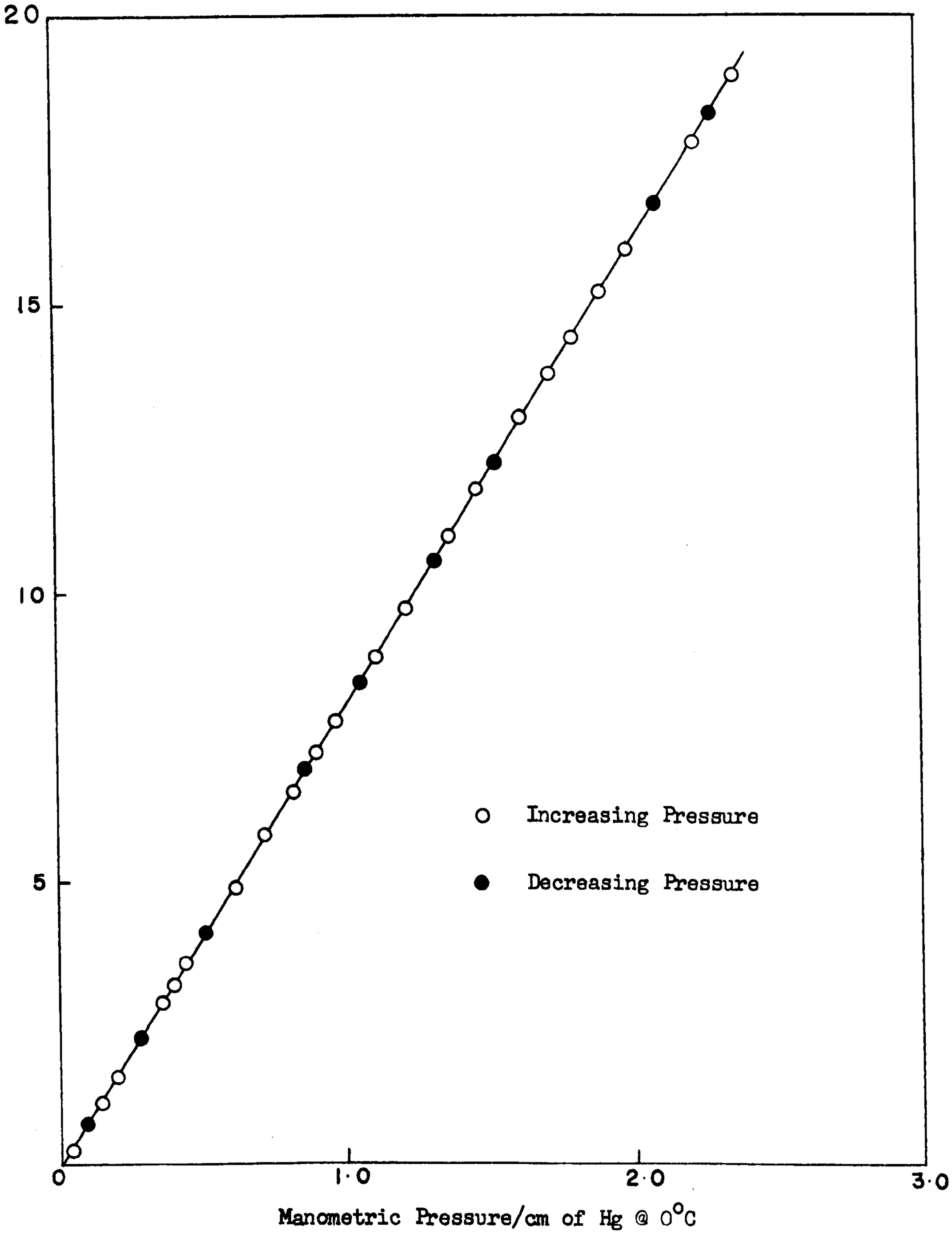

C H A P T E R 4

RESULTS AND DISCUSSION I

GAS ADSORPTION AND RELATED STUDIES ON THE SILICA SAMPLES

The present chapter deals with the analysis and interpretation of the argon, nitrogen and water vapour adsorption data determined on the silica samples, together with their heats of immersion in water. The experimental data are presented in tabular form in Appendices 7, 8 and 9 respectively. Conclusions are drawn concerning the texture and degree of hydroxylation of the silica samples.

4.1 The Adsorption Isotherms

The reversible Type II nitrogen and argon isotherms obtained for Fransil, in the present work, are shown in Fig. 4.1, together with the irreversible water isotherm: the nitrogen and argon isotherms are typical of a non-porous adsorbent. The nitrogen isotherm exhibits a well-defined point B (BET C value of about 138) whereas the argon isotherm gives a more gradual curvature in the region of the statistical monolayer (BET C value of about 32). The water isotherm exhibits hysteresis over the complete range of relative pressure, and indicates that, whilst the sample of Fransil is non-porous, the surface is not fully hydroxylated. The argon isotherm, plotted as a function of P/Po(s) (where Po(s) is the saturated vapour pressure of solid argon), cuts the ordinate P/Po(s) = unity at a finite angle instead of approaching asymptotically. In studies of argon adsorption at -196°C (i.e. below the bulk triple point of argon) it

has been customary to take the value of Po as that of the supercooled liquid.[1-3] Recently, however, Sing and his co-workers[4] have suggested that although this may be justified in the case of certain porous solids,[5] there is no sound reason for making the same assumption with non-porous adsorbents.[6] Consequently, the value of Po used throughout the present work is that of <u>solid</u> argon.

In Fig. 4.2, the nitrogen adsorption data are represented as α_s-plots, the data previously reported for Fransil[7,8] being taken as standard. The α_s-plot is both linear and passes through the origin; this provides useful confirmation of the accuracy of the present measurements (see also Section 3.12, page 60) and demonstrates that the surface properties of this particular sample of Fransil have not changed significantly over the past four or five years.

In confirmation of previous work,[4,8,9] reversible Type II nitrogen and argon isotherms were also obtained on TK 800 outgassed at both 25°C and 140°C; the corresponding water vapour isotherms exhibited hysteresis over the complete range of relative pressure. The hysteresis of the water isotherms was enhanced with increase in temperature of outgassing. In general terms, the picture for the nitrogen, argon and water vapour isotherms respectively, on TK 800 outgassed at either 25°C or 140°C was very similar to that described for Fransil (shown in Fig. 4.1). Replicate water vapour isotherms on the same sample of TK 800 revealed that the degree of hydroxylation of the silica surface was gradually increased with repetitive exposure to water vapour - i.e. water vapour adsorption was enhanced, whilst the degree of irreversibility of the isotherms was progressively reduced.

In order to obtain a fully reversible water isotherm on TK 800 a sample was "soaked" in water vapour, at a relative pressure of about 0.98 at 25°C, over a period of three days: the pressure of water vapour was then

progressively decreased and the "desorption isotherm" obtained. The soaked sample was outgassed at 25°C to constant weight and the complete nitrogen and water vapour isotherms respectively, determined. The isotherms (the uptake expressed in terms of μ mole per unit nitrogen area) are shown in Figs. 4.3 and 4.4 respectively, together with the corresponding isotherms determined on the original, partially hydroxylated, material. It is clear from Fig. 4.3, that the soaking treatment has not significantly affected the subsequent adsorption of nitrogen at relative pressures below about P/Po = 0.5; apart from a slightly more rounded knee of the isotherm, the BET nitrogen area remained virtually unchanged (Table 4.1). At higher relative pressures in the multilayer region, however, the nitrogen isotherm on the soaked material exhibits a small degree of irreversibility, characteristic of capillary condensation. The α_s-plots of the nitrogen adsorption data for the original and soaked materials respectively, are shown in Fig. 4.5. The upward deviation from linearity of the plot for the soaked material is typical of capillary condensation, and is probably a result of a small degree of cementation of particles of TK 800 upon prolonged exposure to water vapour. The fact that the α_s-plots in Fig. 4.5 all show a negative intercept with the ordinate at $\alpha_s = 0$, indicates that Fransil is not a strictly suitable standard adsorbent for comparison with TK 800 adsorption data.

The water vapour isotherms shown in Fig. 4.4 reveal that the soaking treatment of TK 800 resulted in the almost complete hydroxylation of the adsorbent surface. The adsorption of water vapour on the soaked material was considerably enhanced and, apart from a very small degree of hysteresis at high relative pressure (characteristic of capillary condensation), the isotherm was completely reversible below a relative pressure of about P/Po = 0.7. Furthermore, the "desorption isotherm" obtained (in the manner

referred to above) immediately after the soaking treatment at P/Po = 0.98 was virtually coincident with the subsequent adsorption branch of the (almost) reversible isotherm on the soaked material; in addition, the isotherm on the soaked material was reproducible.

The effect on the nitrogen isotherms by outgassing a non-porous silica and two porous silicas at 1000°C, as compared with 25°C, is shown in Figs. 4.6 - 4.8. For ease of comparison the isotherms are plotted as adsorption per unit area (using S^{N}_{BET}); it should be noted, however, that in the case of the microporous gel E the BET nitrogen area is an <u>apparent</u> area.

It is clear from Fig. 4.6, that on outgassing TK 800 at 1000°C, the general shape of the nitrogen isotherm (which was reversible) was changed very little; the reduction in the value of the BET C constant (Table 4.1), indicates that the adsorbent-adsorbate interactions have been reduced by dehydroxylation of the adsorbent surface at 1000°C. The α_s-plot for the high temperature outgassed material, Curve 'C' in Fig. 4.5, is clearly linear over a wide range of relative pressure; although the high temperature treatment has resulted in some sintering of the adsorbent particles (S^{N}_{BET} in Table 4.1 is reduced by about 13% at 1000°C), the texture of the TK 800 sample has remained unchanged after outgassing at 1000°C.

In contrast, however, when the microporous silica, gel E, was outgassed at 1000°C, a small amount of pore-widening occurred as was revealed by the subsequent nitrogen isotherm (Fig. 4.7). The nitrogen isotherm, although still predominantly Type I in character, exhibits an upward swing at relative pressures greater than about P/Po = 0.5 in a manner similar to that of a Type III isotherm.[10] If the adsorption of nitrogen on the dehydroxylated gel E is indeed particle co-operative in nature, it suggests that the adsorbent-adsorbate interactions are reduced by the outgassing at

1000°C whilst the adsorbate-adsorbate interactions have increased. This change is reflected by the drastic reduction in the value of the BET C constant (which is accompanied by a four-fold reduction in the apparent nitrogen area) for the nitrogen isctherm on the high temperature outgassed material (Table 4.1). Kiselev,[11] in studies of nitrogen, benzene and water vapour adsorption, has observed a very similar effect in the cases of hydroxylated and dehydroxylated silicas, and of ungraphitised and graphitised carbons respectively.

The behaviour of the mesoporous silica, gel J, on outgassing at 1000°C was very similar to that for the non-porous TK 800: the texture of the adsorbent remained virtually unchanged, whilst the proportionate loss of nitrogen area (about 12% from Table 4.1) by sintering was almost identical to that for TK 800. The slight enhancement of the hysteresis loop (Type A in the de Boer classification[12,13]) for the nitrogen isotherm on gel J outgassed at 1000°C may , in part, be associated with the slightly higher relative pressure obtained during the determination of this isotherm; otherwise, the Type IV nitrogen isotherms obtained after outgassing at 25°C and 1000°C respectively, are almost completely coincident (Fig. 4.8).

In general, therefore, the nitrogen isotherms determined on the various silicas, reveal that there was very little change in the texture of the adsorbents when outgassed at 1000°C, as compared with 25°C, particularly in the cases of the non-porous TK 800 and the mesoporous gel J. However, the water isotherms, shown in Figs. 4.4, 4.9 and 4.10 for silicas outgassed at 25°C and 1000°C respectively, clearly indicate a substantial change in the chemical nature of the adsorbent surface outgassed at 1000°C. It should be emphasised that the curves in Fig. 4.10 do not necessarily represent equilibrium isotherms for the physical adsorption of water vapour on dehydroxylated silicas; in addition to physical adsorption , irreversible

chemisorption of water vapour also occurred. The rate of chemisorption rapidly increased with increasing relative pressure, whilst the amount of chemisorbed water was dependent on the time of exposure of the adsorbent to water vapour. To minimise the amount of chemisorption, the complete isotherm on a dehydroxylated silica was determined during a continuous period of about 16 hours. Isotherm adsorption points were recorded when a plot of water uptake against time elapsed indicated that the (relative rapid) physical adsorption of water vapour was, for the present purposes, complete at the particular relative pressure; in contrast, during desorption apparent equilibrium was attained relatively quickly (5 - 15 minutes as compared to 20 - 80 minutes for adsorption, in the case of TK 800) and it appeared to represent a genuine state of equilibrium.

The water isotherm on gel E outgassed at 25°C, shown in Fig. 4.9, exhibits a considerable degree of Type IV character, especially in respect of the hysteresis loop; however, the corresponding nitrogen isotherm, shown in Fig. 4.7, demonstrates that gel E is <u>microporous</u>. The hysteresis loop in the water isotherm, Type E in the de Boer clasification,[12,13] is characteristic of pores of the ink-bottle type[14-17] which probably comprise the micropores of the adsorbent; in this instance, the micropores may be visualised as having a neck, too narrow to permit the entry of nitrogen molecules, but sufficiently wide to allow the penetration of water molecules. The water vapour isotherm on gel E (Fig. 4.9) is almost identical with that reported in earlier work by Kiselev et al.[18,19] for water vapour adsorption on a microporous silica gel (with an apparent nitrogen area of 540 $m^2 g^{-1}$); furthermore, Kiselev and his co-workers[20] have also commented on a molecular-sieve effect as between nitrogen and water on such a gel. It is interesting to note that the apparent close similarity of Kiselev's microporous silica gel with gel E studied in the present work, is further

demonstrated by the close similarity in total pore volumes (liquid water): i.e. 0.25 $cm^3\ g^{-1}$ and 0.26 $cm^3\ g^{-1}$ respectively.

When gel E was outgassed at 1000°C the subsequent water isotherm displayed none of the familiar characteristics of a microporous adsorbent; in fact, the adsorption branch was very similar to that of the water isotherm determined on the mesoporous gel J, similarly outgassed at 1000°C (Fig. 4.10).

Water adsorption on all three silicas was much reduced at relative pressures below about 0.35 by outgassing at 1000°C, presumably because the rate of chemisorption (and hence, rehydroxylation)at low relative pressures is practically negligible.[21] Moreover, the adsorption branches of the isotherms at low relative pressures are in very close proximity and may, therefore, be in approximate coincidence with reversible physical adsorption of water on a dehydroxylated silica. Apart from a barely discernible point of inflexion close to the origin (which may be attributed to a small amount of hydroxyl groups remaining on the dehydrated surface), the adsorption branches are essentially Type III in character thereby reflecting the hydrophobicity of the dehydroxylated silicas. Kiselev and his co-workers[21] have observed an identical effect for silicas outgassed at 900°C. The adsorption branch becomes progressively steeper, as the rate of surface rehydration is increased at higher relative pressures; the relative location of the adsorption branches of the isotherms above a pressure of about 0.35 Po is some measure of the ease of rehydration or, conversely, the degree of hydrophobicity of the respective silicas outgassed at 1000°C; i.e. order of hydrophobicity is - TK 800 > gel J > gel E.

The difference between the desorption branch of the water isotherm on gel E outgassed at 1000°C, and those of the corresponding isotherms for gel J and TK 800 respectively, is noteworthy: in the latter cases, the pronounced hysteresis extending to zero pressure is characteristic of

surface rehydration, but for the microporous silica, gel E, the hysterisis is a result of both surface rehydration and pore-emptying. The steep section of the desorption branch, within a very narrow range of relative pressure at about 0.25 Po, is most probably associated with the sudden emptying of the ink-bottle type micropores, mentioned earlier; at relative pressures below about 0.25 Po, the hysteresis is solely associated with surface rehydration. Furthermore, the desorption branch of the water isotherm on gel E outgassed at 1000°C is remarkably similar, in location and shape, to that of the isotherm obtained after outgassing the gel at 25°C (Fig.4.9). Thus, as previously indicated by the general superposability of the corresponding nitrogen isotherms, shown in Fig. 4.7, the pore size distribution for gel E outgassed at 25° and 1000°C respectively, must be fairly similar.

In conclusion to the present discussion on the nitrogen and water vapour isotherms, it is noteworthy that the amount of water remaining after outgassing the respective high-temperature silicas to constant weight at 25°C (expressed as μ mole per m^2 of apparent nitrogen area), is very similar in each case. In fact, it is obvious from Fig. 4.10 that the amount of residual water per unit area is identical for the micro and mesoporous silicas, gels E and J respectively, whilst that for the non-porous TK 800 is about 35% less. This result indicates that the chemical nature of the surfaces of the respective silicas is probably very similar, rehydration of TK 800 being slightly more difficult than for gels E and J respectively.

4.2 Comparison of the Water Adsorption Data

The results of the experiments on nitrogen and on water vapour adsorption respectively, on silicas are summarised in Table 4.1. The values of the BET nitrogen area, S^{N}_{BET}, were calculated by taking 16.2 $Å^2$

TABLE 4.1

Nitrogen and Water Vapour Adsorption on the Silicas

SAMPLE	OUTGASSING TEMPERATURE (°C)	NITROGEN ADSORPTION				WATER ADSORPTION			N_{OH} per 100 Å²	Q_i (erg cm⁻²)
				BET		BET		SORPTION AT P/Po = 0.2		
		TYPE	POROSITY	S^N_{BET} (m^2g^{-1})	C	S^W_{BET} (m^2g^{-1})	C	(μ mole⁻²)		
[a]Fransil	140	II	N	38.6	131	12	19	5.3	4.3	160
[b]TK 800 II	25	II	N	162	84	54	12	5.1	4.1	-
[c]TK 800 II	25	II	N	163	100	40	15	3.8	3.6	251
[c]TK 800 II	140	II	N	164	99	42	11	3.7	2.5	-
[d]TK 800 II	1000	II	N	143	65	11	8	1.0	-	283
Gel E	25	I	Mic	572				11.6	1.8	234
Gel E	1000	I	Mic	150	99	16	3	0.9	-	207
Gel J	25	IV	Me	327				6.4	3.4	266
Gel J	1000	IV	Me	289	72	24	14	1.3	-	247
Column No.	2	3	4	5	6	7	8	9	10	11

N, non-porous; Mic, microporous; Me, mesoporous.

[a] Fransil was outgassed at 140°C for the nitrogen isotherm, but at 25°C for the water isotherm.

[b] Fully hydroxylayed TK 800, i.e. 'soaked'.

[c] Partially hydroxylated TK 800, i.e. as received.

[d] Dehydroxylated TK 800, i.e. outgassed at 1000°C.

as the cross-sectional area of the nitrogen molecule in the completed monolayer; the values of the corresponding BET water area, S^{W}_{BET}, were calculated by taking 10.6 $Å^2$ as the cross-sectional area of the water molecule. However, in view of the fact that the water isotherms did not give a well-defined point B (very low BET C constant in each case), the S^{W}_{BET} values recorded in Table 4.1 are of limited significance. In order to make a more meaningful comparison of the water adsorption data for the various silicas the water uptakes at 0.2 Po, reduced to a unit area basis (using S^{N}_{BET}), are shown in column 9 of Table 4.1.

The amounts of water adsorption per unit area range widely, from 0.9 to 11.6 μ mole m^{-2}. For comparison, an uptake of 15.7 μ mole m^{-2} would correspond to a close-packed water monolayer (taking A_m = 10.6 $Å^2$). In confirmation of previous findings,[4,22] all the silicas gave a lower uptake of water vapour at 0.2 Po than the amount required for the close-packed monolayer coverage. It is noteworthy that the microporous silica, gel E (outgassed at 25°C), gave an appreciably higher level of water adsorption, even though the apparent hydroxyl group population was exceptionally low (Section 4.3), than did the other silicas. As discussed in Section 4.1, this was probably due to the penetration of water into pores (of width about 4 Å) too narrow to accept nitrogen molecules and therefore, the term 'sorption' may be usefully applied to describe such phenomena.[23] In confirmation of the work of Kiselev,[19,21,24] the adsorption of water on the dehydroxylated samples of TK 800 and gels E and J (outgassed at 1000°C) was especially low; about 1 μ mole m^{-2} in each case.

In Fig. 4.11, representative water vapour adsorption isotherms are plotted to 0.4 Po on a unit area basis (by taking the corresponding S^{N}_{BET} value from Table 4.1), along with the standard, reversible,water isotherm

on fully hydroxylated non-porous silica (Kiselev[24]) included as a comparison. Curves lying below the standard isotherm may be interpreted in terms of the chemistry of the adsorbent surface; e.g. increase in the degree of hydroxylation of TK 800 results in the progressive movement of the isotherm towards the standard curve. The fact that the curve for the soaked TK 800 (reversible water isotherm) is markedly displaced from the standard curve, probably indicates that there is a significant difference in the chemistry of the (apparently) fully hydroxylated TK 800 surface and that of the standard. The location of the curve for the microporous silica, gel E, appreciably above the standard curve clearly indicates on the other hand that the texture of the gel is now the over-ruling factor during the sorption of water vapour. The curve for the mesoporous silica, gel J, is located close to the standard curve, and indicates that the chemical nature of the respective surfaces is probably very similar.

4.3 Surface Concentration of Hydroxyl Groups

The apparent number of surface hydroxyl groups per 100 $Å^2$, N_{OH}, shown in column 10 of Table 4.1, was assessed from the weight loss of each silica on outgassing at 1000°C for 2.5 hours. In the assessment of N_{OH} it was assumed that all the physisorbed water was removed[25] by prolonged outgassing of the sample (to constant weight) at 25°C; and furthermore, that the hydroxyl groups remaining were confined to the surface available for nitrogen adsorption. Neither of these assumptions, particularly the latter, is strictly valid: Zhuravlev and Kiselev[25,26] have shown that a thermogravimetric method essentially determines the total content of the "structural water", i.e. that hydroxyl groups are liberated both from the surface and from the bulk of the silica. On the other hand, it is known[24,27] that some hydroxyl groups are retained by a

silica surface, even after outgassing at 1100°C. The fact that some water was physisorbed on the nominally dehydroxylated silicas in the present work (about 1 μ mole per m^2 at 0.2 Po), clearly indicates the presence of residual hydroxyl groups even on the surfaces outgassed at 1000°C. It is to be expected that prolonged outgassing at high temperatures would increase the degree of dehydroxylation; however, under such conditions very fine micropores may develop with a diameter approximating to that of a water molecule.[25,28] In order to reduce the risk of the formation of these very fine pores, a relatively short outgassing period of 2.5 hours at 1000°C was adopted for the present thermogravimetric studies.

The values of the surface concentrations of hydroxyl groups, N_{OH}, obtained for the silicas in the present work, range from 1.8 for the microporous gel E to 4.3 for the non-porous Fransil. In general, the values of N_{OH} are lower than the range reported[25,26] for fully hydroxylated amorphous silica, as determined by a deuterium exchange method,[29] namely 4.2 - 5.7 OH groups per 100 Å² (i.e. 7 - 9.5 μ mole OH per m^2); this range corresponds to approximately one hydroxyl group per surface silicon atom. Water isotherms on the porous silicas, gels E and J (outgassed at 25°C), were reversible below a relative pressure of about 0.3 Po indicating that these gels were probably almost fully hydroxylated: nevertheless, the values of N_{OH} (1.8 and 3.4 respectively) were lower than those reported[22] for a number of microporous and mesoporous silicas (N_{OH} ranging from 5.8 to 11.5), which were determined by a thermogravimetric method. Of course, it is not unexpected that the value of N_{OH} for the microporous gel E is abnormally low, since the apparent nitrogen area (572 m^2g^{-1}, Table 4.1) was employed to express the surface concentration of hydroxyl groups on a unit area basis. However, it is difficult to

account for other apparently low values of N_{OH} for the hydroxylated silicas, e.g. gel J. The present value of N_{OH} should accordingly be interpreted on a semi-quantitative basis only.

Although a plot of weight loss against time elapsed indicated that, in each case, a constant sample weight was achieved, the time of outgassing, 2.5 hours at 1000°C, may be too short. Nevertheless, assuming a consistent error from this cause, it is apparent from Table 4.1 that the soaking treatment of TK 800 did result in an increase in the value of N_{OH}, which closely approached the range reported[25,26] for a fully hydroxylated silica. Although the value of N_{OH} = 4.3 for the Fransil sample does lie within the reported range of 4.2 - 5.7 OH groups per 100 Å^2, the water isotherm exhibited hysteresis over the complete range of relative pressure (Fig. 4.1), indicating that the surface was not fully hydroxylated. With the exception of the porous silicas (gels E and J), it is noteworthy that an increase in the apparent surface concentration of hydroxyl groups was accompanied by an increase in the sorption of water vapour at 0.2 Po for a particular adsorbent.

4.4 Heats of Immersion in Water

The values of Q_i, the heat of immersion of silica in water expressed as erg per cm^2, are given column 11 of Table 4.1 for the various silicas. Each value was calculated from the heat of immersion per gram of outgassed sample (at the temperature indicated in column 2 of Table 4.1), using the corresponding value of S^N_{BET}; it was assumed that the surface area available to adsorbed nitrogen (at the gas-solid interface) and water (at the liquid-solid interface) was the same. For reasons already discussed it is evident that, in a number of cases, this assumption is not fully justified and therefore the values of Q_i determined in the present work do not

always represent the true heats of immersion per unit area.

For Fransil, the value of Q_i determined in the present work (160 erg cm^{-2}) is in excellent agreement with the value of 160 $\pm$ 3 erg cm^{-2} reported by Taylor and Hockey,[30] for the heat of immersion in water of a fully hydroxylated amorphous silica. These workers observed that the value of Q_i was independent of the surface area over the range of 8 - 147 m^2g^{-1} (from Table 4.1, S^N_{BET} = 38.6 m^2g^{-1} for Fransil). All other values of Q_i recorded in Table 4.1 are appreciably higher than 160 erg cm^{-2}. With the exception of TK 800, the value of Q_i decreases with surface dehydroxylation of a particular silica; this result is in accord with the findings of Kiselev and his co-workers.[19,21] It is clear, therefore, that two particular features must be taken into account with the present results: differences in (a) the porosity, and (b) the degree of surface hydroxylation of the silicas. Unfortunately, the two effects cannot be separated, presumably because of the complex nature of the wetting process and the fact that the heat of immersion is directly related to the integral enthalpy of adsorption. These results serve to emphasise the importance of differential enthalpy determination.[31]

4.5 The Frenkel-Halsey-Hill Plots

Representative Frenkel-Halsey-Hill (FHH) plots are shown in Fig. 4.12 - 4.16. The ranges of linearity of the various FHH plots for nitrogen and water vapour respectively, are recorded in Table 4.2, together with the values of r (in the equation $\ln (Po/P) = k/\theta^r$) determined from the slopes of the plots (Section 2.4). Values of r for "ideal" FHH plots[32-34] are also included in the Table for the sake of comparison.

The non-porous texture of both TK 800 and Fransil was confirmed by the fact that the FHH plots (i.e. Curve 'A' in Fig. 4.13 and Fig. 4.15

respectively) for nitrogen adsorption on these samples were linear over a wide range of relative pressure, rarely less than 0.25 to 0.9. It is noteworthy that, for nitrogen adsorption on these adsorbents outgassed at 140°C, r = 2.73 for TK 800 (i.e. the mean of the two values in Table 4.2) whilst for Fransil, r = 2.95. According to Halsey,[35] the magnitude of r characterises the type of interaction between a vapour and the adsorbent surface; in the present instance, the respective values of r indicate the the specific adsorbent-adsorbate interactions of nitrogen with Fransil was greater than that with nitrogen on TK 800. It is interesting to note, by way of comparison, that Halsey[35] (utilising the data of Jura and Harkins[36]) found for nitrogen on a non-porous sample of anatase (TiO_2), a value of r = 2.67. In terms of the FHH Slab Theory[37,38] this would indicate that the surface of the TK 800 and that of anatase are energetically similar, and that both differ significantly from that of Fransil. Furthermore, Pierce[32,33] and Zettlemoyer[34] have suggested that the "ideal" isotherm for nitrogen on a polar surface is represented by a FHH plot for which r = 2.75, i.e. very close to the present value of 2.73 for nitrogen on TK 800.

For water adsorption on Fransil and TK 800 respectively, the contrast between the values of r is even greater. For example, one may take the case when each adsorbent was outgassed at 25°C, i.e. Curve 'B' in Fig. 4.15 and Curve 'A' in Fig. 4.16 respectively: for Fransil, r = 2.03 whilst for TK 800, r = 1.32 (Table 4.2). Clearly, therefore, the difference between the respective magnitudes of the specific adsorbent-adsorbate interactions with Fransil and TK 800 is greater for water than for nitrogen; this is presumably because of the very much greater specificity of water vapour adsorption. In contrast to nitrogen adsorption however, there is a considerable difference between the present values of r for water adsorption

on Fransil (r = 2.03) and on TK 800 (r = 1.32), on the one hand and published data for FHH plots of water vapour isotherms on the other hand: for example, Halsey[35] found r = 2.50 for anatase and similarly, Zettlemoyer[34] found r = 2.49 for a hydroxylated silica, in excellent agreement. Pierce and Ewing[39] have proposed that if an "abnormal" value of r is obtained from a liner FHH plot for a particular adsorbate, then it may be concluded that there was not unrestricted free surface adsorption on the adsorbent. However, in view of the fact that the r values in Table 4.2 are consistently low for water vapour adsorption, and are also located in a relatively narrow range (for TK 800), the question arises as to whether one can accept the limited published data as being representative of water vapour adsorption on a hydroxylated silica. Certainly, the present findings, and the scarcity of published FHH plots for water vapour isotherms, serve to show that a great deal more work is necessary to resolve this anomaly.

It is interesting to note from Table 4.2 that apparently either hydroxylation or dehydroxylation of a partially hydroxylated silica surface results in a reduction in the value of r for the FHH plots for both nitrogen and water vapour isotherms. For example, consider the case of nitrogen adsorption on TK 800 - II, for which the partially hydroxylated surface is represented by the sample outgassed at 25°C (r = 2.73): on soaking the sample in water vapour the degree of hydroxylation was increased (Section 4.3), and it resulted in a value of r = 2.39 (Curve 'A' in Fig. 4.12); on the other hand, when the sample was outgassed at 1000°C the degree of hydroxylation was reduced to almost zero, and a value of r = 2.63 resulted (Curve 'B' in Fig. 4.13). A similar phenomenon was found for water vapour adsorption on TK 800 - II (see Fig. 4.16), although outgassing of the sample

at 1000°C resulted in a greater reduction in the range of linearity of the FHH plot, than that for the corresponding nitrogen FHH plot. The soaking treatment resulted in an increased range of linearity of the FHH plots for the nitrogen and water vapour isotherms respectively, especially in the case of the latter.

The value of r, determined from a FHH plot, is primarily related to the diminution of forces emanating from an adsorbent surface with successive layers in the adsorbed film; i.e. the value of r is established in the multilayer region after the specific effects of the surface are dissipated.[34,35] The downward deviation from linearity of FHH plots below a relative pressure of about 0.15 Po corresponds to the monolayer region and is therefore of little significance. However, as already stated, Halsey[35] has proposed that a high value of r is indicative of specific adsorbent-adsorbate interactions, since the specific effects of the adsorbent surface decay rapidly with distance from the surface. Conversely, a low value of r may indicate that the specific effects of a surface have been reduced by a particular treatment of the adsorbent, so that dispersion forces now predominante. Thus, the above results for partially hydroxylated TK 800 indicate that, for both nitrogen and water vapour adsorption, the specific interactions are reduced by <u>either</u> an enhanced degree of hydroxylation (soaking TK 800 in water vapour) <u>or</u> by drastic dehydroxylation of the surface (outgassing TK 800 at 1000°C). A similar conclusion may be tentatively drawn from a study of the values of the BET C constants, recorded in column 6 of Table 4.1, for nitrogen adsorption on TK 800; the C constants for water adsorption on TK 800 (column 8 of Table 4.1) also show a similar trend.

The FHH plots for nitrogen adsorption on the mesoporous silica,

gel J, are shown in Fig. 4.14 for outgassing of the gel at 25°C (Curve 'A') and 1000°C (Curve 'B') respectively. The upward deviation and restricted range of linearity (Table 4.2) of each plot is clear evidence of capillary condensation. The magnitude of r for each plot was less for gel J than for TK 800 (suggesting that the surface of the mesoporous gel was energetically dissimilar to that of TK 800) but in other respects, gel J appeared to behave in a similar manner to TK 800 when outgassed at 1000°C.

Finally, in the case of argon adsorption on the silicas, the FHH plots were curved over almost the whole of the multilayer region, with a very restricted range of linearity. For example, the FHH plot for argon adsorption on TK 800-II outgassed at 140°C is shown as Curve 'B' in Fig. 4.12: the linearity is restricted to a relative pressure range of 0.35 to 0.65, for which the value of r = 2.39. It is interesting to note that this is identical with the value of r for nitrogen adsorption on fully hydroxylated TK 800 (Table 4.2). Payne[40] has found similar curves for argon adsorption on γ-Al_2O_3. The downward deviation from linearity of the FHH plot for argon above a relative pressure of about 0.65 Po (Curve 'B' in Fig. 4.12), is most probably explained by the particular choice[4] of the solid rather than the liquid as the reference state for the SVP of the adsorptive.

TABLE 4.2

Nitrogen and Water FHH Plots

SAMPLE	OUTGASSING TEMPERATURE (°C)	NITROGEN ADSORPTION		WATER ADSORPTION	
		LINEARITY (P/Po)	r	LINEARITY (P/Po)	r
"Ideal"	-	Polar	2.75	Hydrophilic	2.50
(Refs. 32-34)		Non-polar	2.12	Hydrophobic	1.3-1.9
[a]Fransil	25	0.20-0.85	2.87	0.25-0.75	1.64
Fransil	25	-	-	0.20-0.83	2.03
Fransil	140	0.30-0.90	2.95	-	-
[b]TK 800 II	25	0.20-0.93	2.39	0.20-0.90	1.19
[c]TK 800 II	25	0.20-0.85	2.73	0.15-0.65	1.32
[c]TK 800 II	140	0.25-0.95	2.69	0.20-0.70	1.23
[c]TK 800 III	140	0.30-0.95	2.76	-	-
[d]TK 800 II	1000	0.50-0.92	2.63	0.20-0.60	1.07
Gel J	25	0.05-0.45	2.26		
Gel J	1000	0.08-0.60	1.89	0.35-0.65	0.74

[a] For the purpose of comparison, the FHH plots for this sample of Fransil were constructed using the standard data published[7,8] for nitrogen adsorption, and the standard data tentatively proposed[41] for water adsorption.

[b] Fully hydroxylated TK 800, i.e. 'soaked'.

[c] Partially hydroxylated TK 800, i.e. as received.

[d] Dehydroxylated TK 800, i.e. outgassed at 1000°C.

NB The FHH plots of the nitrogen and water vapour adsorption isotherms on the microporous gel E (outgassed at 25°C and 1000°C) were, as expected, almost entirely non-linear, and were not suitable for analysis.

REFERENCES

1. R.A. Beebe, J.B. Beckwith and J.M. Honig, J. Amer. Chem. Soc., (1945) 67, 1554.
2. G.L. Gaines, J. Phys. Chem., (1958) 62, 1526.
3. G.G. Litvan, J. Phys. Chem., (1972) 76, 2584.
4. J.D. Carruthers, D.A. Payne, K.S.W. Sing and L.J. Stryker, J. Colloid Interface Sci., (1971) 36, 205.
5. M.R. Harris and K.S.W. Sing, Chem. and Ind., (1967) 757.
6. J.H. Singleton and G.D. Halsey, Can. J. Chem., (1955) 33, 184.
7. J.D. Carruthers, P.A. Cutting, R.E. Day, M.R. Harris, S.A. Mitchell and K.S.W. Sing, Chem. and Ind., (1968) 1772.
8. M.R. Bhambhani, P.A. Cutting, K.S.W. Sing and D.H. Turk, J. Colloid Interface Sci., (1972) 38, 109.
9. D.A. Payne, K.S.W. Sing and D.H. Turk, J. Colloid Interface Sci., (1973) 43, 287.
10. S.J. Gregg and K.S.W. Sing, "Adsorption, Surface Area and Porosity"; Academic Press, London, (1967) page 93.
11. A.V. Kiselev, "Proc. 2nd Int. Congr. Surface Activity", London, 1957. Butterworths, London, (1957) 2, 213 and 218.
12. J.H. de Boer, "The Structure and Properties of Porous Materials", Butterworths, London, (1958) page 68.
13. Reference 10, page 172.
14. J.W. McBain, J. Amer. Chem. Soc., (1935) 57, 699.
15. K.S. Rao, J. Phys. Chem., (1941) 45, 506 and 517.
16. S.M. Katz, J. Phys. Chem., (1949) 53, 1166.
17. Reference 10, pages 145 and 177.
18. A.V. Kiselev and E.V. Khrapova, Kolloid. Zh., (1957) 19, 572.
19. O.M. Dzhigit, A.V. Kiselev and G.G. Muttik, Kolloid. Zh., (1962) 24, 15.

20. A.P. Karnaukhov and A.V. Kiselev, Zh. Fiz. Khim., (1960) 34, 2146.

21. O.M. Dzhigit, A.V. Kiselev and G.G. Muttik, Kolloid. Zh., (1961) 23, 553.

22. R. Sh. Mikhail,S. Nashed and K.S.W. Sing, "Proc. Int. Symp. Pore Structure and Properties of Materials", Prague, 1973, In the Press.

23. J.W. McBain, Z. Physik. Chem., 68, 471; Phil. Mag., (1909) 916.

24. A.V. Kiselev, "The Structure and Properties of Porous Materials", Proc. 10th Symp. Colston Res. Soc., Bristol, 1958. Eds. D.H. Everett and F.S. Stone; Butterworths, London, (1958) page 195.

25. A.V. Kiselev, Discussions Faraday Soc., (1971) 52, 14.

26. L.T. Zhuravlev and A.V. Kiselev, "Proc. Int. Symp. Surface Area Determination", Bristol, 1969. Eds. D.H. Everett and R.H. Ottewill; Butterworths, London, (1970) 155.

27. J. Fripiat and J. Uytterhoeven, J. Phys. Chem., (1962) 66, 800.

28. Ya. Ya. Ekabson, A.V. Kiselev, B.V. Kuznetsov and Yu. S. Nikitin, Kolloid. Zh., (1970) 32, 41.

29. R.L. Gorelik, L.T. Zhuravlev, A.V. Kiselev, Yu. S. Nikitin, E.B. Oganesyan and K. Ya. Shengeliya, Kolloid. Zh., (1971) 33, 51.

30. J.A.G. Taylor and J.A. Hockey, J. Phys. Chem., (1966) 70, 2169.

31. K.S.W. Sing and V.R. Ramakrishna, "Colloques Internationaux du C.N.R.S.", Thermochimie, (1971) No 201, 435.

32. C. Pierce, J. Phys. Chem., (1959) 63, 1076; ibid.,

33. C. Pierce, J. Phys. Chem., (1968) 72, 3673; ibid., (1969) 73, 813.

34. A.C. Zettlemoyer, J. Colloid Interface Sci., (1968) 28, 343.

35. G.D. Halsey, J. Chem. Phys., (1948) 16, 931.

36. G. Jura and W.D. Harkins, J.Amer. Chem. Soc., (1944) 66, 1356.

37. T.L. Hill, "Advances in Catalysis", Academic Press, New York, (1952) 4, 211

38. D.M. Young and A.D. Crowell, "Physical Adsorption of Gases", Butterworths, London, (1962) 167.

39. C. Pierce and B. Ewing, J. Amer. Chem. Soc., (1962) 84, 4070.

40. D.A. Payne, Ph.D. Thesis, Brunel University, (1970).

41. J.D. Carruthers, Ph.D. Thesis, Brunel University, (1968).

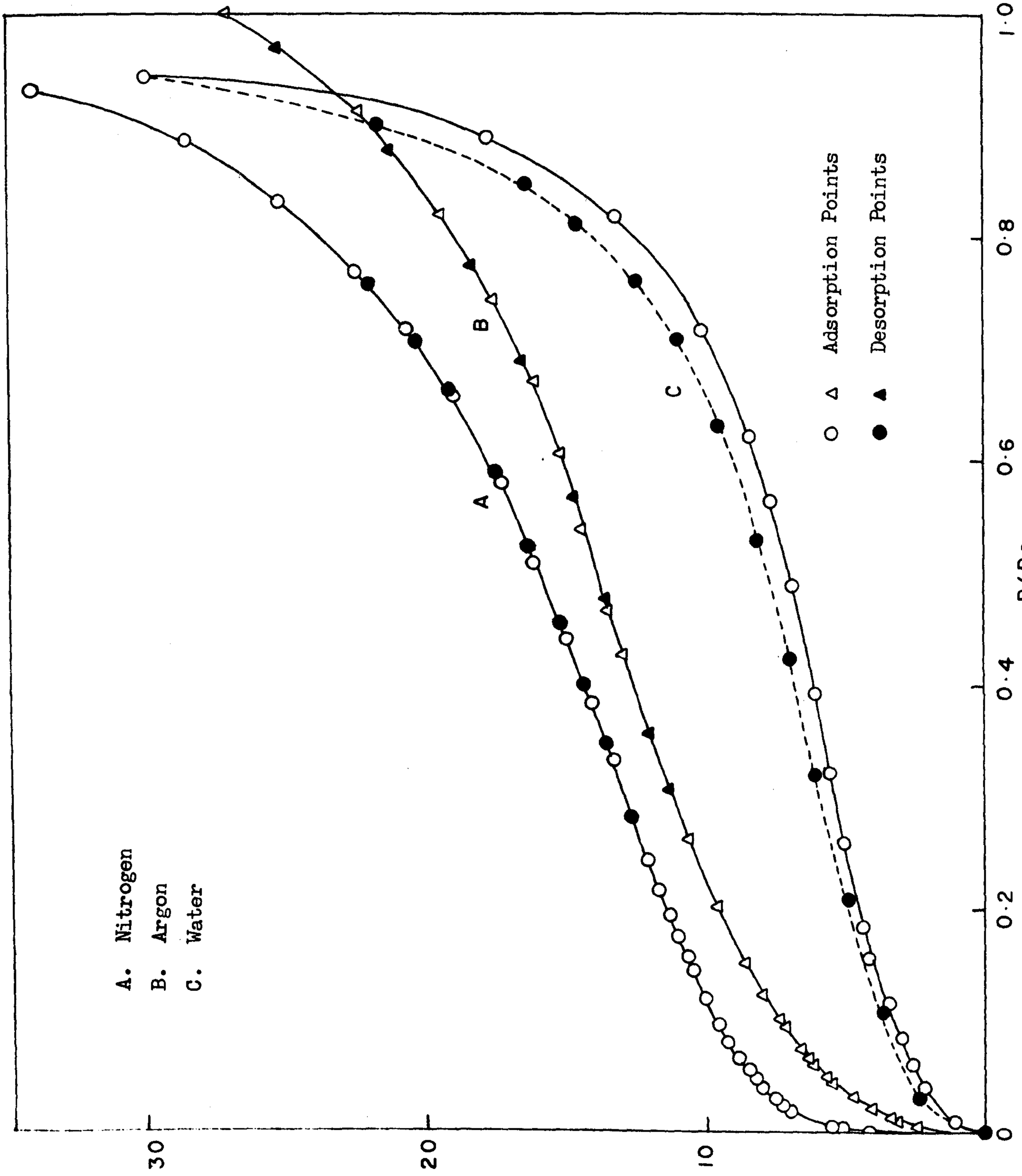

FIG 4.1 Nitrogen, Argon and Water Vapour Isotherms Determined on Transil

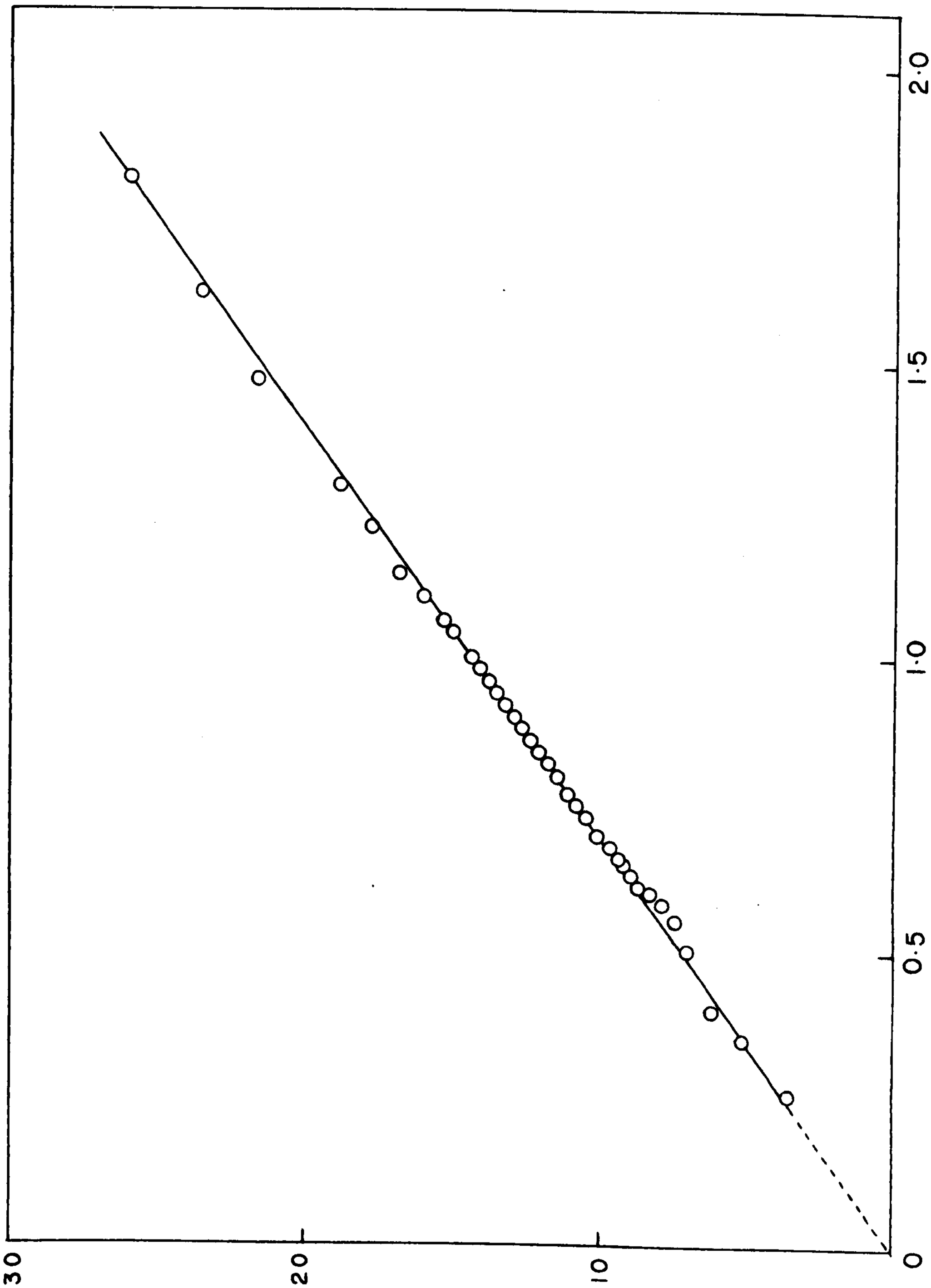

FIG 4.2 α_s-plot for Nitrogen Adsorption on Fransil Outgassed @ 140°C

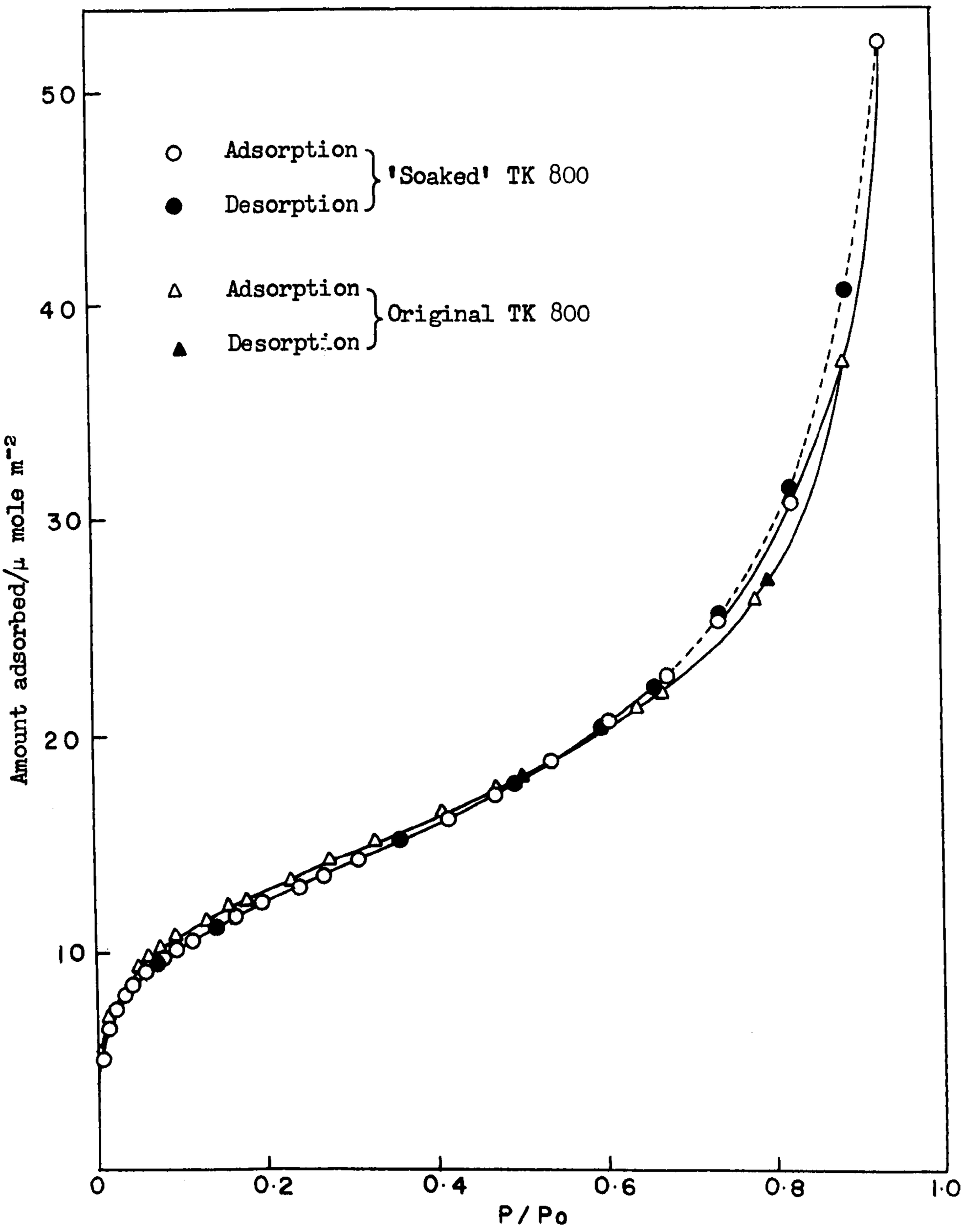

FIG 4.3 Nitrogen Adsorption @ -196°C on TK 800 Outgassed @ 25°C

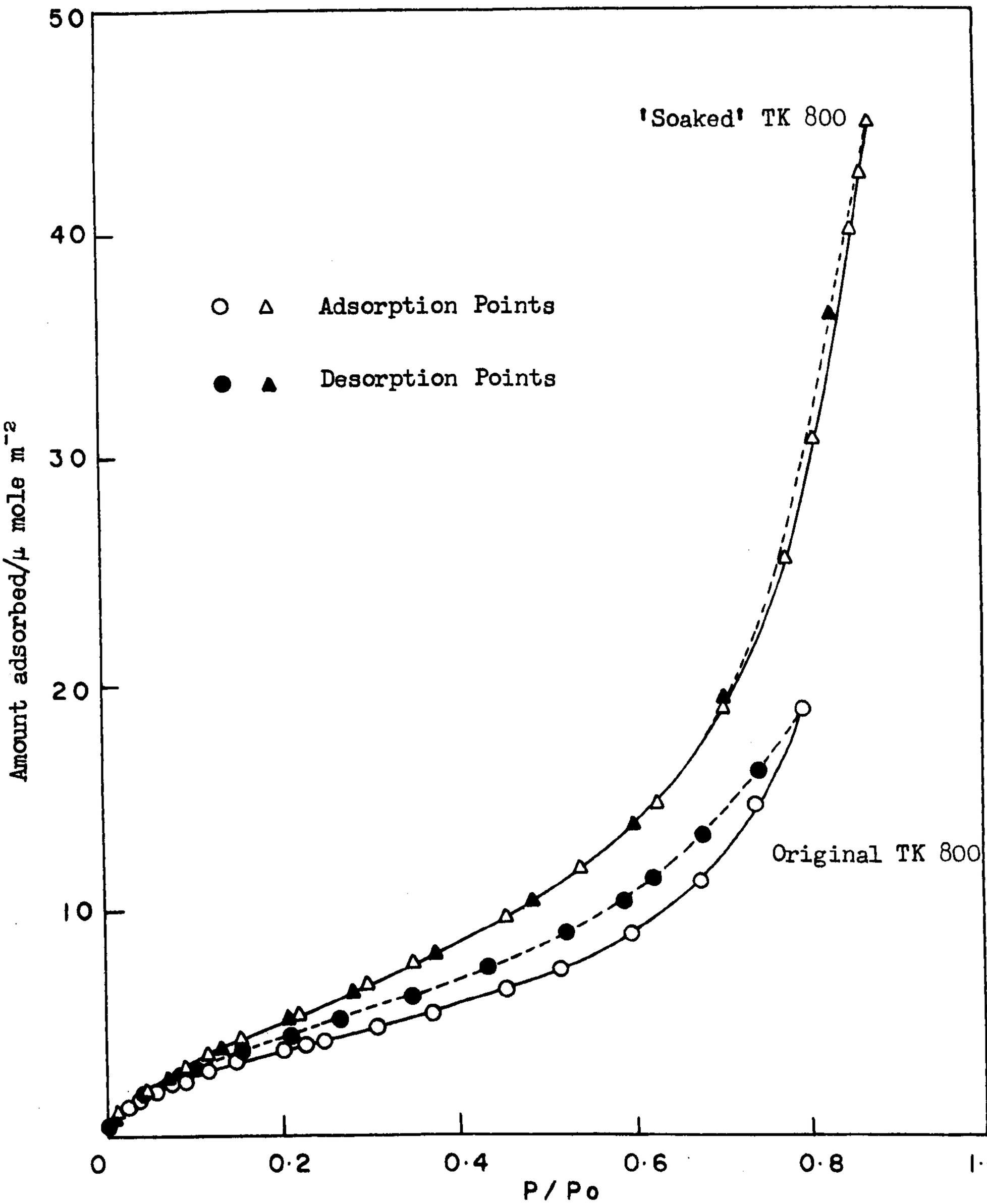

FIG 4.4 **Water Vapour Adsorption** @ 25°C on TK 800 Outgassed @ 25°C

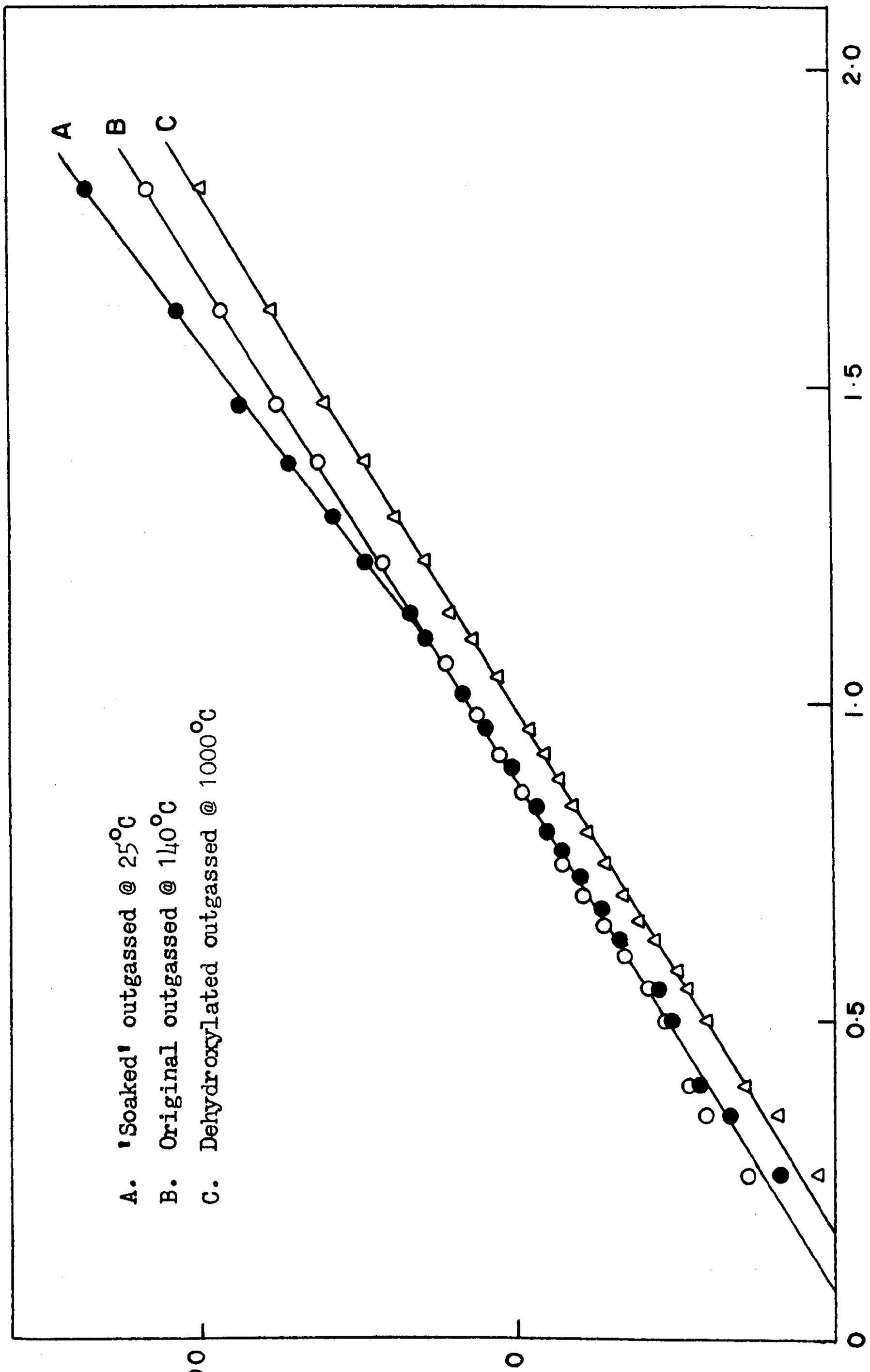

FIG 4.5 α_s-plots for Nitrogen Adsorption on TK 800

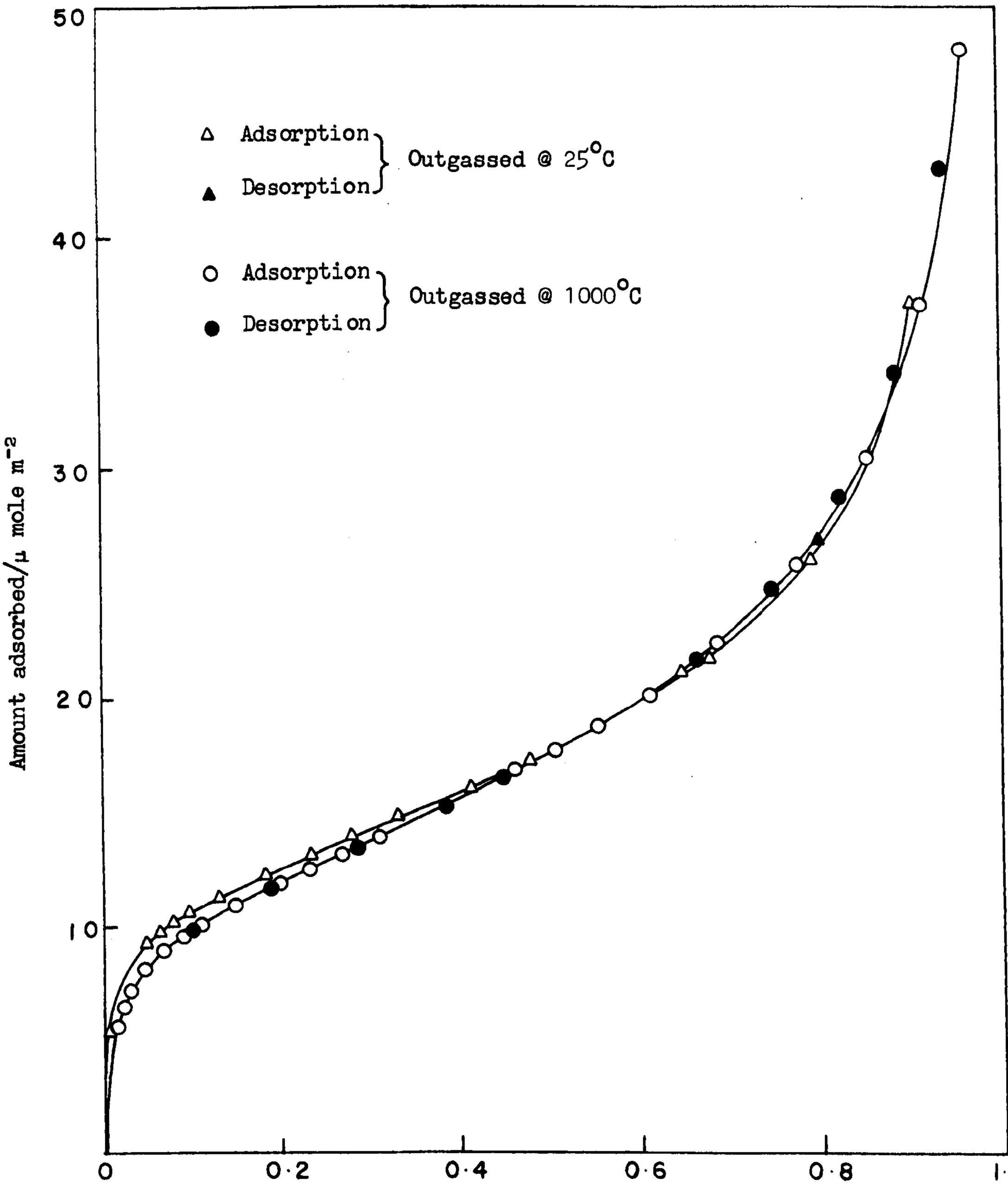

FIG 4.6 Nitrogen Adsorption @ -196°C on TK 800 Outgassed @ 25° and 1000°C respectively

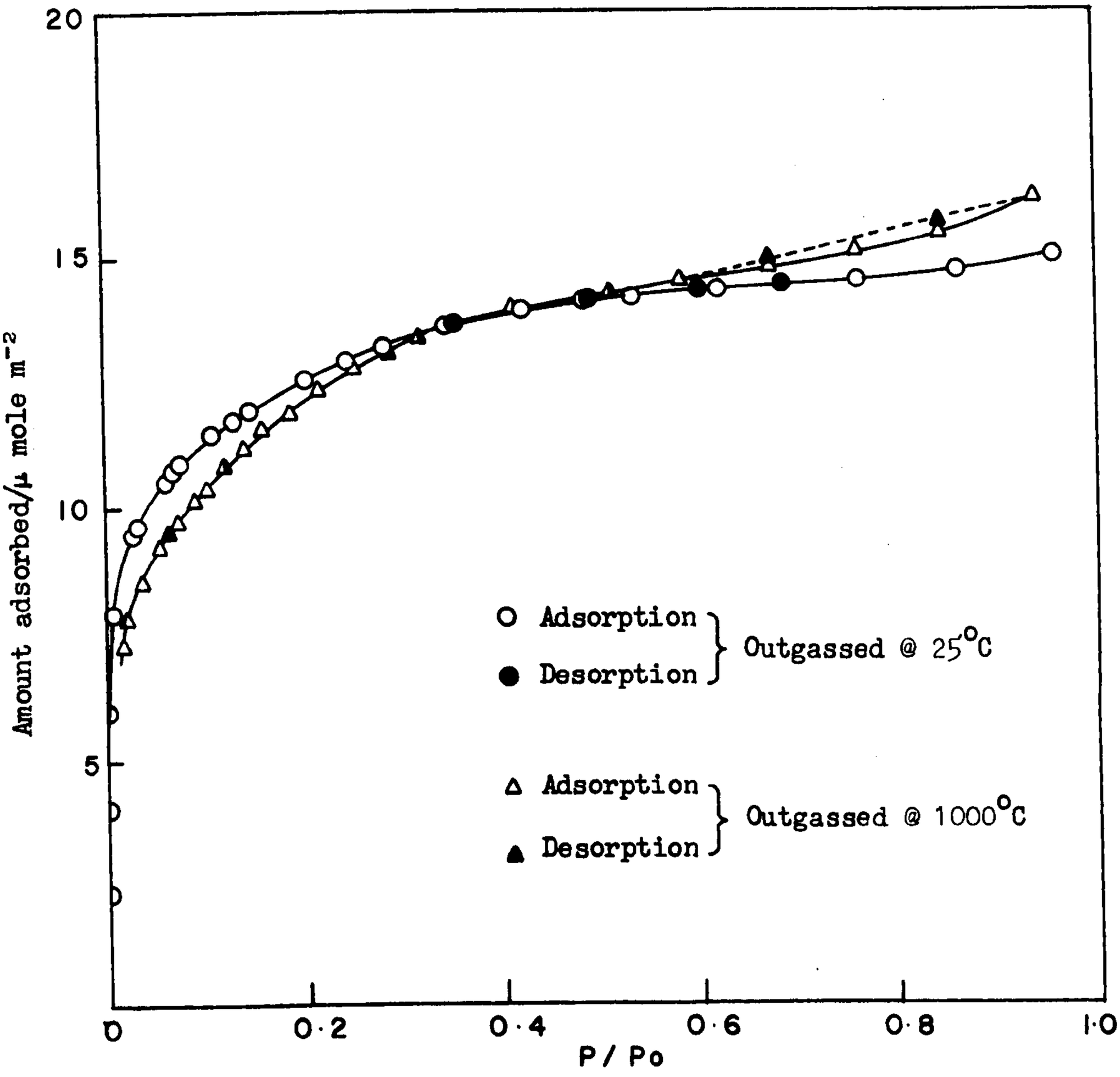

FIG 4.7 Nitrogen Adsorption @ -196°C on Microporous Silica Gel E Outgassed @ 25° and 1000°C respectively

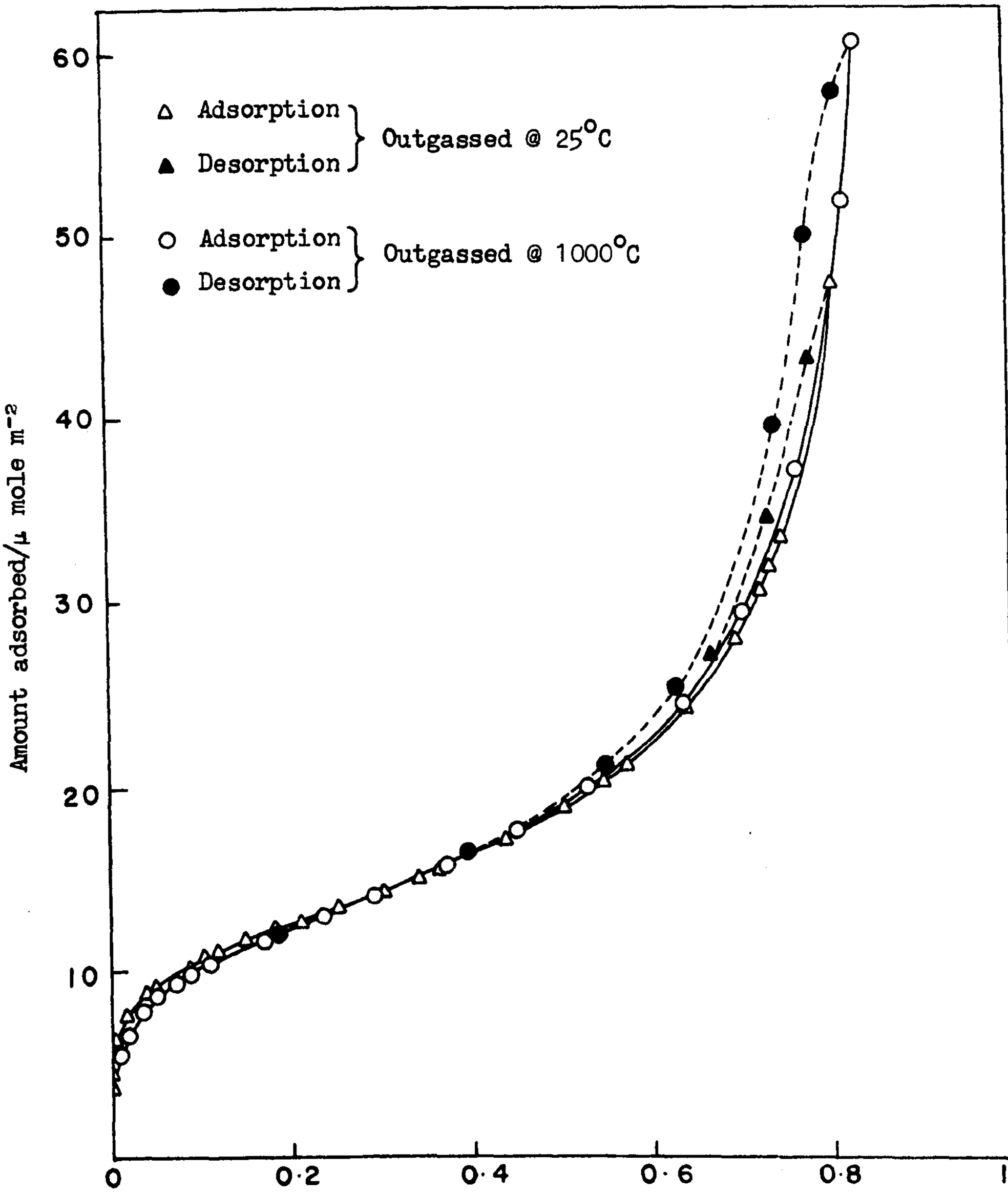

FIG 4.8 Nitrogen Adsorption @ -196°C on Mesoporous Silica Gel J Outgassed @ 25° and 1000°C respectively

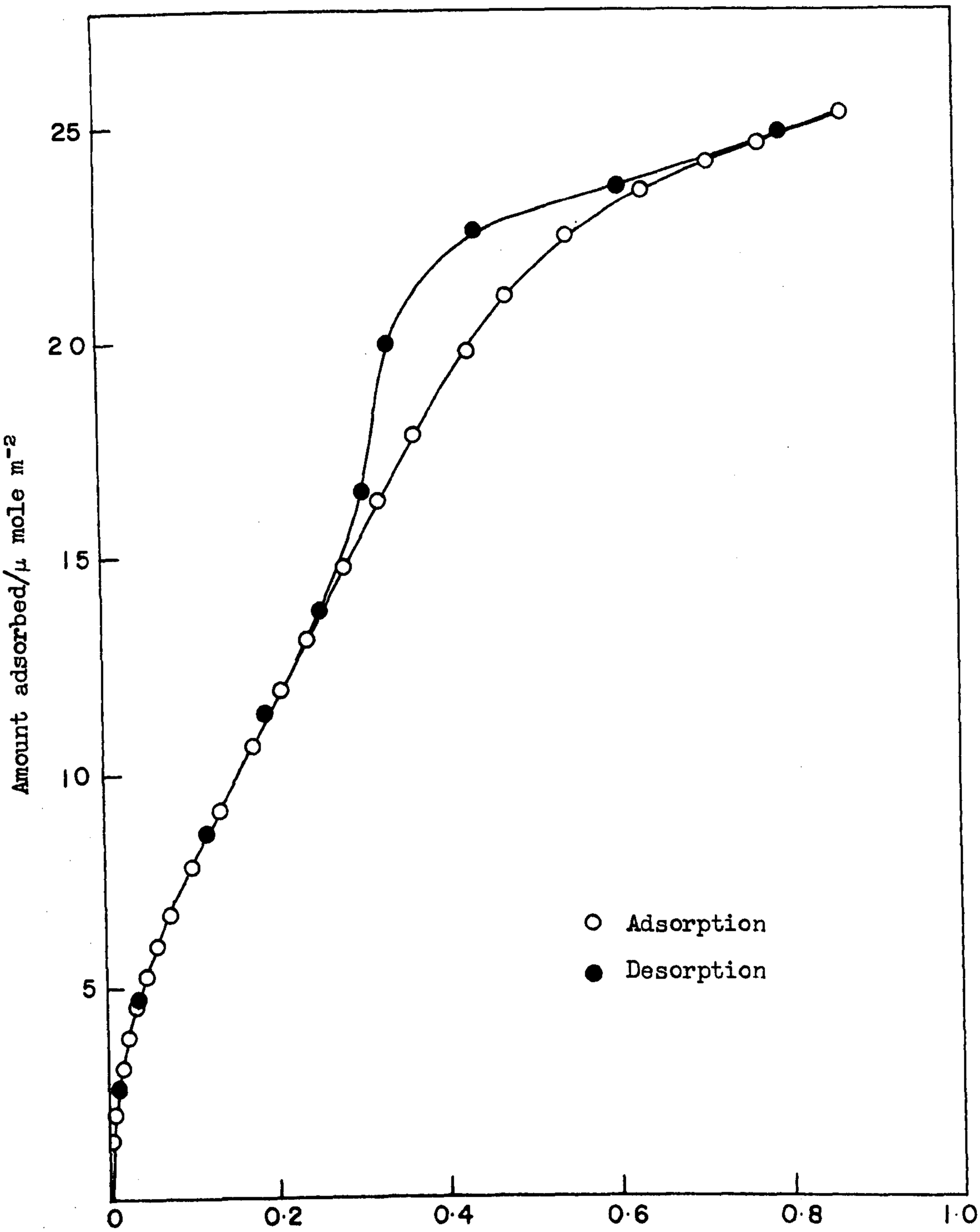

FIG 4.9 Water Vapour Adsorption @ 25°C on Microporous Silica Gel E Outgassed @ 25°C

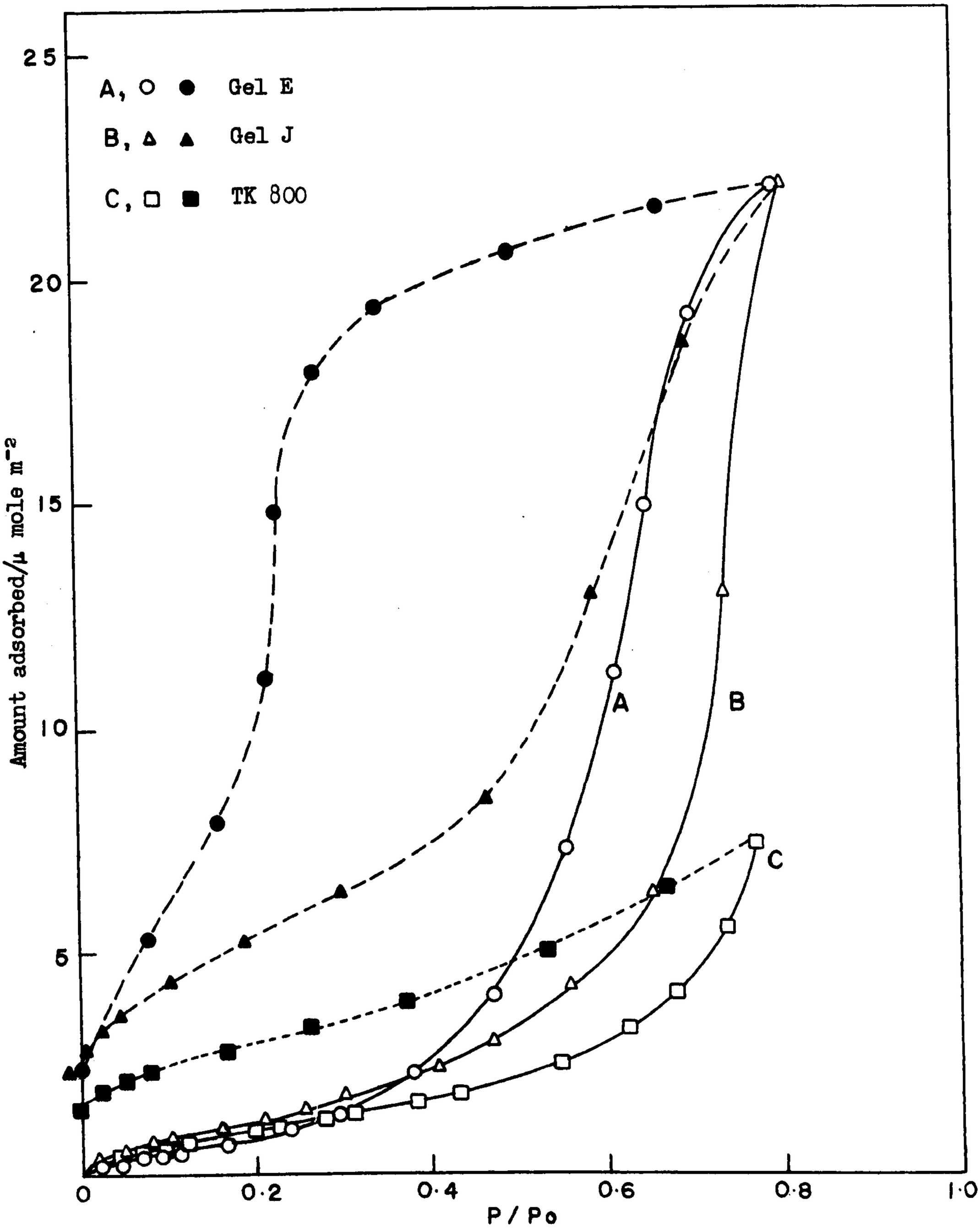

FIG 4.10 Water Vapour Adsorption @ 25°C on Silicas Outgassed @ 1000°C

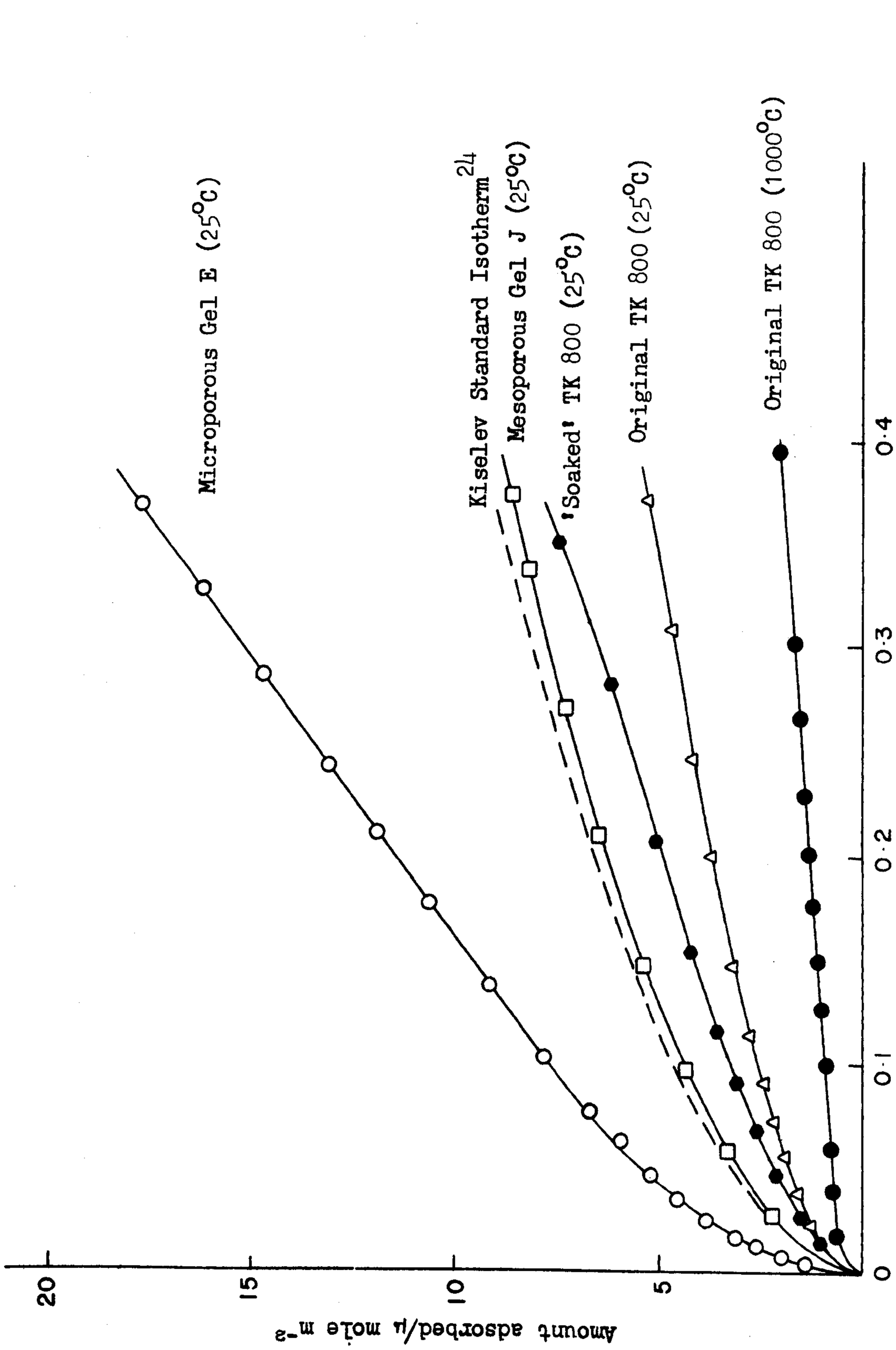

FIG 4.11 Water Vapour Adsorption @ 25°C on Silicas

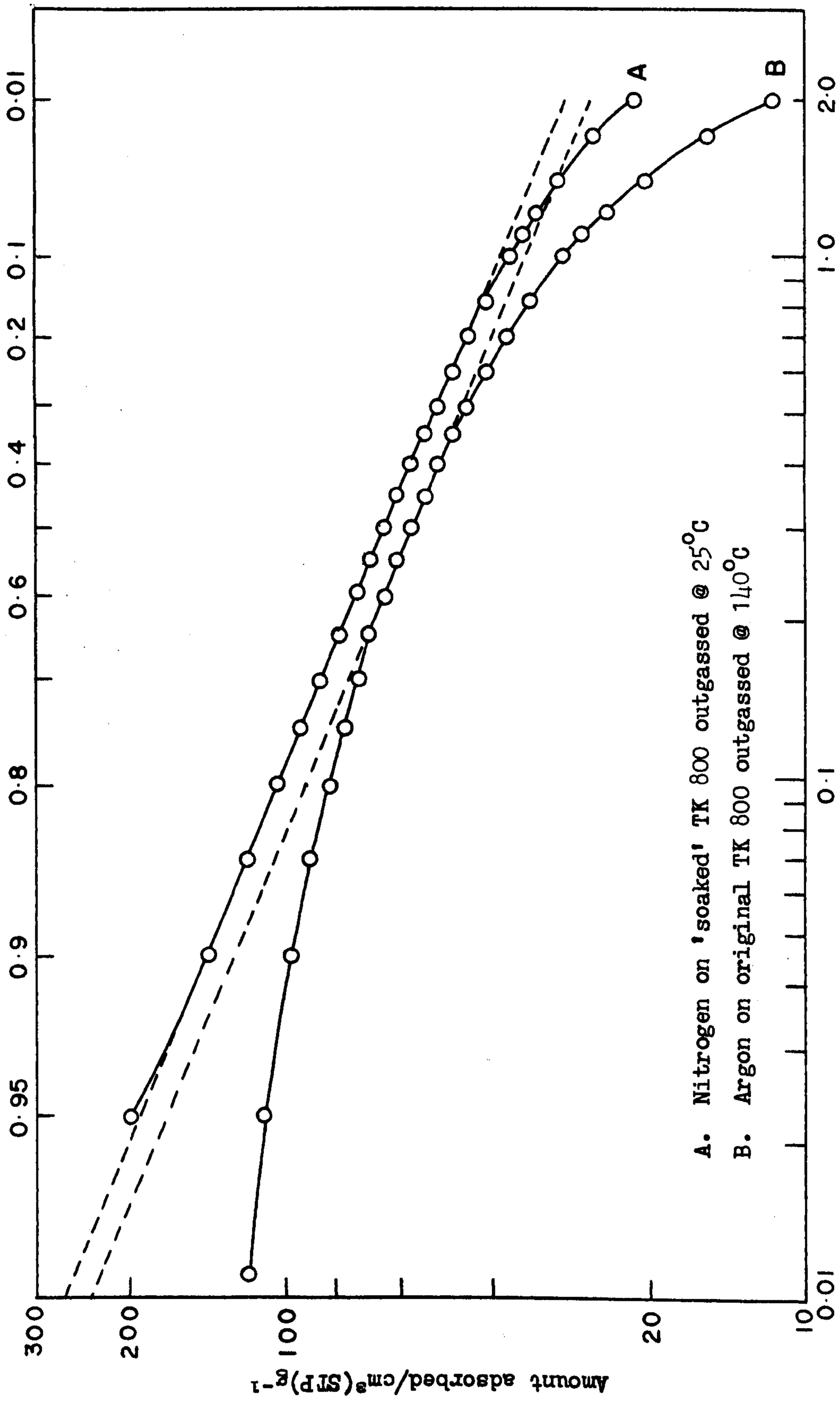

FIG 4.12 FHH Plots for Nitrogen and Argon Adsorption on TK 800

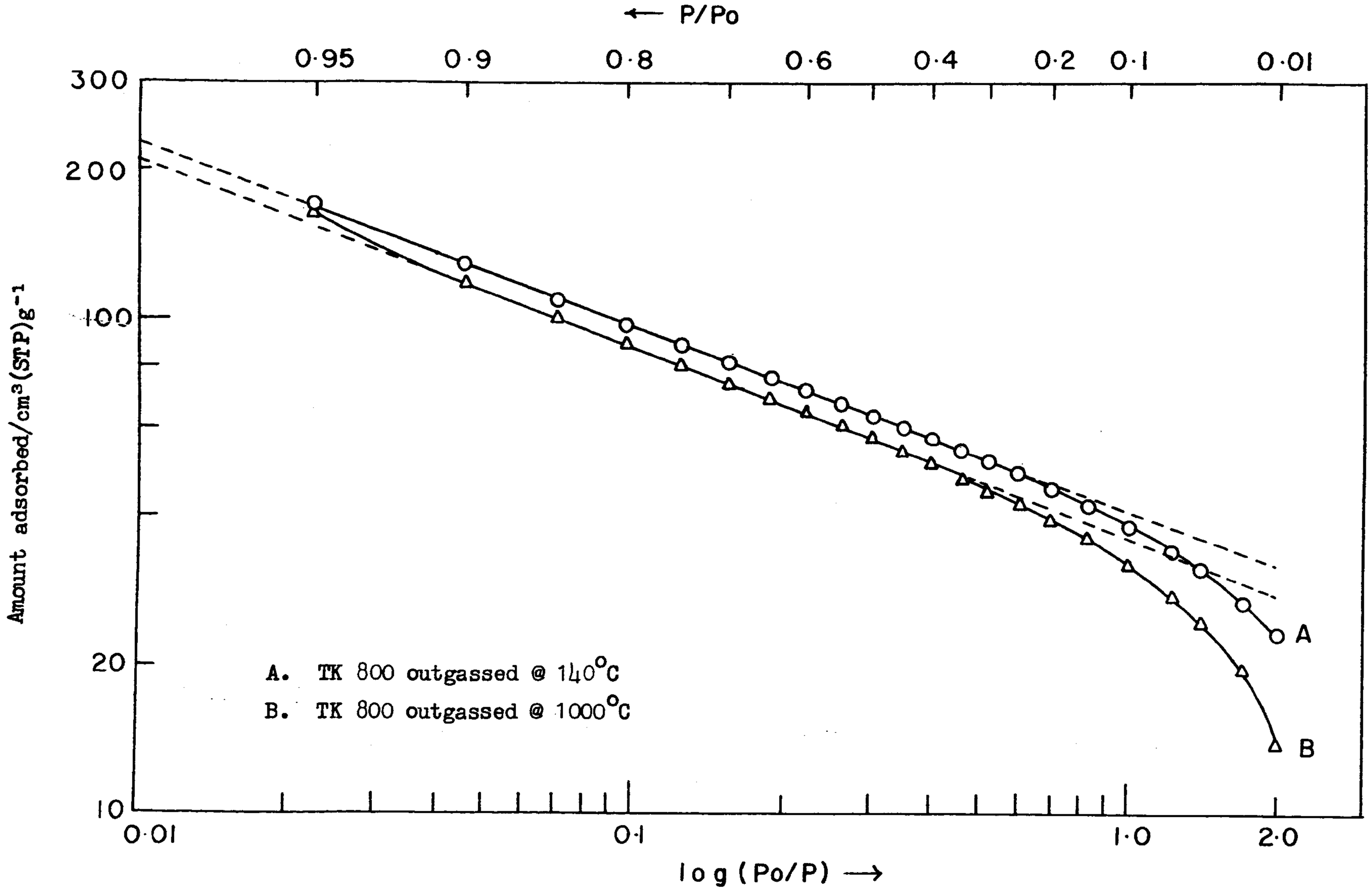

FIG 4.13 FHH Plots for Nitrogen Adsorption on TK 800

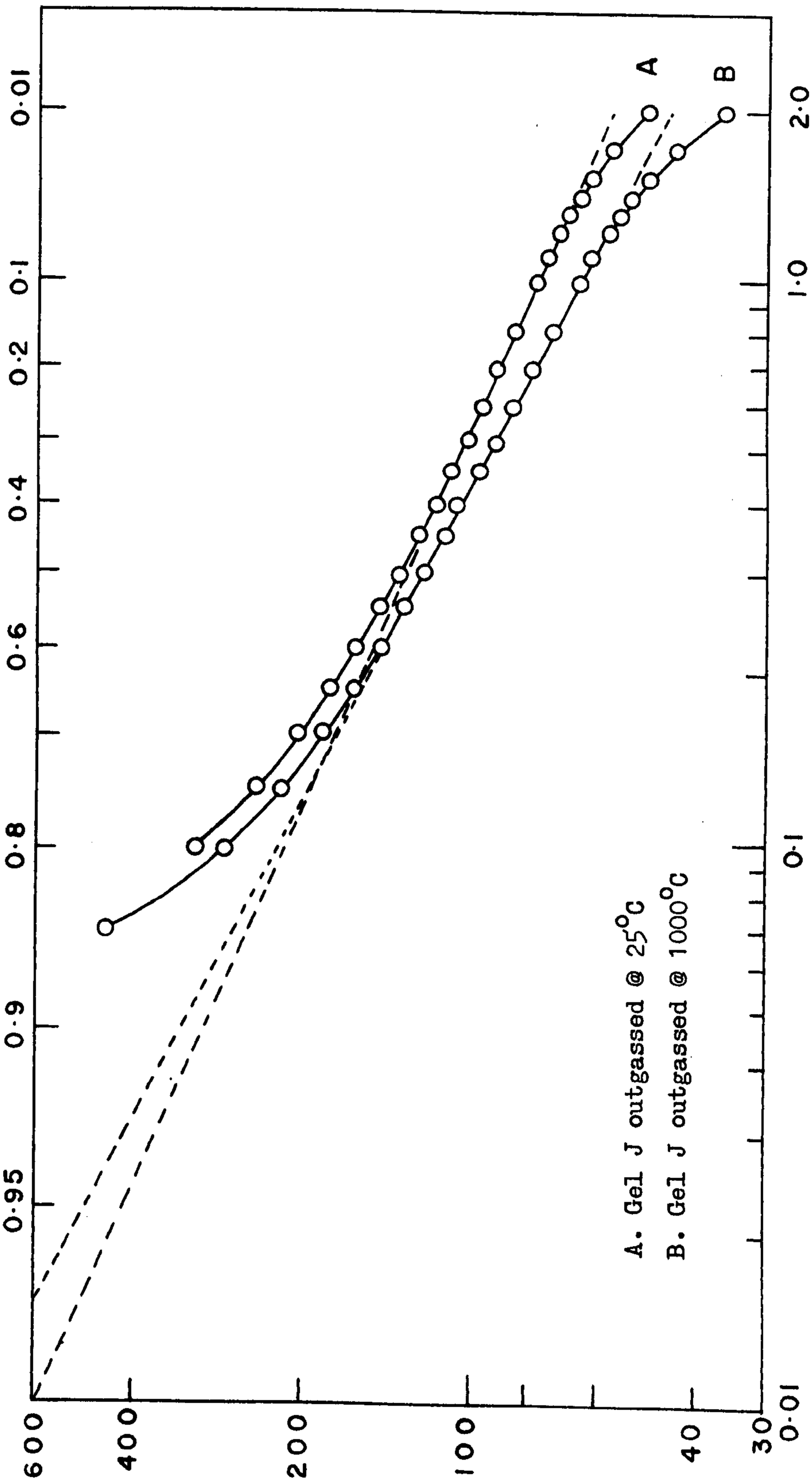

FIG 4.14 FHH Plots for Nitrogen Adsorption on Silica Gel J

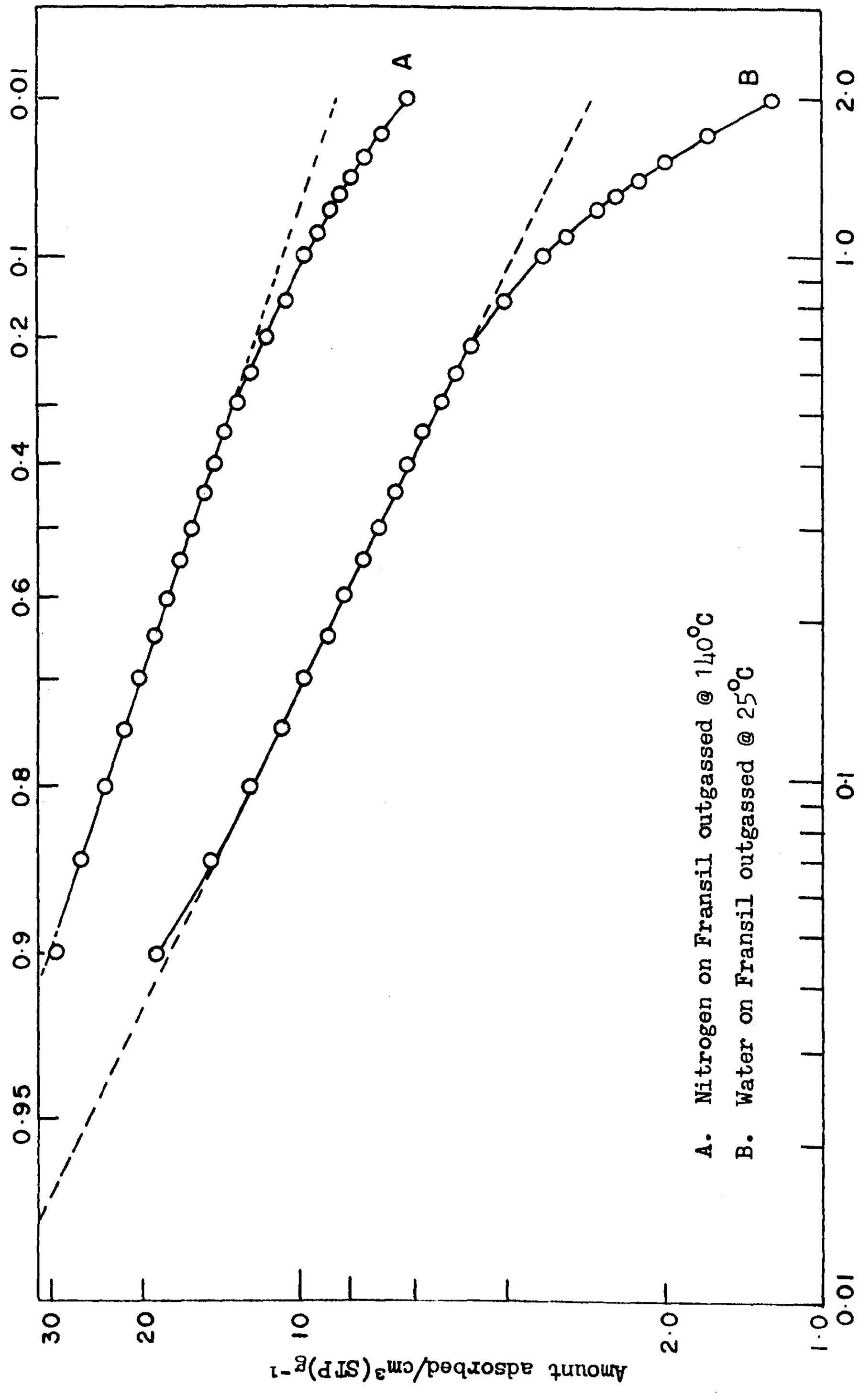

FIG 4.15 FHH Plots for Nitrogen and Water Vapour Adsorption on Fransil

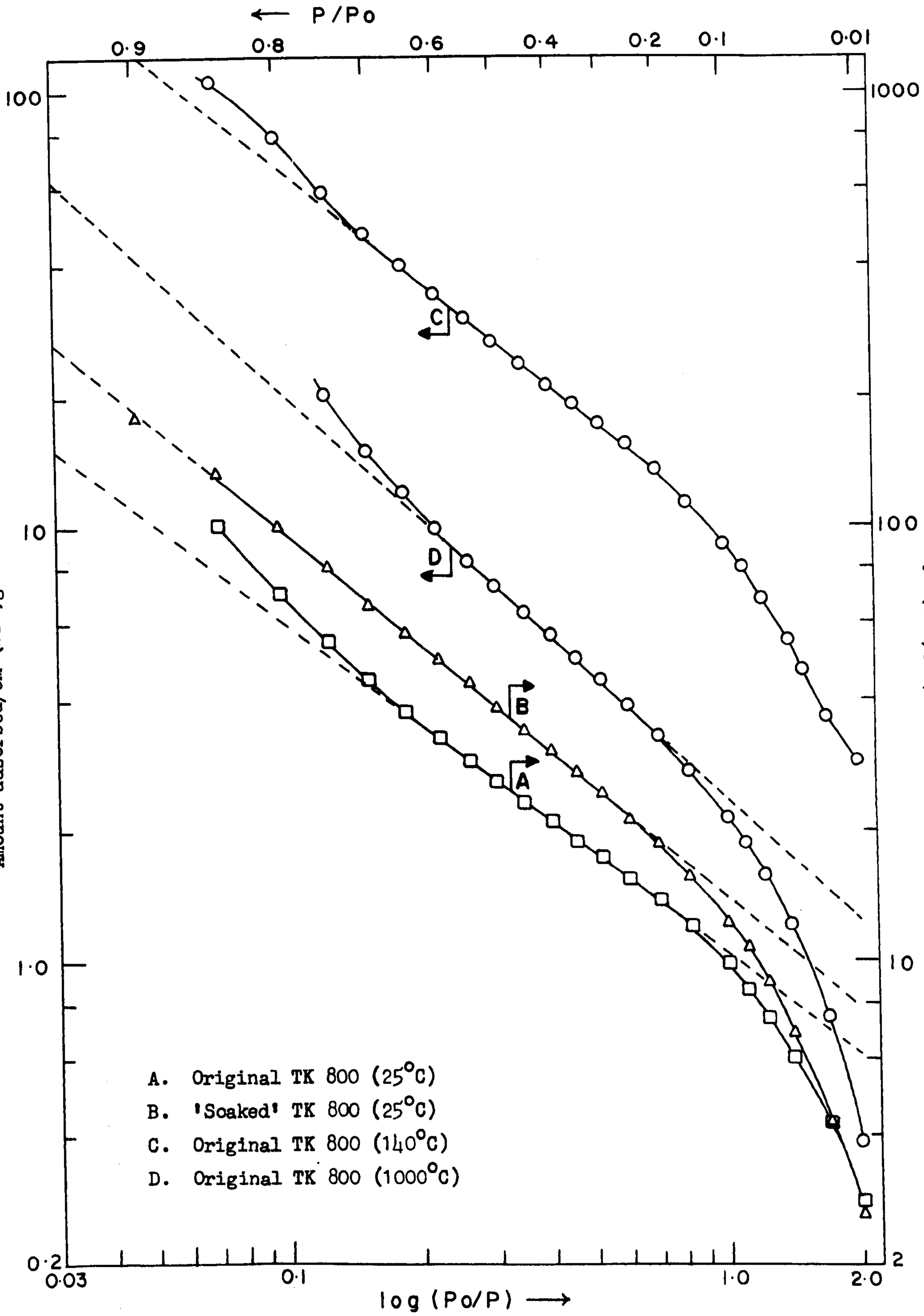

FIG 4.16 FHH Plots of Water Vapour Adsorption on TK 800

C H A P T E R 5

RESULTS AND DISCUSSION II

MERCURY VAPOUR ADSORPTION ON CHROMIUM OXIDES

In the present chapter, the adsorption of mercury vapour on certain chromium oxide surfaces is discussed. An explanation as to why mercury vapour is irreversibly adsorbed is presented. The gravimetric techniques utilised in this study were described in Chapter 3, whilst the relevant mercury adsorption data are tabulated in Appendix 6.

5.1 Mercury Vapour Adsorption on Chromium Oxide Gels

During the prolonged outgassing of certain calcined chromia gels at 25°C, it was observed[1] that the weight of the sample decreased to a minimum (after 2-3 hours) and then underwent a slow but uniform rate of increase. The weight change was arrested by the introduction of a small pressure of a permanent gas (e.g. nitrogen), but the same rate of increase was restored on continuation of the outgassing. When similar experiments were performed using a Gulbransen microbalance (in place of the spring balance) and a mercury-free adsorption system, no increase in weight could be observed. It seemed likely that the weight increase was due to the adsorption of mercury vapour, which originated from various exposed mercury surfaces in the system, e.g. the manometer. To test this hypothesis, a systematic study was undertaken in which mercury vapour was introduced at will into the adsorption system.

A sample of chromia gel A1 was heated in air at 225°C for 16 hours to give gel A1(225)16. In Fig. 5.1, the influence of mercury vapour on the weight of the calcined sample, during outgassing at 25°C, is shown as a function of time. For the sake of convenience, the variable time scale is interrupted between 59 and 75 hours.

The curve lying between points 'A' and 'B' in Fig. 5.1, represents the weight loss of A1(225)16 on outgassing (to about 10^{-4} torr) in the absence of mercury vapour; after a period of about 55 hours, a maximum weight loss was achieved. At point 'B', the sample was exposed to mercury vapour (mercury source at 22°C) and immediately, a steady increase in the weight of the sample was observed: between points 'B' and 'C', the rate of increase was about 2.2 mg g^{-1} h^{-1}.At point 'C', the mercury source was isolated, the weight of the sample then remaining constant over a period of several hours until mercury vapour was re-introduced into the system at point 'D'. To test whether the weight increase of the sample was a function of the pressure of mercury vapour, the temperature of the mercury source was raised to 65°C: between points 'D' and 'E', the rate of increase was now about 3.2 mg g^{-1} h^{-1}. At point 'E', both the mercury source and the pumping system were isolated, and pure oxygen at a pressure of 1 torr introduced to the sample. The small weight increase between points 'E' and 'F' was probably due to the chemisorption of oxygen by A1(225)16: in a similar experiment where pure nitrogen or helium was introduced (in place of oxygen), the sample weight remained constant. At point 'F', the sample was re-exposed to high vacuum, and mercury vapour (from a source at 35°C) re-introduced into the system: between points 'F' and 'G', the rate of increase was about 2.5 mg g^{-1} h^{-1}. Finally, at point 'G', the mercury source was isolated from the system and the sample outgassed (at 25°C and about 10^{-5} torr pressure) over a period of several weeks: no significant weight loss of the sample was observed.

Put in a more succinct manner, these results show that mercury vapour was adsorbed, apparently irreversibly, by gel A1(225)16 and furthermore, that the rate of adsorption was a function of the mercury vapour pressure.

A number of other experiments showed[2] that mercury vapour adsorption was not exhibited by orthorhombic chromium oxy-hydroxide, nor by chromia gels calcined (or outgassed) at temperatures lower than about 150°C, or at temperatures above that of the glow phenomenon.[3] Positive identification of mercury adsorbed on the activated gels after exposure to the vapour, was obtained from the atomic absorption studies described in Section 3.9.

5.2 Mercury Vapour Adsorption on Chromium Dioxide

When a sample of pure chromium dioxide was outgassed, in the presence of mercury vapour, the weight of the sample was observed to increase. The rate of increase was particularly high at pressures less than about 10^{-3} torr. The mercury vapour was irreversibly adsorbed, outgassing at a temperature of 250°C failing to result in a significant weight loss of the sample. To study the effect of mercury vapour adsorption by chromium dioxide, on the subsequent sorptive properties of this oxide, a series of experiments were constructed as follows:

(1) A sample of chromium dioxide was outgassed at 25°C in the complete absence of mercury vapour, and the water vapour adsorption/desorption isotherm determined (shown as Fig. 5.3).

(2) On completion of the first water vapour isotherm, the sample was re-outgassed at 25°C in the presence of mercury vapour until a maximum weight gain was achieved (represented by Curve A in Fig. 5.2): the mercury source was then isolated, the sample further outgassed

at 25°C in order to remove residual mercury vapour from the system, and a second water vapour adsorption/desorption isotherm determined (shown as Fig. 5.4).

(3) On completion of the second isotherm, the sample was again re-outgassed in the presence of mercury vapour until a maximum weight gain was achieved (represented by Curve B in Fig. 5.2): a third water vapour adsorption/desorption isotherm was then determined, but this time in the presence of mercury vapour (shown as Fig. 5.5).

Throughout this series of experiments, the temperature of the mercury vapour source was maintained at 25.0°C, whilst equilibrium pressure measurements were made (to $\pm$ 6 x 10^{-3} torr) using a pressure-sensitive transducer (cf. Sections 3.13 and 3.18).

Curves A and B in Fig. 5.2 represent the uptakes of mercury vapour by the sample of chromium dioxide, on outgassing at 25°C in the interval between the first and second, and between the second and third water vapour isotherms respectively. Limiting values for the uptakes, of about 13.5 mg g^{-1} and 8 mg g^{-1} respectively, were observed after outgassing for about 25 hours. This result, and those of subsequent experiments, showed that after apparent saturation of the chromium dioxide surface with mercury, the surface was re-activated to further mercury vapour adsorption by exposure to water vapour. This effect could be repeated many times;on each subsequent occasion a smaller quantity of mercury vapour was adsorbed. Furthermore, in general, satisfactory agreement was obtained between the values of the mercury vapour uptakes as estimated by the gravimetric studies on the one hand, and the atomic absorption technique on the other: for example, 20.6 mg g^{-1} (gravimetric) and 18.5 mg g^{-1} (atomic absorption).

The water vapour isotherm, determined on the pure chromium dioxide in the complete absence of mercury vapour (Fig. 5.3),exhibited hysteresis over the full range of relative pressure, with some permanent retention of water. Although the adsorption isotherm exhibited some broad stepwise character (where the initial step was located near the monolayer capacity), a nearly linear BET plot was obtained in the relative pressure range of 0.07 to 0.3 Po. From the plot a value of 6.5 m^2g^{-1} was obtained for the apparent BET surface area as measured by water vapour adsorption, whilst the BET C constant was very high at 1800. The high value of the BET C constant implies that there was a strong localisation of the water monolayer on the clean chromium dioxide surface; probably to such an extent that the cross-sectional area of the adsorbed water molecule (an apparent value of 10.6 $Å^2$ was assumed for the purposes of the calculations)was greatly influenced by the nature of the adsorbent. Thus, the value for the apparent BET surface area, S^W_{BET}, may be in error.

By way of comparison, it is interesting to note that in the case of water vapour adsorption on thorium oxide surfaces, Holmes and his co-workers[4] have constructed the BET plots using the desorption branch of the irreversible isotherms. The adsorption branches were not used to calculate BET surface areas because of the initial chemisorption of water vapour by the thorium oxide surfaces. When this procedure was performed in the present case, for water vapour adsorption on the clean chromium dioxide surface, a BET plot showing excellent linearity was obtained in the relative pressure range of 0.05 to 0.3 Po; the corresponding values of S^W_{BET} and the BET C constant, as calculated using this plot, were 8.1 m^2g^{-1} and 620 respectively. Thus, the value of C still reflects the high reactivity of the clean chromium dioxide surface,

whilst the value of S^{W}_{BET} may represent the apparent water BET surface area more realistically.

The water vapour isotherm determined on the mercury-contaminated surface of chromium dioxide (Fig. 5.4), was reversible at high relative pressures but exhibited hysteresis from a relative pressure of about 0.7 Po to zero relative pressure. However, perhaps of greatest significance, is the dramatic change in the shape of the adsorption branch. For ease of comparison, the adsorption branch is also shown superposed (as a dashed line) on the isotherm determined on the clean chromium dioxide surface (Fig. 5.3). The BET plot, constructed using the adsorption data, was reasonably linear in a relative pressure range of 0.1 to 0.3 Po: the apparent BET surface area as measured by water vapour adsorption was 10.4 m^2g^{-1}, whilst the value of the BET C constant was less than 10. From this result it is inferred that the adsorption of mercury vapour has considerably reduced the reactivity of the chromium dioxide surface.

The third water vapour isotherm, determined on the mercury-contaminated surface of chromium dioxide in the presence of mercury vapour (Fig. 5.5), revealed that the general shape of the adsorption branch was further changed very little, as compared to that of the second isotherm (Fig. 5.4). The BET plot, constructed using the adsorption data, was very similar to that described for the second isotherm, yielding identical values of S^{W}_{BET} and C; i.e. 10.4 m^2g^{-1} and < 10 respectively. However, the isotherm exhibited an increased degree of reversibility at high relative pressures, low pressure 'hysteresis' commencing at about 0.45 Po. The interesting, and somewhat unusual, low pressure 'hysteresis loop' was the result of an additional experiment to confirm[2] that the low pressure 'hysteresis' was, in fact, a

consequence of mercury vapour adsorption on the chromium dioxide surface.

At the point on the isotherm where the apparent relative pressure in the system had been reduced to about 0.27 Po (i.e. point 'A' in Fig. 5.5), the chromium dioxide sample was left exposed to the mercury-contaminated atmosphere over a period of 64 hours, adsorption measurements being made at periodic intervals of about 20 hours. The vertical region of the 'hysteresis loop' was interpreted as being a direct consequence of the increased time of exposure of the sample to both mercury vapour (low partial pressure) and water vapour. At point 'B', the pressure in the system was progressively reduced again, each desorption point being recorded after an interval of about 3 hours. At point 'C', outgassing of the chromium dioxide sample at 25°C was commenced, mercury vapour adsorption then becoming particularly pronounced (as indicated by the points located on the ordinate at P/Po = 0 in Fig. 5.5.).

Thus, mercury vapour adsorption on a chromium dioxide surface in the presence of water vapour may well occur over a wide range of relative pressure, the rate of adsorption increasing with the partial pressure of mercury vapour.

The progressive increase in the reversibility, at high relative pressures, of the successive water vapour isotherms probably indicates that mercury, irreversibly adsorbed by the chromium dioxide, was blocking very fine pores which, in the case of the clean surface, were just accessible to penetration by water molecules. In the case of nitrogen adsorption on chromium dioxide, reversible isotherms were obtained with no indication of the presence of porosity.[5] However, it must be borne in mind that a conventional volumetric technique was employed for the

determination of the nitrogen isotherms: i.e. the adsorbent was always exposed to mercury vapour. At the present time, it is not known whether the fine pores present in the chromium dioxide sample (as apparently revealed by water vapour adsorption), were also accessible to penetration by nitrogen molecules.

5.3 Interaction of Chromium Oxides and Mercury Vapour

Samples of chromia gel A1 were calcined in air at selected temperatures between 100° and 1000°C (in 50° increments to 500°C, and 100° increments to 1000°C), and then exposed (in a low vacuum of about 10^{-2} torr) to mercury vapour at 25°C for a period of 5 days. The samples so treated were analysed for mercury content, using the atomic absorption technique described in Section 3.9.

The presence of mercury was found in those samples of gel A1 that had been calcined at temperatures in the range of 150° - 450°C. The greatest mercury content was observed in the case of the sample, A1(300), calcined at 300°C. In order to see if the adsorbed mercury could be removed by outgassing at high temperatures, A1(300) was progressively outgassed at temperatures between 100°C and 1000°C (duration of 2 hours at each temperature), and small samples, at 50°C increments, removed for analysis. Little significant variation in the respective mercury contents were found in the case of those samples outgassed at temperatures up to 350°C; at 400°C, however, the mercury content was considerably reduced (from 80 mg g^{-1} to 15 mg g^{-1}), whilst at temperatures of 500°C and above, the presence of mercury could not be detected.

These results indicated that chromia gels activated towards mercury vapour adsorption when calcined at temperatures in the range of about 150°

to 450°C; particularly so at about 300°C. Furthermore, the species formed as a result of the mercury vapour adsorption appeared to be stable at temperatures up to about 400°C, thereafter presumably decomposing to yield mercury. On the basis of these results, it is tentatively proposed that the adsorption of mercury vapour by certain chromium oxides, leads to the formation of a mercury chromate (or chromates), e.g. $HgCrO_4$, or possibly a 'chromite', e.g. $HgCr_2O_4$.

Aurivillius,[6,7] in a series of extensive studies of mercury (II) salts, prepared the mercury (II) chromate anhydrate, $HgCrO_4$, and the hemihydrate, $HgCrO_4.(H_2O)_{0.5}$, by reaction of mercuric oxide with chromium (VI) oxide and water. Similarly, Lamure and Colas[8] have prepared the mercury 'chromite', $HgCr_2O_4$, (possibly the spinel-type structure,[9] $HgO.Cr_2O_3$) from mercuric oxide and chromium (III) oxide. It is known[3,10,11] that chromium oxide gels calcined at temperatures in the range of about 100° to 400°C, contain appreciable proportions of chromium (VI) oxide in their surface layers, particularly[11] when calcined at 300°C. Furthermore, chromia gels calcined at temperatures above 150°C readily chemisorb oxygen[12] which, according to Narasimha Rao and Kesavulu,[13] is especially pronounced at 300°C; this may facilitate the oxidation of mercury on the surface of the 'activated' chromia. In addition, pure mercury is readily oxidised at 25°C in moist air, whereas this is not the case in the absence of water vapour.[14]

Thus, it seems likely that the surface of an 'activated' chromia will promote the reaction, at 25°C, between mercury and CrO_3 or CrO_2 to yield a mercury chromate and/or a 'chromite'. However, it must also be recognised that the 'adsorbed' mercury may simply be present on the chromium oxide surface, as mercuric oxide. Presumably, the elimination of a mercury compound from the chromium oxide surface, on outgassing at

temperatures above about 350°C, is explained by the decomposition of these compounds at around this temperature. For example: the 'chromite', $HgCr_2O_4$, decomposes[8] at 360°C; the hemihydrate, $HgCrO_4.(H_2O)_{0.5}$, is dehydrated[6] at about 200°C to yield the anhydrate which, in turn, decomposes[15] at about 320°C; whilst the dissociation of mercuric oxide commences[16] at temperatures just above the boiling point of mercury, i.e. 357°C (at 760 torr).

5.4 Mercury Vapour Adsorption on other Adsorbents

Considering the widespread use of mercury as a manometric fluid in gas adsorption systems, there are surprisingly few reported investigations concerning the adsorption of mercury vapour, or its influence on the adsorption of other vapours. Coolidge[17] established that the adsorption of mercury vapour at 20°C on charcoal was negligible, and would not interfere with other charcoal-vapour equilibria. A similar conclusion was reached more recently, by Miles,[18] who showed that the presence of mercury vapour did not affect the adsorption isotherms of hydrocarbon vapours on charcoal. Campbell and Duthie[19] studied the variation in the apparent BET surface area, as measured by krypton adsorption, of a nickel film before, and after, the chemisorption of mercury vapour: they found that the apparent surface area reached a steady value on completion of the third adsorbed layer of mercury. Recently, Liebich and Fink[20] have observed that mercury vapour was adsorbed by certain porous Aerosil silicas (surface areas of 335 m^2g^{-1} and 202 m^2g^{-1}, as measured by nitrogen adsorption).

It is interesting to note, by way of comparison, that Barrer and his co-workers[21,22] have extended the early work of Grandjean[23] and Wyart[24] in connection with the very high uptake (as much as 60% by weight) of mercury vapour by the zeolite, chabazite. Barrer and

Woodhead[21] found that in the presence of air or oxygen, mercury vapour was irreversibly adsorbed by chabazite; i.e. mercury vapour and oxygen underwent at temperatures > 200°C an irreversible intercrystalline chemisorption. In fact, on carrying out successive cycles of exposure to mercury vapour followed by removal of vapour, these workers obtained a picture for the irreversible adsorption of mercury vapour, that is very similar to that shown in Fig. 5.1 in the present work concerning the mercury-chromium oxide system. In contrast, however, mercury vapour was reversibly adsorbed by chabazite in the absence of air or oxygen.

REFERENCES

1. F.S. Baker and K.S.W. Sing, Nature (Phys. Sci.), (1971) 229, 27.
2. M.A. Alario Franco, F.S. Baker and K.S.W. Sing, "Progress in Vacuum Microbalance Techniques", Eds. S.C. Bevan, S.J. Gregg and N.D. Parkyns; Heyden and Son Ltd., London (1973) 2, 51.
3. J.D. Carruthers, J.Fenerty and K.S.W. Sing, Nature, (1967) 213, 66.
4. R.B. Gammage, E.L. Fuller, Jr., and H.F. Holmes, J. Colloid Interface Sci., (1970) 34, 428.
5. F.S. Baker, J.D. Carruthers, R.E. Day, K.S.W. Sing and L.J. Stryker, Discussions Faraday Soc., (1971) No 52, 173.
6. K. Aurivillius and B. Malmros, Acta Chem. Scand., (1961) 15, 1932.
7. K. Aurivillius, Acta Chem. Scand., (1972) 26, 2113.
8. J. Lamure and J.L. Colas, C.R. Acad. Sci., Paris, Ser C, (1969) 268, 57.
9. H. Remy, "Treatise on Inorganic Chemistry", Elsevier, (1956) 2, 136.
10. J. Dereń, J. Haber, A. Podgórecka and J. Burzyk, J. Catalysis, (1963) 2, 161.
11. J.D. Carruthers, J. Fenerty and K.S.W. Sing, "Proc. 6th Int. Symp. Reactivity Solids", Schenectady, 1968. Eds. J.W. Mitchell, R.C. DeVries, R.W. Roberts and P. Cannon; Wiley Interscience, New York, (1969) 127.
12. R.L. Burwell, Jr., G.L. Haller, K.C. Taylor and J.F. Read, "Advances in Catalysis", Academic Press, New York, (1969) 20, 1.
13. T.L. Narasimha Rao and V. Kesavulu, Indian J. Appl. Chem., (1967) 30, 25.
14. Reference 9, page 458.
15. The decomposition temperature of mercury (II) chromate was determined by the present author, for a sample of "Laboratory Reagent" grade material supplied by Hopkins and Williams Ltd.
16. Reference 9, page 464.

17. A.S. Coolidge, J. Amer. Chem. Soc., (1927) 49, 1949.

18. A.J. Miles, Ph.D. Thesis, University of Bristol, (1964).

19. K.C. Campbell and D.T. Duthie, Trans. Faraday Soc., (1965) 61, 558.

20. R. Liebich and P. Fink, Z. Chem., (1971) 11, 34.

21. R.M. Barrer and M. Woodhead, Trans. Faraday Soc., (1948) 44, 1001.

22. R.M. Barrer and J.L. Whiteman, J. Chem. Soc., (A), (1967) No 1, 19.

23. F. Grandjean, Bull. Soc. franc. Mineralog., (1910) 33, 5.

24. J. Wyart, Bull. Soc. franc. Mineralog., (1933) 56, 81 and 142.

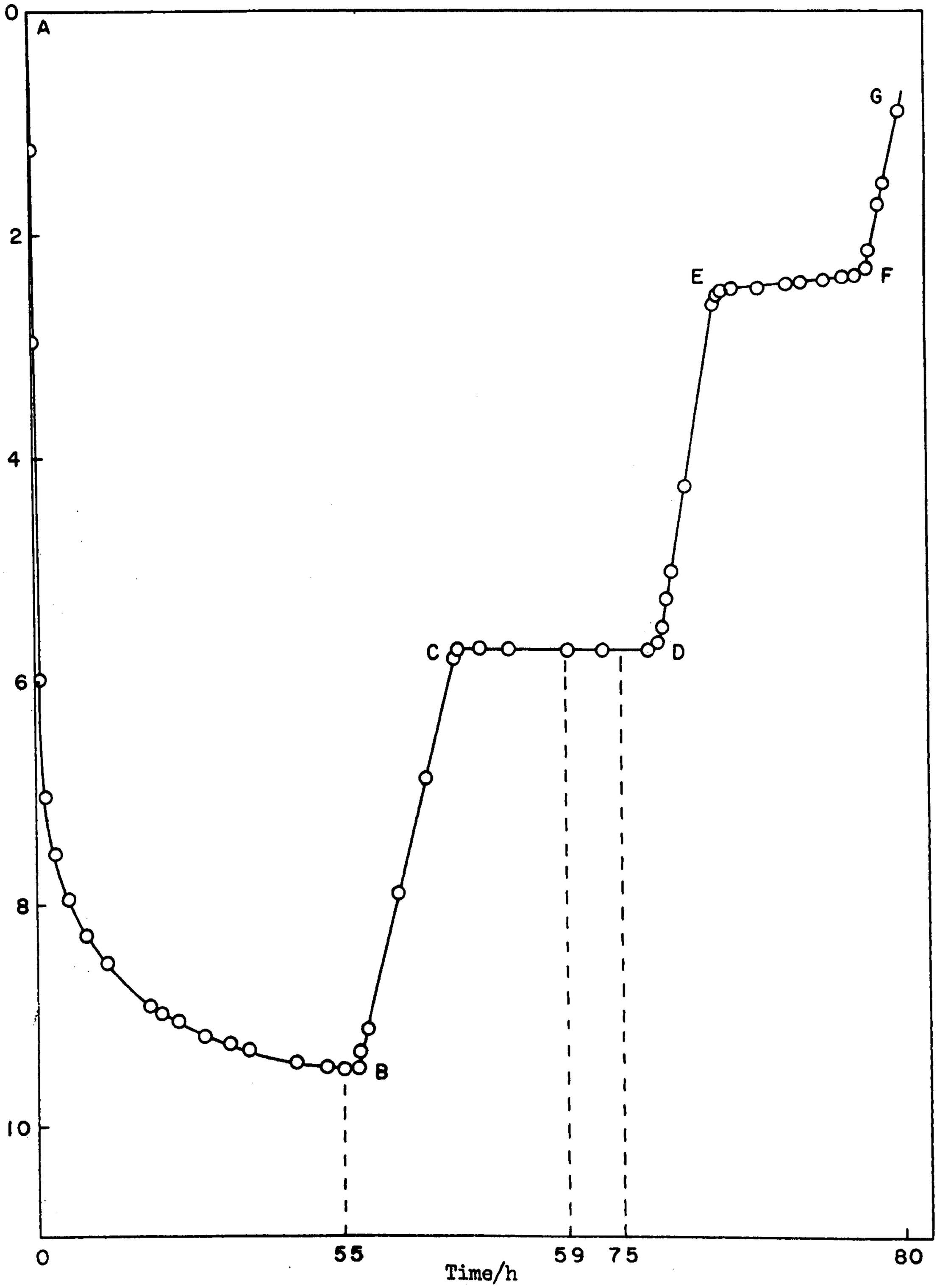

FIG 5.1 Influence of Mercury Vapour During the Outgassing of Chromia Gel A1(225)16 @ 25°C

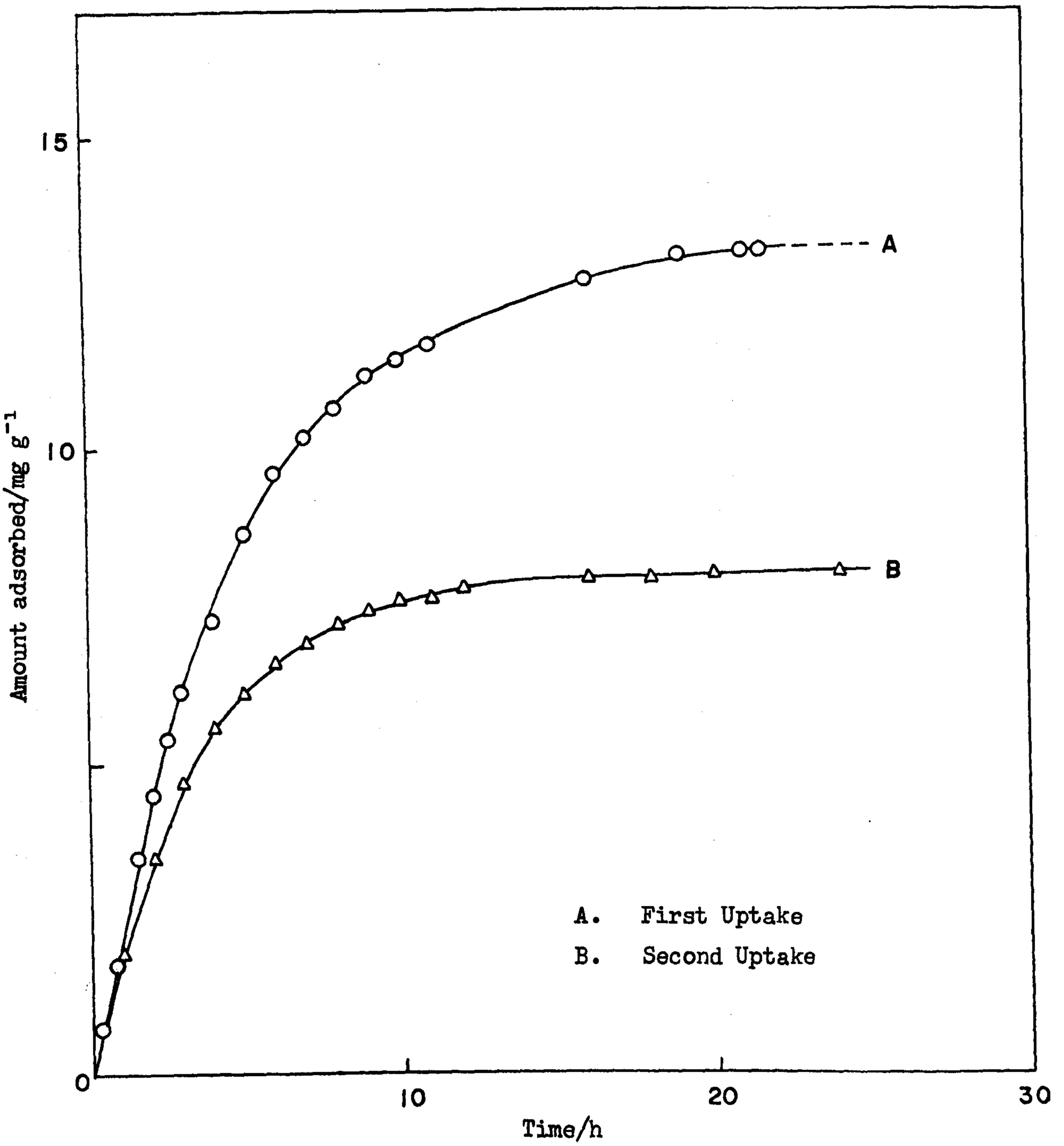

FIG 5.2 Mercury Vapour Adsorption on Chromium Dioxide

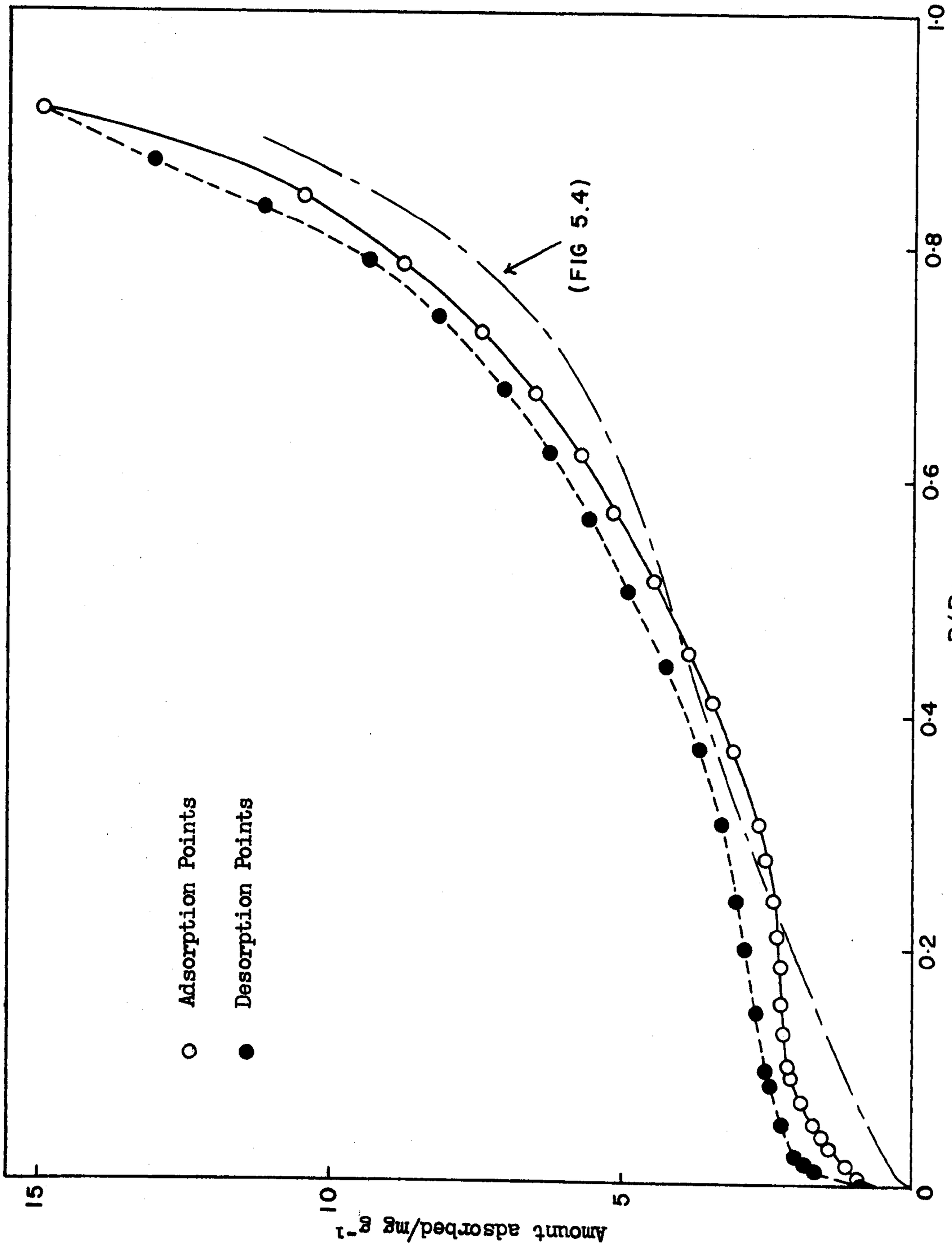

FIG 5.3 Water Vapour Adsorption on Chromium Dioxide in the Absence of Mercury Vapour

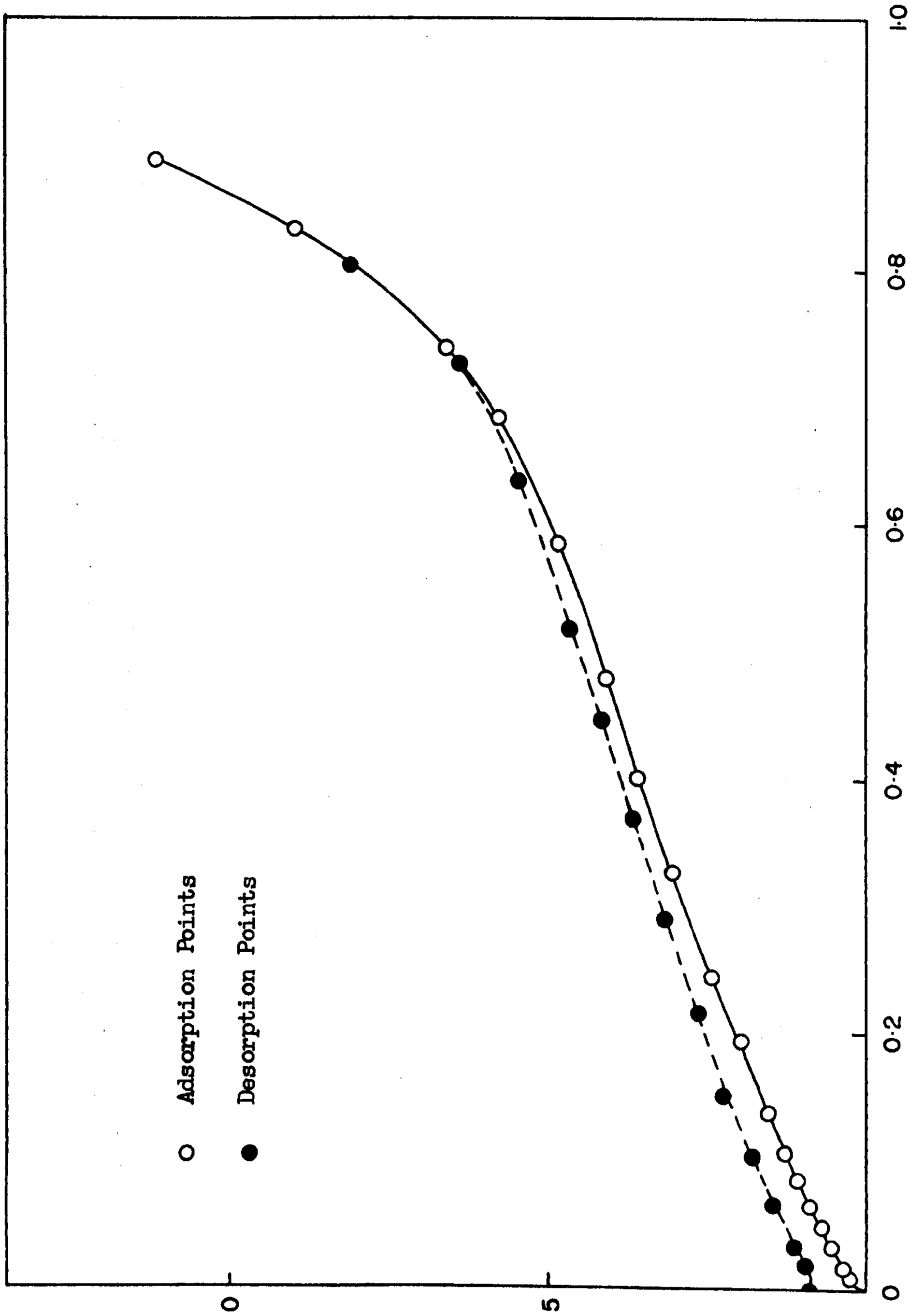

FIG 5.4 Water Vapour Adsorption on Mercury-Contaminated Chromium Dioxide

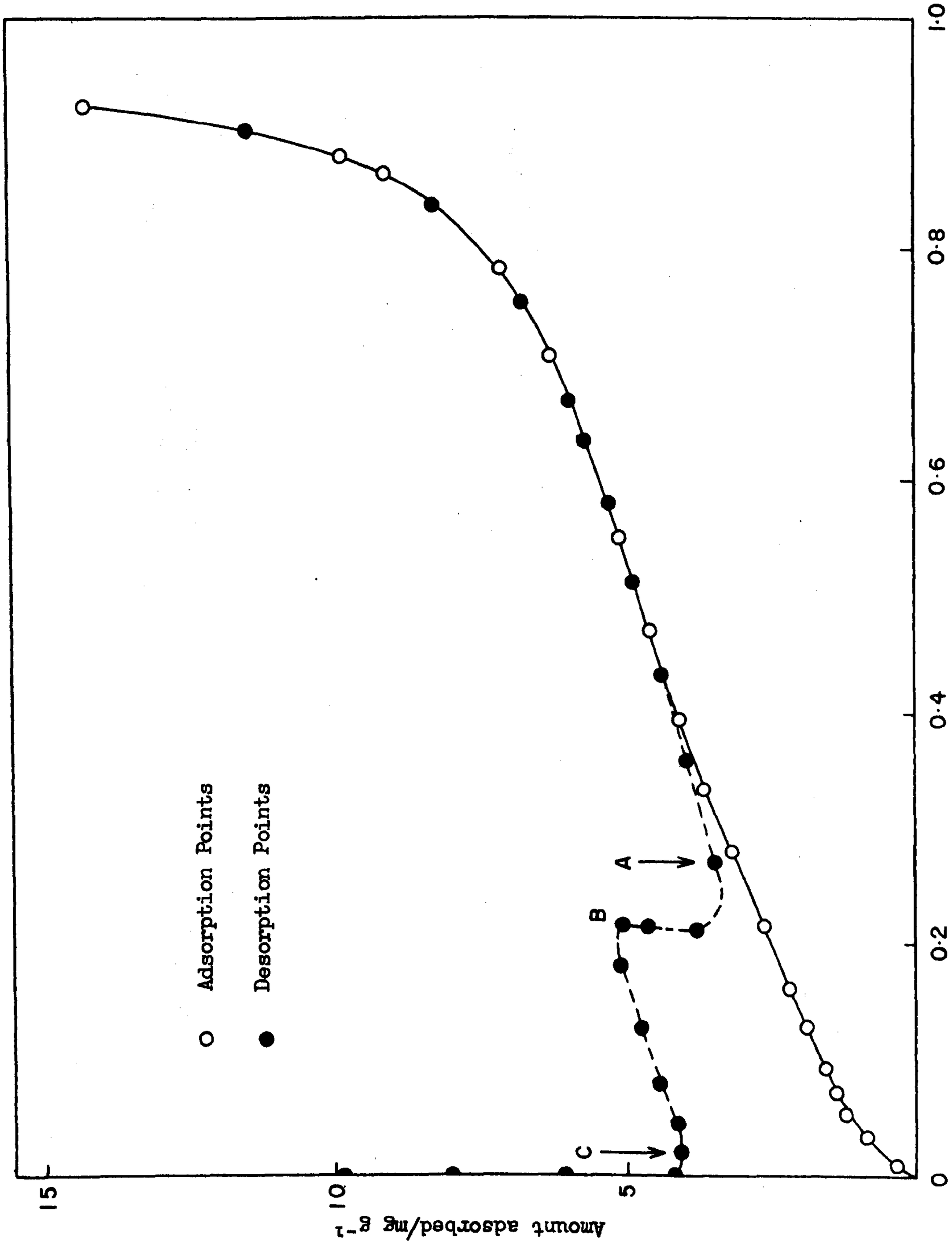

FIG 5.5 Water Vapour Adsorption on Chromium Dioxide in the Presence of Mercury Vapour

C H A P T E R 6

RESULTS AND DISCUSSION III

GAS ADSORPTION AND RELATED STUDIES ON THE CHROMIUM OXIDES

In Sections 6.1 to 6.4 of the present chapter, the characterisation of the hydrous chromium oxides, and the possible role of orthorhombic chromium oxy-hydroxide and of chromium dioxide, are discussed: conclusions are drawn concerning the conditions of gel preparation, particularly in relation to the variation of the precipitation pH. In Sections 6.5 and 6.6, the analysis and interpretation of the nitrogen, argon and water vapour adsorption data are presented: the discussion is primarily concerned with the textural properties of the gels, notably in respect to the pH of precipitation and the effect of subsequent heat treatment of a gel precipitated at high pH.

A. CHARACTERISATION OF THE HYDROUS CHROMIUM OXIDES

6.1 Preparation and Purity of the Chromium Oxide Gels

The conditions of preparation, washing and drying of the chromia gels have been described in Section 3.1; the details are summarised in Table 3.1. The gels were washed until the aqueous eluent was found to be free of ammonium and nitrate ions respectively, as indicated by negative responses to conventional semimicro qualitative tests.[1]

However, it is well known[2-5] that hydrous chromium oxide prepared by precipitation from aqueous solution invariably contains adsorbed impurities which are very difficult to remove. It was therefore to be expected that the chromium oxide gels prepared in this work would be contaminated with ammonium nitrate. This was confirmed by the evolved gas analysis (EGA) using a mass spectrometer to identify some of the gaseous products.

As already explained in Section 3.8 the evolved gas sampling technique (Murphy[6]) was used to characterise the products evolved on heating each gel at 250°C under a partial vacuum. Water and nitrogen were the major constituents, together comprising (on average) about 95% by volume of the total product. In the case of the A-series and S-series gels, small quantities of nitric oxide and nitrous oxide were also found as well as a trace amount of ammonia; for the B-series gels, trace amounts of ammonia and carbon dioxide were found, in addition to the major constituents - water and nitrogen. An earlier detailed mass spectrometric study by Fenerty,[7] of the gaseous products obtained on heating chromium oxide gels, produced similar results.

Fenerty[7] and Friedman and his co-workers[8] have shown that a trace amount of water will initiate the exothermic decomposition of ammonium nitrate at about 180°C: the decomposition products are nitrous oxide and water, with a trace amount of nitric oxide. The evolution of small quantities of nitric and nitrous oxide respectively, from the hydrous gels (A-series and S-series) was thus attributed to the thermal decomposition of ammonium nitrate, present as an adsorbed impurity. In the case of the gels (B-series) prepared using the

Burwell method[9] the trace amounts of ammonia and carbon dioxide present in the evolved gases were attributed to the thermal decomposition of urea, adsorbed on the gels as an impurity. It has been shown[7] that nitrous oxide is not catalytically decomposed (to yield nitrogen and oxygen) at the surface of chromium oxide at 200°C, and furthermore, that ammonia (if originally adsorbed) is neither decomposed nor oxidised. Thus, the relatively large quantities of nitrogen present in the evolved gases were attributed to nitrogen (in the case of the A-series and S-series gels), or air (in the case of the B-series gels), originally adsorbed on, or trapped within, the hydrous chromium oxides.

The conditions of preparation of chromia gel A4 merit particular attention. Gel A4 precipitated slowly from the (originally clear) mother liquor of gel A3 and was, therefore, formed under conditions of both high pH and relatively very high ammonia concentration. Ideally, ammonia should not be employed as a precipitation reagent for chromium oxide gels, since an excess of ammonia may easily lead to the formation of complex ammines.[10] If, in addition, the concentration of ammonium salts is high (as was the case for gel A4), the hydroxide may not be precipitated from such ammines despite the fact[11] that $Cr(OH)_3$ is a dominant form of existence of chromium in aqueous solution of pH value in the range 5 to 13.

Furthermore, as already stated, chromium oxide gels when precipitated from solutions containing alkalis, are apt to contain adsorbed alkali salts; to obtain a hydrous oxide gel in a purer state a milder precipitating reagent, such as potassium iodide-iodate mixture,[12] must be used. However, the present work was directly concerned with the

effect of variation of the pH during precipitation on the subsequent gas adsorption properties of the chromia gels. Ammonia is a convenient reagent for such a purpose.

The fact that any precipitate resulted at all under such conditions would indicate that gel A4 is not wholly a chromium ammine. The violet colour of the mother liquor after filtration of gel A3 (mother liquors from all other gel preparations were colourless) was indicative,[13] however, of either a hexaquochromium (III) compound, e.g. $[Cr(H_2O)_6](OH)_3$ or possibly a lower ammine derivative, e.g. $[Cr(NH_3)_2(H_2O)_4](OH)_3$. The latter compound (insoluble in water) may be formed by the slow progressive replacement of the ammonia ligands in a higher ammine derivative, e.g. $[Cr(NH_3)_6](OH)_3$; such ammines, where the number of NH_3 ligands exceeds two, are soluble in water. However, the violet mother liquor after removal of gel A3 was not consistent with the presence of higher ammine derivatives, namely, orange-yellow.[13] Thus, it seems more likely that the violet colour was due to the presence of the hexaquochromic ion, $[Cr(H_2O)_6]^{3+}$, which slowly changed by a condensation-polymerisation mechanism (cf. Section 1.3) to the blue-grey precipitate designated gel A4, and a colourless mother liquor.

That gel A4 was indeed a hydrous chromium oxide was confirmed by the fact that, in general, the thermograms obtained from the DTA and DSC studies (Section 6.2) were similar to those for the other gels. Furthermore, the fragmentation pattern of the mass spectrum of the gases evolved by gel A4 on heating was very similar to those obtained for the chromia gels of the A-series and S-series respectively, and did not show more than the usual trace amount of ammonia.

6.2 Differential Thermal Analysis (DTA) and Differential Scanning Calorimetry (DSC)

Brief details of the DTA and DSC apparatuses, and the techniques and conditions employed, were given in Sections 3.4 and 3.5 respectively. In confirmation of previous work[7,14] the curves were not significantly changed by a variation in the rate of heating, within the ranges of 2.5° to 10°C per minute and 8° to 32°C per minute, for the DTA and DSC respectively; furthermore, satisfactory reproducibility was obtained with different specimens of the same sample. In the case of chromia gels, the thermal processes occurring below about 250°C are, in general, independent of the nature of the surrounding atmosphere;[7,14,15] nevertheless, peak temperatures on the DTA and DSC thermograms respectively, for a given thermal process were often not identical, temperature differences of about 5° - 15°C being observed. However, it should be noted that DTA and DSC are dynamic techniques, and are therefore dependent on experimental conditions.[16] Above about 250°C, the thermal reactions are generally dependent on the nature of the surrounding atmosphere,[7,14,15] and it was therefore not surprising to observe large differences between the thermograms obtained for the chromia gels, by DTA (static atmosphere of air) on the one hand, and DSC (dynamic atmosphere of nitrogen) on the other. The main purpose of the DSC work was to try to correlate the gases evolved by the gels on heating with particular peaks on the calorimetric curve.

Chromia Gels

In general, the sequence of thermal changes which occurred in the DTA was common to most of the chromia gels studied, although the magnitude of each effect varied from one gel to another; furthermore,

TABLE 6.1

Differential Thermal Analysis of Chromia Gels in Air

GEL		ENDOTHERM		1st EXOTHERM			2nd EXOTHERM		
No	pH	Start (°C)	Max (°C)	M*	Maximum (°C)	(°C)	M	Maximum (°C)	(°C)
A1	10.5	72	162	d	312	357	s	422	-
A2	9.1	65	185	s	323	-	s	403	-
A3	10.5	65	167	s	325	-	s	416	-
A4	10.5	60	185	s	353	-	s	442	-
B6	~6	60	160	s	315	-	d	430	436
B8	~6	75	172	s	325	-	d	432	437
S2	8.6	60	160	**(d)	240	**(325)	s	410	-

* M = peak multiplicity, i.e. s = singlet, d = doublet.

** parentheses used to denote an indistinct broad peak.

the curves were similar to those previously widely reported.[7,14,15,17,18] For this reason, with the exception of an idealised curve shown as Fig. 6.1a, the DTA and DSC thermograms are not reproduced in Figure form here, the relevant data being tabulated for the DTA (Table 6.1) and particular features of each discussed.

A broad endothermic peak was observed in all the DTA and DSC curves (shown in idealised form in Fig. 6.1a), the maxima of which varied between about 160° to 185°C for the DTA and between about 140° to 170°C for the DSC, and was attributed to the loss of 'free' water from the gel leading to the formation of the trihydrate;[18] i.e. the considerable quantity of water that is held by a freshly formed gel in both the form of coordinated water within the bulk and adsorbed water at its surface. The nature of the response of the thermal conductivity gas detector coupled to the DSC apparatus, confirmed that the gas evolved by the gel during the process responsible for the broad endothermic peak probably consisted almost entirely of water vapour and nitrogen. The inference that nitrogen was present is made from the results of the mass spectrometric EGA discussed in Section 6.1; nitrogen was employed as the carrier gas for the thermal conductivity detector and therefore, the relatively small additional amounts of nitrogen evolved by the sample would not have caused a significant effect on the signal from the detector.

The location on the gas detector trace of the maximum of the peak caused by the evolution of free water, appeared to be a function of the pH during precipitation of the gel: thus, progressive increase in this pH appeared to be associated with a displacement of the peak maximum from 152° to 187°C over the pH range investigated. In addition,

the shape of the peak appeared to change with the pH, such that the peak was skewed, and broadened, on the high temperature side of the maximum with increase in the precipitation pH (cf. Fig. 6.1b). These comments are rather tentative, especially as difficulty was occasionally experienced in maintaining balanced gas flows through the thermal conductivity detector system; but they appear to support the views developed in Section 6.3 that the structural water content of the gel is increased with increase in the pH of precipitation. Furthermore,the findings are in keeping with the suggestion by Fenerty[7] that the broad endotherm may in fact be associated with two maxima, at about 120° to 140°C and 180° to 210°C respectively, i.e. with distinct 'types' of free water.

Gel S2 was the only chromia sample to exhibit an exothermic peak (fairly strong) at 240°C in the DTA curve. Sing and his co-workers[15] have suggested that an exothermic peak at about 230°C is associated with the formation of crystalline orthorhombic chromium oxy-hydroxide (CrOOH), which has been identified by electron diffraction studies[15] in chromia gels calcined at 250°C in air; furthermore, it appears that the crystalline monohydrate is only formed if the gel contains sufficient water trapped within large granules. Sing and his co-workers[15] have further suggested that the DTA curve does not depend on the conditions of the formation, but rather on the after-treatment, of the gel. The mechanism of the formation of the oxy-hydroxide structure is suggested to be similar to the hydrothermal process involved in the formation of boehmite, namely that the monohydrate results from the rehydration of a primary decomposition product.[19,20] In partial support of these suggestions

is the recent work of Smyshlyaev and his co-workers,[21] where it has been found that repeated washing of an amorphous (to x-rays) chromia gel with water at 90°C resulted in a discernible x-ray pattern for the washed material. It is the view of the present author, however, that both the conditions during preparation and after-treatment of the gel affect the subsequent DTA curves: this is discussed further.

Many studies[17,18,22,23] of chromia gels, including the majority of those described in the present work, have not revealed the presence of the exothermic peak at about 230°C in the DTA curves; on the other hand, a number of studies have revealed (almost without exception, on gels prepared using the Burwell method[9]) the presence of a strong exothermic peak in this region.[7,14,15] However, it is possible that the relative intensities of endothermic (dehydration) and exothermic (oxidation) processes, proceeding simultaneously, are such that the processes effectively neutralise one another and a discernible peak is not observed. This may be particularly the case in the present work: the gel preparation conditions were varied (notably the pH) in an attempt to increase the 'structural' water (i.e. water bound as hydroxyl groups) content of the gel; such water would undoubtably be removed from the gel, on heating, at a higher temperature than that for the 'free' water. For the latter type of water, its removal leaves an unstable structure which either collapses, or crystallises, to a more stable phase, i.e. the monohydrate, and an exothermic peak is observed at about 230°C. In those cases where an exothermic peak at about 230°C is not observed, the implication may be that the monohydrate, albeit not crystalline,

is already present in the gel (probably confined to the surface layers).

It is difficult, of course, to apply a similar agreement to gels B6 and B8 to explain the absence of the exothermic peak at about 230°C, especially in view of the presence of the peak obtained in previous work on gels prepared using the Burwell method. However, a possible clue to the reasons for the observed difference in this respect may be found in work relating to the conditions of preparation of gels using the Burwell method. For example: Krleza and Sljukic[24] have found that the geometry of the reaction vessel and the occurrence of localised heating, affect the form of the precipitate; similarly, Cross and Leach[25] have commented on the varying degrees of stirring efficiency of different gel preparations. In the present instance, the reaction mixture for gels B6 and B8 respectively, was stirred extremely vigorously - a practice that was seldom adopted in earlier published work.

From Table 6.1, it will be seen that all gels exhibited an exothermic peak (generally broad, but fairly strong) in the range 312° to 353°C. This exothermic change was enhanced in an oxygen atmosphere, but considerably reduced, or even absent, in reducing or inert atmospheres. Detailed studies by Fenerty[7] and Carruthers[14] have shown that this peak can be attributed to the oxidation of surface Cr^{3+} ions to chromium (VI) oxide; furthermore, the oxidation is not confined to the surface but extends appreciably into the bulk.

In the case of gel A4, the oxidation of surface Cr^{3+} ions apparently occurred at a relatively high temperature, the maximum of the exothermic peak being observed at about 353°C; presumably, this is due to the fact that the surface area of this gel is relatively low (S^{N}_{BET} = 13 m^2g^{-1}), and therefore more energy is required to initiate

the oxidation in depth. Sorrentino and his co-workers[26] have also stressed a relationship between the surface area of hydrous oxides (including chromia) and their DTA curves.

For Gel A1, the exothermic peak corresponding to the oxidation of surface Cr^{3+} ions is recorded in Table 6.1 as a doublet, with fairly strong peaks of equal intensity at about 312°C and 357°C respectively; the implication would be either that the surface oxidation of Cr^{3+} is a two stage process, or that another, different, stage is also involved. Alternatively (and more probably), the exothermic peak represented as a doublet may in fact be a broad single peak, with a sharp endotherm (at about 335°C) superposed; in support of this view, Fenerty[7] has observed a prominent maximum at about 337°C on the EGA curve for a chromia gel (determined using mass spectrometry), due to the evolution of water; furthermore, concurrent magnetic susceptibility measurements have indicated that ferromagnetic CrO_2 is present in chromia gels calcined in air at about this temperature. Thus, an endothermic peak at 335°C (superposed on an exothermic peak centred at about the same temperature) may possibly be attributed to the endothermic reaction:

$$2\ CrOOH + \tfrac{1}{2}\ O_2 \longrightarrow 2\ CrO_2 + H_2O$$

This reaction is discussed in more detail later, but here it is interesting to note that at temperatures in the range of 500°C to 600°C, CrO_2 undergoes an endothermic decomposition[27] to α-Cr_2O_3. It is noteworthy that several of the DTA curves (including that for gel A1) obtained in the present work exhibited a broad and shallow endotherm at about 550°C; thereby supporting the contention that CrO_2 was formed by oxidation of orthorhombic CrOOH at about 335°C, on

calcination of gel A1 in air. Sing and his co-workers[27] have shown that an alternative source of CrO_2, namely the decomposition of CrO_3 at about 350°C, probably contributes no more than a few percent to the total amount of CrO_2 found in some calcined gels.

We turn now to the final thermal effect which occurred on heating the hydrous chromium (III) oxide: that which is usually referred to as the "glow phenomenon", and characterises[28] the transformation of amorphous chromium (III) oxide into crystalline α-Cr_2O_3. The glow phenomenon occurs at about 400°C in air; heating in an atmosphere of hydrogen or nitrogen, or under vacuum, serves to delay the glow exotherm until a higher temperature (up to about 600°C),but it does not eliminate the effect.[7,15,28]. The exotherm is especially strong when oxygen is re-admitted to the system, and it has been concluded[7] that the exothermic crystallisation is associated, to some extent, with oxidation-reduction processes.

From Table 6.1, it will be seen that the variation in the temperature at which the exothermic peak was observed for the various gels (in air), covered the range of 403°C to 442°C. As already discussed in relation to the oxidation of surface Cr^{3+} ions, the unusually high temperature of 442°C for the glow of gel A4 may possibly be attributed to its relatively low surface area. In the case of gels B6 and B8 respectively, the glow temperature was also relatively high, but in addition, the exothermic transformation was resolved into two peaks indicating a two stage process. Although the <u>apparent</u> surface area of these gels was very high (S^N_{BET} about 500 m^2g^{-1}), it should be noted that the gels were essentially microporous and that the <u>external</u> surface area was very low, which may account for the relatively high

glow temperature. Of particular interest is the case of gels B6 and B8 however, was the occurrence of the exothermic peak as a doublet, the spacing of the individual peaks corresponding to about 5°C. It has been observed[7] that this phenomenon occurs for gels with relatively large amounts of chromium in the Cr^{6+} state; the first peak (associated with a slight decrease in sample mass) has been attributed to the decomposition of CrO_3 which, in turn, initiates in some way the sudden strongly exothermic transformation to α-Cr_2O_3, thereby giving rise to the second peak.

Orthorhombic Chromium Oxy-Hydroxide and Chromium Dioxide

As already mentioned, previous investigations of the bulk and surface properties of hydrous chromium (III) oxides have revealed the formation of the orthorhombic chromium oxy-hydroxide, CrOOH, and the ferromagnetic chromium dioxide, CrO_2, in certain cases when chromia gels are calcined under hydrothermal and oxidising conditions.[7,14,15,28] It was considered that an investigation of the thermal decomposition of these oxides in various atmospheres, using the DTA technique, might clarify the relationship between the oxides, and also their possible role in the calcination of chromia gels.

Preliminary DTA experiments in which pure samples of orthorhombic CrOOH and CrO_2 respectively, were heated in atmospheres of air, oxygen, nitrogen and hydrogen revealed that these oxides were easily interconverted under normal atmospheric pressure. However, it was later decided to carry out a more detailed study of these interesting oxides, and the work was therefore handed over to Dr. M.A. Alario Franco (Brunel University). In addition to confirming[29] the present author's earlier DTA work (described below), the results of this study provided

the major evidence for the nature of the interconversion reaction of orthorhombic CrOOH and CrO_2. Alario Franco's contribution to the subject matter of the present thesis comprised the characterisation of the various substances involved in the overall reaction (by x-ray powder diffraction and magnetic susceptibility measurements).

In air, the decomposition of the orthorhombic CrOOH occurred in three stages: a pronounced exotherm at about 255°C, a pronounced endotherm at about 500°C, and a smaller, broader endotherm at about 550°C. The exothermic reaction was enhanced in oxygen (peak at 240°C), but was suppressed in both nitrogen and hydrogen; in vacuum, the exotherm was delayed until a temperature of about 365°C. In air, no change in crystal structure could be detected by x-ray diffraction, but after heating to 400°C in oxygen the strongest lines of CrO_2 were apparent (sample nearly black in colour), in addition to the CrOOH x-ray pattern. These results indicate that the exothermic peak at 240°C (255°C in air) corresponds to the decomposition and oxidation of some CrOOH to CrO_2, probably in the surface layers.

The endothermic peak at about 500°C in air was associated with the formation of CrO_2 and some Cr_2O_3. In oxygen, the endotherm was enhanced and was observed at 450°C; the product was now CrO_2, with no detectable Cr_2O_3. The endothermic peak was absent in an atmosphere of nitrogen or hydrogen and the original orthorhombic structure appeared to remain unchanged until about 600°C.

The decomposition of CrO_2 to α-Cr_2O_3 caused the second endotherm at about 550°C in air or oxygen. In vacuum, the endotherm was very pronounced, whereas in nitrogen or hydrogen it was broadened, reduced in intensity, and delayed until about 600°C, when the conversion of

the CrOOH to α-Cr_2O_3 occurred.

The thermal decomposition of CrO_2 in air or oxygen occurred in two stages, broad endothermic peaks being observed at about 510°C and 550°C respectively. X-ray diffraction revealed that the first stage did not produce any detectable change in the crystal structure, whereas the second led to a rearrangement of the lattice to the stable α-Cr_2O_3. In nitrogen, the DTA curve revealed barely discernible endotherms at about 460°C and 570°C respectively, whereas in vacuum, only one endothermic peak was observed at about 560°C. These results indicate that the tetragonal CrO_2 (rutile) structure is stabilised to some extent in an oxidising atmosphere.

The DTA curve obtained on heating CrO_2 in hydrogen proved especially interesting. A very pronounced exothermic peak at about 315°C corresponded to the quantitative reduction of CrO_2 to the orthorhombic CrOOH, as characterised by x-ray diffraction. At about 600°C, a broad and shallow endothermic peak revealed that the CrOOH so formed was decomposed to α-Cr_2O_3. If, however, the DTA run was interrupted immediately after the occurrence of the exothermic peak at 315°C, the CrOOH behaved in an analogous manner to that already described for pure orthorhombic CrOOH, when subjected to calcination in air or oxygen, i.e. it was reconverted to CrO_2.

Thus, the interconversion of bulk orthorhombic CrOOH and CrO_2, and their decomposition to α-Cr_2O_3, under normal atmospheric pressure may be summarised by the scheme:

$$\text{CrOOH} \underset{\text{H}_2\ (315^\circ\text{C})}{\overset{\text{Air (500}^\circ\text{C)}\ \text{or}\ \text{O}_2\ (450^\circ\text{C})}{\rightleftharpoons}} \text{CrO}_2 \xrightarrow[(\text{air or O}_2)]{> 550^\circ\text{C}} \alpha\text{-Cr}_2\text{O}_3$$

Furthermore, the solid-state interconversion of orthorhombic chromium oxy-hydroxide (green) and tetragonal chromium dioxide (black) is an example of a topotactic reaction,[15,30] where a three-dimensional similarity exists between the structures of the starting material and the product. Although Shannon[31] has postulated that the decomposition of CrO_2 (tetragonal rutile structure) to α-Cr_2O_3 (rhombohedral corundum structure) at 550°C is also an example of a topotactic reaction, the structure of α-Cr_2O_3 is too compact to permit the entry of H atoms into the lattice and therefore it cannot be converted to orthorhombic CrOOH (as in the case of CrO_2).[29]

Finally, it should be noted that the DTA curves discussed here for CrOOH and CrO_2 respectively, were quite different from those discussed earlier for hydrous chromium (III) oxides. The very pronounced exotherm associated with the glow phenomenon was not observed in the course of transformation of CrO_2 to α-Cr_2O_3. On this evidence, therefore, it seems likely that even under the most favourable conditions (e.g. preparation at high pH or heating in oxygen), the formation of CrOOH and CrO_2 is probably restricted to the surface layers of a chromia gel.

6.3 Thermal Dehydration of the Chromia Gels

Samples of the chromia gels were outgassed, to constant weight, at various temperatures up to 250°C and the weight loss of each gel plotted as a function of the temperature. In this section, the weight loss plots so obtained are discussed.

In order to make a comparison between all the chromia gels under identical outgassing conditions, the plots were constructed by

simultaneously outgassing the gels at selected temperatures in a vacuum oven: the weight loss at a particular temperature was determined by periodically removing the samples (into a desiccator) and weighing them on a manual balance as rapidly as possible; the process was repeated until constant weight was achieved (generally after about 48 hours), the weight loss being entirely attributed to the removal of water. The outgassed pressure at each point was about 10^{-2} torr. Ideally, the weight loss of the gels ought to have been determined in situ using the spring balance (outgassing to lower than 10^{-4} torr). However, it was not, of course, possible to study more than one sample at a time in such a manner, using the spring balance described in Section 3.17.

In the discussion of these results it is helpful to recall that the precipitation of hydrous metal oxides is more complicated than most precipitation processes because the nucleation and growth cannot be described simply by deposition of ionic or molecular species.[32] Instead, a variety of chemical reactions occur, e.g. hydrolysis, condensation and formation of polynuclear species involving different ligands (in addition to OH^-), which may all be very sensitive to small changes in pH. Hydrogels, or hydrous oxide precipitates, freshly formed from highly solvated Cr^{3+} ions, are usually poorly ordered and retain considerable amounts of 'free' water (sorbed and coordinated molecules). As the localised hydroxide or oxy-hydroxide structure develops with ageing, water molecules are replaced by OH^- and O^{2-} ions.[33] Furthermore, the presence of the concentrated atmosphere of water ligands around each Cr^{3+} ion, both in solution and in the freshly formed precipitate, has been shown[34] to have a great effect on the process of formation and ageing of a chromia gel.

Thus,it was expected that an increase in the pH of precipitation (or gelation) would provide an effective means of displacing the coordinated water during the formation of a chromia gel. It was already known[35] that in the case of precipitated hydrous alumina, the formation of the oxy-hydroxide (boehmitic) structure is facilitated by an increase in the pH of precipitation. Similarly, in the case of silica gels, Halberstadt and his co-workers[36] have observed that the pH of precipitation has a profound influence on the gel structure. The results of the present work about to be discussed serve to show that a similar effect is to be observed in the case of hydrous chromium oxides.

Representative weight loss/temperature plots for the chromia gels are shown in Fig. 6.2. Virtually identical plots were found for gels B7, B8 and B9 respectively, which in turn, were rather similar to Curve 1 in Fig. 6.2 for gel B6: there was no detectable difference in the nature of the water contents of these gels despite the fact that the initial drying out of the gels can scarcely have been uniform (see B-series gels, Section 3.1). In a similar manner, the plots (represented by Curve 2 in Fig. 6.2) for gels A1 and A3 respectively, each precipitated at pH 10.5, were also virtually identical up to a temperature of about 250°C. Unfortunately, there was insufficient sample available to carry out a weight loss study on gel S2 (pH 8.6), to complete the set.

It is clear from Fig. 6.2 that an increase in the pH of precipitation of the gel is associated with a decrease in the removal of water from the gel, at least at temperatures of up to about 170°C. This result would indicate that, with increase in the precipitation pH, a greater proportion of the 'water' in the gel is present as 'structural

water', i.e. as hydroxyl groups. A similar finding was discussed in relation to the DTA and DSC studies on the gels (Section 6.2).

Ignition of the gels at 1100°C revealed that the overall weight loss of each gel was about 46% w/w. Assuming that this overall loss is entirely due to the removal of water, then the remaining water associated with a gel outgassed at about 170°C (from Fig. 6.2) corresponds closely, with the exception of gel A4, to a molecular formula for the outgassed gel of $Cr_2O_3.H_2O$, i.e. the monohydrate, CrOOH. On outgassing the gels above about 250°C, the weight loss plots become fairly similar, the loss presumably being associated with the removal of structural water: however, it is interesting to note that at about 170°C, the plots in Fig. 6.2 intersect, such that for a given temperature <u>above</u> 170°C, the weight loss of the high pH gels (particularly gel A3) is greater. This higher loss is almost certainly associated with the greater proportion of structural water in the high pH gels; for the gels precipitated below pH 10.5, a higher weight loss is observed <u>below</u> about 170°C, i.e. due to a greater proportion of 'free' water.

Finally, in the present discussion, we turn to the particularly noteworthy behaviour of gel A4 on outgassing at temperatures of up to 250°C. It will be recalled that this gel precipitated very slowly at pH 10.5, over a period of about 3 days, from the mother liquor remaining after the rapid precipitation (and isolation) of gel A3 (see Sections 3.1 and 6.1). Chalyi and his co-workers[37] have found that slowly precipitated chromia gel contains less non-structural water than rapidly precipitated chromia gel. The appreciable difference between Curve 1 (slowly precipitated gel A4) and Curve 2 (rapidly

precipitated gel A3) in Fig. 6.2, clearly supports this view: the weight loss of gel A4, due to the removal of the non-structural water content of the gel, was, on average, about 7% less than that for gel A3 at temperatures up to about 180°C.

In addition, the weight loss plot for gel A4 (Curve 1 in Fig. 6.2) exhibits an inflexion at about 125°C, followed by a steep rise to about 200°C; i.e. indicative of a two stage process. In this context, it is interesting to note that Fenerty[7] has suggested that the initial broad endotherm observed in the DTA curve of a chromia gel, may be associated with the removal of two types of non-structural water: at about 120° - 140°C and at about 180° - 210°C respectively. This view is supported by the extensive investigations by Chalyi and his co-workers[38] that the non-structural water in chromia gels is present in the adsorbed and absorbed states respectively.

6.4 X-ray Powder Diffraction and Electron Microscopy Studies

The techniques employed for the x-ray powder diffraction and electron microscope studies were briefly described in Sections 3.6 and 3.7 respectively. Unfortunately, the results of these studies proved to be of little assistance to the present work.

X-ray Powder Diffraction Studies

Well-defined x-ray diffraction patterns were observed in the case of the pure crystalline samples of orthorhombic CrOOH and CrO_2, the d-spacings of which were in reasonable agreement with those previously reported for these oxides.[39,40] However, no discernible patterns were obtained for any of the chromia gels, after exposure of the samples to CuK_α radiation for varying periods of up to 12 hours. In the case of a sample of gel A3 which was progressively outgassed at

various temperatures up to 1000°C (and held at this temperature for 17 hours), the crystallite size of the α-Cr_2O_3 so formed was still too small to result in anything more than a diffraction pattern in which extremely broadened lines were just visible. Giovanoli[41] has commented on a similar difficulty in the study of chromia gels by x-ray powder diffraction, failing to find the slightest trace of crystalline phases in gels even after prolonged treatment of samples in oxygen at 380°C. By way of contrast, however, it is interesting to note that Ratnasamy and Leonard[42], using x-ray scattering techniques particularly suitable for the study of amorphous materials, claimed to have identified crystalline $Cr(OH)_3$ in a chromia gel dried in air at 25°C: particularly pertinent to the present work is the fact that the gel was prepared at pH 10.5, using the method developed by the present author;[43] namely that described in Section 3.1 for the A-series chromia gels. Thus, it is possible that some of the chromia gels studied in the present work, particularly those prepared at high pH, may in fact have contained crystalline phases but that the crystallites were far too small (and contained a high density of imperfections) to be detected by x-ray powder diffraction techniques, the gels therefore appearing to be amorphous.

Electron Microscopy

Transmission electron microscopy of the chromia gels at various magnifications up to about 50,000x proved especially disappointing, the subsequent micrographs revealing little detail. Immediately a sample was subjected to the electron beam the gel was rapidly dehydrated, the particles coalescing to form a mass that was virtually opaque to the electron beam. Under such conditions, the temperature of the

specimen may rise by several hundred degrees,[44] resulting in drastic changes in the gel; any information concerning the original texture of the gel would almost certainly be lost.

The examination of labile materials using a scanning electron microscope, however, is not, by virtue of the different techniques employed, prone to the same undesirable side effects such as beam heating. On the other hand, the magnifications obtainable with such instruments are, at present, relatively very low; in the present work, the highest satisfactory magnification attained was 14,000x. Although the definition of the electron micrographs so obtained was excellent, with little or no obvious signs of change in the texture etc. of the gels, the information derived from the photographs was little more than of a general nature.

Little difference was observed between gels A1, A2, A3 and S2; the gels appeared to posses an 'open' texture, with well dispersed particles of a small size. In the case of gel A4, the appearance was very similar, but the texture of the gel appeared to be more open, with less aggregation of the particles.

No differences in appearance were observed between gels B7, B8 and B9 (for which no organic solvents were used in the washing process), the gels consisting of large vitreous angular particles. In the case of gel B6, however, where organic solvents were employed in the washing process, the particle size was very much smaller, the particles being fairly divided and more rounded; in fact, rather similar to the A-series gels.

The scanning electron micrographs (mags. 1000 - 14,000x) of gel A3 outgassed at 1000°C for 17 hours, did not reveal any particles with sharply defined edges that could be associated with the presence of a crystalline solid.

B. GAS ADSORPTION ON THE HYDROUS CHROMIUM OXIDES

The experimental techniques employed for the gas adsorption measurements were described in Sections 3.16 (for nitrogen and argon adsorption) and 3.20 (for water vapour adsorption). The experimental data for nitrogen, argon and water vapour adsorption on the chromium oxides are presented, in tabulated form, in Appendices 3,4 and 5 respectively. Representative isotherms are shown in Figures 6.3 to 6.8, and 6.12 to 6.18; whilst typical α_s-plots of the adsorption data are shown in Figures 6.9, 6.10, 6.19 and 6.20 respectively.

6.5 Sorptive Properties of Chromia Gels Outgassed at 25°C

The BET surface areas, S^{N}_{BET}, S^{Ar}_{BET} and S^{W}_{BET} respectively, together with the corresponding BET C constants, of various gels (CrOOH and CrO_2 are included for purposes of comparison) outgassed at 25°C are summarised in Table 6.2. The BET method, and the value of the cross-sectional area (A_m) of the adsorbate for nitrogen and water respectively, were described in Section 2.3, where reference was made to the uncertainty concerning the respective values of A_m and Po (the saturation vapour pressure SVP) of argon at -196°C. For reasons discussed in Section 4.1, the value of Po used throughout the present work for argon adsorption at -196°C (i.e. below the bulk triple point of argon) is that of solid argon (e.g. 190.6 torr at -196.0°C[45]).

Although a number of comparisons have been reported[46,47] between BET areas calculated from nitrogen and argon isotherms, the findings are largely inconclusive presumably because the adsorbents were not

sufficiently well characterised. However, the effective value of A_m for argon must depend to some extent on the nature of the adsorbent. Recent investigations[48,49] of argon and nitrogen adsorption on non-porous oxides have revealed that a value of $A_m = 18.2$ Å^2 for argon should be adopted, for non-porous oxide and hydroxylated oxide surfaces, in order to obtain agreement with the nitrogen area. Such an ad hoc approach may not be wholly acceptable[46] since argon isotherms frequently display an indistinct point B. Furthermore, it has been found[49,50] that the apparent cross-sectional area of argon is reduced if the adsorbent is microporous. Thus, the value of $A_m = 18.2$ Å^2 adopted in the present work for the apparent cross-sectional area of argon, though suspect in absolute validity is acceptable for comparative purposes.

The Adsorption Isotherms

With the exception of gels B6 and B8, the nitrogen isotherms determined on the chromia gels outgassed at 25°C were Type II in the Brunauer classification[51] (Section 2.1, Fig. 2.1); nitrogen adsorption on gel B2 (Carruthers[14]) was very low in the BET region (Section 2.3), the surface area, S^N_{BET}, being less than 1 m^2g^{-1}. In the case of gel B6, the steep initial part of the nitrogen isotherm was characteristic of an adsorbent possessing both micropores and mesopores, i.e. Type I and IV character; whilst in the case of gel B8, the isotherm was predominantly Type I in character.

The nitrogen isotherm on gel A1 (Curve A in Fig. 6.3), precipitated at pH 10.5, exhibited a narrow hysteresis loop in the capillary condensation range, indicating the presence of a small amount of mesoporosity, whilst the nitrogen isotherms on gels A2 and S2 (Curves

B and C respectively, in Fig. 6.3) were reversible. When, however, these isotherms were compared with the isotherm determined on a non-porous chromium oxide reference adsorbent,[43] using the empirical α_s-method (Section 2.4), it was seen that gel A2 (precipitated at pH 9.1) also possessed a small degree of mesoporosity. Thus, the α_s-plot for gel S2 (Curve D in Fig. 6.9), precipitated at pH 8.6, is linear over a wide range of relative pressure, viz. 0.05 - 0.85; whereas the α_s-plots on gels A1 and A2 (Curves B and C respectively, in Fig. 6.9) are linear in the monolayer range and thereafter show a slight upward deviation (more pronounced in the case of gel A1) - due to capillary condensation. For purposes of comparison, the α_s-plot for nitrogen adsorption on orthorhombic CrOOH is included in Fig. 6.9 (Curve A): the wide range of linearity clearly demonstrates that the sample of CrOOH outgassed at 25°C was non-porous and therefore suitable as a reference adsorbent.

The respective shapes of the nitrogen isotherms determined on gels B6 and B8, precipitated at about pH 6 using the Burwell method,[9] are in sharp contrast to those determined on both the A-series and on the S-series gels. The isotherm on gel B6 (Curve A in Fig. 6.4) indicates that the gel is predominantly microporous, but in addition, that it probably contains some pores in the mesopore range: the well-defined hysteresis loop, Type E in the de Boer classification,[52] is characteristic of ink-bottle type pores[53] suggesting that the pores in gel B6 are mixed, in both shape and size. In contrast, the typically Type I isotherm obtained on gel B8 (Curve B in Fig. 6.4) is reversible over the complete range of relative pressure. Clearly, both gels are microporous (gel B6 containing mesopores in addition) but, although the

gels originate from a single preparation, the different after-treatment of the two portions of the fresh gel has resulted in a striking modification of the texture of the fresh gel. It will be recalled (Section 3.1, B-series gels) that the portion designated gel B6 was washed with aliquots of water, acetone and ether, whilst the portion designated gel B8 was washed with water only; each was then dried at room temperature in a current of dry air. In the former case, the replacement of the gel water, before drying of the gel, by a liquid with a lower surface tension than that of water, namely acetone or ether, has resulted in an apparent increase in both the surface area, S^{N}_{BET}, (cf. Table 6.2) and pore volume, V^{N}_{P}, of the gel. Taylor[54] has observed a very similar effect when chromia gels were washed with pentane prior to drying.

The values of V^{N}_{P}, about 0.33 $cm^3\,g^{-1}$ and 0.12 $cm^3\,g^{-1}$ for gels B6 and B8 respectively, were assessed from the plateau of the Type I isotherms in Fig. 6.4 (assuming that the uptake at saturation represented the pore volume[55]). However, it should be noted that these values of V^{N}_{P} do not necessarily represent the true pore volume of the gels, but only the volume available to nitrogen. Thus, from a consideration of the <u>apparent</u> values of S^{N}_{BET} and S^{W}_{BET} for gels B6 and B8 (recorded in Column Nos. 5 and 9 of Table 6.2), it is evident that there is a molecular sieve effect[43,56] as between nitrogen and water in the case of gel B8 but not in the case of gel B6: the nitrogen area is about 35% less than that as measured by water, whereas the apparent nitrogen and water areas are very similar in the case of gel B6.

Thus, the method of washing of a chromia gel may radically change, or eliminate, the molecular sieve properties of the freshly formed gel.

The surface area of gel B8 was probably entirely associated with micropores, whereas for gel B6, precipitated under identical conditions to gel B8 but washed with organic solvents prior to drying, a more open texture resulted. From the slope of the upper linear region of the α_s-plot (Curve A in Fig. 6.10) of the nitrogen isotherm on gel B6, it was found that this gel possesed a small external area of about 21 m^2g^{-1}, (by application of equation 2.14 in Section 2.4).

In general, the argon isotherms on the gels (where determined) were very similar to the corresponding nitrogen isotherms. An exception was observed in the case of the argon isotherm determined on gel A2: the isotherm (shown in Fig. 6.5) exhibited a broad and well-defined hysteresis loop (Type E in the de Boer classification[52]) which closed abruptly at a relative pressure of 0.35 Po, whereas the nitrogen isotherm (Curve B in Fig. 6.3) was completely reversible; furthermore, the apparent argon area, S_{BET}^{Ar}, was 300 m^2g^{-1} as compared to the nitrogen area, S_{BET}^{N}, of 82 m^2g^{-1} (Table 6.2). However, it must be noted that whereas the nitrogen isotherm was determined on the fresh gel, the argon isotherm was determined eighteen months later. This may well be the result of drastic ageing of the gel, with the development of mesoporosity. However, in the absence of an argon isotherm determined on the fresh gel, and a nitrogen isotherm determined after eighteen months, it cannot be ruled out that a genuine difference in the sorptive properties of gel A2, between nitrogen and argon, existed in the fresh gel.

In the case of the Type II argon isotherms, because the uptake was plotted as a function of P/Po(s) (where Po(s) was the SVP of <u>solid</u> argon), the isotherm crossed the ordinate at unity relative pressure instead of approaching it asymptotically: examples are provided by

Fig. 6.5, and Curve A in Fig. 6.7.

Representative water vapour isotherms determined on chromia gels outgassed at 25°C are shown in Fig. 6.6 All the water isotherms exhibited hysteresis extending over the full range of relative pressure but, in general, little or no permanent retention of water by the sample was observed on re-outgassing the gels at 25°C. The hysteresis was almost certainly, therefore, associated with the penetration of water vapour into the bulk of the gel, rather than a chemical change of the surface of the gel. In general, the shapes of the water vapour adsorption isotherms were very similar to those for the corresponding nitrogen adsorption isotherms.

In the case of gel B6, the Type IV character of the isotherm was more pronounced for water vapour adsorption (Curve C in Fig. 6.6) than for nitrogen adsorption (Curve A in Fig. 6.4); i.e. the presence of mesopores in gel B6, in addition to micropores, was more apparent from the water vapour isotherm. The hysteresis exhibited by the water isotherm on gel B6 comprised two main types: high pressure hysteresis, similar to a Type E loop[52] (characteristic of ink-bottle type pores and which, but for the occurrence of a penetration effect, would probably have closed at about 0.35 Po), followed by low pressure hysteresis extending to zero relative pressure and associated with the penetration of water vapour into the bulk of the gel.

In Fig. 6.7, the Type II nitrogen, argon and water vapour isotherms respectively, determined on gel A4 outgassed at 25°C are shown: the isotherms for nitrogen and argon adsorption were completely reversible, whereas the water isotherm exhibited hysteresis extending to zero relative pressure with, on this occasion, some permanent retention

of water. The interesting feature revealed by these isotherms is the large difference between the BET surface areas for both nitrogen and argon on the one hand, and water vapour on the other: whereas the nitrogen and argon areas were in substantial agreement at about 13 m^2g^{-1}, with water the apparent area was about 215 m^2g^{-1} (Table 6.2).

It will be recalled (Section 3.1, A-series gels) that gel A4 precipitated relatively very slowly and it seems likely, therefore, that large particles were formed. Consequently, nitrogen or argon adsorption took place on a small external area, whereas water sorption took place within fine micropores that were too narrow to permit the entry, to any appreciable extent, of nitrogen (or argon) molecules. The α_s-plot for nitrogen adsorption on this gel is shown as Curve B in Fig. 6.10: the deviation from linearity at low relative pressures supports the view that gel A4 contained pores in the micropore range (width < 20 Å).

Finally, we turn briefly to a general problem encountered during gas adsorption studies on chromia gels (and on many other gel systems); namely the labile nature of the gels, and the associated difficulty in obtaining reproducible isotherms on chromia gels outgassed at 25°C.

In Fig. 6.8, Curve A represents the nitrogen isotherm determined after outgassing gel A1 at 25°C for 32 hours; on completion of the isotherm (duration one day) the gel was re-outgassed for a further period of 18 hours and the isotherm re-determined (Curve B in Fig. 6.8). The rapid ageing process of gel A1 during this short period has resulted in a substantial displacement of the multilayer region of the second isotherm to higher relative pressure: furthermore, this change was accompanied by a reduction in the nitrogen area of the gel; from about 144 m^2g^{-1} to about 128 m^2g^{-1}.

Clearly, outgassing of gel A1 at 25°C led to a metastable structure of the gel, which changed both whilst a given isotherm was being determined and also on outgassing prior to the determination of a further isotherm. A similar effect was observed in the case of the other chromia gels which exhibited Type II isotherms, including chromia gels studied by other workers,[57,58] but was less noticeable in the case of the microporous gels, e.g. gels B6 and B8.

Comparison of the Nitrogen, Argon and Water BET Surface Areas of the Gels

In the previous section, reference was made to the fact that certain of the chromia gels, when outgassed at 25°C, exhibited molecular sieve properties: in these cases, the water vapour sorption capacity was high, whereas the pore volume available to nitrogen (and occasionally argon) was comparatively small, or almost non-existent. The results of certain experiments on nitrogen, argon and water vapour adsorption respectively, summarised in Table 6.2, help to illustrate why the surface properties of hydrous chromium oxides are so sensitive to the conditions of preparation and the removal of water.

In Section 6.3, it was mentioned that hydrous chromium oxide precipitates,freshly formed from hexaquo Cr^{3+} ions, are usually poorly ordered and retain considerable amounts of free water. When the gel is outgassed at 25°C, however, the free water (sorbed and coordinated) is removed without a drastic structural change or collapse of the solid framework; although, as shown in Fig. 6.8,

some changes in the textural properties of the gel occur. The gel then appears to act as a molecular sieve, the cavities remaining in the vicinity of the cations on removal of the ligand water being available for the sorption of water vapour, but not for nitrogen (and presumably, larger adsorbate molecules). It has been shown[14,43] that on heating a gel which exhibited a molecular sieve effect to about 280°C, the small cavities appeared to migrate and aggregate with the increase in thermal energy: the gel became mesoporous, as indicated by a change in the isotherm shape, good agreement being obtained between the values of pore volume as assessed by nitrogen and water sorption.

The molecular sieve character of the chromia gels (B-series), prepared at about pH 6 using the Burwell method, is especially interesting. In the extreme case, nitrogen uptake on gel B2 (prepared by Carruthers[14]) was barely detectable ($S^{N}_{BET} < 1\ m^2g^{-1}$), whereas the apparent water area was about 286 m^2g^{-1}. Similarly, but to a lesser degree, gel B8 exhibited a preferential affinity for water vapour;whilst in the case of gel B6,replacement of the gel water by acetone prior to drying led to a pore-widening process and consequently, good agreement between the apparent values of S^{N}_{BET} and S^{W}_{BET}.

The relationship between variation of the pH of the precipitation medium and the sorptive properties of the gel, has been examined in the case of hydrous aluminium oxide[59-61] and of silica gels:[62,63] it was found that these gel systems, when outgassed at room temperature, exhibited the greatest preferential affinity for water vapour sorption when precipitated at the lowest pH values; furthermore, in general,

the isotherms were characteristic of microporous solids, i.e. Type I. In the case of hydrous chromium oxides a similar study does not appear to have been made, although molecular sieve effects, as between nitrogen and water vapour, have been reported.[57,64] The results summarised in Table 6.2 serve to show that, in general, the nature of the porosity in chromia gels is closely associated with the pH of precipitation.

Although gels A2 (pH 9.1) and S2 (pH 8.6) showed some molecular sieve character, gel A1 (pH 10.5) did not appear to have any significant preferential affinity for water vapour rather than nitrogen. The nature of the α_s-plots for the nitrogen isotherms determined on these gels (shown in Fig. 6.9), shows that the increase in the value of S^{N}_{BET} with pH was associated with the development of mesoporosity in gels A1 and A2. Cross and Leach[25] have similarly found that the precipitation of chromia gels at low pH (about pH 5) results in a microporous gel, whilst at higher pH the gel tends to be mesoporous. This type of secondary pore structure is probably formed as a result of aggregation-cementation, an ageing process which is promoted by the reduction in the degree of solvation at the solid-liquid interface.[65]

When comparing the results for water sorption by the silica samples (Section 4.2, Table 4.1), it proved helpful to express the uptake of water vapour, at a relative pressure of 0.2 Po, on a unit area basis (using the corresponding S^{N}_{BET} value). In Column 11 of Table 6.2 the results for water sorption by the chromia gels is expressed in a similar manner. Thus, it will be seen that, with the exception of gels A4, B6 and B8 (discussed in the previous Section), an increase in the pH of the gel precipitation is

accompanied by a decrease in the sorption of water vapour per unit area of the gel.

In the case of gels A1 and A3 (each precipitated at pH 10.5) the significant difference bewteen the water uptakes at 0.2 Po, i.e. 21.8 and 32.1 μ mole m^{-2} respectively, may be associated with the four-fold increase in the concentration of ammonia solution employed for gel A3 (Section 3.1, Table 3.1). It is known that the sorptive properties of outgassed hydrous chromium oxides are particularly sensitive in respect of the concentration of the reactants,[14,15] including the sequence and rate at which the solutions are mixed,[66,67] used in the preparation of the gels: in a manner similar to that found for alumina gels,[61] an increase in concentration led to a marked decrease in the S^{N}_{BET} value of the chromia gel. The change in the conditions of preparation of gel A4, relative to those of the other gels, was particularly marked; this may explain why gel A4, prepared at high pH, exhibited a high preferential affinity for water vapour.

In all cases, water sorption by the chromia gels outgassed at 25°C was very much greater than in the case of silica gels similarly outgassed (cf. silica gels E and J in Table 4.1, Chapter 4). It seems likely that the high affinity for water, exhibited by chromia, is associated with a marked tendency for hydration in depth of poorly ordered cations, e.g. Cr^{3+} originally solvated and not fully coordinated in the oxide structure. Sing and his co-workers[60] have found that certain hydrous alumina gels, outgassed at room temperature, exhibit similar high preferential affinities for water vapour.

TABLE 6.2

Nitrogen, Argon and Water Vapour Adsorption on Chromium Oxides Outgassed at 25°C

SAMPLE	pH	NITROGEN				ARGON		WATER		
				BET		BET		BET		SORPTION AT 0.2 Po
		TYPE	POROSITY	S^{N}_{BET} (m^2g^{-1})	C	S^{Ar}_{BET} (m^2g^{-1})	C	S^{W}_{BET} (m^2g^{-1})	C	(μ mole m^{-2})
A1	10.5	II	Me	144	46	-	-	174	36	21.8
A3	10.5	II	N	132	144	152	51	233	48	32.1
A4	10.5	II	N	13.0	335	12.6	75	215	138	313
A2	9.1	II	N	82	155	300	49	172	31	36.5
S2	8.6	II	N	49	216	-	-	172	45	63.3
B2	~6	II	N	<1	-	-	-	286	120	> 3000
B6	~6	I & IV	Mic & Me	485	100	618	44	470	16	15.2
B8	~6	I	Mic	271	163	351	280	421	46	27.7
CrOOH	-	II	N	16.2	105	-	-	3.1	37	3.4
CrO_2	-	II	N	14.1	115	-	-	12.4	36	15.7
Col.No.	2	3	4	5	6	7	8	9	10	11

N, non-porous; Me, mesoporous; Mic, microporous

In contrast, the non-porous sample of crystalline orthorhombic chromium oxy-hydroxide exhibited much less affinity for water vapour, the uptake at a relative pressure of 0.2 Po corresponding to 3.4 μ mole m^{-2}. In the case of the sample of CrO_2, believed to be essentially non-porous,[43] the uptake of water vapour at 0.2 Po corresponded to a close-packed water monolayer; i.e. 15.7 μ mole m^{-2} (taking the molecular cross-sectional area of water as 10.6 $Å^2$). It should be noted, however, that the results recorded in Table 6.2 of certain experiments on nitrogen and water vapour adsorption on CrO_2, were obtained after the occurrence of mercury adsorption on the surface of the CrO_2 sample (cf. Section 5.2).

6.6 Sorptive Properties of Chromia Gel A3 Outgassed at Various Temperatures up to 1000°C

The sample outgassing procedure was described in Sections 3.15 and 3.19 for the volumetric and gravimetric techniques respectively. Mercury vapour was present, both during the outgassing and the determination of the isotherm, in the case of nitrogen and argon adsorption respectively, but absent throughout the determination of the water vapour isotherms. Where reference is made to a particular specimen of gel A3, the temperature and the duration of the outgassing treatment of the gel is designated as indicated in the following examples: A3(25)64V was a sample of gel A3 outgassed at 25°C for 64 hours; whilst A3(1000)17V was a sample of gel A3 outgassed at 1000°C for 17 hours. In a similar manner, B3(880)2 was a sample of gel B3 calcined at 880°C for 2 hours in air, the sample being subsequently outgassed at 25°C prior to the isotherm determination

(Carruthers[14]). The outgassing of gel A3 at the temperatures indicated in Table 6.3 was carried out sequentially, without exposure of the sample to air at any stage during the determination of the isotherms: nitrogen and argon isotherms were determined consecutively on the same specimen of gel A3, whilst the water vapour isotherms were determined on another sample of the gel similarly treated.

The BET surface areas, S^{N}_{BET}, S^{Ar}_{BET} and S^{W}_{BET} for nitrogen, argon and water vapour adsorption respectively, together with the corresponding BET C constants, of gel A3 outgassed at selected temperatures up to 1000°C are summarised in Table 6.3: the variation of the BET surface area of the gel, as a function of outgassing temperature, is presented for each adsorbate in graphical form as Fig. 6.11. Representative nitrogen isotherms determined on gel A3 are analysed as α_s-plots in Figs. 6.9 and 6.20, whilst Frenkel-Halsey-Hill (FHH) plots are summarised in Tables 6.4 and 6.5.

Interpretation and Analysis of the Adsorption Isotherms

Isotherms representative of nitrogen, argon and water vapour adsorption respectively, determined on gel A3 outgassed at various temperatures up to 1000°C, are reproduced as Figs. 6.12 - 6.18: the general shape of the curves is similar to that of a Type II isotherm.[51] In the case of nitrogen and argon adsorption, the majority of the isotherms were completely reversible. In contrast, however, all the water vapour isotherms, with the exception of the repeat determination on gel A3 outgassed at 1000°C (Curve C in Fig. 6.18), exhibited hysteresis extending over the complete range of relative pressure: in the case of the repeat water vapour isotherm determined

on A3(1000)17V, a hysteresis loop was obtained which closed at a relative pressure of about 0.3 Po. Furthermore, on re-outgassing, at 25°C, of a specimen of gel A3 after the determination of a particular water vapour isotherm, some permanent retention of water by the specimen was observed, the degree of which decreased with increase in temperature of outgassing: i.e. in addition to the usual penetration of water into the bulk of a chromia gel (Section 6.5), surface rehydration of gel A3 occurred on exposure of a specimen to water vapour. Permanent retention of water was not observed in the case of gel A3 initially outgassed at 25°C, i.e. Curve C in Fig. 6.12.

The nitrogen, argon and water vapour adsorption isotherms determined on A3(150)15V were initially identical (up to relative pressures of about 0.9 Po) to the corresponding isotherms determined on the gel outgassed at 25°C, i.e. A3(25)64V: practically no significant change was observed in the respective values of the BET surface areas, or those of the BET C constants (cf. Table 6.3 and Fig. 6.11). This result indicates that there was little disturbance of the gel structure on outgassing the gel at 150°C.

From Fig. 6.11 it is apparent, however, that in the case of A3(300)20V, the nitrogen and argon BET surface areas were each increased by about 30%, whilst the area as measured by water adsorption decreased by about 35%; indicating that some rearrangement of the gel structure occurred on outgassing gel A3 at 300°C. The nature of this change is indicated by the α_s-plots shown in Figs. 6.19 and 6.20. The selection of suitable non-porous reference surfaces poses a special problem with chromium oxide gels, because heat treatment leads to changes in both the texture and the chemical structure. Ideally, a different standard isotherm should be employed for each well-characterised

oxide, or hydroxide, structure (e.g. CrOOH, Cr_2O_3, CrO_2, CrO_3). In the present instance, however, the purpose of an analysis of the isotherms using the α_s-method was to detect the changes which occurred on progressively outgassing gel A3 at increasing temperatures; it was felt that this was best served by comparing the nitrogen isotherms (for example) determined on the heat treated material, with that determined on the gel outgassed at 25°C, i.e. A3(25)64V.

In order to establish the nature of any porosity present in A3(25)64V, the nitrogen isotherm determined on this specimen was compared, as an α_s-plot, with that determined on the pure sample of orthorhombic chromium oxy-hydroxide - an adsorbent which was established (Section 6.5) as being non-porous. Accordingly, the α_s-plot of the nitrogen isotherm determined on A3(25)64V is shown as Curve A in Fig. 6.19. The plot is linear in a relative pressure range of 0.1 to 0.75; but the slight deviations from linearity at low, and at high, relative pressures are indicative of a small degree of microporosity and mesoporosity respectively, in gel A3(25)64V. The positive intercept (in association with the wide range of linearity) of Curve B in Fig. 6.19 indicates that the degree of microporosity was increased on outgassing gel A3 at 300°C, whereas further outgassing at 440°C resulted in a loss of microporosity to a degree similar to that originally found in A3(25)64V (cf. Curve C in Fig. 6.19). The increase in the degree of microporosity of A3(300)20V, together with the enhanced values of S^{N}_{BET} and S^{Ar}_{BET} respectively, is probably associated with the removal of water molecules, present in the adsorbed and absorbed states, from the gel (cf. Sections 6.2 and 6.3).

In Fig. 6.20, the nitrogen isotherms determined on the heat treated samples of gel A3 are compared, as α_s-plots, with that determined on A3(25)64V. The comments made concerning the α_s-plots in Fig. 6.19 are reinforced by Curves A, B and C respectively in Fig. 6.20: the wide range of linearity of the α_s-plots, extending to relative pressures of about 0.9 Po, suggests that there was no increase in the degree of mesoporosity originally present in A3(25)64V, on outgassing gel A3 at temperatures up to 440°C. It is interesting to note, however, that although Curves A and B in Fig. 6.20 are parallel (indicating that the surfaces of A3(150)15V and A3(300)20V were probably similar) the downward deviation from linearity of Curve B at relative pressures below about 0.1 Po, is indicative of a disturbance of the nitrogen monolayer on A3(300)20V. It would appear that there is a greater enthalpy of adsorption in the case of A3(300)20V than for A3(150)15V. This result may be associated with the fact that mercury vapour was almost certainly chemisorbed on the surface of A3(300)20V, during the determination of the nitrogen and argon isotherms (cf. Section 5.1).

For nitrogen adsorption on gel A3 outgassed at 600°, 800° and 1000°C respectively, the relatively complex nature of the α_s-plots (shown as Curves D, E and F respectively, in Fig. 6.20) confirm that a change in the chemistry of these surfaces resulted, after occurrence of the glow phenomenon at a temperature between 440° and 600°C: with the exception of the plot for A3(1000)17V, the range of linearity is restricted to a very narrow range of relative pressure. The deviation from linearity at high relative pressures in the case of Curves E and F, may be associated with the collapse

of the mesopore structure on outgassing gel A3 at 800° and 1000°C respectively. Certainly, the results summarised in Table 6.3 (and represented graphically in Fig. 6.11) serve to show that the occurrence of the glow phenomenon is accompanied by a drastic reduction in the surface area of gel A3; thereby confirming previous findings.[14,43,68]

During the progressive outgassing of gel A3, the sample bulk was observed to decrease considerably after outgassing at 150°C, i.e. the particles of gel A3 compacted. This apparent change in the bulk density was reflected by the presence of a small degree of high pressure hysteresis in the nitrogen and argon isotherms respectively, (cf. Figs. 6.13 and 6.15) first becoming apparent in the case of A3(150)15V, then carrying through the sequential isotherm determinations to A3(600)16V. Further outgassing at 800°C and 1000°C respectively, resulted in reversible nitrogen and argon isotherms (cf. Figs. 6.14 and 6.16 respectively). These results suggest that the compaction of the gel created an ill-defined pore structure, thereby allowing a small degree of inter-particle condensation of nitrogen (and argon) to occur. With collapse of the gel structure to α-Cr_2O_3, this pore structure was removed.

Carruthers and Sing[68] have found that, in the case of a microporous chromia gel prepared using the Burwell method, the drastic ageing which occurred in the low temperature range (i.e. less than about 200°C) was avoided by heating the gel in a vacuum; a large reduction in the value of S^N_{BET} was delayed until an outgassing temperature of about 250°C. A similar situation has been encountered with hydrous aluminium oxides[59,65] and with other inorganic gels.[69,70]

In the present work, it is noteworthy that a large reduction in the surface area of gel A3 (containing little microporosity) was not observed until an outgassing temperature of 440°C was exceeded. Low temperature ageing depends on the presence of free water in the gel, and presumably this water is removed more easily from a non-porous gel than that from a microporous gel.

The values of the BET C constants for nitrogen adsorption on gel A3 outgassed at temperatures of 440°C, and above, are recorded in Table 6.3 enclosed by parentheses to indicate that the validity of these values is suspect. It is apparent from the corresponding nitrogen isotherms, shown in Figs. 6.13 and 6.14, that the knee of the isotherm is both progressively sharpened and displaced towards very low relative pressures. This is indicative of a high degree of specific adsorbent-adsorbate interaction, localised nitrogen adsorption taking place on highly energetic sites. In order to obtain more meaningful values of the BET C constants, the BET analysis should be performed, for the nitrogen isotherms in question, in a narrow range of relative pressure lying outside the usual BET region of 0.05 Po to 0.3 Po. In the present work, however, insufficient experimental data were available at very low relative pressures to permit such an analysis.

With the exception of A3(600)16V, the argon isotherms determined on gel A3 (Figs. 6.15 and 6.16) exhibited curves in the monolayer region of the isotherm, that essentially retained the character of a Type II isotherm. Although it is frequently found that for argon adsorption on many surfaces the statistical monolayer is not a well-defined point on the isotherm,[48] it would appear that, in the

present instance, this is not the case for argon adsorption on certain chromium oxides: the BET C constants recorded in Table 6.3 for argon adsorption on gel A3 are all greater than 50, and therefore it would appear that the BET procedure may be used with reasonable confidence to locate the value of the monolayer capacity, and thence the argon BET surface area (bearing in mind the uncertainty concerning the cross-sectional area of the adsorbed argon molecule[46,47]). Thus, the fact that the interactions of the argon molecule with solid surfaces are essentially non-specific, appears to offer it an advantage over nitrogen in the present study of chromia gels outgassed at high temperatures.

The argon isotherms determined on gel A3 outgassed at temperatures of 600°C and above (Figs. 6.15 and 6.16), exhibited some stepwise character, albeit poorly-defined. To a lesser extent, stepwise character was also apparent in the case of the corresponding water vapour isotherms, whilst for nitrogen adsorption such an effect was barely discernible. Pierce and Ewing[71] investigated the requirements for the occurrence of stepwise isotherms: they concluded, that in addition to the need for a homogeneous surface, there must be strong lateral interactions between adsorbed molecules, and that the temperature of adsorption should be low enough to inhibit the thermal agitation of the adsorbate molecules. However, Zettlemoyer and his co-workers[72] have shown that the geometry and chemical nature of the adsorbate are more essential requirements than that of low temperature.

Almost certainly, the surface of a chromia gel outgassed at temperatures between 600° and 1000°C, is predominantly heterogeneous

in the energetic sense, although prolonged treatment at high temperature of the α-Cr_2O_3 so formed probably results in an increased uniformity of the surface. However, it is interesting to note that Selim and his co-workers[73] have reported the presence of well-defined steps in the water vapour isotherms determined (at 35°C) on a chromia gel that was heated in air at 320°C for 3 hours. These workers have proposed that the presence of strong lateral interactions between adsorbate molecules is more important than the presence of surface homogeneity, in order for stepwise adsorption to occur. For the formation of the first water layer on the surface of certain chromia gels, the adsorbent-adsorbate interactions are probably stronger than the lateral interactions between the adsorbate molecules; when the surface becomes covered by the adsorbate, then adsorbate-adsorbate interactions will predominate, e.g. intermolecular hydrogen bonding.

The Frenkel-Halsey-Hill (FHH) Plots

The ranges of linearity of the various FHH plots for nitrogen, argon and water vapour adsorption respectively, on gel A3, are recorded in Table 6.4, together with the corresponding values of 'r' determined from the slopes of the plots (Section 2.4). For purposes of comparison, the FHH plots for nitrogen and for water vapour adsorption on orthorhombic CrOOH, CrO_2 and chromia gel B3(880)2 respectively, are summarised in Table 6.5.

Although the ranges of linearity of the FHH plots for nitrogen adsorption on gel A3 were not quite so wide as those found for nitrogen on non-porous silicas (cf. Table 4.2, Section 4.5), the plots nevertheless confirmed that the various samples of gel A3 (outgassed at temperatures between 25° and 1000°C) contained only a small amount

of porosity. In general, the values of r (mean = 2.7) correspond fairly closely to the range of 2.5 - 2.75 reported[74] as typical for nitrogen adsorption on a polar surface. For nitrogen adsorption on the well-characterised reference chromium oxides, orthorhombic CrOOH, CrO_2 and gel B3(880)2 respectively, the FHH plots were linear over a wide range of relative pressure with very close agreement between the values of r (cf. Table 6.5). In the case of nitrogen and water vapour adsorption respectively, the values of r recorded in Tables 6.4 and 6.5 are characteristic[75] of specific adsorbent-adsorbate interactions.

In the case of argon adsorption on gel A3, the FHH plots exhibited severelyrestricted ranges of linearity, although in comparison to argon adsorption on the silicas, the upper limit was located at higher relative pressures (at about 0.9 Po). The high values of r in the case of argon adsorption, on gel A3, therefore, probably possess little meaning.

The ranges of linearity of the FHH plots for water vapour adsorption on gel A3 were slightly more restricted than in the case of water adsorption on the silicas. However, the values of r (mean = 2.7) were characteristic of water vapour adsorption on hydrophilic surfaces, i.e. r = about 2.5 (Zettlemoyer[74]), whereas the value of r in the case of the hydroxylated silicas were consistently much lower. The greater hydrophilicity of a chromia surface (even after prolonged outgassing at 1000°C), as compared to a hydroxylated silica surface, is also reflected by the much higher uptakes of water vapour at an arbitrary relative pressure of 0.2 Po (expressed, in Tables 6.3 and 4.1 respectively, on a unit area basis using the corresponding nitrogen BET surface areas).

TABLE 6.3

Nitrogen, Argon and Water Vapour Adsorption on Chromia Gel A3 Outgassed at Temperatures up to 1000°C

OUTGASSING TEMPERATURE (°C)	NITROGEN		ARGON		WATER		
	BET		BET		BET		SORPTION AT 0.2 Po
	S^{N}_{BET} (m^2g^{-1})	C	S^{Ar}_{BET} (m^2g^{-1})	C	S^{W}_{BET} (m^2g^{-1})	C	(μ mole m^{-2})
25	132	144	152	51	233	48	32.1
150	130	167	148	70	218	48	30.3
300	168	216	197	155	130	18	12.2
440	136	(94)	152	72	66	27	8.4
600	67	(54)	59	118	43	481	12.5
800	36.0	(42)	31.0	122	19	196	10.5
1000	12.0	(46)	10.7	92	7.5	10	8.7
[a]1000	-	-	-	-	6.4	14	8.1

[a]Repeat water vapour isotherm determination: the nitrogen BET surface area was assumed to remain constant.

TABLE 6.4

FHH Plots of Nitrogen, Argon and Water Vapour Adsorption Isotherms on Chromia Gel A3

OUTGASSING TEMPERATURE (°C)	NITROGEN		ARGON		WATER	
	LINEARITY (P/Po)	r	LINEARITY (P/Po)	r	LINEARITY (P/Po)	r
25	0.08 - 0.8	2.4	0.75 - 0.9	3.3	0.35 - 0.8	3.0
150	0.08 - 0.8	2.4	0.40 - 0.85	2.9	0.35 - 0.6	3.6
300	0.15 - 0.75	2.9	0.65 - 0.9	3.8	0.30 - 0.7	2.2
440	0.35 - 0.75	2.5	0.50 - 0.9	3.1	0.40 - 0.63	1.7
600	0.25 - 0.7	2.8	0.65 - 0.95	3.8	0.35 - 0.68	3.1
800	0.25 - 0.92	3.2	0.55 - 0.86	4.4	0.65 - 0.82	3.3
1000	0.25 - 0.8	2.7	0.45 - 0.8	4.0	0.40 - 0.76	2.4
[a]1000	-	-	-	-	0.35 - 0.78	2.3

[a] Repeat water vapour isotherm determination.

TABLE 6.5

FHH Plots of Nitrogen and Water Vapour Adsorption Isotherms on Chromium Oxides

SAMPLE	OUTGASSING TEMPERATURE (°C)	NITROGEN		WATER	
		LINEARITY (P/Po)	r	LINEARITY (P/Po)	r
CrOOH	25	0.15 - 0.9	2.4	0.45 - 0.82	1.3
CrO_2	25	0.15 - 0.9	2.5	0.60 - 0.90	2.3
[a]Gel B3	[a]880	0.25 - 0.9	2.5	-	-

[a]An 'aged' chromia sample calcined at 880°C for 2 hours in air, previously adopted[43] as a non-porous reference adsorbent.

REFERENCES

1. A.I. Vogel, "Macro and Semimicro Qualitative Inorganic Analysis, Longmans, 4 Edt., (1964) pages 318 and 363.
2. K.C. Sen, J. Phys. Chem., (1927) 31, 922.
3. S.W. Weller and S.E. Voltz, J. Amer. Chem. Soc., (1954) 76, 4695.
4. H. Remy, "Treatise on Inorganic Chemistry", Elsevier (1956) 2, 135.
5. S.J. Teichner, U.S. 2,888,323 (1959).
6. C.B. Murphy, J.A. Hill and G.P. Schacher, Analyt. Chem., (1960) 32, 1374.
7. J. Fenerty, Ph.D. Thesis,Liverpool Polytechnic, (1971).
8. L. Friedman and J. Bigeleisen, J. Chem. Phys., (1950) 18, 1325.
9. R.L. Burwell, Jr., and H.S. Taylor, J. Amer. Chem. Soc., (1936) 58, 679; R.L. Burwell, Jr., ibid. (1937) 59, 1609.
10. Reference 4, page 136.
11. V.P. Tolstikov, Zh. Obshch. Khim., (1969) 39(2), 240.
12. H. Remy, "Treatise on Inorganic Chemistry", Elsevier, (1956) 1, 813.
13. Reference 4, page 146.
14. J.D. Carruthers, Ph.D. Thesis, Brunel University, (1968).
15. J.D. Carruthers, J. Fenerty and K.S.W. Sing, "Proc. 6th Int. Symp. Reactivity Solids", Schenectady, 1968. Eds. J.W. Mitchell, R.C. DeVries, R.W. Roberts and P. Cannon; Wiley Interscience, New York, (1969) 127.
16. P.D. Garn, "Thermoanalytical Methods of Investigation", Academic Press, (1965).
17. T.L. Narasimha Rao and V. Kesavulu, Indian J. Appl. Chem., (1967) 30, 25.
18. J. Dereń and J. Haber, Ceramika, (1969) No 13, 5.

19. J.H. deBoer, J.J. Steggerda, J.M.H. Fortuin and P.Zwietering, "Proc. 2nd Int. Congr. Surface Activity", London, 1957. Butterworths, London, (1957) 2, 93.

20. R. Tertian and D. Papée, J. Chem. Phys., (1958) 55, 341.

21. S.I. Smyshlyaev, E.P. Tsymbal and L.A. Simonova, Izv. Vyssh. Ucheb. Zaved., Khim. Khim. Teknol., (1972) 15(8), 1252.

22. J. Dereń, J. Haber, A. Podgórecka and J. Burzyk, J. Catalysis, (1963) 2, 161.

23. S.K. Bhattacharyya and V.S. Ramachandran, Bull. Nat. Inst. Sci. (India), (1959) 12, 23.

24. F. Krleza and M. Sljukic, Kolloid Zh., (1962), 182, 145.

25. N.E. Cross and H.F.Leach, J. Catalysis, (1971) 21, 239.

26. M. Sorrentino, L. Steinbrecher and F. Hazel, J. Colloid Interface Sci., (1969) 31, 307.

27. M.A.Alario Franco, J. Fenerty and K.S.W. Sing, "Proc. 7th Int. Symp. Reactivity Solids", Bristol, 1972. Eds. J.S. Anderson, M.W. Roberts and F.S. Stone; Chapman and Hall, London, (1972) 327.

28. J.D. Carruthers, K.S.W. Sing and J. Fenerty, Nature (1967) 213, 66.

29. M.A. Alario Franco and K.S.W. Sing, J. Thermal Analysis, (1972) 4, 47.

30. Y. Shibasaki, Mat. Res. Bull., (1972) 7, 1125.

31. R.D. Shannon, J. Amer. Ceram. Soc., (1967) 50, 56.

32. K.H. Leisser, Angew. Chem. Int. Edt., (1969) 8, 188.

33. W. Feitknecht, Kolloid. Zh. (1954) 136, 52.

34. M.S. Kovel, Tr. Ural. Politekh. Inst., (1966) No 152, 5.

35. D. Aldcroft and G.C. Bye, Proc. Brit. Ceram. Soc., (1969) 125.

36. E.S. Halberstadt, H.K. Henisch, J. Nickl and E.W. White, J. Colloid Interface Sci., (1969) 29, 469.

37. V.P. Chalyi, S.P. Rozhenko and Z. Ya. Makarova, Ukr. Khim. Zh., (1962) 28, 921.

38. V.P. Chalyi, Z. Ya. Makarova and V.T. Zorya, Kolloid. Zh., (1964) 26, 263.

39. N.C. Tombs, W.J. Croft, J.R. Carter and J.F. Fitzgerald, Inorg. Chem., (1964) 3, 1791.

40. R. Wilhelmi and O. Johnsson, Acta. Chem. Scand., (1958) 12, 1532.

41. R. Giovanoli, in "Proc. 7th Int. Symp. Reactivity Solids", Bristol, 1972. Eds. J.S. Anderson, M.W. Roberts and F.S. Stone; Chapman and Hall, London, (1972) 335.

42. P. Ratnasamy and A.J. Léonard, J. Phys. Chem., (1972) 76, 1838.

43. F.S. Baker, J.D. Carruthers, R.E. Day, K.S.W. Sing and L.J. Stryker, Discussions Faraday Soc., (1971) No 52, 173.

44. A. Gosnold, National Physical Laboratory, Teddington, England. Personal Communication.

45. "Handbook of Chemistry and Physics", The Chemical Rubber Co., Ohio, 46th Edt. (1965-1966) page D124.

46. S.J. Gregg and K.S.W. Sing, "Adsorption, Surface Area and Porosity", Academic Press, London, (1967) page 90.

47. A.L. McClellan and H.F. Harnsberger, J. Colloid Interface Sci., (1967) 23, 577.

48. J.D. Carruthers, D.A. Payne, K.S.W. Sing and L.J. Stryker, J. Colloid Interface Sci., (1971) 36, 205.

49. D.A. Payne, K.S.W. Sing and D.H. Turk, J. Colloid Interface Sci., (1973) 43, 287.

50. M.R. Harris and K.S.W. Sing, Chem. and Ind., (1967) 757.

51. S. Brunauer, "The Adsorption of Gases and Vapours", Oxford University Press, London, (1944).

52. J.H. de Boer, "The Structure and Properties of Porous Materials", Proc. 10th Symp. Colston Res. Soc., Bristol, 1958. Eds. D.H. Everett and F.S. Stone; Butterworths, London, (1958) page 68.

53. Reference 46, pages 145 and 177.

54. K.C. Taylor, Ph.D. Thesis. Northwestern University, Evanston, Illinois, U.S.A., (1968).

55. Reference 46, page 195.

56. F.S. Baker, K.S.W. Sing and L.J. Stryker, Chem. and Ind., (1970) 718.

57. Yu. A. Eltekov, Izv. Akad. Nauk, S.S.S.R., Otd. Khim. Nauk, (1960) 2236.

58. Yu. A. Eltekov, T.R. Brueva and A.M. Rubinshtein, Izv. Akad. Nauk S.S.S.R., Otd. Khim. Nauk, (1961) 560.

59. M.R. Harris and K.S.W. Sing, J. Appl. Chem., (1957) 7, 397.

60. M.R. Harris and K.S.W. Sing, "Proc. 3rd Int. Congr. Surface Activity", Cologne, 1960. University Press, Mainz, (1960) 2, 42.

61. J.W. Lucas, G.W. Newton and K.S.W. Sing, J. Appl. Chem., (1963) 13, 265.

62. K.S.W. Sing and J.D. Madeley, J. Appl. Chem., (1953) 3, 549.

63. A.G. Foster and J.M. Thorp, "The Structure and Properties of Porous Materials", Proc. 10th Symp. Colston Res. Soc., Bristol, 1958. Eds. D.H. Everett and F.S. Stone; Butterworths, London, (1958) page 227.

64. K.S.W. Sing, R.E. Day and L.J. Stryker, in "Proc. Int. Symp. Surface Area Determination", Bristol, 1969. Eds. D.H. Everett and R.H. Ottewill; Butterworths, London, (1970) 84.

65. G.C. Bye, J.G. Robinson and K.S.W. Sing, J. Appl. Chem., (1967) 17, 138.

66. N.F. Ermolenko and S.A. Levina, Kolloid, Zh., (1959) 21, 564.

67. N.F. Ermolenko and G.A. Popkovich, Vestsi Akad. Navuk Belarus. S.S.S.R., Ser Khim. Navuk (1966) 102.

68. J.D. Carruthers and K.S.W. Sing, Chem. and Ind., (1967) 1919.

69. P.J. Anderson and P.L. Morgan, Trans. Faraday Soc., (1964) 60, 930.

70. P.J. Anderson, R.F. Horlock and R.G. Avery, Proc. Brit. Ceram. Soc., (1965) 3, 33.

71. C. Pierce and B. Ewing, J. Amer. Chem. Soc., (1962) 84, 4070.

72. D.R. Bassett, E.A. Boucher and A.C. Zettlemoyer, J. Phys. Chem., (1967) 71, 2787.

73. S.A. Selim, R. Sh. Mikhail and R.I. Razouk, J. Phys. Chem., (1970) 74, 2944.

74. A.C. Zettlemoyer, J. Colloid Interface Sci., (1968) 28, 343.

75. G.D. Halsey, J. Chem. Phys., (1948) 16, 931.

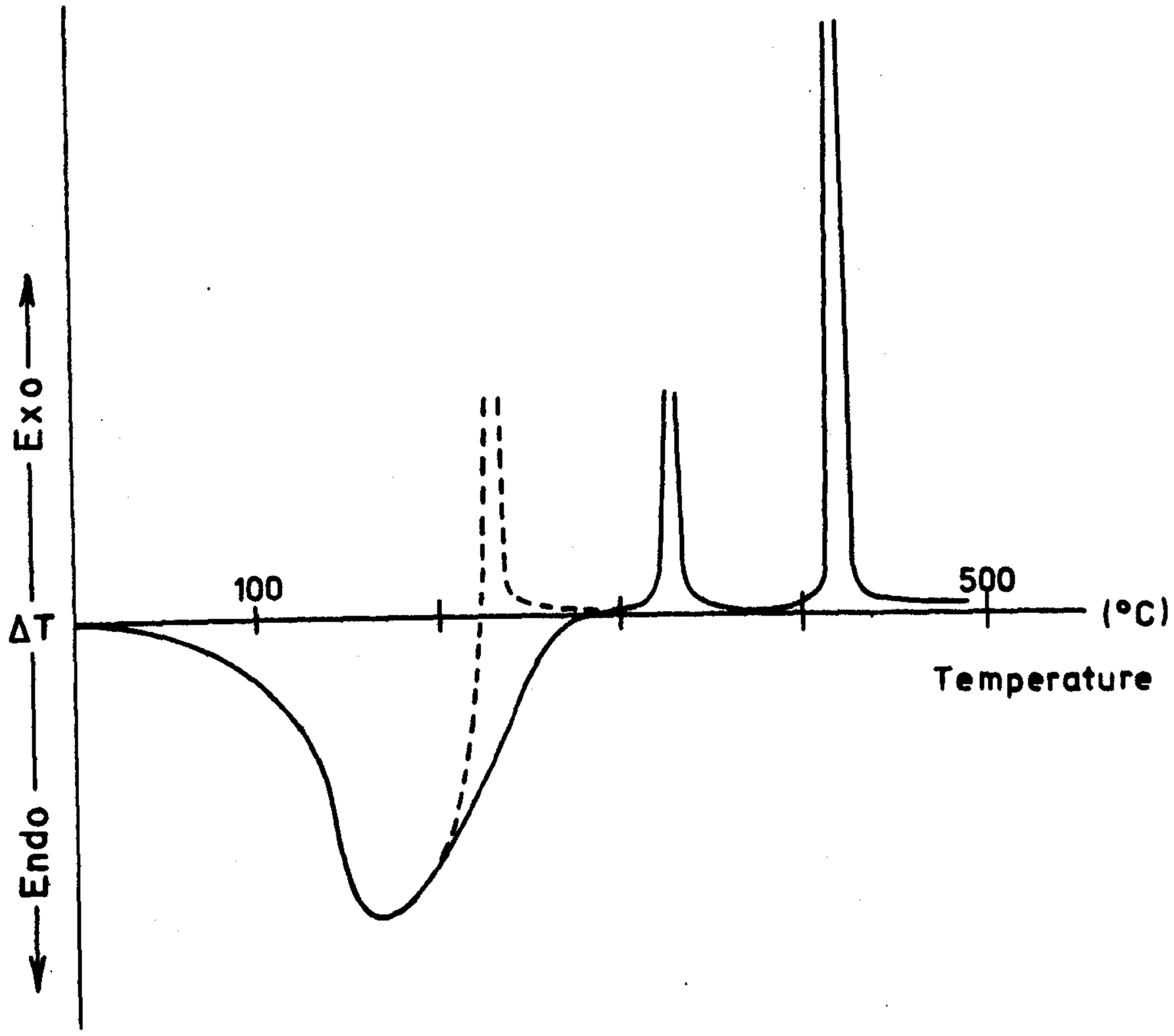

FIG 6.1a "Idealised" DTA Curve

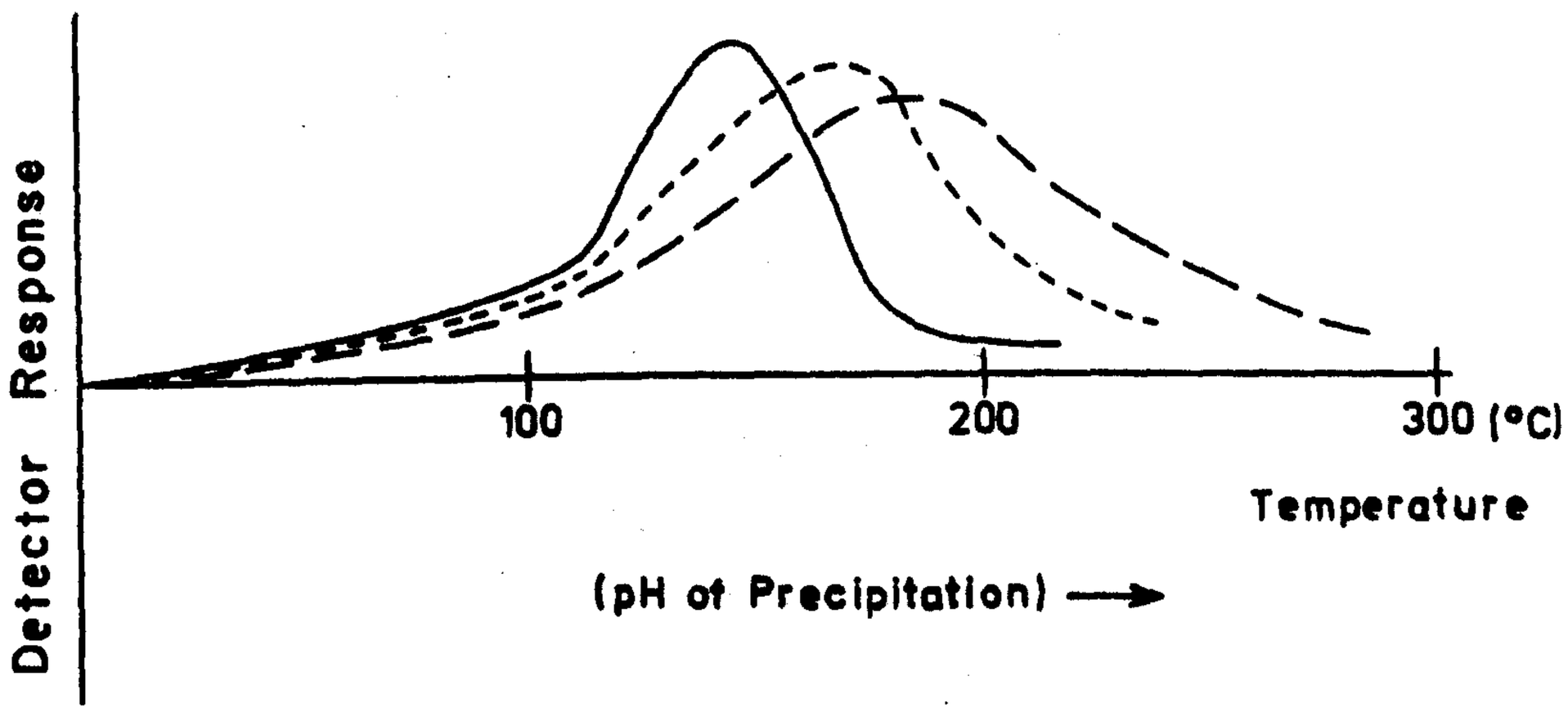

FIG 6.1b Progressive Change of Shape of the Peak on the Gas Detector Trace Associated with the Evolution of 'Free' Water from Chromia Gels (Idealised Representation)

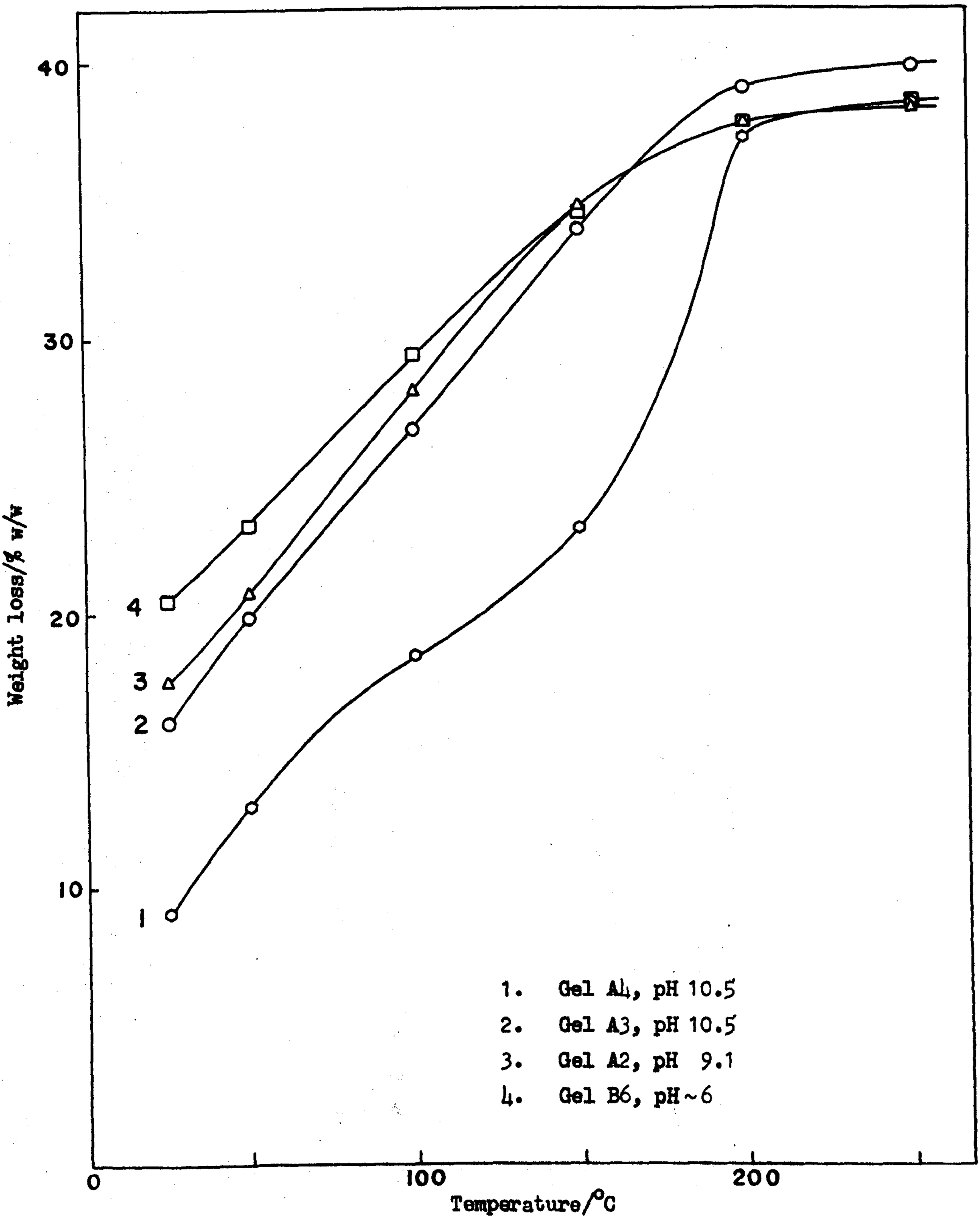

FIG 6.2 Weight Loss of Chromia Gels as a Function of Outgassing Temperature

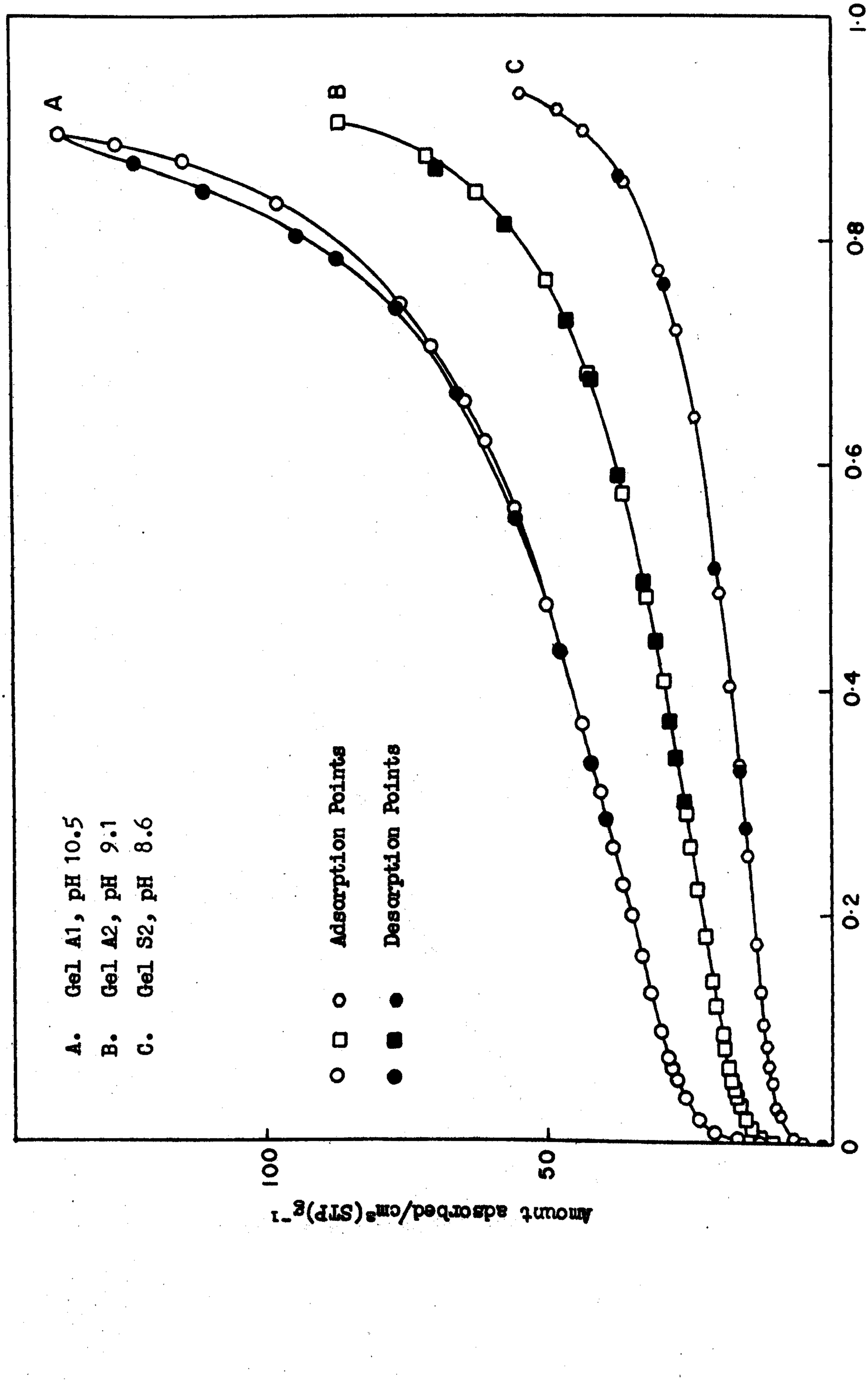

FIG 6.3 Nitrogen Isotherms Determined on Chromia Gels Outgassed @ 25°C

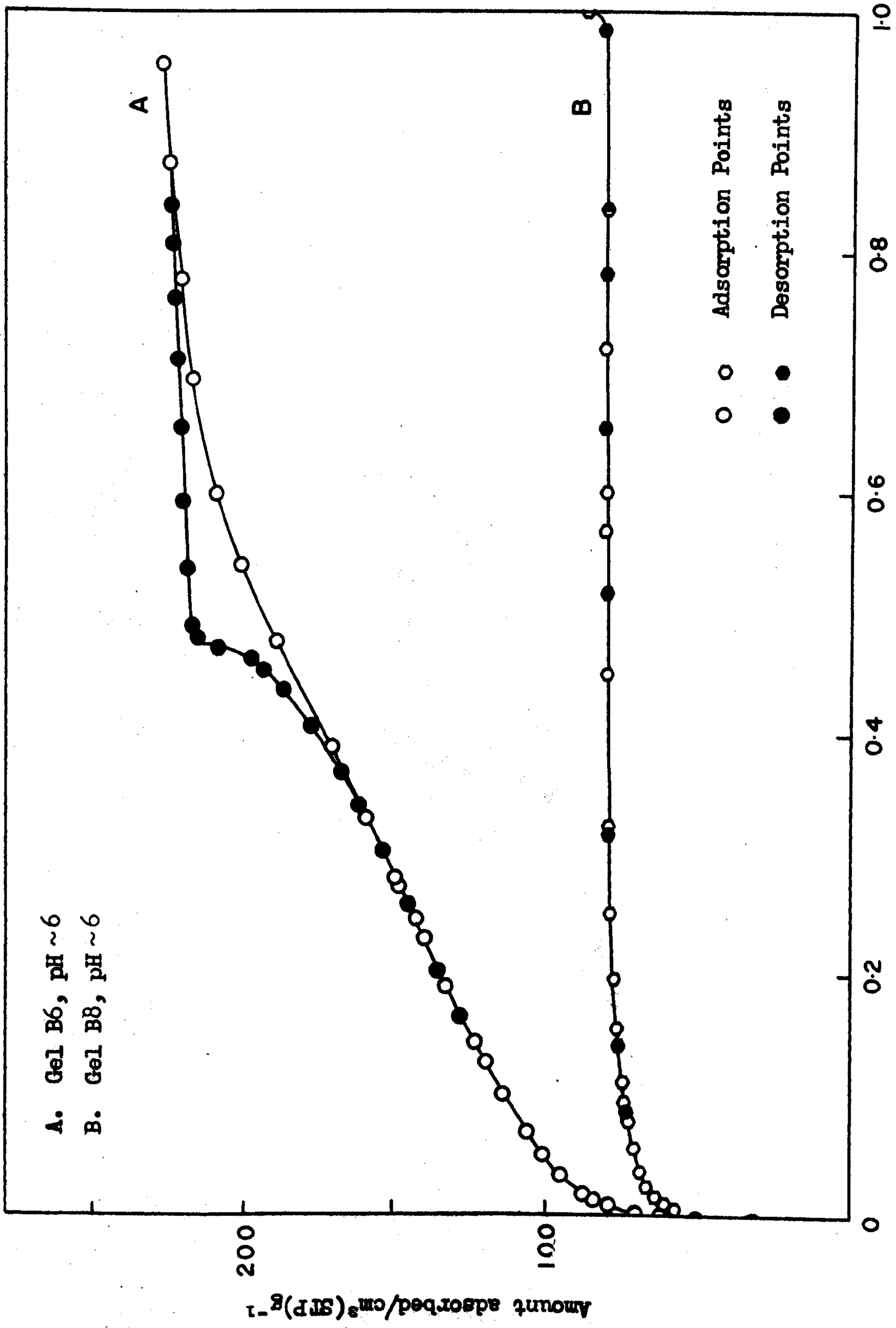

FIG 6.4 Nitrogen Isotherms Determined on Chromia Gels Outgassed @ 25°C

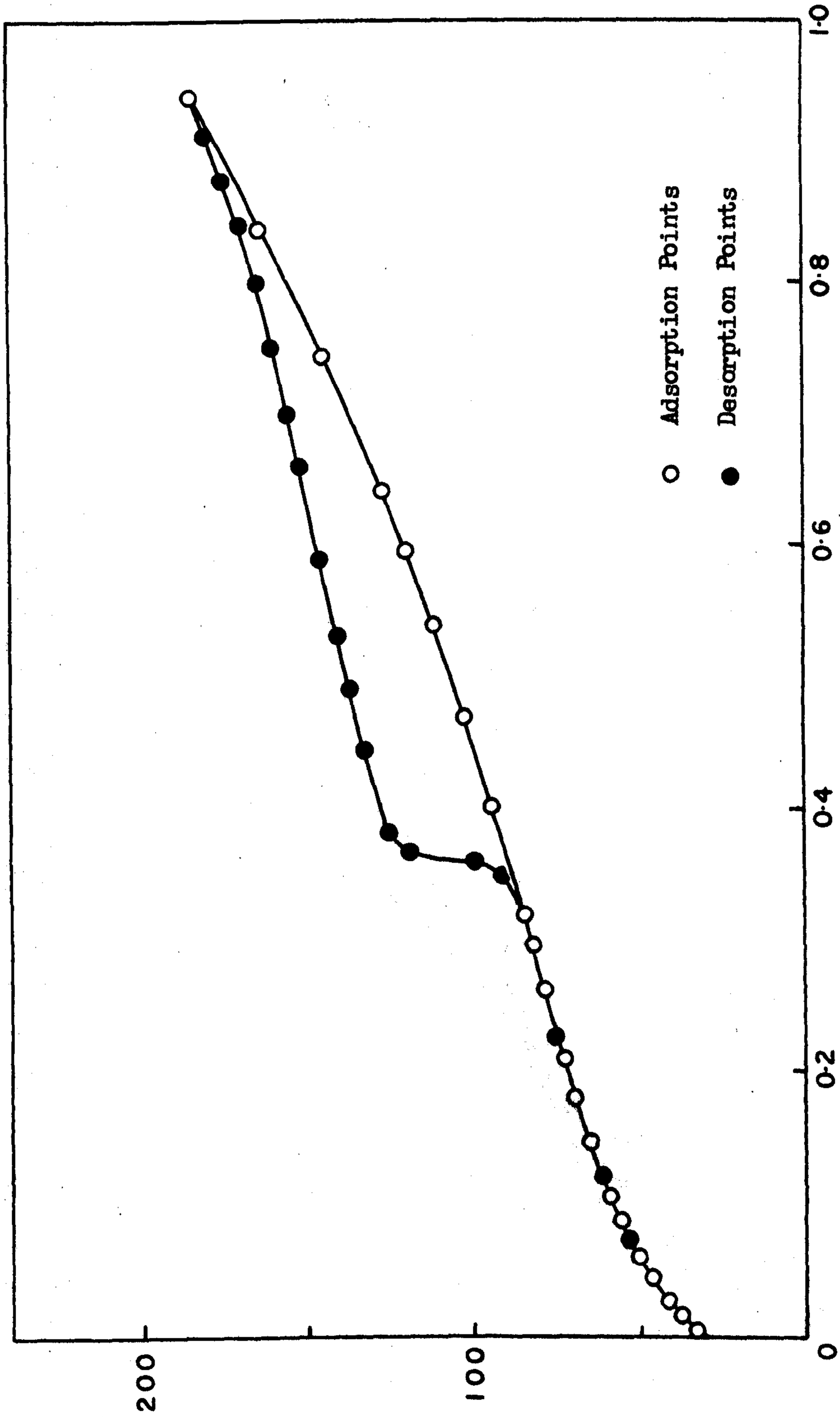

FIG 6.5 Argon Isotherm Determined on Chromia Gel A2 Outgassed @ 25°C

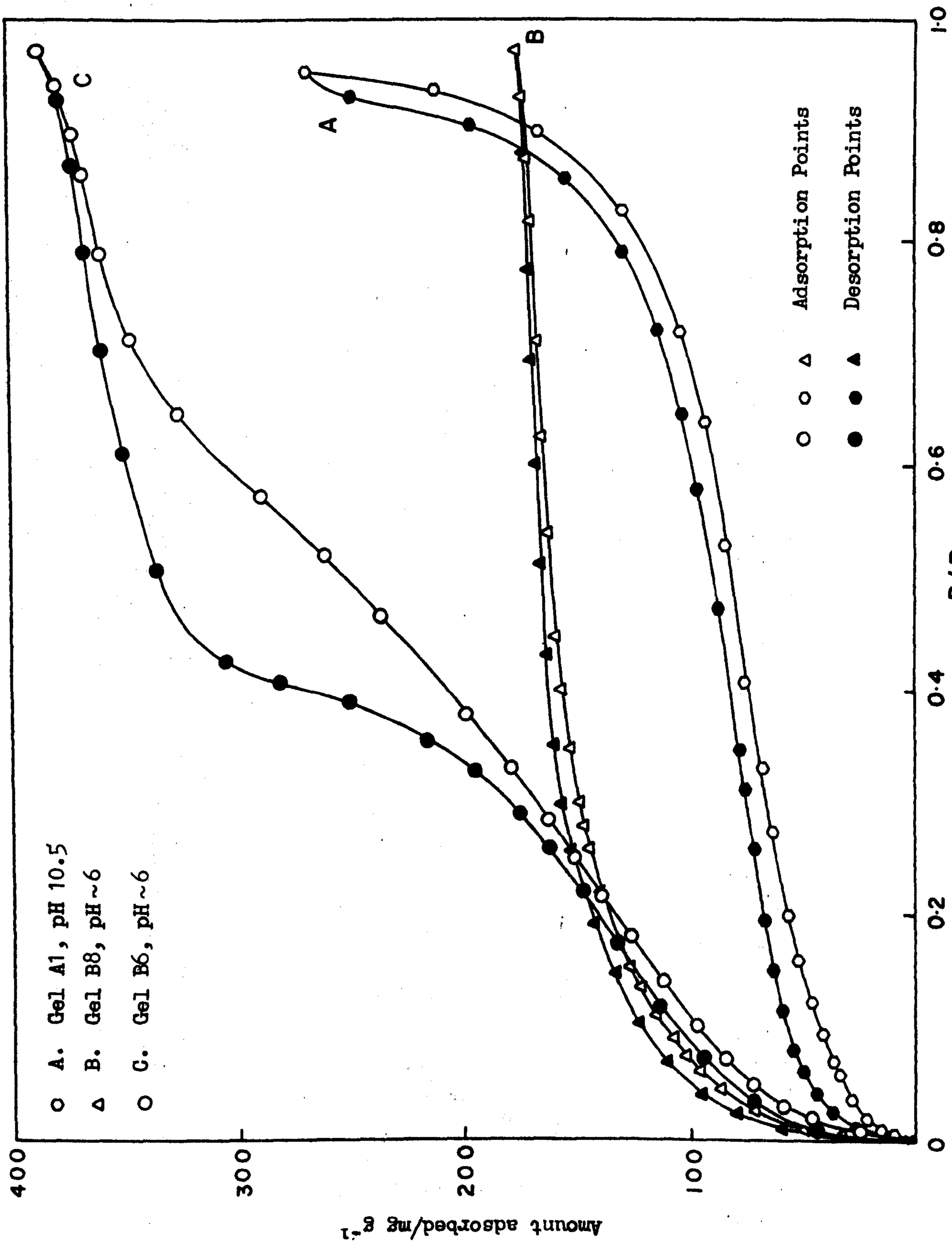

FIG 6.6 Water Vapour Isotherms Determined on Chromia Gels Outgassed @ 25°C

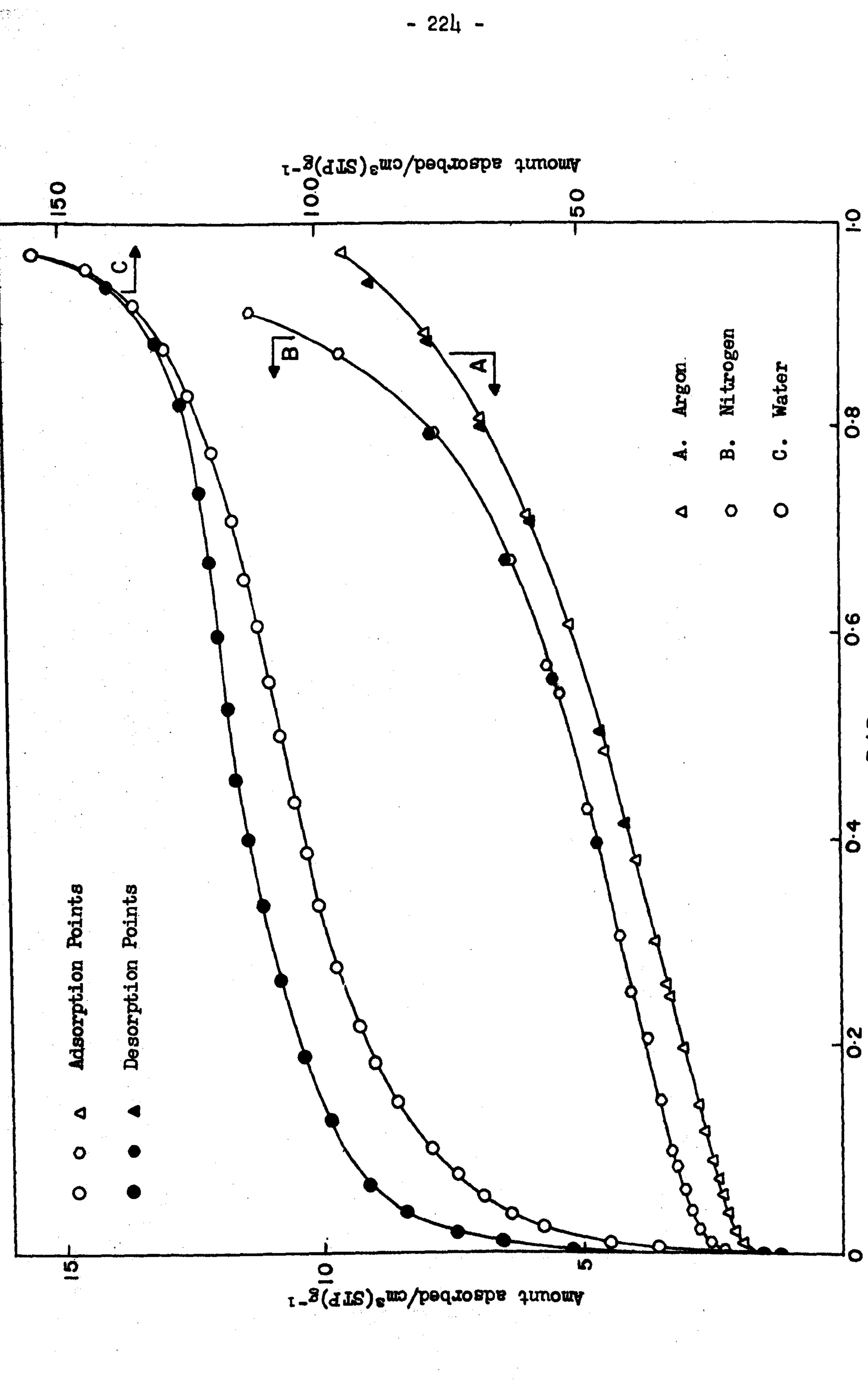

FIG 6.7 Nitrogen, Argon and Water Vapour Isotherms Determined on Chromia Gel At Outgassed @ 25°C

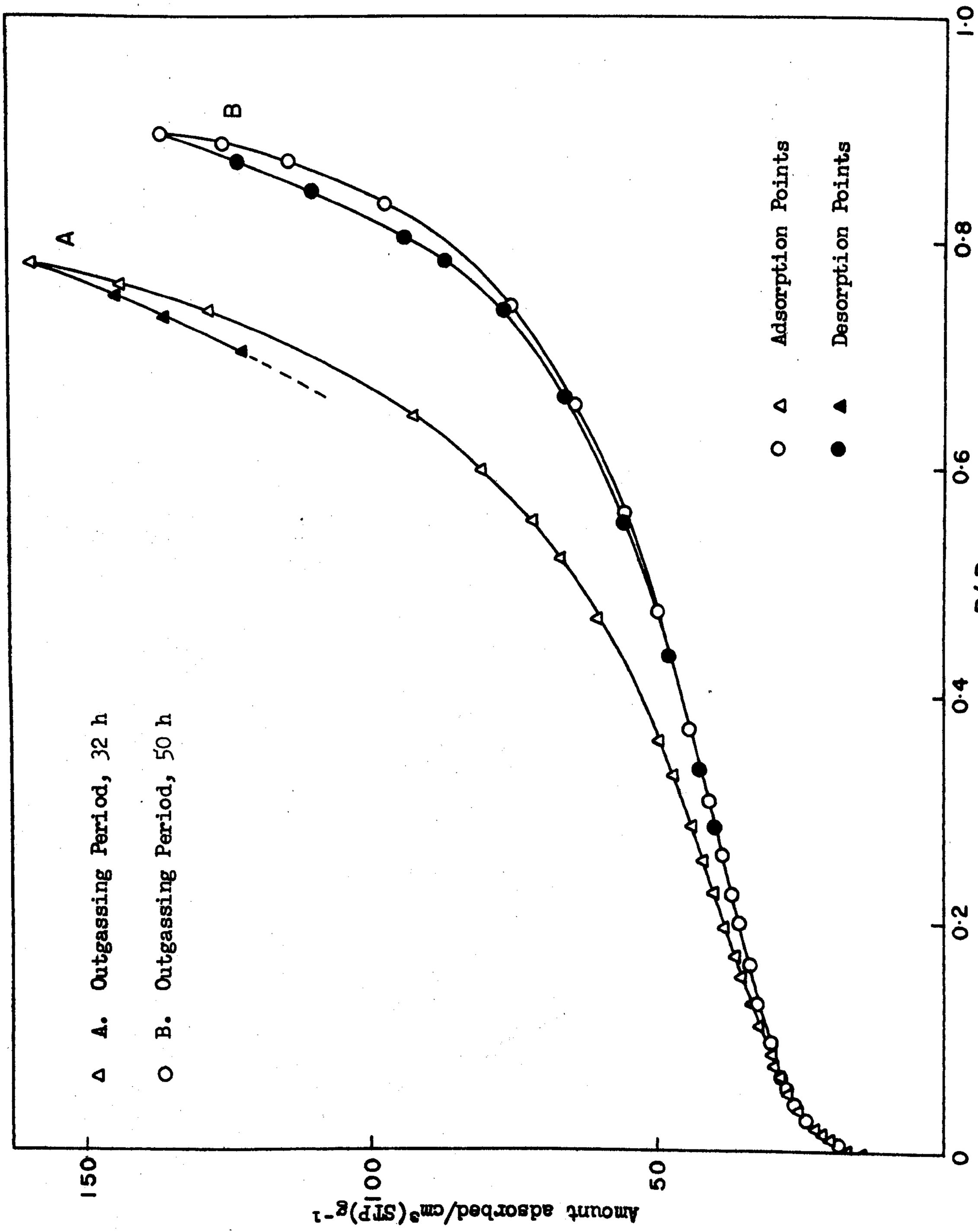

FIG 6.8 Nitrogen Isotherms Determined on Chromia Gel A1
Outgassed @ 25°C for Different Periods of Time

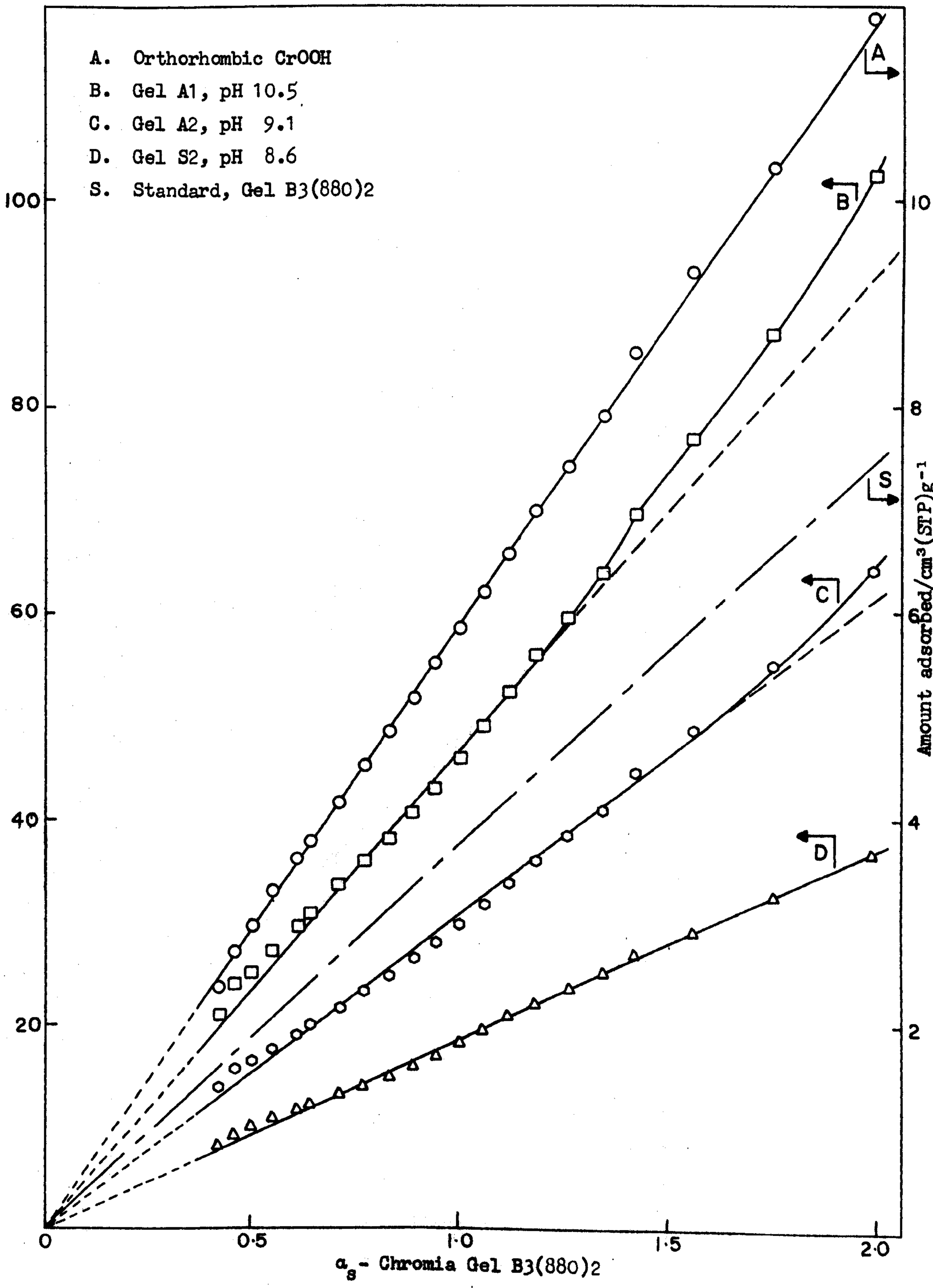

FIG 6.9 α_s-Plots for Nitrogen Adsorption on Chromia Gels @ 25°C

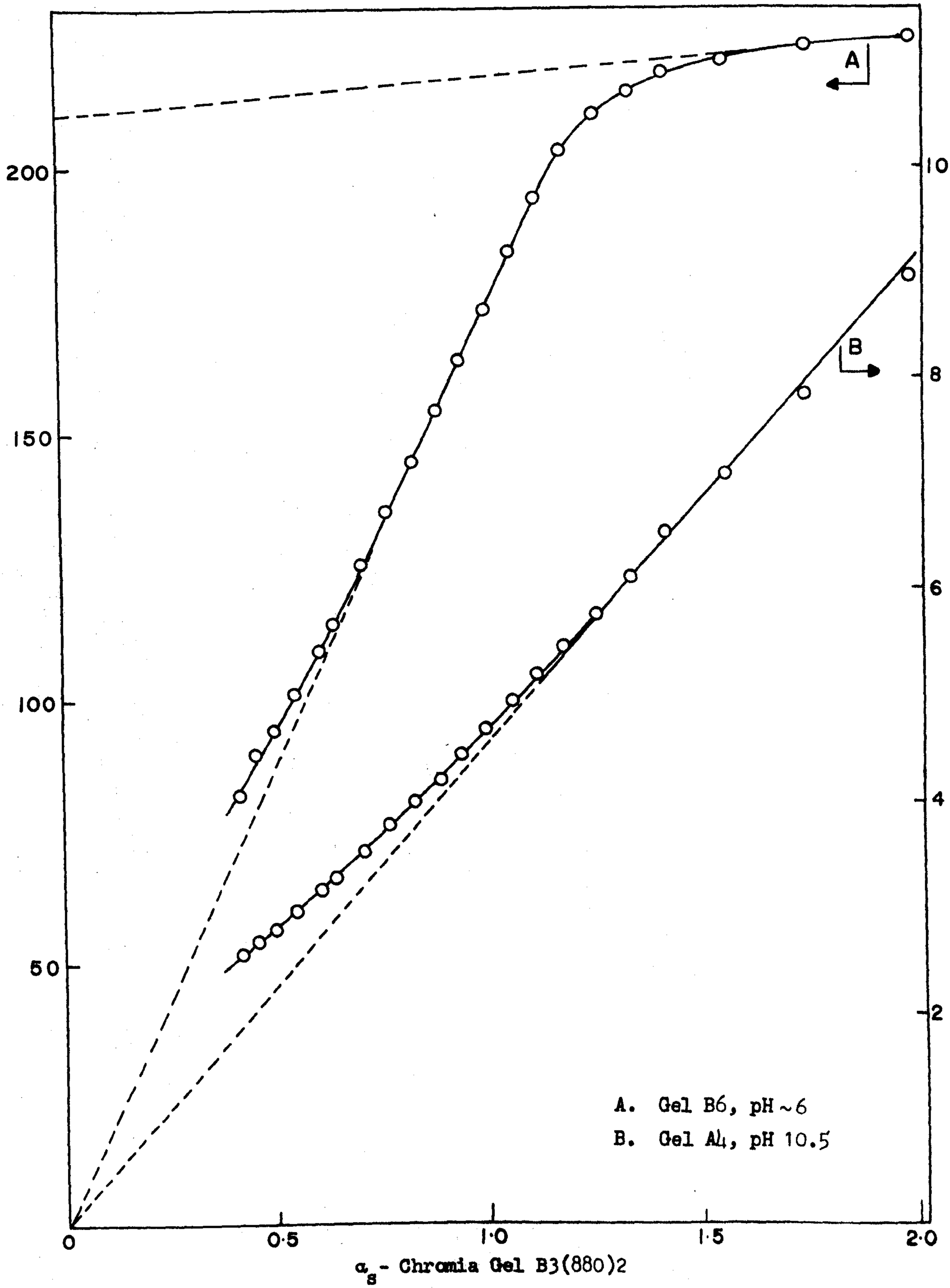

FIG 6.10 α_s-Plots for Nitrogen Adsorption on Chromia Gels Outgassed @ 25°C

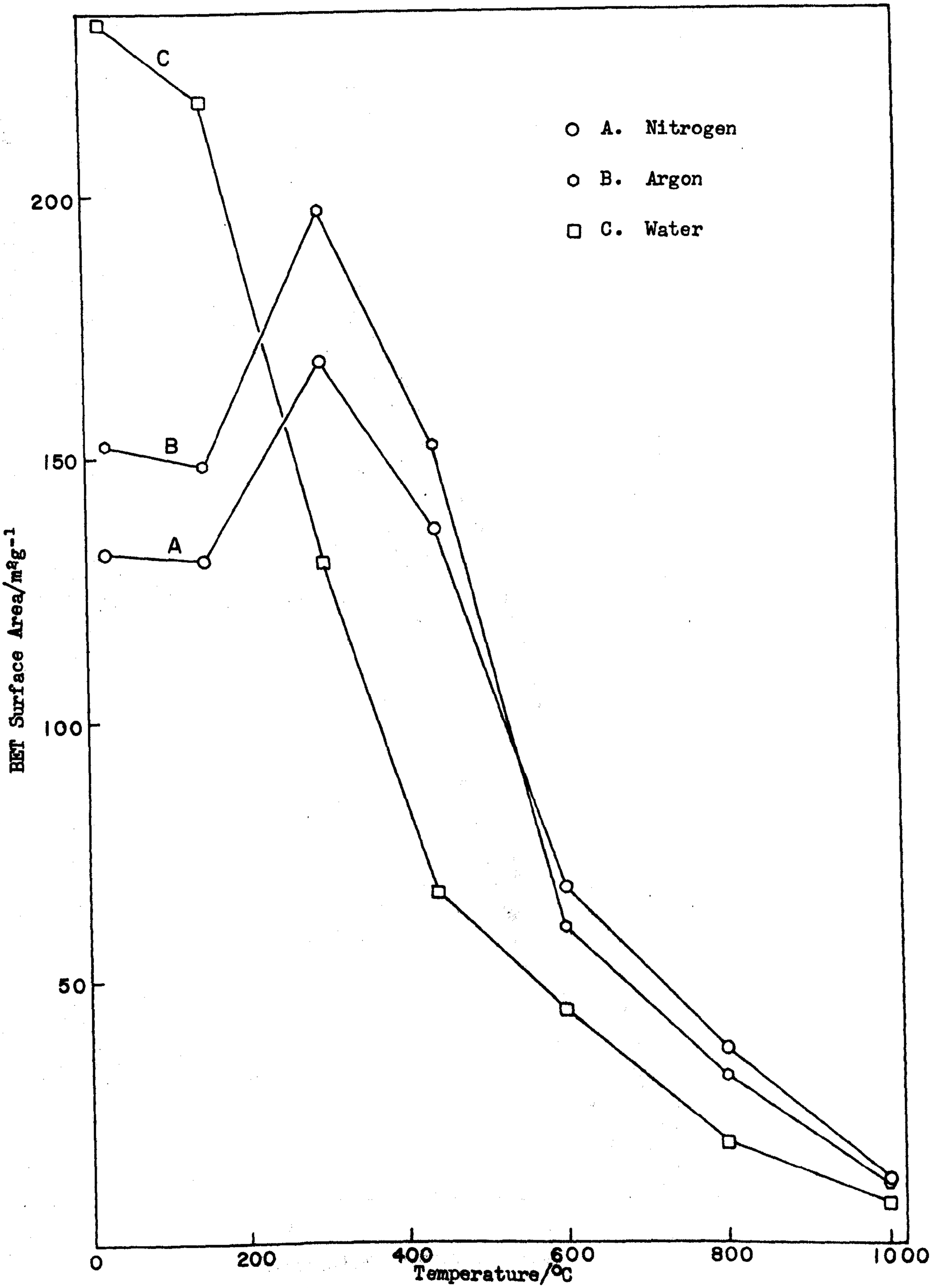

FIG 6.11 Variation of the BET Surface Area with the Temperature of Outgassing for Nitrogen, Argon and Water Vapour Adsorption on Chromia Gel A3

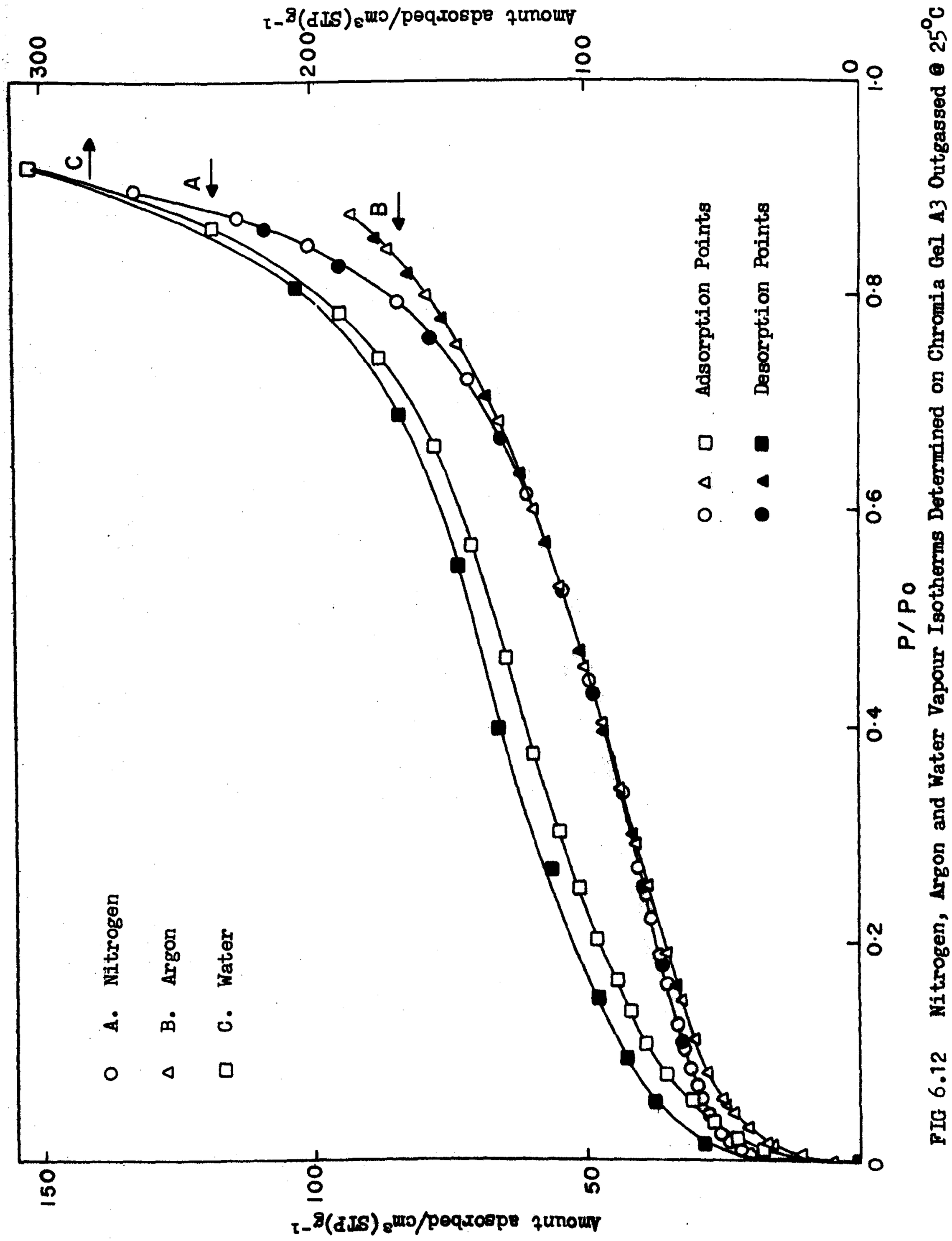

Nitrogen, Argon and Water Vapour Isotherms Determined on Chromia Gel A3 Outgassed @ 25°C

FIG 6.12

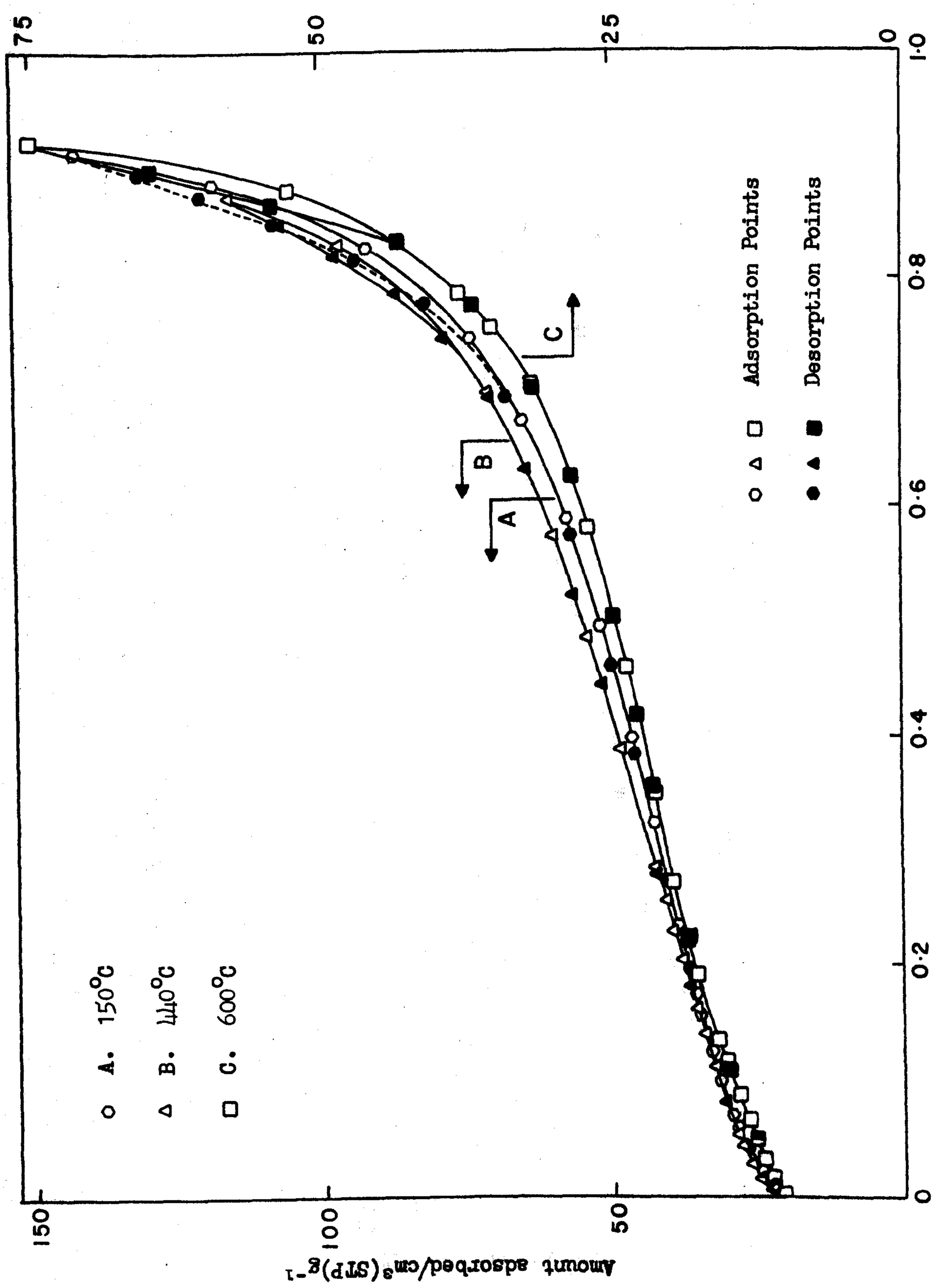

FIG 6.13 Nitrogen Isotherms Determined on Chromia Gel A3 Outgassed @ 150°, 440° and 600°C

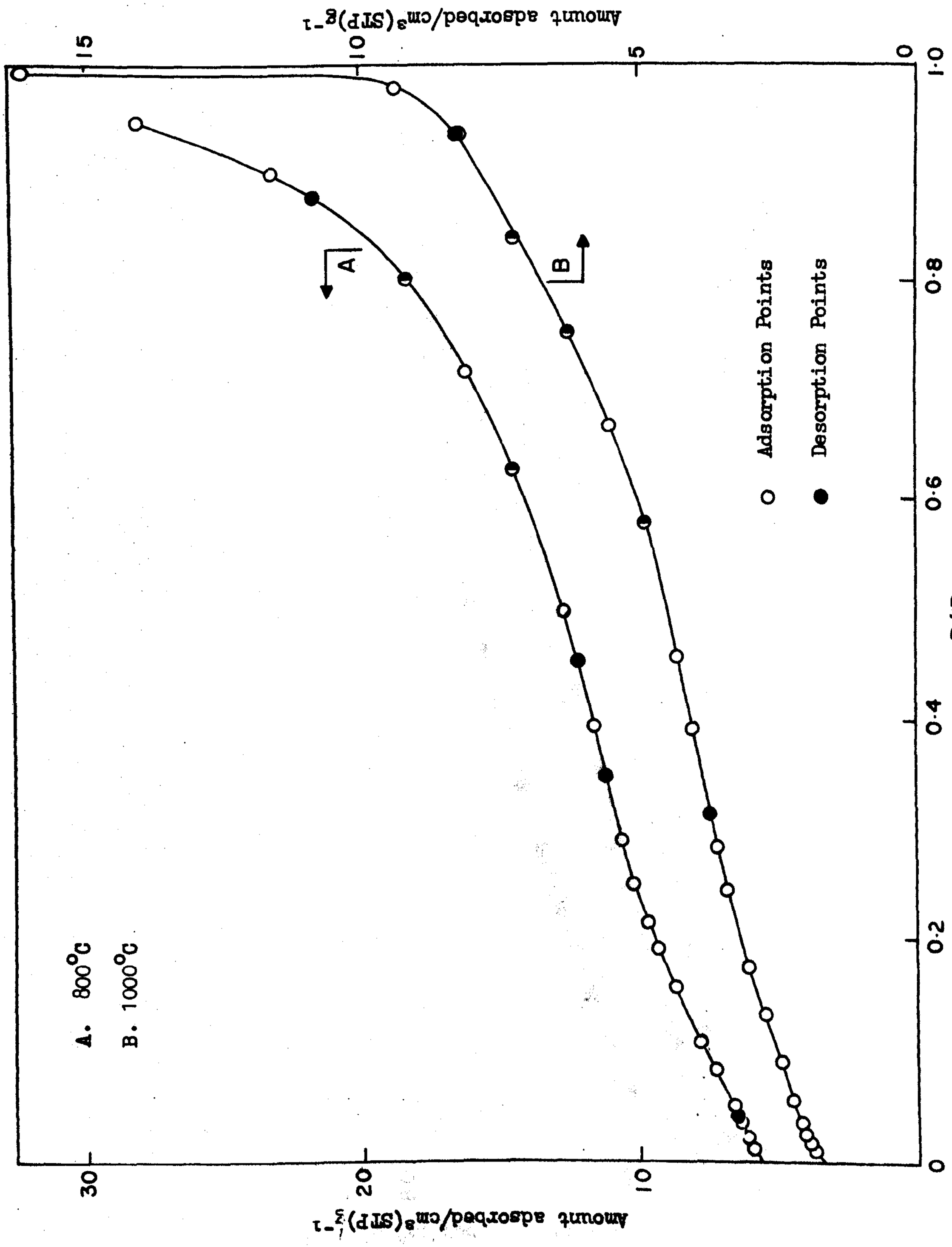

FIG 6.14 Nitrogen Isotherms Determined on Chromia Gel A3 Outgassed @ 800° and 1000°C

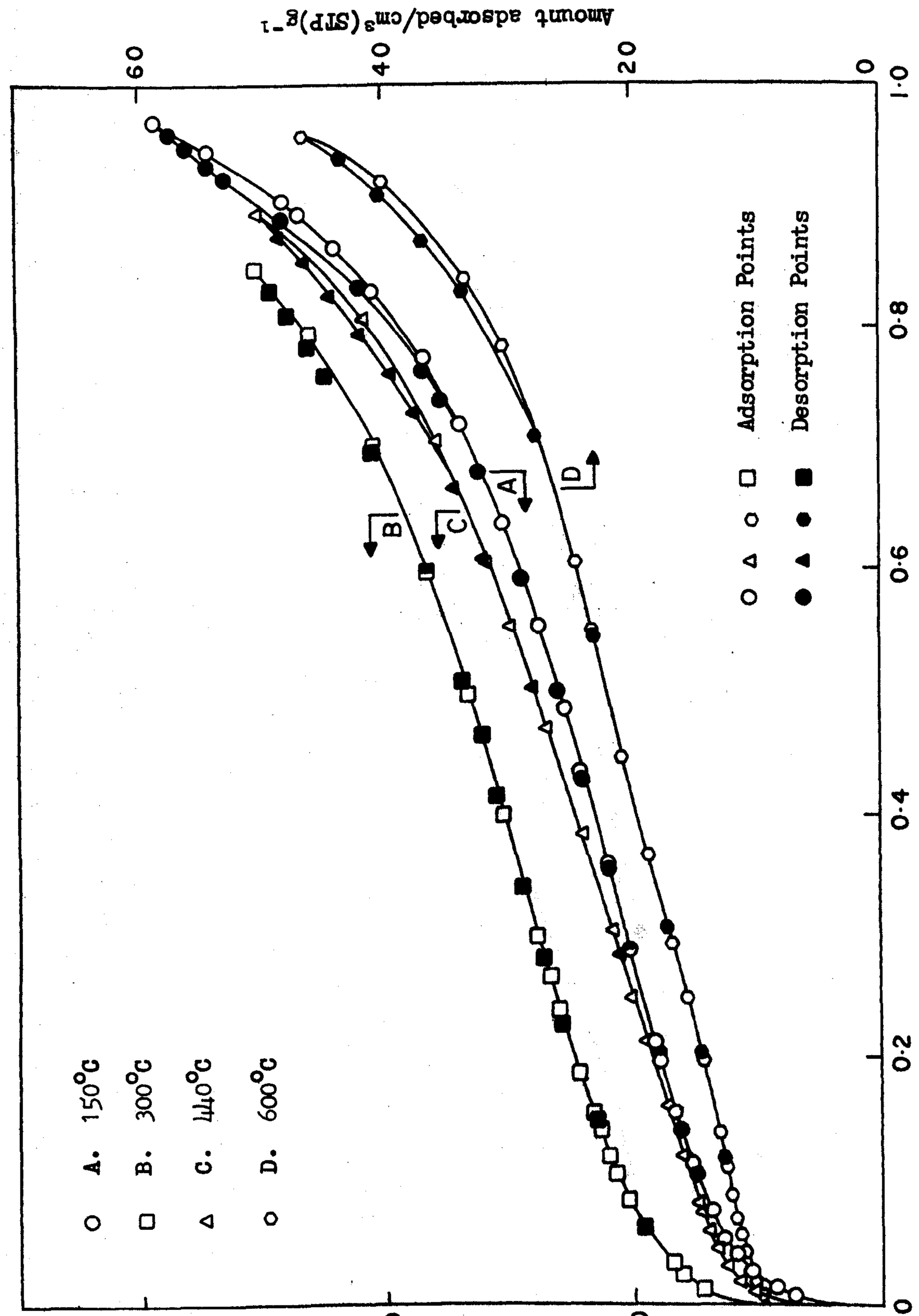

Argon Isotherms Determined on Chromia Gel A3 Outgassed @ 150°, 300°, 440° and 600°C

FIG 6.15

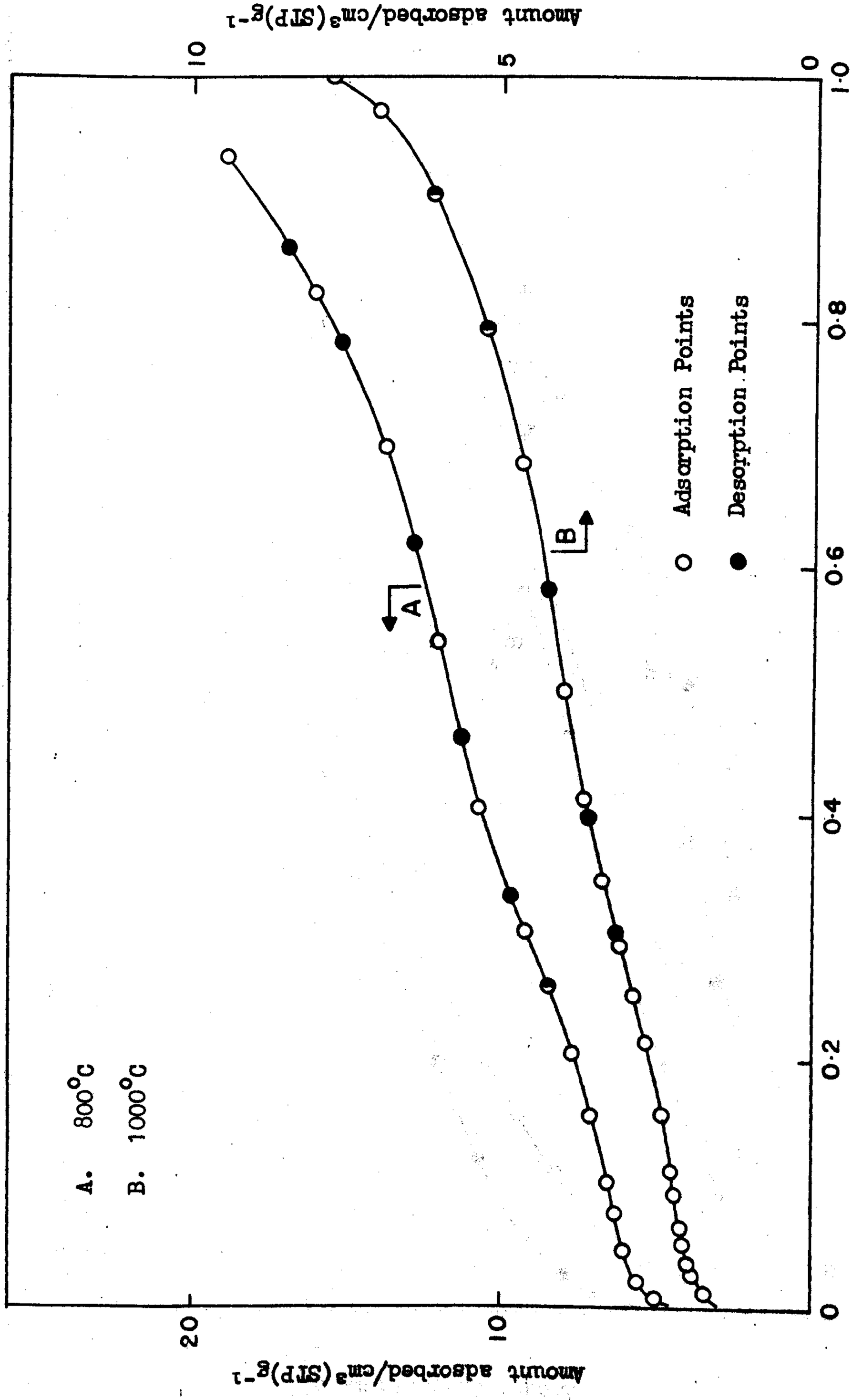

FIG 6.16 Argon Isotherms Determined on Chromia Gel A3 Outgassed @ 800° and 1000°C

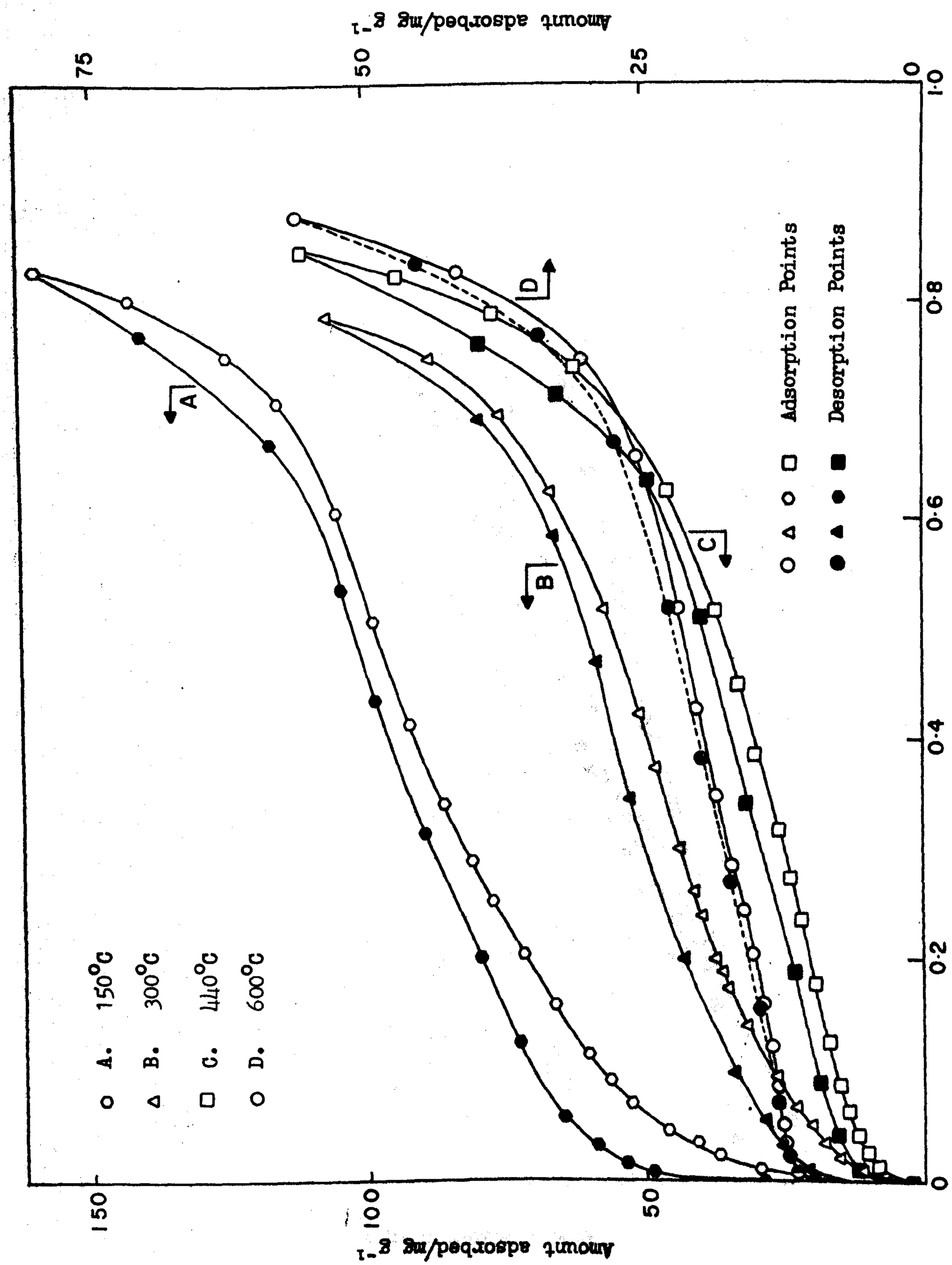

FIG 6.17 Water Vapour Isotherms Determined on Chromia Gel A3 Outgassed @ 150°, 300°, 440° and 600°c

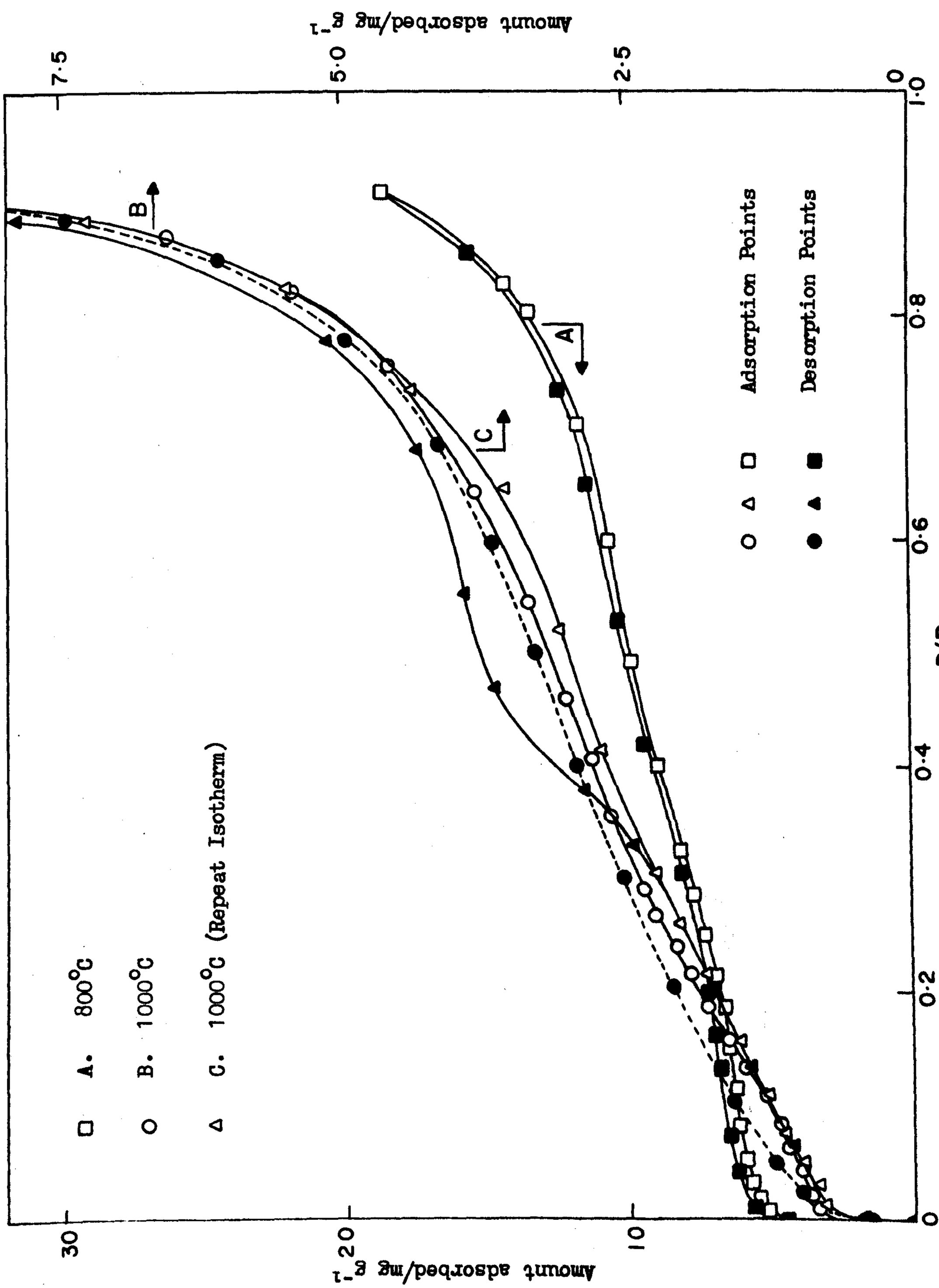

FIG 6.18 Water Vapour Isotherms Determined on Chromia Gel A3 Outgassed @ 800° and 1000°C

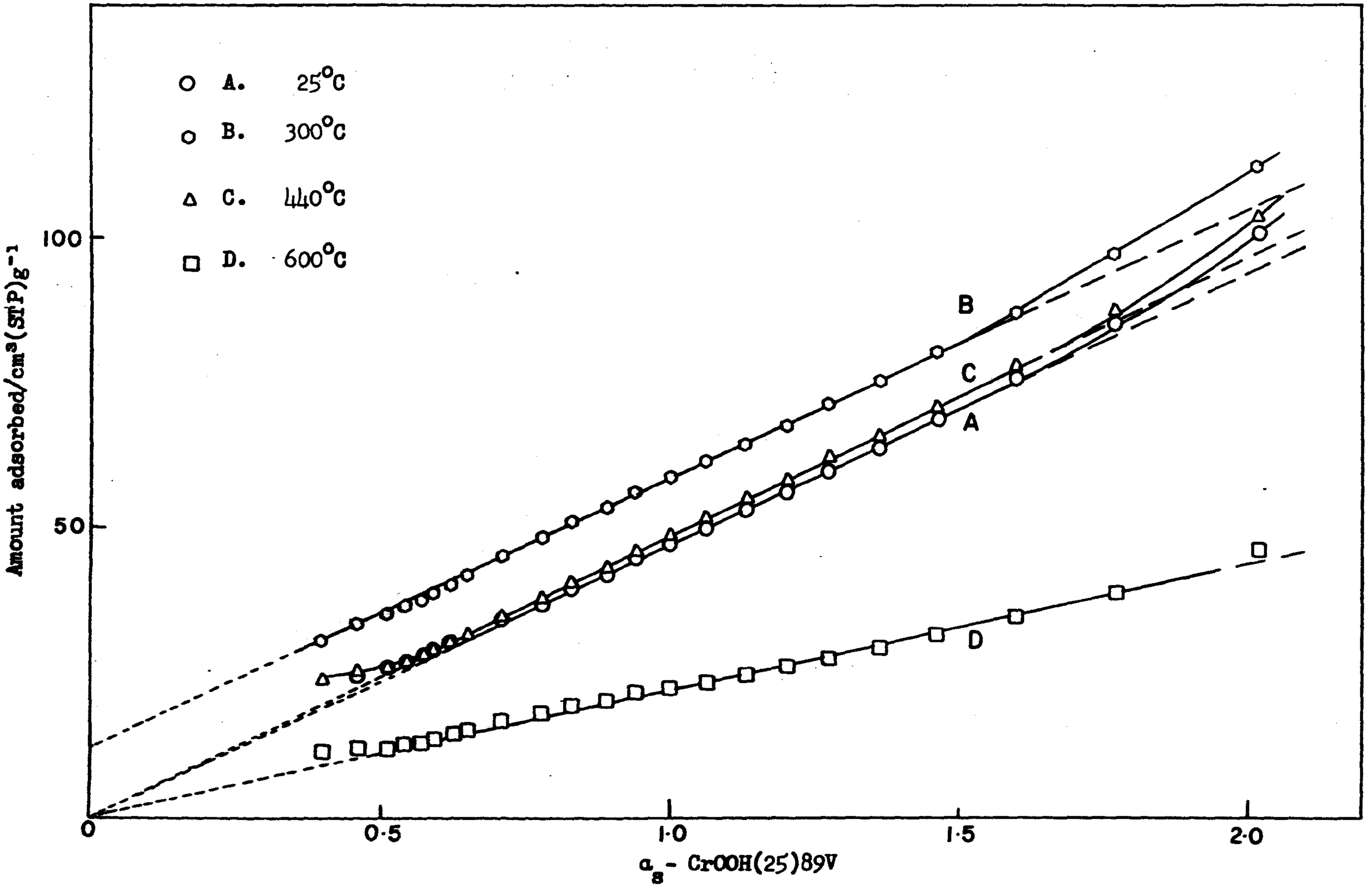

FIG 6.19 a_s-Plots for Nitrogen Adsorption on Chromia Gel A3 Outgassed @ 25°, 300°, 440° and 600°C

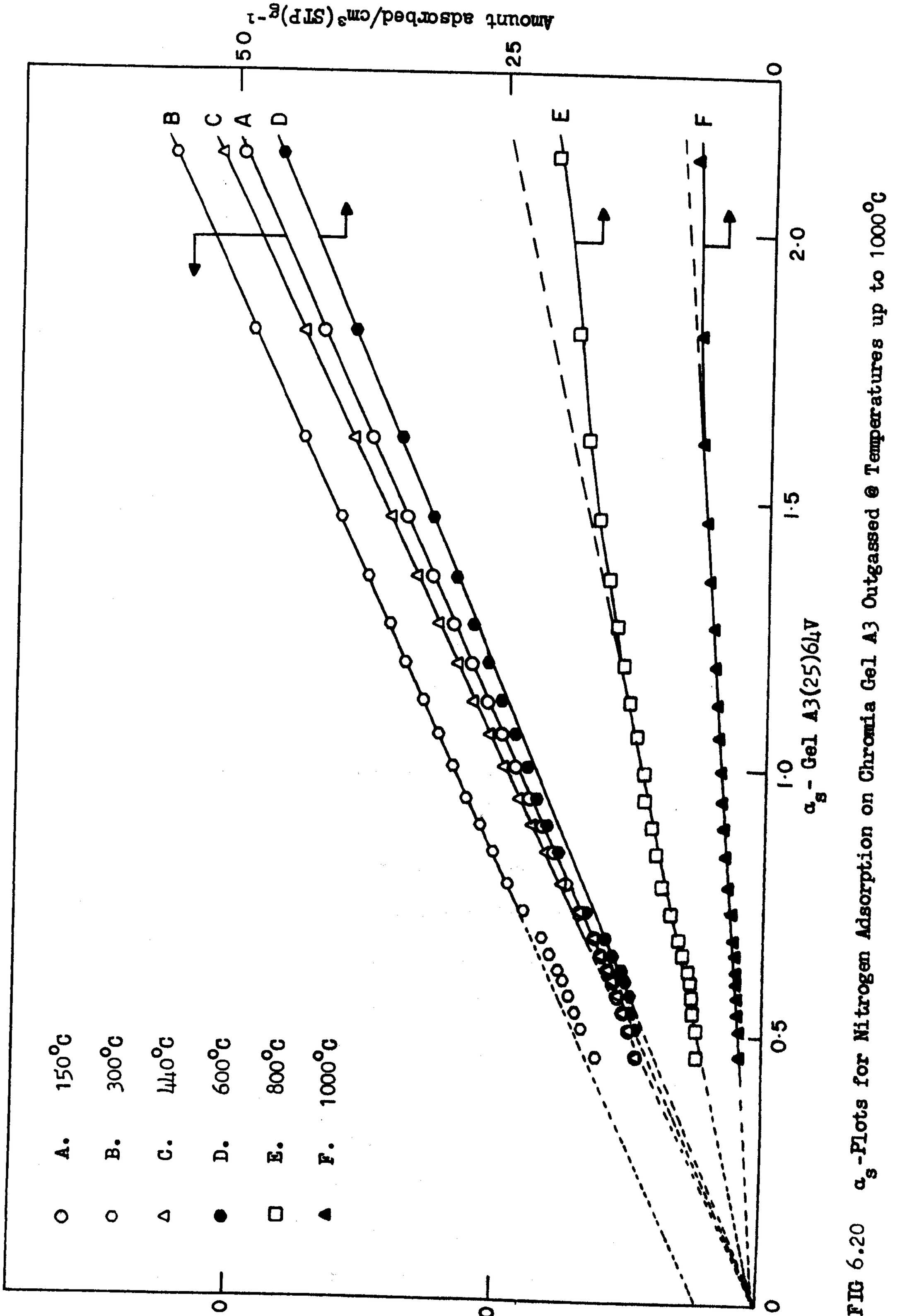

FIG 6.20 α_s-Plots for Nitrogen Adsorption on Chromia Gel A3 Outgassed @ Temperatures up to 1000°C

C H A P T E R 7

GENERAL DISCUSSION AND CONCLUSIONS

The term "ageing" is used to connote all those irreversible structural or textural changes in the colloidal system which may occur after flocculation or gelation.[1-3] Ageing occurs when an "active" solid (i.e. one that is thermodynamically unstable in respect of surface area) is left in contact with an aqueous medium and also when the liquid phase is removed. It is now recognised[3] that water plays a key role in the ageing of hydroxides and hydrous oxides. The poorly organised flocculated hydroxide prepared from salts of hydrated cations usually contains large quantities of molecular water; this is partly sorbed (trapped within the framework and held at the gel surface) and partly associated with the cations.[3,4] Fenerty,[5] using diffuse reflectance spectra measurements, has shown that a considerable number of water molecules remain coordinated to chromium (III) ions in hydrous chromium oxides. The displacement of these water ligands is a prerequisite for the development of the hydroxide or oxy-hydroxide structure. Hydrous oxides of aluminium and iron (III) prepared under similar conditions to those of hydrous chromium (III) oxides, contain well defined oxy-hydroxide structures.[6,7] The formation of the hydroxide or oxy-hydroxide structures is facilitated[8] if hydrous aluminium oxide is precipitated at a high pH. The results discussed in Section 6.3 indicate that the development of an oxy-hydroxide structure (e.g. chromium

oxy-hydroxide, CrOOH) is more pronounced in the case of a chromia gel precipitated at pH 10.5, than that of a gel precipitated at about pH 6.

Hydrous chromium (III) oxide may be regarded as a condensation polymer of $Cr(H_2O)_3(OH)_3$ in which hydroxide, or oxide, ions act as bridges linking the chromium ions.[5,9,10] The pH of an aqueous suspension of a freshly formed chromia gel was observed to decrease with the time of ageing. Bye and Simpkin[11] have observed a similar effect, which has been attributed[5] to the continued growth of the polymer after precipitation. The decrease in pH of the gel suspension appears to be associated with a dehydration process occurring at the oxide-water interface, similar to that observed in the case of a hydrous iron (III) oxide.[12]

In the present work, gas adsorption measurements have indicated that in the case of hydrous chromium oxides outgassed at temperatures lower than about 150°C, the coordinated water is apparently removed with little structural change, the original solid framework remaining intact (for example, see Tables 6.3 and 6.4, and Curve 'A' in Fig. 6.20). Chromia gels precipitated at about pH 6 were found to be microporous. These gels, outgassed at 25°C, possessed molecular sieve properties; the sorption capacity for water was high, whereas the pore structure available to nitrogen (and presumably most other adsorbates) was small. A similar result has been reported in the case of certain hydrous aluminas.[13] The molecular sieve effect is attributed to the cavities remaining in the vicinity of the cations after removal of the ligand water. In contrast, however, the replacement of ligand molecules from the chromium (III) octahedra by hydroxide ions was facilitated by

precipitation of the gel at high pH i.e. 10.5. These gels, which possessed very little microporosity, did not exhibit a significant molecular sieve effect. The results summarised in Table 6.2 indicate that an increase in the pH of precipitation is accompanied by a decrease in the degree of the molecular sieve character of the chromia gels.

Carruthers[14] tentatively suggested that the conditions of mixing of the reactants are more important than the pH during the precipitation of a chromia gel. Although the manner in which the reactants are mixed undoubtedly plays an important role in controlling the properties of a chromia gel (particularly[15] in the case of a gel prepared using the Burwell method), the bulk and surface properties of chromia gels are especially sensitive to the pH of precipitation. The results of Cross and Leach[16] confirm this view: chromia gels prepared at about pH 5 possessed pore structures consisting almost entirely of micropores, whereas a gel prepared at pH 8.5 contained both micropores and mesopores.

It has been found[17,18] that the surface properties of silica gels are also profoundly influenced by the pH of precipitation; in this case, however, the mechanism is probably rather different, involving the catalytic action of hydroxyl ions. Thus, the size and degree of packing of the polysilicic acid units are influenced by the pH of formation of the silica hydrogel, but crystalline oxide or hydroxide structures do not develop.

The textural properties of a chromia gel, notably in the case of microporous gels, may be drastically changed according to the method employed to wash and 'dry' the gel. The use of acetone and

and diethyl ether to displace the gel water, for example, resulted in a marked change in the character of the nitrogen (Fig. 6.4) and water vapour isotherms (Curves B and C in Fig. 6.6) respectively, accompanied by an increase in the total pore volume of the gel. Taylor[19] reported a similar result when chromia gels were washed with pentane prior to drying; whilst Foster and Thorp[18] observed a pore-widening effect when silica gels were dried rapidly. The increased pore volume of the chromia gels is associated with a reduction in the capillary forces acting in the gel, achieved by replacing the gel water by a liquid of lower surface tension, e.g. acetone. If this liquid is removed above its critical temperature (by autoclaving), or the water removed from the wet gel by a process of freeze-drying then a chromia aerogel may be obtained.[19]

During the calcination of hydrous chromium oxides in air, the overall oxidation process $Cr^{3+} \longrightarrow Cr^{6+}$ is generally accompanied by micropore widening, whereas the reduction stage $Cr^{6+} \longrightarrow Cr^{3+}$, which involves the crystallisation of α-Cr_2O_3, is accompanied by the removal of pores and the loss of surface area.[5,14] Gels calcined in nitrogen (up to temperatures of about 600°C) remain mesoporous because the crystal growth of α-Cr_2O_3 is delayed in an inert atmosphere.[20] The drastic low temperature ageing (< 200°C) that occurs in the case of many microporous chromias, due to the large amount of residual water assisting the formation of crystalline oxy-hydroxide, may be delayed until about 250°C by heating the gel in vacuum.[20,21]

The rigorous exclusion of water vapour from an oxide xerogel prevents further ageing at room temperature[22] and also considerably retards thermal ageing. However, water appears to play a dual role in the ageing

of hydrous oxides. Thus, the presence of a certain level of residual water appears to offer a measure of protection to the particles of a partially dried gel. For example, in the case of certain hydrous aluminas,[3] the surface area (S^{N}_{BET} ~ 300 m^2g^{-1}) was stabilised over periods of about a year - provided that the ratio of H_2O : Al_2O_3 remained greater than 6 : 1. However, exposure of the outgassed gel to water vapour resulted in a drastic reduction in the surface area. Sing and Bye[3] proposed that the removal of water allowed a closer particle-particle contact so that ageing, presumably by a surface diffusion mechanism, was facilitated when water vapour was re-admitted to the system.

Nitrogen, argon and water vapour isotherms respectively, were determined on gel A3 outgassed at various temperatures between 25° and 1000°C. Gel A3, precipitated at pH 10.5, was found to contain small amounts of both microporosity and mesoporosity (using the α_s-method; Curve A in Fig. 6.19). The degree of microporosity was increased at 300°C, but returned to the original (25°C) level after outgassing the gel at 440°C. The ill-defined mesopore structure which developed at temperatures between 150° and 600°C appeared to be associated with compaction and the cementation between neighbouring particles. This was removed at higher temperatures when the drastic reduction of surface area was accompanied by the crystallisation of α-Cr_2O_3 (Fig. 6.11). The mesoporous structure finally collapsed at about 800°C. The isotherms obtained after outgassing the gel at 600°, 800° and 1000°C respectively, exhibited some stepwise character; this may be associated with a progressive increase in the homogeneity of the α-Cr_2O_3 surface. The original (25°C) surface area of the gel was preserved up to temperatures of about 440°C.

The nitrogen isotherms determined on gel A3 outgassed at temperatures above 440°C, were found to exhibit a sharp knee at very low relative pressures. This indicated that some nitrogen molecules were adsorbed on highly energetic sites (possibly exposed Cr^{3+} ions) whilst the remainder of the surface was covered at higher pressures. The values of the BET C constants (Table 6.3), which were unusually low for nitrogen adsorption, were related to the surface coverage in the normal BET region only, and therefore do not reflect the strong adsorbent-adsorbate interactions which occur at low surface coverage. On the other hand, the adsorbent-adsorbate interactions of argon are essentially non-specific, and therefore less sensitive to changes in the chemistry of the surface. In this respect, the argon BET C constants may provide a more reliable guide to the overall adsorbent-adsorbate interactions, than do the corresponding nitrogen values.

The adsorption of water vapour on oxides and other solids is known to be highly specific.[23,24] This appears to be due to the large field-dipole energy contribution to the total gas-solid interaction energy.[24] When this specific contribution is removed, or reduced, (e.g. by the dehydroxylation of silica) the water uptake is diminished, i.e. the surface tends to become hydrophobic. Zettlemoyer[25] and others[23,26] have concluded that on such surfaces adsorbed water molecules form clusters around residual or impurity polar sites.

It is clear that dehydrated chromium oxide surfaces do not exhibit the type of hydrophobic character displayed by a dehydroxylated silica, e.g. TK 800 outgassed at 1000°C. There seems

to be a closer similarity between chromium oxide and alumina, which has been shown[27] to develop hydrophilic character on dehydration. Kiselev and his co-workers[23,28] found that the surface rehydration of silica is a slow process and that a reversible water vapour isotherm was restored only after soaking the silica in liquid water, or by repeated adsorption and desorption experiments. A similar result was found in the case of TK 800 'soaked' in water vapour at a relative pressure of about 0.98 Po (cf. Fig. 4.4). In contrast, however, the surface of clean α-Al_2O_3 has a high affinity for water, with chemisorption taking place at low pressure, and physical adsorption on the hydrated surface.[29]

The results obtained in this work and in other related investigations[29,30] have provided evidence for the identification of six different mechanisms for the sorption of water by oxides:-

(1) Hydrogen bonding between adsorbed water molecules and surface hydroxyl groups.

(2) Hydrogen bonding between sorbed water molecules and hydroxyl groups in micropores.

(3) Hydration of exposed surface cations by adsorbed water molecules.

(4) Dissociative chemisorption of water with the formation of hydroxyl groups.

(5) Hydration in depth of poorly ordered cations.

(6) Hydroxide or oxy-hydroxide formation in depth.

Process 1 results in a 'standard' water isotherm and heat of immersion, but process 2 gives rise to abnormally high values of water uptake and heat of immersion - especially when the micropores are too narrow to accommodate other sorbate molecules. Process 3 is important

with alumina (and titania etc.), but is not operative with amorphous silica. Process 4 is fast with alumina, but slow with dehydroxylated silica. Processes 5 and 6 are always associated with ageing and are important with both alumina and chromia.

Finally, the occurrence and significance of mercury vapour adsorption should be noted. Chromium dioxide, and hydrous chromium oxides calcined (or outgassed) at temperatures between about 150° and 450°C, were found to exhibit a high affinity for mercury vapour. In the case of chromium dioxide, the adsorption of water vapour was significantly affected by the irreversible adsorption of mercury vapour on the surface. It seems likely that such effects may have passed unnoticed in earlier work. For example Taylor[19] studied the chemisorption of pure oxygen, at 25°C, on the surface of a chromium oxide gel previously activated at 400°C; the system was then evacuated to 5×10^{-5} torr with the aid of a mercury diffusion pump. Mercury was also employed as a manometric fluid in the system. It was observed that the weight of the catalyst continued to rise during the evacuation, a phenomenon that was tentatively ascribed to the desorption of water from the walls of the system. Furthermore, the weight increase was arrested when the system was flushed with pure helium at a pressure of 100 torr, but was reinstated when the system was re-evacuated to 10^{-5} torr. In the light of the present work, it seems likely that Taylor was observing a weight increase due to mercury vapour adsorption by the activated chromia.

It is evident that in adsorption studies of vapours on chromium oxide, and perhaps other transition metal oxide gel systems, one is not entitled to assume that mercury vapour adsorption is negligible in the case of an adsorbent exposed to the vapour.

REFERENCES

1. I.M. Kolthoff, Analyst, (1952) 77, 1000.
2. V.P. Chalyi, Zh. Neorgan. Khim., (1963) 8,(2), 269.
3. G.C. Bye and K.S.W. Sing, "Particle Growth in Suspensions", Proc. Symp. Soc. Chem. and Ind., Colloid and Surface Chemistry Group, Brunel, 1972. Ed. A.L. Smith; Academic Press, London, (1973) 29.
4. V.P. Chalyi, Z. Ya. Makorova and V.T. Zorya, Kolloid. Zh., (1964) 26(2), 263.
5. J. Fenerty, Ph.D. Thesis, Liverpool Polytechnic, (1971).
6. L.L. Van Reijen, Ph.D. Thesis, Technische Hogeschool, Eindhoven, (1964).
7. F.A. Cotton and G. Wilkinson, "Advanced Inorganic Chemistry", Interscience, London, (1966) page 858,
8. D. Aldcroft and G.C. Bye, Proc. Brit. Ceram. Soc., (1965) 125.
9. J.C. Bailar, in "Preparative Inorganic Reactions", Ed. W.M. Jolly, Wiley and Sons, (1964) 1, 3.
10. R.L. Burwell, Jr., G.L. Haller, K.C. Taylor and J.F. Reid, "Advances in Catalysis", Academic Press, New York, (1969) 20, 1.
11. G.C. Bye and G.T. Simpkin, Chem. and Ind., (1970) 532.
12. G.A. Parks, Chem. Rev., (1965) 65, 177.
13. M.R. Harris and K.S.W. Sing, "Proc. 3rd Int. Congr. Surface Activity", Cologne, 1960. University Press, Mainz, (1960) 2, 42.
14. J.D. Carruthers, Ph.D. Thesis, Brunel University, (1968).
15. F. Krleza and M. Sljukic, Kolloid. Zh., (1962) 182, 145.
16. N.E. Cross and H.F. Leach, J. Catalysis, (1971), 21, 239.
17. K.S.W. Sing and J.D. Madeley, J. Appl. Chem., (1953) 3, 549.
18. A.G. Foster and J.M. Thorp, "The Structure and Properties of Porous Materials", Proc. 10th Symp. Colston Res. Soc., Bristol, 1958. Eds. D.H. Everett and F.S. Stone; Butterworths, London, (1958) page 227.

19. K.C. Taylor, Ph.D. Thesis, Northwestern University, Evanston, Illinois, U.S.A., (1968).

20. J.D. Carruthers, J. Fenerty amd K.S.W. Sing, "Proc. 6th Int. Symp. Reactivity Solids", Schenectady, 1968. Eds. J.W. Mitchell, R.C. DeVries, R.W. Roberts and P. Cannon; Wiley Interscience, New York, (1969) 127.

21. J.D. Carruthers and K.S.W. Sing, Chem. and Ind., (1967) 1919.

22. M.R. Harris and K.S.W. Sing, J. Appl. Chem., (1957) 7, 397.

23. A.V. Kiselev, "The Structure and Properties of Porous Materials", Proc. 10th Symp. Colston Res. Soc., Bristol, 1958. Eds. D.H. Everett and F.S. Stone; Butterworths, London, (1958) page 195.

24. R.M. Barrer, J. Colloid Interface Sci., (1966) 21, 415.

25. A.C. Zettlemoyer, J. Colloid Interface Sci., (1968) 28, 343.

26. J.W. Whalen, J. Phys. Chem., (1961) 65, 1676.

27. D.A. Payne, Ph.D. Thesis, Brunel University, (1970).

28. O.M. Dzhigit, A.V. Kiselev and G.G. Muttik, Kolloid. Zh., (1961) 23, 553; ibid. (1962) 24, 15.

29. J.D. Carruthers, D.A. Payne, K.S.W. Sing and L.J. Stryker, J. Colloid Interface Sci., (1971) 36, 205.

30. K.S.W. Sing, "Colloques Internationaux du C.N.R.S.", Thermochimie, (1971) No 201, 601.

A P P E N D I X 1

COMPUTER PROGRAMS

```
::ADSORPTION PROCESSING MANOMETRIC PRESSURE DNW/FSP NOV 1977

SETV RC(5)D(2)GH(2)NPTV(4)W(2)XY(1)Z(10)
SETS K(1)Q
SETR 3
SET C(1:5)=13.5955,13144.01,.7016,.0028625,.000002617

2)READ V2::VOLUME ABOVE NITROGEN LEVEL
READ V3::VOLUME BELOW NITROGEN LEVEL
READ W1::SAMPLE WEIGHT
READ W2::WOOL WEIGHT
READ D1::SAMPLE DENSITY
READ D2::WOOL DENSITY
READ G::ADSORBATE FACTOR

Z4=W2/D2
Z4=V2-Z4
Z5=W1/D1
Z5=V3-Z5
LINE
TITLE     P/PO      V ADS       P/V(PO-P)
Z7=0
3)READ Q
LINE
SUBR 1
V=Z2*Z8
V1=V+Z7
CHECK V1
CYCLE K1=2:1:Q
SUBR 1
Z6=G*Z9
Z6=1+Z6
Z=Z3*Z5
Z=Z*Z6
Z10=Z2*Z4
Z10=Z+Z10
V=Z2*Z8
V4=V+Z10
CHECK V4
Z7=V1-V4
Z7=Z7+Z10

X=Z9/P
Y=V1-V4
W=W1*3.7825
Y=Y/W
Z=P-Z9
V=Y*Z
Y1=Z9/V
LINE
PRINT X,5
PRINT Y
PRINT Y1
REPEAT K1
JUMP @3
```

```
1)READ H1::MERCURY HEIGHT 1
READ H2::MERCURY HEIGHT 2
READ B::BURETTE READING
READ T::TEMP CENTIGRADE
READ N::APPARATUS BULB VOLUME
READ P::SAT VAP PRESSURE

D=C5
CYCLE K=4:-1:2
D=D*T
D=D+CK
REPEAT K
D=D*T
D=D*.00000001
D=D+1
D=C1/D
CHECK D
Z9=H2-H1
Z1=Z9*D
Z2=T+273.16
Z2=Z1/Z2
Z3=Z1/77.4
Z8=B+N
EXIT

START 2
```

```
::ADSORPTION PROCESSING TRANSDUCER PRESSURE DNW/FSR NOV/15/2

  T  :CD(2:GHNPTV(4)W(2)XY(1)Z(10)
SETS K(1)0
SETR 3

2)READ V2::VOLUME ABOVE NITROGEN LEVEL
READ V3::VOLUME BELOW NITROGEN LEVEL
READ W1::SAMPLE WEIGHT
READ W2::WOOL WEIGHT
READ D1::SAMPLE DENSITY
READ D2::WOOL DENSITY
READ C::TRANSDUCER CALIBRATION FACTOR
READ G::ADSORBATE FACTOR

Z4=W2/D2
Z4=V2-Z4
Z5=W1/D1
Z5=V3-Z5
LINE
TITLE     P/P0      V ADS      P/V(P0-P)
Z7=0
3)READ 0
LINE
SUBR 1
V=Z2*Z8
V1=V+Z7
CYCLE K1=2:1:Q
SUBR 1
Z6=G*Z9
Z6=1+Z6
Z=Z3*Z5
Z=Z*Z6
Z10=Z2*Z4
Z10=Z+Z10
V=Z2*Z8
V4=V+Z10
Z7=V1-V4
Z7=Z7+Z10

X=Z9/P
Y=V1-V4
W=W1*3.7825
Y=Y/W
Z=P-Z9
V=Y*Z
Y1=Z9/V
LINE
PRINT X,5
PRINT Y
PRINT Y1
REPEAT K1
JUMP @3
```

```
1)READ H::TRANSDUCER DVM READING IN MILLIVOLTS
READ B::BURETTE READING
READ T::TEMP CENTIGRADE
READ N::APPARATUS BULB VOLUME
READ P::SAT VAP PRESSURE

Z9=H*C
Z1=Z9*13.5955
Z2=T+273.16
Z2=Z1/Z2
Z3=Z1/77.4
Z8=B+N
EXIT

START 2
```

```
SILICA SPRING BALANCE PROGRAM. GENERAL USE. TRANSDUCER AND DVM
PRESSURE MEASUREMENT. FOR BALANCE BUILT BY F.S.BAKER, UXBRIDGE 72'
BEGIN
COMMENT. THIS IS A GENERAL PROGRAM FOR WATER ADSORPTION AT 25.0 C
FOR COMPUTING THE ADSORPTION DATA FROM THE REBUILT, RECALIBRATED
SILICA SPRING BALANCE. PRESSURE MEASUREMENT IS BY THE TRANSDUCER
AND DIGITAL MILLI-VOLTMETER. THE TRANSDUCER, DVM AND SPRING WERE
CALIBRATED DURING MARCH 1972 BY F.S.B. TRANSDUCER (SERIAL NO 5574)
CALIBRATION FACTOR = 0.12411: SPRING CALIBRATION FACTOR = 10.7776.
THIS PROGRAM CONVERTS READINGS FROM THE SILICA SPRING BALANCE IN
LAB NO 120 TO P, LN P, P/PO, P/V(PO-P), TOTAL WEIGHT INCREASE AND
TOTAL WEIGHT INCREASE PER GRAM. THE DATA TAPE SHOULD BE AS FOLLOWS.
1. NUMBER OF FIXED POINTS 2. FIRST FIXED POINT 3. NUMBER OF
READINGS FOR THAT FIXED POINT 4. SPRING EXTENSION READINGS
5. SECOND FIXED POINT ETC., 6. SAMPLE WEIGHT, SAMPLE DENSITY,
BUCKET WEIGHT, INITIAL SPRING POSITION, PO VALUE, THEN DIGITAL
VOLTMETER READINGS IN MILLIVOLTS TERMINATED BY 0. THE PROGRAM
PRINTS OUT P, LN P, P/PO, P/V(PO-P), TOTAL WEIGHT INCREASE,
WEIGHT IFCREASE PER GRAM, THE BET XM AND C VALUES TOGETHER WITH
THE SURFACE AREA, SLOPE, INTERCEPT AND REGRESSION COEFFICIENT.'
ARRAY SER,SERC(1:50,1:50),DVM,BET,POPO,FP,CSER,WI,WIT,
WIG(1:50)'
REAL SW,SD,BW,ISP,PO,A,B,C,D,E,F,G,H,AB,AC,AD,AE,AF,AG,
SUMP,SUMB,SUMP2,SUMBP,SLOPE,INTERCEPT,AREA,XM,P,BC'
INTEGER N1,K,I,J,L1,N3,L2,N4,N5,L3,N6,T'
INTEGER ARRAY N2(1:100),AA(1:25)'
SWITCH SX:=S1,S2,S3'
REAL PROCEDURE SIGMA(X,I,A,B)'
COMMENT THIS PROCEDURE EVALUATES SIGMA X FROM LIMITS A TO B'
REAL X'
      INTEGER I,A,B'
      BEGIN REAL S'
      S:=0'
      FOR I:=A STEP 1 UNTIL B DO S:=S+X'
      SIGMA:=S'
      END'
T:=1'
INSTRING(AA,T)'
T:=1'
OUTSTRING(AA,T)'
READ N1'
K:=0'
FOR I:=1 STEP 1 UNTIL N1 DO
      BEGIN READ FP(I)'
      READ N2(I)'
      FOR J:=1 STEP 1 UNTIL N2(I) DO
            BEGIN
            READ SER(I,J)'
            SERC(I,J):=FP(I)-SER(I,J)'
            K:=K+1'
            CSER(K):=SERC(I,J)'
            END'
      END'
READ SW,SD,BW,ISP,PO'
PRINT SAL?
      P          LN P          P/PO          P/V(PO-P)    TOTAL W.I.   W.I./G?'
L1:=0'
FOR K:=1 STEP 1 UNTIL 100 DO
      BEGIN
      READ DVM(K)'
      IF DVM(K)=0 THEN GOTO S1 ELSE L1:=L1+1'
      END'
```

```
S1:N3:=L1'
FOR K:=1 STEP 1 UNTIL N3 DO
      BEGIN
      WI(K):=(CSER(K)-(FP(1)-ISP))*10.7776'
      P:=DVM(K)*0.12411'
      BC:=((SW/SD)+(PW/2.21)+(WI(K)/997.044))*(0.96896-5*P)'
      WIT(K):=WI(K)+BC'
      WIG(K):=WIT(K)/SW'
      POPO(K):=P/PO'
      BET(K):=POPO(K)/(WIG(K)*(1.0-POPO(K)))'
      PRINT ΣΣL??,P,SAMELINE,ΣΣS3??,ALIGNED(1,4),LN(P),ΣΣS3??,
      FREEPOINT(8),POPO(K),ΣΣS3??,BET(K),ΣΣS3??,
      FREEPOINT(6),WIT(K),ΣΣS3??,WIG(K)'
      END'
L2:=0'
FOR K:=1 STEP 1 UNTIL N3 DO
      BEGIN
      IF POPO(K) GR 0.05 THEN GOTO S2 ELSE L2:=L2+1'
      END'
S2:N4:=L2+1'
IF N4=0 THEN N5:=1 ELSE N5:=N4'
L3:=0'
FOR K:=1 STEP 1 UNTIL N3 DO
      BEGIN
      IF POPO(K) GR 0.3 THEN GOTO S3 ELSE L3:=L3+1'
      END'
S3:N6:=L3'
SUMP:=SIGMA(POPO(K),K,N5,N6)'
SUMB:=SIGMA(BET(K),K,N5,N6)'
SUMP2:=SIGMA(POPO(K)*POPO(K),K,N5,N6)'
SUMBP:=SIGMA(POPO(K)*BET(K),K,N5,N6)'
A:=(N6-N5)*SUMBP'
B:=SUMP*SUMB'
G:=(N6-N5)*SUMP2'
D:=SUMP*SUMP'
E:=SUMP2*SUMB'
F:=SUMP*SUMBP'
AB:=SUMP/(N6-N5+1)'
AC:=SUMB/(N6-N5+1)'
AD:=SIGMA((POPO(K)-AB)*(BET(K)-AC),K,N5,N6)'
AE:=SIGMA((POPO(K)-AB)**2,K,N5,N6)'
AF:=SIGMA((BET(K)-AC)**2,K,N5,N6)'
AG:=AD/SQRT(AE*AF)'
SLOPE:=(A-B)/(G-D)'
INTERCEPT:=(E-F)/(G-D)'
XM:=1.0/(SLOPE+INTERCEPT)'
AREA:=XM*6.024*10.6/18.01534'
C:=1.0/(XM*INTERCEPT)'
H:=0.3*SLOPE+INTERCEPT'
PRINT
ΣΣL4?SLOPE= ?,SAMELINE,SLOPE,ΣΣL2?INTERCEPT= ?,SAMELINE,
INTERCEPT,ΣΣL2?XM= ?,SAMELINE,XM,ΣΣL2?C= ?,SAMELINE,C,
ΣΣL2?SURFACE AREA= ?,SAMELINE,AREA,ΣΣS?SQUARE METERS PER GRAM?,
ΣΣL2?P/V(PO-P)= ?,SAMELINE,H,Σ WHEN P/PO=0.3?,ΣΣL2?REGRESSION
COEFFICIENT = ?,SAMELINE,ALIGNED(1,4),AG,Σ FOR ?,DIGITS(1),
N6-N5-1,Σ DEGREES OF FREEDOM ?'
END'
```

A P P E N D I X 2

CONVERSION TABLES FOR VOLUMETRIC AND GRAVIMETRIC APPARATUSES

Conversion Factors:

1 torr = 1 mm Hg @ $0^{o}C$

= 1.333×10^{2} Nm^{-2}

= 1.933×10^{-2} psi

1 psi = 51.71 torr

= 6.89×10^{3} Nm^{-2}

1 Nm^{-2} = 7.5×10^{-3} torr

= 1.45×10^{-4} psi

Quartz Spring Balance Conversion Table

Water Vapour Adsorption at 25.0°C

P/Po	MANOMETRIC (cm @ 22.5°C)		DVM (mV)
	Mercury	Oil	
0.01	0.02	0.31	0.19
0.02	0.05	0.61	0.38
0.03	0.07	0.92	0.57
0.04	0.10	1.23	0.77
0.05	0.12	1.53	0.96
0.06	0.14	1.84	1.15
0.07	0.17	2.14	1.34
0.08	0.19	2.45	1.53
0.09	0.21	2.76	1.72
0.10	0.24	3.06	1.91
0.15	0.36	4.60	2.87
0.20	0.48	6.13	3.83
0.25	0.60	7.66	4.79
0.30	0.72	9.19	5.74
0.35	0.83	10.72	6.70
0.40	0.95	12.26	7.66
0.45	1.07	13.79	8.61
0.50	1.19	15.32	9.57
0.55	1.31	16.85	10.53
0.60	1.43	18.38	11.48
0.65	1.55	19.92	12.44
0.70	1.67	21.45	13.40
0.75	1.79	22.98	14.36
0.80	1.91	24.51	15.31
0.85	2.03	26.04	16.27
0.90	2.15	27.58	17.23
0.95	2.27	29.11	18.18
1.00	2.39	30.64	19.14

Calibration Factors

SVP of water at 25.0°C = 2.3756 cm of Hg at 0°C
= 2.3853 cm of Hg at 22.5°C

Quartz spring calibration factor = 10.7776 mg/cm at 26.5°C

Silicone oil manometer calibration factor:

= 0.07753 cm of Hg at 0°C per cm of oil at 22.5°C
= 0.07785 cm of Hg at 22.5°C per cm of oil at 22.5°C

Transducer/DVM calibration factor:

= 0.12411 cm of Hg at 0°C per mV
= 0.12462 cm of Hg at 22.5°C per mV

Serial No. of Transducer = 2574

Serial No. of DVM = 4451

LEFT HAND VOLUMETRIC APPARATUS

Equivalent Hg Manometer & Transducer Pressure Data

P/Po	cm Hg		mV DVM	
	Nitrogen	Argon	Nitrogen	Argon
0.01	0.77	0.20	0.37	0.10
0.02	1.54	0.41	0.74	0.19
0.03	2.31	0.61	1.11	0.29
0.04	3.08	0.81	1.48	0.39
0.05	3.85	1.01	1.85	0.49
0.06	4.62	1.22	2.22	0.58
0.07	5.39	1.42	2.59	0.68
0.08	6.16	1.62	2.96	0.78
0.09	6.93	1.82	3.33	0.88
0.10	7.70	2.03	3.70	0.97
0.15	11.55	3.04	5.55	1.46
0.20	15.40	4.05	7.40	1.95
0.25	19.25	5.06	9.25	2.43
0.30	23.10	6.08	11.10	2.92
0.35	26.95	7.09	12.95	3.41
0.40	30.80	8.10	14.80	3.89
0.45	34.65	9.11	16.65	4.38
0.50	38.50	10.13	18.50	4.86
0.55	42.35	11.14	20.35	5.35
0.60	46.20	12.15	22.20	5.84
0.65	50.05	13.16	24.05	6.32
0.70	53.90	14.18	25.90	6.81
0.75	57.75	15.19	27.74	7.30
0.80	61.60	16.20	29.59	7.78
0.85	65.45	17.21	31.44	8.27
0.90	69.30	18.23	33.29	8.76
0.95	73.15	19.24	35.14	9.24
1.00	77.00	20.25	36.99	9.73

Equivalent SVP Data taken as follows:

N_2 = 77.00 cm Hg @ 0°C

Ar = 20.25 cm Hg

O_2 = 15.83 cm Hg

Serial No of Transducer = L36647

Serial No of DVM = 5111

Transducer Calibration factor:

1 cm Hg = 0.48043 mV @ 26.7°C

1 mV = 2.08146 cm Hg

RIGHT HAND VOLUMETRIC APPARATUS

Equivalent Hg Manometer & Transducer Pressure Data

P/Po	cm Hg		mV DVM	
	Nitrogen	Argon	Nitrogen	Argon
0.01	0.77	0.20	0.40	0.10
0.02	1.54	0.41	0.80	0.21
0.03	2.31	0.61	1.20	0.32
0.04	3.08	0.81	1.60	0.42
0.05	3.85	1.01	2.00	0.53
0.06	4.62	1.22	2.40	0.63
0.07	5.39	1.42	2.81	0.74
0.08	6.16	1.62	3.21	0.84
0.09	6.93	1.82	3.61	0.95
0.10	7.70	2.03	4.01	1.06
0.15	11.55	3.04	6.01	1.58
0.20	15.40	4.05	8.01	2.11
0.25	19.25	5.06	10.02	2.63
0.30	23.10	6.08	12.02	3.16
0.35	26.95	7.09	14.03	3.69
0.40	30.80	8.10	16.03	4.22
0.45	34.65	9.11	18.03	4.74
0.50	38.50	10.13	20.04	5.27
0.55	42.35	11.14	22.04	5.80
0.60	46.20	12.15	24.04	6.32
0.65	50.05	13.16	26.05	6.85
0.70	53.90	14.18	28.05	7.38
0.75	57.75	15.19	30.06	7.91
0.80	61.60	16.20	32.06	8.43
0.85	65.45	17.21	34.06	8.96
0.90	69.30	18.23	36.07	9.49
0.95	73.15	19.24	38.07	10.01
1.00	77.00	20.25	40.07	10.54

Equivalent SVP Data taken as follows:

N_2 = 77.00 cm Hg @ 0°C

Ar = 20.25 cm Hg @ 0°C

O_2 = 15.83 cm Hg @ 0°C

Serial No of Transducer = L36971

Serial No of DVM = 5111

Transducer Calibration factor:

1 cm Hg = 0.52044 mV

1 mV = 1.92144 cm Hg

@ 24.6°C

A P P E N D I X 3

NITROGEN ADSORPTION ON CHROMIUM OXIDES

EXPERIMENTAL DATA

S^{N}_{BET} = Nitrogen BET Surface Area - m^2g^{-1}

C^{N}_{BET} = Nitrogen BET C Constant

V ads = Amount Adsorbed - $cm^3(STP)g^{-1}$

NITROGEN ADSORPTION DATA

A1(25)32V
(FSB 9)

P/Po	V ads $cm^3(STP)g^{-1}$
0.0024	13.84
0.0065	18.11
0.0110	19.93
0.0200	22.31
0.0354	25.20
0.0512	27.10
0.0647	28.21
0.0753	29.16
0.0844	29.84
0.1110	32.13
0.1305	33.32
0.1533	34.96
0.1714	36.23
0.1952	38.15
0.2251	40.01
0.2540	42.01
0.2843	43.79
0.3275	47.00
0.3593	49.48
0.5221	66.88
0.5542	72.02
0.5985	80.59
0.6458	92.73
0.6657	100.65
0.7389	128.68
0.7628	144.13
0.7825	159.21
0.7530	145.32
0.7348	136.41
0.7046	122.93
** 0.4681	60.33

S^N_{BET} = 143.8 m^2g^{-1}

C^N_{BET} = 46

A1(25)50V
(FSB 10)

P/Po	V ads $cm^3(STP)g^{-1}$
0.0025	16.63
0.0026	16.73
0.0081	18.00
0.0161	21.03
0.0280	23.81
0.0411	25.91
0.0546	27.42
0.0651	28.19
0.0738	28.80
0.0971	30.40
0.1304	32.40
0.1639	33.79
0.1982	35.47
0.2259	36.85
0.2591	38.42
0.3085	40.87
0.3685	43.97
0.4751	50.00
0.5613	55.87
0.6572	64.34
0.7439	75.68
0.8353	97.54
0.8721	114.50
0.8867	126.43
0.8964	137.06
0.8717	123.42
0.8464	110.56
0.8052	94.06
0.7864	86.86
0.7405	76.80
0.6626	66.11
0.5515	55.86
0.4363	48.14
0.3351	42.71
0.2851	40.02

S^N_{BET} = 128.1 m^2g^{-1}

C^N_{BET} = 117

** Adsorption Point

NITROGEN ADSORPTION DATA

A1(114)16V
(FSB 11)

P/Po	V ads $cm^3(STP)g^{-1}$
0.0008	14.47
0.0050	20.95
0.0131	23.40
0.0251	25.11
0.0364	26.43
0.0430	27.06
0.0489	27.54
0.0866	30.13
0.1060	31.24
0.1229	32.13
0.1851	35.28
0.2255	37.19
0.2574	38.82
0.3500	43.61
0.4434	48.49
0.5246	53.55
0.6240	61.27
0.7222	72.80
0.7797	82.55
0.8369	98.57
0.8730	118.82
0.8399	104.35
0.8095	93.56
0.7310	75.61
0.6806	68.39
0.6000	60.10
0.5210	54.21
0.3983	46.64
0.2974	40.96
0.1563	33.92

S^N_{BET} = 128.8 m^2g^{-1}

C^N_{BET} = 149

NITROGEN ADSORPTION DATA

A2(25)47V
(FSB 25)

P/Po	V ads $cm^3(STP)g^{-1}$	P/Po	V ads $cm^3(STP)g^{-1}$
0.0004	6.71	0.1419	21.24
0.0009	8.12	0.1810	22.45
0.0016	9.58	0.2234	23.73
0.0017	9.63	0.2578	24.86
0.0034	11.26	0.2897	25.87
0.0035	11.37	0.4076	29.90
0.0068	12.89	0.4815	32.69
0.0071	13.02	0.5738	36.75
0.0074	13.10	0.6789	42.92
0.0132	14.46	0.7638	50.11
0.0144	14.68	0.8096	56.32
0.0155	14.83	0.8431	62.46
0.0177	15.14	0.8754	71.08
0.0199	15.41	0.9062	86.57
0.0217	15.61	0.8643	69.89
0.0335	16.68	0.8140	57.68
0.0399	17.08	0.7276	46.83
0.0450	17.40	0.6738	42.62
0.0549	17.96	0.5894	37.63
0.0673	18.51	0.4945	33.21
0.0780	18.96	0.4433	31.10
0.0809	19.11	0.3734	28.59
0.0966	19.74	0.3411	27.47
0.1206	20.55	0.3012	26.14

S^N_{BET} = 82.4 m^2g^{-1}

C^N_{BET} = 155

NITROGEN ADSORPTION DATA

A3(25)64V
(FSB 54)

P/Po	V ads $cm^3(STP)g^{-1}$
0.0039	18.55
0.0047	19.29
0.0101	21.50
0.0183	23.51
0.0251	24.75
0.0434	27.31
0.0570	28.57
0.0686	29.47
0.0850	30.60
0.1031	31.76
0.1247	33.01
0.1622	34.84
0.1875	36.12
0.2216	37.80
0.2432	38.87
0.2715	40.22
0.3397	43.54
0.4452	49.21
0.5331	54.27
0.6174	60.40
0.7237	71.25
0.7981	84.05
0.8501	100.15
0.8762	113.50
0.9011	132.91
0.8652	108.60
0.8300	94.61
0.7627	78.15
0.6677	65.33
0.5303	54.10
0.4323	48.31
0.3382	43.62
0.2524	39.25
0.1819	36.91
0.1087	32.32
0.0693	29.71
0.0336	26.23

S^N_{BET} = 131.6 m^2g^{-1}

C^N_{BET} = 144

A3(150)15V
(FSB 58)

P/Po	V ads $cm^3(STP)g^{-1}$
0.0051	20.00
0.0103	22.58
0.0198	24.67
0.0401	27.01
0.0579	28.62
0.0668	29.27
0.0789	30.12
0.0976	31.23
0.1110	32.03
0.1248	32.77
0.1389	33.53
0.1563	34.42
0.1743	35.32
0.1947	36.32
0.2358	38.38
0.2736	40.21
0.3247	42.63
0.3979	46.37
0.4959	51.60
0.5901	57.71
0.6762	65.00
0.7502	74.02
0.8299	91.65
0.8847	118.81
0.9097	142.57
0.8931	131.32
0.8746	120.39
0.8522	107.67
0.8209	93.44
0.7820	81.90
0.6982	67.94
0.5747	56.94
0.4621	50.40
0.3855	46.01
0.2794	40.72
0.1979	36.80
0.1428	34.03
0.0496	28.00
0.0367	26.81

S^N_{BET} = 130.2 m^2g^{-1}

C^N_{BET} = 167

NITROGEN ADSORPTION DATA

A3(300)20V
(FSB 62)

P/Po	V ads $cm^3(STP)g^{-1}$
0.0010	23.93
0.0102	31.05
0.0262	34.59
0.0464	37.14
0.0769	39.87
0.1326	43.74
0.1844	46.81
0.2036	47.95
0.2293	49.41
0.2619	51.15
0.2946	52.88
0.3671	56.69
0.4491	61.08
0.6014	70.58
0.7303	83.35
0.8201	101.91
0.8602	115.81
0.9051	147.00
0.9237	184.15
0.9084	169.64
0.8949	155.61
0.8762	138.72
0.8497	119.42
0.7740	92.45
0.6854	78.71
0.6039	71.21
0.4799	63.10
0.3541	56.22
0.2485	50.55
0.1436	44.50
0.1133	42.52
0.0912	41.04
0.0584	38.25
0.0357	36.01
0.0140	32.35

S^N_{BET} = 168.3 m^2g^{-1}

C^N_{BET} = 216

A3(440)18V
(FSB 68)

P/Po	V ads $cm^3(STP)g^{-1}$
0.0051	22.50
0.0173	24.77
0.0279	26.04
0.0431	27.46
0.0531	28.28
0.0810	30.28
0.1128	32.33
0.1410	33.99
0.1615	35.18
0.1824	36.38
0.2035	37.64
0.2296	39.10
0.2565	40.57
0.2863	42.27
0.3881	48.05
0.4862	53.83
0.5764	59.60
0.7022	70.46
0.8326	96.11
0.8748	115.66
0.8500	106.35
0.8231	96.98
0.7896	86.71
0.7507	72.28
0.6983	70.71
0.6331	64.29
0.5241	56.30
0.4457	51.52
0.3869	47.91
0.2787	42.12
0.1771	36.36
0.0786	30.40

S^N_{BET} = 135.6 m^2g^{-1}

C^N_{BET} = 94

NITROGEN ADSOPRTION DATA

A3(600)16V
(FSB 71)

P/Po	V ads $cm^3(STP)g^{-1}$
0.0014	10.35
0.0150	11.30
0.0297	12.08
0.0482	12.73
0.0651	13.28
0.0861	14.03
0.1157	15.08
0.1338	15.78
0.1898	17.66
0.2243	18.45
0.2720	19.74
0.3484	21.13
0.4604	23.51
0.5822	26.76
0.7101	31.62
0.7901	37.80
0.8802	52.63
0.9178	74.87
0.8948	64.47
0.8681	54.20
0.8337	43.07
0.7786	36.75
0.7078	32.26
0.6274	28.40
0.5048	24.81
0.4199	22.75
0.3574	21.50
0.2181	18.51
0.1077	15.00
0.0496	12.83

S^N_{BET} = 66.8 m^2g^{-1}

C^N_{BET} = 54

A3(800)16V
(FSB 76)

P/Po	V ads $cm^3(STP)g^{-1}$
0.0108	5.87
0.0208	6.12
0.0340	6.39
0.0491	6.64
0.0601	6.82
0.0819	7.27
0.1079	7.73
0.1556	8.72
0.1900	9.30
0.2135	9.69
0.2504	10.18
0.2907	10.58
0.3963	11.61
0.5003	12.66
0.6295	14.53
0.7191	16.27
0.8044	18.25
0.9001	23.20
0.9469	28.14
0.8787	21.68
0.8038	18.35
0.6293	14.58
0.4538	12.16
0.3497	11.18
0.0390	6.50

S^N_{BET} = 36.1 m^2g^{-1}

C^N_{BET} = 42

NITROGEN ADSORPTION DATA

A3(1000)17V
(FSB 79)

P/Po	V ads $cm^3(STP)g^{-1}$
0.0085	1.86
0.0169	1.97
0.0242	2.04
0.0354	2.12
0.0555	2.24
0.0895	2.43
0.1328	2.75
0.1749	3.05
0.2446	3.43
0.2843	3.60
0.3927	4.05
0.4592	4.34
0.5797	4.88
0.6689	5.52
0.7567	6.25
0.8419	7.24
0.9358	9.19
0.9791	9.36
0.9922	16.05
0.9353	9.28
0.8419	7.30
0.7571	6.25
0.5797	4.98
0.3147	3.75

S^N_{BET} = 12.0 m^2g^{-1}

C^N_{BET} = 46

A4(25)64V
(FSB 75)

P/Po	V ads $cm^3(STP)g^{-1}$
0.0030	2.29
0.0101	2.57
0.0224	2.78
0.0393	2.91
0.0591	3.02
0.0812	3.18
0.0962	3.31
0.1440	3.35
0.2037	3.73
0.2501	4.04
0.3047	4.27
0.4281	4.87
0.5391	5.37
0.5668	5.62
0.6700	6.29
0.7947	7.75
0.8730	9.60
0.9129	11.34
0.7939	7.86
0.6690	6.43
0.5527	5.52
0.3960	4.69
0.0582	3.02

S^N_{BET} = 13.0 m^2g^{-1}

C^N_{BET} = 335

NITROGEN ADSORPTION DATA

B6(25)24V
(FSB 47)

P/Po	V ads $cm^3(STP)g^{-1}$
0.0000	1.81
0.0000	5.40
0.0000	13.08
0.0000	33.42
0.0005	51.01
0.0015	62.62
0.0032	71.15
0.0035	71.49
0.0080	80.29
0.0088	81.11
0.0188	90.59
0.0221	92.49
0.0309	97.20
0.0356	99.19
0.0383	100.25
0.0512	104.82
0.0612	108.00
0.0675	109.77
0.0862	114.97
0.0969	117.48
0.1155	121.80
0.1209	123.07
0.1673	132.58
0.1959	138.33
0.2382	146.61
0.2451	147.85
0.3048	159.39
0.3899	176.31

S^N_{BET} = 497 m^2g^{-1}

C^N_{BET} = 144

NITROGEN ADSORPTION DATA

B6(25)58V
(FSB 57)

P/Po	V ads $cm^3(STP)g^{-1}$	P/Po	V ads $cm^3(STP)g^{-1}$
0.0000	18.26	0.8396	224.80
0.0000	29.85	0.8070	224.49
0.0005	51.12	0.7622	223.90
0.0081	80.57	0.7108	222.92
0.0149	86.36	0.6535	221.86
0.0174	87.89	0.5933	220.64
0.0320	95.11	0.5371	218.86
0.0502	101.23	0.4904	218.37
0.0678	106.14	0.4787	215.80
0.1003	114.19	0.4726	209.18
0.1273	120.04	0.4616	197.72
0.1443	123.69	0.4529	193.84
0.1892	132.50	0.4369	186.92
0.2277	139.97	0.4056	178.10
0.2446	143.14	0.3895	173.04
0.2726	148.50	0.3694	168.31
0.2804	149.96	0.3410	162.82
0.3304	159.49	0.3022	154.81
0.3881	170.74	0.2829	151.20
0.4775	189.92	0.2574	146.39
0.5402	202.01	0.2375	142.18
0.5995	209.55	0.2015	136.00
0.6950	217.04	0.1649	128.06
0.7792	222.13	0.1377	123.01
0.8752	226.11	0.1088	116.09
0.9559	228.30	0.0765	108.17

S^N_{BET} = 485 m^2g^{-1}

C^N_{BET} = 100

NITROGEN ADSORPTION DATA

B8(25)6$\frac{1}{4}$V
(FSB 70)

P/Po	V ads $cm^3(STP)g^{-1}$
0.0089	61.48
0.0147	64.03
0.0230	66.61
0.0364	68.95
0.0541	70.98
0.0755	72.83
0.0951	74.13
0.1084	74.79
0.1538	76.58
0.1944	77.64
0.2504	78.72
0.3186	79.41
0.4486	80.14
0.5664	80.59
0.5965	80.82
0.7193	81.00
0.8339	81.07
1.0095	88.18
0.9839	81.82
0.8340	81.07
0.7808	81.26
0.6521	81.06
0.5159	80.63
0.3149	79.60
0.1397	76.41
0.8480	73.92

S^N_{BET} = 271 m^2g^{-1}

C^N_{BET} = 163

S2(25)20V
(FSB 3)

P/Po	V ads $cm^3(STP)g^{-1}$
0.0002	1.48
0.0003	2.94
0.0021	5.43
0.0049	6.91
0.0225	9.53
0.0266	9.81
0.0301	10.02
0.0521	10.82
0.0656	11.23
0.0835	11.70
0.1025	12.13
0.1325	12.70
0.1742	13.48
0.2519	14.89
0.3329	16.45
0.4012	17.98
0.4835	19.95
0.6413	24.35
0.7197	27.42
0.7733	30.36
0.8523	36.88
0.8959	43.88
0.9115	48.08
0.9310	54.95
0.8561	37.40
0.7583	29.53
0.5060	20.79
0.3293	16.58
0.2761	15.40

S^N_{BET} = 49.3 m^2g^{-1}

C^N_{BET} = 216

NITROGEN ADSORPTION DATA

S2(25)31V
(FSB 4)

P/Po	V ads $cm^3(STP)g^{-1}$
0.0021	5.01
0.0071	7.13
0.0077	7.26
0.0083	7.34
0.0202	8.53
0.0242	8.77
0.0279	8.95
0.0404	9.62
0.0551	9.98
0.0654	10.19
0.0842	10.60
0.1023	10.93
0.1250	11.27
0.1541	11.72
0.1802	12.08
0.2111	12.63
0.2321	12.98
0.2640	13.57
0.2901	14.09
0.3551	15.02
0.4295	16.45
0.5735	19.50
0.6534	21.80
0.7779	26.96
0.8576	33.18
0.8900	41.50
0.8993	54.56
0.8527	33.35
0.7593	26.06
0.7178	24.18
0.6399	21.41
0.5090	18.19
0.4019	15.96
0.2742	13.73

S^N_{BET} = 44.0 m^2g^{-1}

C^N_{BET} = 254

S2(120)17V
(FSB 5)

P/Po	V ads $cm^3(STP)g^{-1}$
0.0005	7.22
0.0070	8.20
0.0150	9.15
0.0231	9.91
0.0350	10.99
0.0454	11.35
0.0554	11.66
0.0958	12.64
0.1256	13.25
0.1540	13.78
0.1775	14.15
0.1975	14.54
0.2187	14.95
0.2388	15.35
0.2625	15.89
0.2937	16.64
0.3763	18.05
0.5127	20.89
0.6346	24.25
0.7260	27.71
0.8022	32.46
0.8551	38.60
0.9104	48.37
0.9418	65.71
0.9144	53.35
0.8742	42.13
0.7799	31.21
0.6630	25.48
0.5821	22.92
0.4729	20.28
0.3907	18.46
0.3295	17.21

S^N_{BET} = 51.8 m^2g^{-1}

C^N_{BET} = 233

NITROGEN ADSORPTION DATA

CrOOH(25)113V
(FSB 19)

P/Po	V ads $cm^3(STP)g^{-1}$
0.0015	1.41
0.0016	1.43
0.0094	2.32
0.0109	2.40
0.0122	2.47
0.0438	3.22
0.0574	3.39
0.0710	3.54
0.1147	3.91
0.1512	4.15
0.1851	4.37
0.2925	5.06
0.3662	5.51
0.4256	5.93

S^N_{BET} = 16.1 m^2g^{-1}

C^N_{BET} = 106

CrOOH(25)89V
(FSB 20)

P/Po	V ads $cm^3(STP)g^{-1}$
0.0043	1.91
0.0046	1.96
0.0049	1.99
0.0143	2.58
0.0170	2.68
0.0196	2.76
0.0375	3.15
0.0485	3.31
0.0594	3.44
0.0724	3.57
0.0955	3.77
0.1182	3.95
0.1543	4.21
0.2006	4.50
0.2420	4.76
0.3339	5.38
0.4136	5.89
0.4758	6.38
0.5548	7.02
0.6645	8.09
0.8100	10.60
0.8657	12.34
0.9382	18.68
0.9269	17.00
0.8783	13.04
0.7688	9.69
0.7104	8.73
0.6313	7.78
0.5531	7.02
0.4190	5.99

S^N_{BET} = 16.2 m^2g^{-1}

C^N_{BET} = 105

NITROGEN ADSORPTION DATA

CrO_2(25)161V
(FSB 17)

P/Po	V ads $cm^3(STP)g^{-1}$
0.0000	0.69
0.0051	2.04
0.0061	2.12
0.0104	2.27
0.0151	2.40
0.0204	2.53
0.0301	2.69
0.0411	2.81
0.0511	2.92
0.0612	3.00
0.0823	3.21
0.1037	3.36
0.1326	3.55
0.1760	3.78
0.2158	4.00
0.2499	4.19
0.3182	4.57
0.3758	4.90
0.4261	5.18
0.5508	5.87
0.6351	6.50
0.7014	7.11
0.7588	7.89
0.8482	9.72
0.9207	12.97
0.9671	21.12
0.9323	14.23
0.8719	10.48
0.7520	7.80
0.7097	7.24
0.5838	6.11
0.4750	5.41
0.4230	5.13

S^N_{BET} = 14.1 m^2g^{-1}

C^N_{BET} = 115

CrO_2(25)20V
(FSB 27)

P/Po	V ads $cm^3(STP)g^{-1}$
0.0020	1.77
0.0027	1.82
0.0075	2.08
0.0096	2.15
0.0117	2.21
0.0219	2.41
0.0294	2.52
0.0376	2.62
0.0536	2.80
0.0730	2.97
0.0929	3.13
0.1027	3.20
0.1544	3.54
0.2071	3.83
0.2562	4.11
0.3043	4.33

S^N_{BET} = 13.8 m^2g^{-1}

C^N_{BET} = 84

CrO_2(100)17V
(FSB 28)

0.0087	2.42
0.0111	2.50
0.0137	2.56
0.0270	2.80
0.0364	2.93
0.0464	3.05
0.0654	3.25
0.0888	3.44
0.0952	3.50
0.1229	3.68
0.1601	3.93
0.2142	4.23
0.2635	4.56
0.3203	4.81
0.4764	5.79
0.5961	6.57
0.6851	7.67

S^N_{BET} = 15.1 m^2g^{-1}

C^N_{BET} = 100

A P P E N D I X 4

ARGON ADSORPTION ON CHROMIUM OXIDES

EXPERIMENTAL DATA

S_{BET}^{Ar} = Argon BET Surface Area - m^2g^{-1}

C_{BET}^{Ar} = Argon BET C Constant

V ads = Amount Adsorbed - $cm^3(STP)g^{-1}$

ARGON ADSORPTION DATA

A2(25)47V
(FSB 83)

P/Po	V ads $cm^3(STP)g^{-1}$
0.0045	33.50
0.0150	37.95
0.0281	42.00
0.0403	44.81
0.0438	45.74
0.0603	50.11
0.0881	56.02
0.1061	58.69
0.1468	64.48
0.1804	68.74
0.2100	72.82
0.2637	78.13
0.2972	82.04
0.3200	84.47
0.4033	93.80
0.4712	102.33
0.5406	111.08
0.5950	119.10
0.6425	126.37
0.7462	144.24
0.8411	162.76
0.9416	183.26
0.9140	178.88
0.8785	173.82
0.8443	169.32
0.8025	164.40
0.7506	159.12
0.7013	154.61
0.6598	150.96
0.5885	144.75
0.5307	139.64
0.4905	135.73
0.4470	131.73
0.3833	125.01
0.3701	119.02
0.3606	99.29
0.3503	91.02
0.2265	74.94
0.1213	61.99
0.0740	54.10

S_{BET}^{Ar} = 300 m^2g^{-1}

C_{BET}^{Ar} = 49

A3(25)64V
(FSB 56)

P/Po	V ads $cm^3(STP)g^{-1}$
0.0024	5.06
0.0058	10.53
0.0062	10.83
0.0148	15.93
0.0162	16.69
0.0310	20.50
0.0430	22.98
0.0503	24.08
0.0573	25.08
0.0801	27.85
0.1114	30.24
0.1456	32.62
0.1889	35.34
0.2523	38.82
0.2912	40.93
0.3431	43.77
0.4042	47.03
0.4553	49.98
0.5299	54.35
0.6014	59.18
0.6829	65.71
0.7556	72.97
0.8022	78.89
0.8451	85.49
0.8782	92.30
0.8664	90.28
0.8543	88.14
0.8376	85.01
0.8211	81.98
0.7786	75.61
0.7074	68.01
0.6340	61.75
0.5705	57.02
0.4701	51.00
0.3964	46.59
0.3423	43.71
0.2996	41.58
0.1902	35.73
0.1606	33.91
0.1073	30.12

S_{BET}^{Ar} = 152 m^2g^{-1}

C_{BET}^{Ar} = 51

ARGON ADSORPTION DATA

A3(150)15V
(FSB 60)

P/Po	V ads $cm^3(STP)g^{-1}$
0.0051	14.05
0.0125	17.02
0.0250	20.99
0.0398	23.64
0.0520	25.41
0.0563	25.89
0.0751	27.60
0.1130	30.77
0.1547	33.37
0.1944	35.64
0.2130	36.64
0.2889	40.42
0.3600	43.90
0.4375	48.12
0.4872	50.90
0.5546	55.00
0.6390	60.75
0.7223	67.68
0.7766	73.63
0.8308	81.45
0.8667	87.87
0.8949	93.50
0.9062	95.96
0.9449	108.40
0.9690	117.45
0.9592	114.80
0.9494	111.97
0.9345	108.57
0.9231	105.19
0.8904	96.38
0.8328	83.81
0.7662	73.74
0.7423	70.91
0.6820	64.85
0.5927	58.00
0.5014	52.01
0.4286	48.05
0.3557	43.81
0.2888	40.01
0.2052	36.20
0.1400	32.82
0.1036	30.09

S_{BET}^{Ar} = 148 m^2g^{-1}

C_{BET}^{Ar} = 70

A3(300)20V
(FSB 65)

P/Po	V ads $cm^3(STP)g^{-1}$
0.0100	28.40
0.0228	31.87
0.0305	33.54
0.0832	40.59
0.1054	42.57
0.1192	43.73
0.1394	45.24
0.1527	46.16
0.1850	48.20
0.2384	51.47
0.2664	53.01
0.2999	55.00
0.4004	60.57
0.4983	66.24
0.6009	72.58
0.7034	81.25
0.7972	91.74
0.8491	100.88
0.8315	98.14
0.8109	95.33
0.7857	92.12
0.7619	89.10
0.6977	81.69
0.5969	73.11
0.5100	67.10
0.4653	64.21
0.4172	61.79
0.3407	57.68
0.2807	54.31
0.2267	51.03
0.1493	46.17
0.1078	43.15
0.0614	38.00

S_{BET}^{Ar} = 197 m^2g^{-1}

C_{BET}^{Ar} = 155

ARGON ADSORPTION DATA

A3(440)18V
(FSB 69)

P/Po	V ads $cm^3(STP)g^{-1}$
0.0095	20.57
0.0181	23.05
0.0300	24.85
0.0437	26.36
0.0586	27.75
0.0736	28.90
0.0806	29.41
0.1189	31.91
0.1596	34.36
0.2115	37.46
0.2489	39.75
0.3051	43.13
0.3826	47.86
0.4714	53.52
0.5548	59.49
0.6059	63.17
0.7076	71.15
0.8085	82.66
0.8974	100.30
0.8763	96.40
0.8546	92.65
0.8271	88.39
0.7967	83.28
0.7639	78.71
0.7324	74.96
0.6685	68.74
0.6081	64.06
0.5025	56.00
0.3824	48.01
0.2841	42.14

S^{Ar}_{BET} = 152 m^2g^{-1}

C^{Ar}_{BET} = 72

A3(600)16V
(FSB 74)

P/Po	V ads $cm^3(STP)g^{-1}$
0.0071	9.80
0.0170	10.16
0.0406	11.10
0.0558	11.46
0.0685	11.77
0.0880	12.17
0.1108	12.61
0.1388	13.16
0.1971	14.41
0.2477	15.60
0.2944	16.85
0.3681	18.79
0.4484	20.86
0.5500	23.14
0.6048	24.41
0.7150	27.51
0.7860	30.29
0.8432	33.23
0.9201	39.81
0.9582	46.39
0.9395	43.18
0.9101	40.06
0.8716	36.66
0.8312	33.63
0.7113	27.65
0.5437	23.12
0.4345	20.60
0.3069	17.26
0.2016	14.57
0.1185	12.81

S^{Ar}_{BET} = 59 m^2g^{-1}

C^{Ar}_{BET} = 118

ARGON ADSORPTION DATA

A3(800)16V
(FSB 78)

P/Po	V ads $cm^3(STP)g^{-1}$
0.0089	5.03
0.0226	5.57
0.0467	5.97
0.0755	6.26
0.1012	6.54
0.1558	7.10
0.2064	7.70
0.2608	8.54
0.3049	9.22
0.4064	10.71
0.5411	12.00
0.6201	12.79
0.6988	13.74
0.7846	15.21
0.8250	16.00
0.9344	18.94
0.8620	16.90
0.7844	15.21
0.6203	12.78
0.4641	11.31
0.3326	9.70
0.2608	8.53

S_{BET}^{Ar} = 31.0 m^2g^{-1}

C_{BET}^{Ar} = 122

A3(1000)17V
(FSB 81)

0.0123	1.72
0.0259	1.91
0.0345	1.99
0.0511	2.05
0.0628	2.10
0.0913	2.20
0.1094	2.25
0.1541	2.40
0.2136	2.67
0.2511	2.85
0.2915	3.09
0.3459	3.39
0.4112	3.68
0.4985	3.99
0.5791	4.27
0.6844	4.69
0.7935	5.28
0.9029	6.12
0.9701	7.00
1.0190	7.73
0.9017	6.16
0.7937	5.29
0.5791	4.28
0.3965	3.66
0.3013	3.19

S_{BET}^{Ar} = 10.7 m^2g^{-1}

C_{BET}^{Ar} = 92

A4(25)64V
(FSB 77)

0.0082	1.90
0.0204	2.08
0.0366	2.19
0.0550	2.29
0.0704	2.38
0.0881	2.49
0.1161	2.63
0.1411	2.75
0.1959	3.03
0.2460	3.29
0.2593	3.36
0.2986	3.57
0.3780	3.93
0.4827	4.56
0.6067	5.18
0.7145	5.95
0.8914	7.89
0.9436	8.89
0.9701	9.48
0.9395	8.96
0.8826	7.85
0.8009	6.84
0.7056	5.91
0.6013	5.14
0.5027	4.60
0.4795	4.44
0.4136	4.13
0.2963	3.53
0.0596	2.32
** 0.8094	6.84

S_{BET}^{Ar} = 12.6 m^2g^{-1}

C_{BET}^{Ar} = 75

** Adsorption Point

ARGON ADSORPTION DATA

B6(25)58V
(FSB 61)

P/Po	V ads $cm^3(STP)g^{-1}$	P/Po	V ads $cm^3(STP)g^{-1}$
0.0000	13.14	0.5991	247.01
0.0032	40.17	0.6488	253.44
0.0055	51.80	0.7080	260.29
0.0116	63.46	0.7373	262.36
0.0142	68.95	0.9751	270.00
0.0205	77.42	1.0158	294.01
0.0206	77.98	1.0138	279.84
0.0343	87.84	0.8846	268.71
0.0364	88.76	0.8042	267.32
0.0570	100.12	0.6810	264.63
0.0613	101.65	0.5488	261.18
0.0953	113.77	0.4496	257.61
0.0992	116.35	0.4105	255.40
0.1416	128.74	0.3733	251.47
0.1568	132.50	*0.5163	241.38
0.2047	145.93	0.4886	238.60
0.2186	148.81	0.4453	233.86
0.2286	151.37	0.4086	229.36
0.2937	167.70	0.3682	218.25
0.3195	173.84	0.3555	207.41
0.3245	175.51	0.3422	196.97
0.4156	200.83	0.3316	186.85
0.4421	206.71	0.3136	177.33
0.4645	211.87	0.2957	168.35

S_{BET}^{Ar} = 618 m^2g^{-1}

C_{BET}^{Ar} = 44

* Genuine increase in pressure; an apparent condition of supersaturation existed.

ARGON ADSORPTION DATA

B8(25)64V
(FSB 72)

P/Po	V ads $cm^3(STP)g^{-1}$
0.0153	65.44
0.0178	66.80
0.0344	73.01
0.0472	75.89
0.0716	79.77
0.1023	82.79
0.1323	84.92
0.1931	87.93
0.2374	88.98
0.3005	89.83
0.3788	90.46
0.4548	90.94
0.5315	91.32
0.6121	91.66
0.7241	91.95
0.8387	92.15
0.9823	92.57
0.9073	92.38
0.8095	92.16
0.7086	91.90
0.6041	91.46
0.5092	91.08
0.4232	90.54
0.3351	89.86
0.2514	89.17
0.1642	86.80
0.1372	85.31
0.1222	84.40
0.1055	83.17
0.0980	82.52
0.0744	80.13
0.0596	78.05

$S_{BET}^{Ar} = 351\ m^2g^{-1}$

$C_{BET}^{Ar} = 280$

A P P E N D I X 5

WATER ADSORPTION ON CHROMIUM OXIDES

EXPERIMENTAL DATA

S^{W}_{BET} = Water BET Surface Area - $m^2 g^{-1}$

C^{W}_{BET} = Water BET C Constant

W ads = Amount Adsorbed - mg g^{-1}

WATER ADSORPTION DATA

A1(25)64V
(FSB 12)

P/Po	W ads mg g^{-1}
0.0035	10.00
0.0080	15.21
0.0191	21.89
0.0351	28.11
0.0570	33.20
0.0692	36.18
0.0931	40.57
0.1220	45.21
0.1580	52.60
0.1983	56.30
0.2743	62.49
0.3301	66.81
0.4071	75.00
0.5304	83.41
0.6386	92.63
0.7202	103.91
0.8280	129.50
0.9001	166.48
0.9361	212.00
0.9524	268.52
0.9310	249.20
0.9049	195.89
0.8570	153.51
0.7931	129.04
0.7230	114.01
0.6460	102.40
0.5800	95.87
0.4722	86.81
0.3471	76.93
0.3119	75.11
0.2560	70.90
0.1931	67.00
0.1494	62.81
0.1140	58.98
0.1022	57.19
0.0781	53.50
0.0603	49.89
0.0390	44.00
0.0240	37.03
0.0171	32.81
0.0101	27.05
0.0000	15.00

S^{W}_{BET} = 174 $m^2 g^{-1}$

C^{W}_{BET} = 36

A2(25)47V
(FSB 26)

P/Po	W ads mg g^{-1}
0.0013	7.43
0.0037	11.31
0.0060	14.20
0.0089	16.69
0.0131	18.96
0.0173	21.46
0.0226	23.51
0.0299	25.78
0.0375	28.50
0.0467	31.00
0.0582	33.71
0.0671	35.93
0.0797	38.26
0.0944	40.70
0.1191	44.25
0.1490	48.19
0.2007	54.17
0.2508	59.11
0.3006	63.66
0.3572	68.15
0.4286	73.25
0.4900	77.96
0.5923	85.61
0.6473	90.88
0.7197	99.14
0.7900	109.90
0.8483	124.65
0.8876	141.34
0.9133	160.08
0.8677	134.13
0.8215	119.66
0.7612	107.52
0.6862	98.92
0.6001	92.05
0.5157	86.94
0.4202	80.90
0.3415	75.19
0.2974	71.36
0.2287	65.43
0.1684	59.72
0.1165	53.84
0.0619	46.97
0.0325	40.31
0.0100	28.78
0.0000	0.00

S^{W}_{BET} = 172 $m^2 g^{-1}$

C^{W}_{BET} = 31

WATER ADSORPTION DATA

A2(130)20V
(FSB 29)

P/Po	W ads mg g^{-1}
0.0029	18.52
0.0084	24.96
0.0191	31.60
0.0294	35.85
0.0393	39.10
0.0616	44.08
0.0755	46.47
0.0942	49.12
0.1167	51.71
0.1569	55.49
0.2062	59.54
0.2791	64.66
0.3121	66.78
0.3903	72.22
0.4792	77.27
0.5429	82.71
0.6434	89.48
0.7328	97.85
0.8076	109.66
0.8700	127.50
0.9101	149.00
0.9332	173.06
0.9138	158.12
0.8225	122.47
0.7449	106.61
0.6799	99.57
0.6185	94.79
0.5482	90.54
0.4627	86.83
0.3746	83.51
0.2885	77.80
0.2083	72.16
0.1128	64.66
0.0955	62.00
0.0619	58.42
0.0420	54.30
0.0215	50.78
0.0115	47.26
0.0000	25.89

S^{W}_{BET} = 179 m^2g^{-1}

C^{W}_{BET} = 68

A3(25)64V
(FSB 66)

P/Po	W ads mg g^{-1}
0.0089	28.60
0.0199	36.32
0.0338	42.75
0.0535	48,72
0.0779	56.95
0.1062	63.33
0.1350	67.20
0.1634	70.89
0.2025	77.12
0.2505	81.69
0.2801	85.50
0.3043	87.25
0.3746	95.79
0.4648	103.46
0.5681	113.44
0.6610	124.75
0.7441	140.65
0.7869	151.81
0.8651	190.01
0.9191	243.44
0.8105	164.26
0.6909	134.53
0.5495	117.14
0.4003	106.03
0.2660	89.56
0.1477	75.93
0.0934	68.63
0.0506	60.19
0.0144	46.09
0.0000	0.00

S^{W}_{BET} = 233 m^2g^{-1}

C^{W}_{BET} = 48

WATER ADSORPTION DATA

A3(150)15V
(FSB 73)

P/Po	W ads mg g^{-1}
0.0100	29.65
0.0220	37.00
0.0344	40.61
0.0451	46.25
0.0682	52.53
0.0913	56.00
0.1154	60.11
0.1582	66.20
0.2056	71.91
0.2547	77.29
0.2909	81.02
0.3431	86.00
0.4176	92.13
0.5115	99.00
0.6117	105.56
0.7113	116.01
0.7528	125.42
0.8050	143.00
0.8315	159.04
0.7724	140.85
0.6725	117.41
0.5416	104.55
0.4401	98.59
0.3168	89.59
0.2028	79.64
0.1256	72.36
0.0585	64.69
0.0307	58.61
0.0155	53.54
0.0079	48.72
0.0000	38.70

S^{W}_{BET} = 218 m^2g^{-1}

C^{W}_{BET} = 48

A3(300)20V
(FSB 82)

P/Po	W ads mg g^{-1}
0.0105	11.13
0.0218	15.10
0.0341	17.74
0.0496	20.04
0.0661	22.50
0.0934	26.00
0.1385	31.21
0.1868	36.03
0.1978	37.02
0.2397	39.45
0.2612	40.84
0.3003	43.28
0.3750	47.80
0.4228	50.51
0.5180	56.78
0.6248	66.38
0.6971	75.40
0.7507	87.04
0.7879	106.80
0.6945	79.60
0.5865	65.82
0.4721	58.31
0.3462	52.32
0.2004	42.70
0.0973	33.95
0.0540	28.25
0.0315	25.33
0.0105	20.60
0.0000	6.75

S^{W}_{BET} = 130 m^2g^{-1}

C^{W}_{BET} = 18

WATER ADSORPTION DATA

A3(440)18V
(FSB 84)

P/Po	W ads mg g^{-1}
0.0126	8.11
0.0247	10.06
0.0399	11.87
0.0624	13.32
0.0855	14.98
0.1235	16.94
0.1768	19.33
0.2340	21.71
0.2733	23.83
0.3168	25.70
0.3871	29.97
0.4501	33.10
0.5172	36.99
0.6269	45.60
0.7407	62.18
0.7900	77.00
0.8251	94.02
0.8472	111.47
0.7633	79.55
0.7170	65.50
0.6361	49.07
0.5099	39.59
0.3407	31.78
0.1883	23.02
0.0860	18.67
0.0420	15.71
0.0123	11.65
0.0026	8.11
0.0000	2.39

S^{W}_{BET} = 66 m^2g^{-1}

C^{W}_{BET} = 27

A3(600)16V
(FSB 86)

P/Po	W ads mg g^{-1}
0.0100	11.38
0.0241	11.90
0.0346	12.27
0.0514	12.57
0.0852	13.10
0.1207	13.62
0.1603	14.30
0.2051	15.19
0.2434	16.09
0.2848	17.21
0.3499	18.49
0.4302	20.21
0.5235	21.93
0.6602	25.45
0.7512	30.39
0.8300	41.49
0.8797	56.06
0.8378	45.13
0.7701	34.20
0.6730	27.39
0.5220	22.68
0.3832	19.83
0.2704	17.29
0.1540	14.67
0.0700	13.25
0.0231	12.27
0.0102	11.83
0.0045	11.60
0.0029	11.23
0.0000	9.95

S^{W}_{BET} = 43 m^2g^{-1}

C^{W}_{BET} = 481

WATER ADSORPTION DATA

A3(800)16V
(FSB 88)

P/Po	W ads mg g^{-1}
0.0063	5.12
0.0168	5.42
0.0307	5.65
0.0506	5.87
0.0810	6.10
0.1146	6.25
0.1513	6.40
0.1862	6.63
0.2153	6.85
0.2473	7.31
0.2846	7.68
0.3247	8.08
0.4013	8.89
0.4936	9.79
0.5991	10.54
0.7037	11.60
0.8034	13.26
0.8278	14.20
0.9112	18.45
0.8572	15.40
0.7331	12.29
0.6465	11.31
0.5290	10.25
0.4205	9.32
0.3043	8.13
0.1618	6.85
0.1314	6.78
0.0732	6.40
0.0399	6.18
0.0102	5.65
0.0021	5.50
0.0000	4.40

S^{W}_{BET} = 18.7 m^2g^{-1}

C^{W}_{BET} = 196

A3(1000)17V
(FSB 89)

P/Po	W ads mg g^{-1}
0.0066	0.83
0.0129	0.90
0.0197	0.90
0.0401	0.98
0.0614	1.08
0.0818	1.17
0.1070	1.30
0.1335	1.45
0.1563	1.60
0.1847	1.81
0.2135	1.96
0.2379	2.11
0.2885	2.35
0.3557	2.64
0.4047	2.82
0.4585	3.04
0.5445	3.35
0.6424	3.83
0.7549	4.59
0.8200	5.44
0.8705	6.55
0.9448	15.59
0.8860	7.46
0.8493	6.10
0.7785	4.97
0.6854	4.14
0.5962	3.69
0.5002	3.31
0.3992	2.94
0.3001	2.53
0.2025	2.10
0.1015	1.58
0.0480	1.21
0.0223	0.98
0.0000	0.38

S^{W}_{BET} = 7.5 m^2g^{-1}

C^{W}_{BET} = 10

WATER ADSORPTION DATA

A3(1000)17V
(FSB 90)

Repeat Isotherm

P/Po	W ads mg g^{-1}
0.0131	0.83
0.0289	0.83
0.0511	0.96
0.0774	1.13
0.1089	1.26
0.1574	1.52
0.2140	1.81
0.2602	2.03
0.3032	2.18
0.4155	2.71
0.5225	3.09
0.6463	3.54
0.7355	4.37
0.8250	5.47
0.8861	7.26
0.9458	11.97
0.9290	10.77
0.8871	7.88
0.7795	5.12
0.6812	4.32
0.5545	3.91
0.4700	3.66
0.3803	2.86
0.3301	2.44
0.2014	1.73
0.1341	1.42
0.0646	1.05
0.0047	0.45
0.0000	0.00

S^{W}_{BET} = 6.4 m^2g^{-1}

C^{W}_{BET} = 14

A3(1060)7V
(FSB 63)

P/Po	W ads mg g^{-1}
0.0123	0.53
0.0215	0.59
0.0328	0.62
0.0422	0.65
0.0813	0.76
0.1002	0.83
0.1220	0.91
0.1571	1.03
0.1850	1.16
0.2100	1.28
0.2370	1.40
0.2610	1.51
0.2871	1.65
0.3045	1.73
0.4013	2.21
0.4989	2.67
0.6004	3.08
0.7252	3.78
0.8021	4.57
0.8433	5.18
0.9054	6.97
0.8469	5.45
0.7321	4.10
0.5944	3.35
0.4039	2.54
0.3272	2.19
0.2201	1.73
0.0606	1.08
0.0296	0.98
0.0101	0.80
0.0000	0.11

S^{W}_{BET} = 5.2 m^2g^{-1}

C^{W}_{BET} = 9

WATER ADSORPTION DATA

A4(25)64V (FSB 92)

P/Po	W ads mg g^{-1}
0.0047	28.53
0.0094	36.05
0.0236	46.29
0.0362	51.29
0.0551	55.54
0.0748	59,55
0.1023	63.80
0.1466	68.79
0.1849	72.14
0.2224	74.82
0.2778	78.29
0.3391	80.77
0.3900	82.79
0.4378	84.45
0.5010	86.47
0.5555	88.29
0.6090	90.14
0.6536	91.88
0.7119	93.98
0.7780	97.29
0.8341	100.67
0.8779	104.27
0.9220	109.14
0.9550	116.45
0.9604	124.54
0.9380	112.98
0.8834	105.59
0.8249	101.91
0.7402	99.23
0.6709	97.70
0.6001	96.21
0.5298	94.89
0.4606	93.49
0.4021	91.71
0.3339	89.98
0.2660	86.55
0.1909	83.21
0.1280	79.08
0.0669	73.25
0.0380	67.27
0.0197	59.79
0.0121	52.77
0.0039	41.95
0.0000	12.59
0.0000	9.62

S^{W}_{BET} = 215 m^2g^{-1}

C^{W}_{BET} = 138

B6(25)75V (FSB 91)

P/Po	W ads mg g^{-1}
0.0092	24.92
0.0189	45.37
0.0294	58.44
0.0488	72.07
0.0724	83.81
0.1012	96.21
0.1422	111.41
0.1799	125.21
0.2156	138.17
0.2518	150.35
0.2880	162.59
0.3339	179.12
0.3819	199.07
0.4679	237.29
0.5209	261.26
0.5739	289.81
0.6484	327.35
0.7150	348.41
0.7905	361.10
0.8614	369.59
0.8970	374.28
0.9401	380.65
0.9715	387.86
0.9275	379.37
0.8698	373.78
0.7932	368.14
0.7040	360.93
0.6122	351.93
0.5067	337.07
0.4278	305.73
0.4076	280.92
0.3929	250.30
0.3572	216.39
0.3300	195.38
0.2925	174.93
0.2610	162.31
0.2198	147.28
0.1749	131.86
0.1180	113.08
0.0713	93.31
0.0346	69.39
0.0102	43.86
0.0000	0.00

S^{W}_{BET} = 470 m^2g^{-1}

C^{W}_{BET} = 16

WATER ADSORPTION DATA

B8(25)64V
(FSB 93)

P/Po	W ads mg g^{-1}
0.0037	32.72
0.0092	48.60
0.0254	70.55
0.0438	84.92
0.0603	94.64
0.0740	100.71
0.0923	107.30
0.1099	113.80
0.1338	120.91
0.1521	125.18
0.1697	129.30
0.2193	137.98
0.2578	143.05
0.2809	145.57
0.3019	147.75
0.3499	151.73
0.4018	155.43
0.4490	158.04
0.5401	161.50
0.6253	164.01
0.7121	166.52
0.8183	169.84
0.8750	171.60
0.9301	173.54
0.9713	174.96
0.8816	172.50
0.7748	170.46
0.6951	168.85
0.6020	166.95
0.5125	165.01
0.4328	162.59
0.3528	159.41
0.3001	156.00
0.2570	151.73
0.2240	147.08
0.1923	141.11
0.1479	132.20
0.1033	121.53
0.0679	109.53
0.0399	93.98
0.0231	78.62
0.0100	59.74
0.0000	26.55
0.0000	11.38
0.0000	3.37

S^{W}_{BET} = 421 m^2g^{-1}

C^{W}_{BET} = 46

S2(25)65V
(FSB 6)

P/Po	W ads mg g^{-1}
0.0012	6.69
0.0056	12.11
0.0149	21.67
0.0356	29.32
0.0598	38.45
0.1030	46.47
0.1660	52.90
0.2485	59.80
0.3120	63.79
0.3741	69.36
0.4946	76.32
0.6198	83.12
0.7172	89.33
0.8700	102.72
0.9147	111.16
0.7676	95.07
0.6276	89.44
9.4544	84.02
0.2985	70.53
0.1355	56.88
0.0604	47.69
0.0000	18.48
0.0000	6.37
0.0000	5.58

S^{W}_{BET} = 172 m^2g^{-1}

C^{W}_{BET} = 45

WATER ADSORPTION DATA

$CrOOH(25)89V$ (FSB 21)

P/Po	W ads mg g^{-1}
0.0010	0.35
0.0238	0.59
0.0340	0.70
0.0471	0.83
0.0739	0.83
0.1026	0.83
0.1472	0.83
0.1988	0.98
0.2529	1.14
0.3161	1.19
0.3956	1.34
0.4827	1.55
0.5759	1.91
0.6938	2.63
0.7835	3.56
0.8937	5.84
0.9510	8.20
0.9865	11.57
0.9068	7.08
0.8238	4.90
0.7180	3.51
0.6340	2.84
0.5495	2.47
0.4489	2.21
0.3636	2.07
0.2888	2.01
0.1964	1.91
0.1[illegible]	1.70
0.0640	1.50
0.0439	1.24
0.0260	1.03
0.0128	0.77
0.0001	0.41
0.0000	0.21

S^{W}_{BET} = 3.1 m^2g^{-1}

C^{W}_{BET} = 37

*$CrO_2(25)260V$ (FSB 18)

P/Po	W ads mg g^{-1}
0.0210	1.86
0.0299	2.06
0.0463	2.39
0.0722	2.67
0.1022	3.03
0.1400	3.47
0.1826	3.75
0.2168	4.20
0.2792	4.52
0.3446	4.92
0.4112	5.29
0.5024	5.65
0.6437	6.37
0.7346	7.29
0.8005	8.38
0.9239	13.52
0.8636	10.25
0.6748	6.69
0.4948	5.61
0.3762	5.12
0.2208	4.40
0.1367	3.91
0.0773	3.59
0.0237	3.19
0.0000	3.43
0.0000	7.34
0.0000	17.99

* Mercury Vapour Present: cf. Appendix 6.

S^{W}_{BET} = 12.4 m^2g^{-1}

C^{W}_{BET} = 36

A P P E N D I X 6

MERCURY VAPOUR ADSORPTION ON CHROMIUM OXIDES

(Including Water Vapour Isotherms
Determined on Chromium Dioxide)

EXPERIMENTAL DATA

S^{W}_{BET} = Water BET Surface Area - m^2g^{-1}

C^{W}_{BET} = Water BET C Constant

W ads = Amount Adsorbed - mg g^{-1}

MERCURY VAPOUR ADSORPTION DATA

Weight Change of A1(225)16 on Outgassing at 25°C (Fig. 5.1)

(FSB 14)

Time (h)	Overall Weight Loss (mg g^{-1})
Mercury Vapour Absent	
0	0
0.25	1.25
0.5	2.96
0.75	5.99
1.75	7.05
3.5	7.56
6.0	7.97
9.0	8.30
12.5	8.55
20.5	8.92
22.5	8.98
25.5	9.07
30.5	9.18
34.5	9.25
38.0	9.31
46.5	9.43
52.0	9.47
55.0	9.50
55.25	9.50
Mercury Vapour Present (22°C)	
55.33	9.31
55.42	9.14
56.00	7.92
56.50	6.89
57.00	5.82
Mercury Vapour Absent	
57.08	5.74
57.17	5.76
57.50	5.74
58.00	5.74
59.50	5.74
70.00	5.74
75.50	5.74
Mercury Vapour Present (65°C)	
75.67	5.67
75.75	5.54
75.83	5.30
75.92	5.06
76.17	4.27
76.67	2.64
Mercury Vapour Absent; Oxygen Present (1 torr)	
76.75	2.55
76.83	2.51
77.00	2.51
77.50	2.49
78.00	2.48
78.25	2.46
78.67	2.45
79.00	2.41
79.25	2.38
Mercury Vapour Present (35°C)	
79.42	2.32
79.50	2.16
79.67	1.75
79.75	1.55
80.00	0.93
Mercury Vapour Absent	
95.0	0.87
263.0	0.85
599.0	0.84

MERCURY VAPOUR ADSORPTION DATA

Mercury Vapour Adsorption on Chromium Dioxide (Fig. 5.2)

First Uptake
CrO_2(25)23V
(FSB 23-a)

Time (h)	Uptake (mg g^{-1})
0.25	0.75
0.75	1.76
1.5	3.51
2.0	4.51
2.5	5.39
3.0	6.14
4.0	7.27
5.0	8.65
6.0	9.59
7.0	10.16
8.0	10.66
9.0	11.16
10.0	11.41
11.0	11.66
16.0	12.70
19.0	13.10
21.0	13.16
21.5	13.16

Second Uptake
CrO_2(25)40V
(FSB 23-b)

Time (h)	Uptake (mg g^{-1})
1	1.97
2	3.46
3	4.70
4	5.55
5	6.10
6	6.60
7	6.90
8	7.20
9	7.40
10	7.55
11	7.60
12	7.70
16	7.90
18	7.90
20	8.00
24	8.00
39	8.50

MERCURY VAPOUR ADSORPTION DATA

Water Vapour Adsorption on Chromium Dioxide

Systematic mercury vapour adsorption experiment (FSB 23) constructed as follows:

23-1 - Hg vapour completely absent during both outgassing and isotherm.
23-2 - Hg vapour present during outgassing but absent during isotherm.
23-3 - Hg vapour present, both during outgassing and isotherm.

CrO_2(25)14V

(FSB 23-1)

P/Po	W ads mg g^{-1}	P/Po	W ads mg g^{-1}
0.0084	0.94	0.7837	8.78
0.0173	1.13	0.8420	10.47
0.0315	1.44	0.9154	14.98
0.0414	1.57	0.8708	13.04
0.0519	1.69	0.8325	11.16
0.0614	1.82	0.7858	9.34
0.0713	1.88	0.7391	8.15
0.0818	2.01	0.6772	7.02
0.0918	2.07	0.6222	6.21
0.1012	2.13	0.5660	5.58
0.1285	2.19	9.5046	4.89
0.1542	2.26	0.4417	4.26
0.1841	2.26	0.3714	3.64
0.2104	2.32	0.3069	3.26
0.2413	2.38	0.2413	3.01
0.2765	2.51	0.1993	2.88
0.3069	2.63	0.1464	2.70
0.3709	3.07	0.0965	2.51
0.4118	3.45	0.0829	2.44
0.4538	3.82	0.0525	2.26
0.5130	4.45	0.0247	2.01
0.5697	5.14	0.0178	1.82
0.6201	5.70	0.0131	1.69
0.6725	6.46	0.0000	0.88
0.7260	7.40		

S^W_{BET} = 6.5 m^2g^{-1}

C^W_{BET} = 1800

MERCURY VAPOUR ADSORPTION DATA

Water Vapour Adsorption on Chromium Dioxide

$CrO_2(25)23V$ (FSB 23-2)

P/Po	W ads mg g^{-1}
0.0079	0.25
0.0173	0.37
0.0325	0.56
0.0477	0.68
0.0656	0.87
0.0850	1.05
0.1091	1.24
0.1385	1.55
0.1925	1.98
0.2439	2.41
0.3273	3.03
0.4018	3.59
0.4789	4.08
0.5849	4.82
0.6841	5.75
0.7386	6.55
0.8325	8.96
0.8876	11.19
0.8063	8.10
0.7265	6.37
0.6342	5.44
0.5183	4.64
0.4469	4.14
0.3693	3.65
0.2896	3.15
0.2146	2.66
0.1521	2.23
0.1044	1.79
0.0661	1.42
0.0346	1.11
0.0184	0.93
0.0000	0.87

S^W_{BET} = 10.4 m^2g^{-1}

C^W_{BET} = < 10

$CrO_2(25)40V$ (FSB 23-3)

P/Po	W ads mg g^{-1}
0.0110	0.36
0.0346	0.85
0.0546	1.21
0.0734	1.39
0.0934	1.58
0.1285	1.88
0.1616	2.18
0.2135	2.61
0.2786	3.15
0.3326	3.64
0.3940	4.06
0.4700	4.54
0.5513	5.09
0.6332	5.64
0.7077	6.24
0.7837	7.15
0.8803	9.82
0.8645	9.09
0.9233	14.24
0.9033	11.45
0.8383	8.24
0.7538	6.73
0.6683	5.94
0.5791	5.27
0.5115	4.85
0.4333	4.36
0.3588	3.94
0.2707	3.45
0.2109	3.76
0.2135	4.61
0.2146	5.03
0.1810	5.09
0.1269	4.73
0.0803	4.42
0.0451	4.12
0.0210	4.06
0.0000	4.12
0.0000	6.06
0.0000	8.00
0.0000	9.88

S^W_{BET} = 10.4 m^2g^{-1}

C^W_{BET} = < 10

A P P E N D I X 7

NITROGEN ADSORPTION ON SILICAS

EXPERIMENTAL DATA

S^{N}_{BET} = Nitrogen BET Surface Area - m^2g^{-1}

C^{N}_{BET} = Nitrogen BET C Constant

V ads = Amount Adsorbed - $cm^3(STP)g^{-1}$

NITROGEN ADSORPTION DATA

*TK 800-II(25)13V
(FSB 50)

P/Po	V ads $cm^3(STP)g^{-1}$
0.0100	21.50
0.0229	26.83
0.0327	29.05
0.0420	30.80
0.0079	32.87
0.0798	35.18
0.0947	36.49
0.1137	38.20
0.1653	42.07
0.1963	44.17
0.2407	46.93
0.2705	48.66
0.3105	51.63
0.4172	58.13
0.4724	62.15
0.5394	67.91
0.6062	74.56
0.6774	82.19
0.7367	91.06
0.8261	110.73
0.8800	129.71
0.9210	157.00
0.9455	190.24
0.8927	147.41
0.8237	113.70
0.7362	92.20
0.6582	80.13
0.5958	73.77
0.4864	64.00
0.4231	59.01
0.3602	54.70
0.2659	48.52
0.1416	40.31
0.0739	34.62
0.0463	31.00
0.0143	23.51
0.0074	18.49

S^N_{BET} = 161.7 m^2g^{-1}

C^N_{BET} = 84

* "soaked" material

TK 800-II(140)16V
(FSB 34)

P/Po	V ads $cm^3(STP)g^{-1}$
0.0049	19.78
0.0106	23.85
0.0342	30.51
0.0399	31.80
0.0485	32.92
0.0620	34.75
0.0727	35.87
0.0841	37.04
0.0968	38.16
0.1136	39.57
0.1329	41.01
0.1570	42.69
0.1932	45.08
0.2285	47.33
0.2559	48.83
0.2835	50.50
0.3637	55.22
0.4227	58.83
0.4825	62.73
0.5442	66.40
0.6145	72.58
0.6829	79.28
0.7521	88.11
0.7941	95.48
0.8636	112.63
0.9132	135.93
0.9469	165.74
0.9328	156.64
0.8940	130.15
0.8437	108.81
0.7751	93.12
0.7078	83.13
0.6344	75.15
0.5566	68.36
0.4928	63.62
0.4411	60.27
0.4036	57.86
0.3680	55.51
0.3380	53.81
0.3127	52.41
0.2708	49.89
0.2043	46.00
0.1341	41.02

S^N_{BET} = 164.1 m^2g^{-1}

C^N_{BET} = 99

NITROGEN ADSORPTION DATA

TK 800-II(RT)16V*
(Data for Fig.3.6)

P/Po	V ads $cm^3(STP)g^{-1}$
0.0005	11.10
0.0036	18.63
0.0143	25.53
0.0165	26.38
0.0186	26.96
0.0487	33.16
0.0616	34.72
0.0733	36.09
0.1136	39.58
0.1456	4.97
0.1746	43.96
0.2038	45.74
0.2293	47.37
0.2880	50.43
0.3357	53.26
0.3854	56.13
0.4741	61.52
0.5433	66.07
0.5650	68.04
0.6761	77.61
0.7520	87.35
0.8563	110.01
0.7085	81.79
0.3910	56.51
0.3177	52.54

* D.H. Turk, Ph.D. Thesis,
Brunel University, (1972).

TK 800-II(1000)2.5V
(FSB 41)

P/Po	V ads $cm^3(STP)g^{-1}$
0.0146	17.73
0.0222	20.65
0.0314	23.10
0.0463	25.84
0.0668	28.71
0.0871	30.75
0.1084	32.61
0.1473	35.29
0.1971	38.40
0.2309	40.31
0.2678	42.39
0.3114	44.99
0.3908	49.29
0.4585	54.24
0.5016	57.15
0.5498	60.51
0.6079	65.08
0.6818	72.25
0.7685	82.90
0.8444	97.76
0.9039	118.94
0.9469	154.20
0.9255	137.51
0.8745	109.55
0.8144	92.21
0.7413	79.66
0.6591	70.09
0.5344	59.70
0.4473	53.72
0.3834	49.10
0.2853	43.59
0.1894	38.01
0.0993	31.61
0.0769	29.50

S^N_{BET} = 142.6 m^2g^{-1}

C^N_{BET} = 65

NITROGEN ADSORPTION DATA

TK 800-III(140)15V
(FSB 43)
(Manometric Pressure)

P/Po	V ads $cm^3(STP)g^{-1}$
0.0060	21.08
0.0106	23.95
0.0134	24.98
0.0266	28.49
0.0334	30.08
0.0404	31.29
0.0458	32.02
0.0528	32.96
0.0600	33.90
0.0678	34.77
0.0782	35.78
0.0896	36.79
0.1033	37.99
0.1268	39.84
0.1494	41.47
0.1812	43.51
0.2310	46.42
0.2678	48.62
0.3058	50.75
0.3453	52.87
0.3925	55.92
0.4419	58.69
0.4951	62.27
0.5770	68.16
0.6340	72.86
0.7052	80.47
0.7867	91.70
0.8556	106.96
0.9083	127.25
0.9458	158.04
0.8963	123.01
0.8452	105.04
0.7770	90.49
0.7002	79.78
0.6295	72.70
0.5735	68.12
0.5257	64.53
0.4829	61.58
0.4461	59.10
0.4148	57.05
0.3664	54.19
0.2853	49.75
0.1920	44.30
0.1301	40.08
0.0913	36.81

S^N_{BET} = 161.0 m^2g^{-1}

C^N_{BET} = 97

TK 800-III(140)15V
(FSB 43)
(Transducer Pressure)

P/Po	V ads $cm^3(STP)g^{-1}$
0.0053	21.48
0.0101	23.78
0.0126	24.81
0.0258	28.59
0.0330	29.66
0.0401	30.79
0.0455	31.50
0.0525	32.38
0.0599	33.27
0.0679	34.10
0.0778	35.21
0.0892	36.22
0.1031	37.38
0.1266	38.98
0.1491	40.54
0.1811	42.51
0.2306	45.58
0.2677	47.58
0.3057	49.74
0.3445	52.09
0.3914	55.19
0.4398	58.16
0.4932	61.63
0.5745	67.34
0.6313	72.03
0.7018	79.88
0.7826	91.29
0.8513	106.45
0.9027	127.11
0.9396	158.05
0.8903	123.11
0.8400	104.60
0.7714	89.59
0.6959	79.03
0.6260	71.60
0.5707	67.48
0.5235	64.01
0.4810	61.05
0.4443	58.78
0.4137	57.00
0.3660	54.02
0.2852	48.80
0.1925	43.73
0.1304	39.52
0.0915	36.58

S^N_{BET} = 155.0 m^2g^{-1}

C^N_{BET} = 122

NITROGEN ADSORPTION DATA

Fransil(140)15V
(FSB 30)

P/Po	V ads $cm^3(STP)g^{-1}$
0.0564	8.20
0.0624	7.65
0.0676	8.54
0.0752	8.78
0.0844	8.94
0.0960	9.23
0.1134	9.27
0.1373	9.46
0.1617	10.37
0.1908	10.79
0.2307	11.38
0.2768	11.95
0.3344	12.73

S^N_{BET} = 38.6 m^2g^{-1}

C^N_{BET} = 131

Fransil(140)31V
(FSB 31)

P/Po	V ads $cm^3(STP)g^{-1}$
0.0025	4.31
0.0050	5.20
0.0071	5.59
0.0212	7.00
0.0251	7.29
0.0310	7.59
0.0405	8.08
0.0486	8.30
0.0574	8.61
0.0676	8.88
0.0816	9.26
0.0989	9.61
0.1220	10.06
0.1463	10.53
0.1592	10.63
0.1748	10.99
0.1937	11.27
0.2158	11.65
0.2434	12.11
0.2816	12.65
0.3320	13.29
0.3851	14.07
0.4406	14.95
0.5901	16.18
0.5795	17.43
0.6577	19.08
0.7186	20.71
0.7724	22.55
0.8348	25.28
0.8892	28.58
0.9345	34.04
0.7589	22.10
0.7072	20.39
0.6645	19.25
0.5900	17.55
0.5227	16.35
0.4560	15.25
0.4019	14.40
0.3493	13.63

S^N_{BET} = 41.2 m^2g^{-1}

C^N_{BET} = 110

NITROGEN ADSORPTION DATA

Gel E(1000)2V
(FSB 46)

P/Po	V ads $cm^3(STP)g^{-1}$
0.0570	30.93
0.0735	32.60
0.0906	34.09
0.1048	34.72
0.1215	36.30
0.1405	37.47
0.1605	38.77
0.1881	40.04
0.2187	41.34
0.2566	42.80
0.3210	44.73
0.4169	46.79
0.5142	48.03
0.5858	48.72
0.6753	49.69
0.7638	50.81
0.8504	52.10
0.9497	54.60
0.8506	52.93
0.6746	50.28
0.5148	48.09
0.4175	46.88
0.3215	44.82
0.2903	43.77
0.1203	36.32
0.0639	31.97
0.0360	28.58
0.0223	26.03
0.0166	24.36

S^N_{BET} = 150 m^2g^{-1}

C^N_{BET} = 99

Gel J(1000)2V
(FSB 48)

P/Po	V ads $cm^3(STP)g^{-1}$
0.0115	36.34
0.0199	43.09
0.0370	51.11
0.0528	56.00
0.0730	60.60
0.0900	63.74
0.1116	67.10
0.1711	75.15
0.2379	83.37
0.2950	90.49
0.3737	100.91
0.4529	113.08
0.5308	127.98
0.6382	156.98
0.7055	189.04
0.7699	238.63
0.8284	335.09
0.8451	391.84
0.8197	374.17
0.7849	323.07
0.7453	254.97
0.6321	162.94
0.5521	136.00
0.3969	105.60
0.2326	83.97
0.1831	77.89

S^N_{BET} = 289 m^2g^{-1}

C^N_{BET} = 72

A P P E N D I X 8

ARGON ADSORPTION ON SILICAS

EXPERIMENTAL DATA

S_{BET}^{Ar} = Argon BET Surface Area - m^2g^{-1}

C_{BET}^{Ar} = Argon BET C Constant

V ads = Amount Adsorbed - $cm^3(STP)g^{-1}$

ARGON ADSORPTION DATA

TK 800-II(140)20V
(FSB 36)

P/Po	V ads $cm^3(STP)g^{-1}$
0.0050	9.00
0.0151	14.01
0.0236	16.99
0.1329	19.24
0.0442	21.71
0.0580	23.91
0.0659	24.91
0.0757	26.25
0.0901	27.96
0.1003	29.04
0.1100	30.09
0.1200	31.06
0.1441	33.24
0.1809	35.98
0.2086	38.12
0.2474	40.59
0.3038	44.51
0.3446	47.14
0.4239	52.52
0.5058	57.72
0.5582	61.57
0.6147	65.83
0.6874	71.63
0.7866	80.99
0.8431	88.14
0.9014	97.99
0.9460	108.38
0.9799	118.68
0.9643	114.41
0.9267	103.79
0.8808	94.21
0.8254	85.58
0.7710	79.10
0.6768	70.51
0.6488	68.28
0.5945	64.00
0.5431	60.52
0.4431	53.51
0.3503	47.48
0.2844	43.30
0.2405	40.21
0.2079	37.99
0.1744	35.72
0.1306	32.11
0.0884	27.78
0.0678	25.50

S_{BET}^{Ar} = 162.6 m^2g^{-1}

C_{BET}^{Ar} = 33

Fransil(140)51V
(FSB 32)

P/Po	V ads $cm^3(STP)g^{-1}$
0.0061	2.40
0.0122	3.11
0.0134	3.30
0.1210	4.01
0.0311	4.62
0.0428	5.39
0.0478	5.60
0.0572	5.97
0.0652	6.24
0.0742	6.58
0.0927	7.10
0.1003	7.32
0.1199	7.91
0.1502	8.47
0.2043	9.49
0.2596	10.49
0.3046	11.16
0.3555	11.88
0.4189	12.73
0.4626	13.43
0.5356	14.37
0.6043	15.11
0.6681	16.00
0.7451	17.50
0.8196	19.41
0.9110	22.32
1.0025	27.17
0.9674	25.31
0.8761	21.21
0.7734	18.19
0.6867	16.42
0.5645	14.61
0.4746	13.48
0.4253	12.90

S_{BET}^{Ar} = 41.4 m^2g^{-1}

C_{BET}^{Ar} = 32

A P P E N D I X 9

WATER VAPOUR ADSORPTION ON SILICAS

EXPERIMENTAL DATA

S^{W}_{BET} = Water BET Surface Area - m^2g^{-1}

C^{W}_{BET} = Water BET C Constant

W ads = Amount Adsorbed - mg g^{-1}

WATER ADSORPTION DATA

TK 800-II(25)19V
(FSB 40)

P/Po	W ads mg g^{-1}
0.0144	3.07
0.0244	3.84
0.0380	4.76
0.0561	5.76
0.0727	6.60
0.0910	7.29
0.1146	8.37
0.1482	9.60
0.2007	11.13
0.2460	12.44
0.2264	11.67
0.3074	13.97
0.3704	15.81
0.4538	18.81
0.5117	21.34
0.5959	25.95
0.6757	32.93
0.7381	41.30
0.7984	55.19
0.7449	47.13
0.6804	38.84
0.6229	33.24
0.5894	30.32
0.5241	36.10
0.4341	21.65
0.3494	18.19
0.2662	15.19
0.2098	13.20
0.1553	11.13
0.1033	9.06
0.0837	8.14
0.0706	7.52
0.0514	6.52
0.0312	5.14
0.0210	4.45
0.0105	3.53
0.0092	2.84
0.0000	1.15
0.0000	1.07
0.0000	1.07

S^{W}_{BET} = 40 m^2g^{-1}

C^{W}_{BET} = 15

TK 800-II(25)10V*
(FSB 44)

P/Po	W ads mg g^{-1}
0.0144	3.14
0.0270	4.44
0.0472	6.20
0.0679	7.66
0.0913	9.12
0.1159	10.57
0.1540	12.49
0.2190	15.46
0.2980	19.25
0.3499	21.98
0.4548	27.96
0.5419	34.16
0.6277	42.67
0.7069	54.69
0.7790	73.92
0.8147	89.55
0.8608	117.35
0.8737	124.63
0.8826	131.14
0.8362	105.78
0.7071	56.38
0.6033	39.53
0.4850	29.95
0.3756	22.90
0.3812	18.23
0.2069	14.94
0.1322	11.11
0.0708	7.58
0.0551	6.28
0.1130	10.11
0.0407	5.51
0.0202	3.45
0.0089	2.14
0.0000	0.00

S^{W}_{BET} = 54 m^2g^{-1}

C^{W}_{BET} = 12

* "soaked" material

WATER ADSORPTION DATA

TK 800-II(1/40)17V
(FSB 35)

P/Po	W ads mg g^{-1}
0.0094	2.08
0.0233	3.29
0.0357	4.41
0.0498	5.02
0.0650	5.80
0.0776	6.40
0.0910	6.83
0.1036	7.35
0.1309	8.39
0.1537	9.43
0.1844	10.29
0.2143	11.42
0.2534	12.54
0.2898	13.58
0.3488	15.40
0.4055	17.30
0.4606	19.46
0.5309	22.66
0.6198	28.89
0.6809	35.38
0.7593	48.87
0.7816	56.00
0.7759	54.21
0.8661	92.90
0.8414	79.32
0.8071	70.58
0.7509	57.87
0.6806	46.36
0.6712	45.32
0.5697	34.60
0.4782	28.37
0.4123	24.74
0.3224	20.93
0.2193	16.61
0.1466	12.97
0.1081	11.59
0.8068	10.47
0.0671	9.34
0.0511	8.39
0.0357	7.27
0.0241	6.31
0.0163	5.45
0.0079	4.50
0.0000	2.51

S^{W}_{BET} = 42 m^2g^{-1}

C^{W}_{BET} = 11

Fransil(25)16V
(L.J. Stryker)

P/Po	W ads mg g^{-1}
0.0090	0.95
0.0379	1.77
0.0598	2.09
0.0842	2.44
0.1128	2.84
0.1555	3.29
0.1822	3.55
0.2567	4.06
0.3195	4.53
0.3923	4.90
0.4884	5.52
0.5620	6.19
0.6215	6.74
0.7171	8.12
0.8192	10.56
0.8882	14.30
0.9428	24.20
0.9004	17.46
0.8461	13.20
0.8127	11.70
0.7617	10.01
0.7099	8.87
0.6327	7.72
0.5292	6.62
0.4244	5.64
0.3193	4.93
0.2072	3.98
0.1064	2.96
0.0292	1.93
0.0000	0.39
0.0000	0.12
0.0000	0.08

S^{W}_{BET} = 12.4 m^2g^{-1}

C^{W}_{BET} = 19

WATER ADSORPTION DATA

TK 800-II(1000)2.5V (FSB 38)

P/Po	W ads mg g^{-1}
0.0197	1.75
0.0407	2.02
0.0598	2.10
0.1002	2.54
0.1272	2.80
0.1506	3.07
0.1768	3.33
0.2020	3.68
0.2290	3.94
0.2662	4.19
0.3024	4.56
0.3950	5.52
0.5023	6.66
0.4391	6.57
0.3268	6.05
0.2198	5.52
0.1062	4.56
0.0535	4.12
0.0113	3.86
0.0000	3.33
0.0000	3.33

S^{W}_{BET} = 13.5 m^2g^{-1}

C^{W}_{BET} = 13

TK 800-II(1000)2.5V (FSB 39)

P/Po	W ads mg g^{-1}
0.0157	0.53
0.0420	1.05
0.0682	1.32
0.0949	1.67
0.1233	1.93
0.1603	2.28
0.1967	2.72
0.2256	2.89
0.2471	3.16
0.2791	3.33
0.3124	3.68
0.3835	4.30
0.4312	4.82
0.5464	6.58
0.6243	8.59
0.6757	10.61
0.7344	14.38
0.7664	19.38
0.6686	16.75
0.5317	13.07
0.3738	10.08
0.2636	8.59
0.1663	7.19
0.0800	6.14
0.0519	5.52
0.0205	4.91
0.0000	3.86

S^{W}_{BET} = 11.4 m^2g^{-1}

C^{W}_{BET} = 8

WATER ADSORPTION DATA

Gel E(1000)2V
(FSB 45)

P/Po	W ads mg g^{-1}
0.0205	0.48
0.0433	0.59
0.0703	1.07
0.0908	1.28
0.1112	1.39
0.1663	1.92
0.2400	3.00
0.2935	3.85
0.3801	6.36
0.4721	10.91
0.5513	19.94
0.6101	30.39
0.6361	40.36
0.6950	51.81
0.7934	59.50
0.6605	58.22
0.4928	55.60
0.3447	52.34
0.2751	48.49
0.2302	40.01
0.2167	30.10
0.1600	21.49
0.0792	14.38
0.0000	6.52

S^{W}_{BET} = 16 m^2g^{-1}

C^{W}_{BET} = 3

Gel J(1000)2V
(FSB 49

P/Po	W ads mg g^{-1}
0.0189	2.26
0.0477	3.29
0.0816	4.09
0.1065	4.76
0.1618	5.86
0.2111	6.89
0.2560	8.23
0.3019	9.76
0.4076	12.56
0.4716	15.80
0.5582	22.63
0.6521	33.61
0.7321	68.68
0.7987	114.79
0.6904	96.55
0.5857	67.70
0.4661	44.22
0.3001	33.18
0.1883	27.39
0.1044	22.75
0.0472	18.85
0.0254	17.08
0.0073	14.82
0.0000	12.44

S^{W}_{BET} = 24 m^2g^{-1}

C^{W}_{BET} = 14

Aerosil 200(1000)2V
(FSB 51)

0.0118	0.57
0.0286	0.73
0.0472	0.81
0.0858	0.97
0.1351	1.37
0.1750	1.70
0.2046	1.86
0.2502	2.28
0.2862	2.59
0.3261	3.00
0.3635	3.39
0.4309	4.28
0.5196	5.74
0.6030	8.16
0.6896	14.30
0.7856	23.75
0.6547	22.62
0.5526	19.07
0.4732	16.40
0.3798	13.98
0.2990	12.04
0.2203	10.58
0.1613	9.37
0.0808	7.68
0.0546	7.19
0.0173	6.22
0.0000	5.49

S^{W}_{BET} = 10.1 m^2g^{-1}

C^{W}_{BET} = 5

A P P E N D I X 10

STANDARD DATA

Nitrogen Adsorption on Gel B3(880)2 *

P/Po	V $cm^3 g^{-1}$	α_s
0.01	1.57	0.42
0.02	1.72	0.46
0.03	1.87	0.50
0.04	1.98	0.53
0.05	2.05	0.55
0.06	2.15	0.58
0.07	2.23	0.60
0.08	2.28	0.61
0.09	2.35	0.63
0.10	2.39	0.64
0.15	2.65	0.71
0.20	2.87	0.77
0.25	3.10	0.83
0 30	3.32	0.89
0.35	3.51	0.94
0.40	3.73	1.00
0.45	3.95	1.06
0.50	4.18	1.12
0.55	4.40	1.18
0.60	4.70	1.26
0.65	5.00	1.34
0.70	5.30	1.42
0.75	5.82	1.56
0.80	6.53	1.75
0.85	7.42	1.99

S^{N}_{BET} = 11.0 $m^2 g^{-1}$

* J.D. Carruthers, Ph.D. Thesis, Brunel University, (1968).